UNIVERSITY OF LIVERPOOL

Investigating the relationship between vitamin C, cGMP and Ca^{2+} with regard to hepatoprotection

Bright Ozuruoke Enyindah

Thesis submitted in accordance with the requirements of the University of Liverpool for the degree of Doctor in Philosophy

April 2020

Declaration

I **Bright Ozuruoke Enyindah** confirm that the work presented in this thesis is all my own work and has not been submitted for any other degree.

Table of Contents

Abstract

Elevated intracellular calcium ion concentration ($[Ca^{2+}]_i$) is a key event in the development of a cytotoxic response in hepatocytes. One molecule that appears to interfere with the calcium ion (Ca^{2+})-mediated cell damage is Cyclic guanosine 3',5'-monophosphate (cGMP). Agents that elevate cellular cGMP have been reported to reduce $[Ca^{2+}]_i$ and protect hepatocytes against Ca^{2+}-mediated cell death. There is evidence of vitamin C (Vit C) elevating cGMP in certain cell types, however, whether this can be achieved in human hepatocytes has not been investigated. In addition, the underlying mechanism is still not clear, but there are some indications of the involvement of cell surface protein disulphide isomerase (csPDI). PDI was traditionally thought to be an ER-resident protein, however, studies suggest that it is expressed on the surface of certain cell types where it colocalizes with and modulates the action of the membrane associated particulate guanylyl cyclase (pGC).

In this study, whether Vit C has the ability, like atrial natriuretic peptide (ANP) and sodium nitroprusside (SNP), to elevate cGMP, decrease $[Ca^{2+}]_i$ and protect human hepatocytes against the damage induced by harmful $[Ca^{2+}]_i$ elevations was investigated using the human liver cancer cell line HepG2 and where possible primary human hepatocytes (PHHs). Using human embryonic kidney 293 (HEK293) cells as a non-hepatic model cell line, the ability of Vit C to elevate cGMP and decrease $[Ca^{2+}]_i$ in non-hepatic cells was also confirmed. Finally, the functional involvement of PDI in these mechanisms, its cellular presence and localization/colocalization with the natriuretic peptide receptor type A (NPRA), as well as its externalization route in human hepatocytes was investigated.

Vit C, like ANP and SNP elevated cGMP and attenuated thapsigargin (Tg)-induced $[Ca^{2+}]_i$ elevations in HepG2 cells. The Vit C and ANP, but not SNP-mediated cGMP elevations and attenuation of $[Ca^{2+}]_i$ signal was downregulated by the inhibition of PDI with the PDI inhibitor bacitracin (Bac) and the anti-PDI monoclonal antibody RL90. The ability of Vit C to elevate cGMP and attenuate $[Ca^{2+}]_i$ signal was also observed in HEK293 cells, and the mechanisms appeared to be regulated by PDI. Using immunofluorescence, we found that HepG2 and HEK293 cells expressed membrane PDI and NPRA and cytoplasmic localized (most likely ER) PDI and NPRA. In HepG2 cells, the two membrane proteins were observed to colocalize. Importantly, the presence of PDI and its colocalization on the cell membrane with NPRA was also observed in PHHs. In both HepG2 and PHHs, obstruction of the endoplasmic reticulum (ER)-golgi protein translocation route inhibited PDI externalization. Finally,

Vit C, like ANP and SNP was observed to protect HepG2 cells and PHHs against Tg-induced cell death. The Vit C-mediated protection was attenuated by the cGMP-dependent protein kinase (PKG) inhibitor 8-bromo-guanosine cyclic 3',5'-[(R)-(hydrogen phosphorothioate)] (Rp-8-Br-cGMP) and modulated by PDI as demonstrated with RL90 and Bac.

These findings suggest that Vit C, like other cGMP elevators, stimulates cGMP generation, reduces $[Ca^{2+}]_i$ and through PKG protects hepatocytes against Tg-induced cell death. The data is consistent with Vit C and ANP mediating their effects via the same route since their actions appeared to be modulated by PDI, unlike the actions of SNP which was unaffected.

Acknowledgements

Firstly, I want to thank my supervisors Dr Alec Simpson and Prof Chris Goldring for giving me the opportunity to undertake this PhD. Especially to Alec, I want to say special thanks to you for all the support. Indeed, you have been more than just a supervisor. I am eternally grateful to you and I will greatly miss you. Special thanks also go to Jill Bubb for her support. I would also like to thank all my colleagues in the lab. In Particular, I would like to say a big thank you to Dr Monday Ogese who was not only academically helpful but also a source of motivation. To Dr Mingming Yang, Dr Joseph Zeguer, Dr Jing Zhou, Dr Will Talbot, Saajid Purohoo and everyone in the department that made my PhD enjoyable, I say big thanks to you all.

To the friends I made outside the University, especially my wonderful flatmates Dr Matthew Agwae and Augustine Amakiri and to the wonderful friends and brothers I met in church, especially uncle Gift, I appreciate you all for being there for me. To my friends and brothers Kenneth Amadi (Kento) and Paul Akanji (Pablo), I can never thank you enough. Thank you for being true friends.

Special thanks to Total E and P Nigeria (TEPNG) Ltd who partly funded this project. Without your support, this dream would never have become a reality.

Harold Orisa, John Amadi and Chidi Anthony, who also contributed immensely in their own ways to make this come through, I cannot thank you all enough.

I reserve special thanks to my family for all the love they have shown me. To my late father and mother, I want to say special thanks to them for setting me on the right path. I must additionally thank my big brother Barr. John Kennedy Enyindah and my late brother-in-law Sam Egbua, both of whom took up the

fatherly role after the death of my father and executed it perfectly. To my wonderful sisters Flora, Grace, Ngozi, Chimele, my aunty Ihuoma, my brother Henry and my brother-in-law Chinedu who became more than a biological brother, without whom my life story would never be complete, I wish I had the right words to express my deep and sincere gratitude for your support and care.

Abbreviations

ANP	Atrial natriuretic peptide
ATP	Adenosine triphosphate
Bac	Bacitracin
BFA	Brefeldin A
BNP	B-type natriuretic peptide
Ca^{2+}	Ionised calcium
$[Ca^{2+}]_c$	Cytosolic Ca^{2+}
$[Ca^{2+}]_i$	Intracellular Ca^{2+}
CNP	C-type natriuretic peptide
DEX	Dexamethasone
DNA	Deoxyribonucleic acid
DMEM	Dulbecco's modified Eagle medium
DMSO	Dimethyl sulfoxide
EC	Endothelial cell
EDTA	Ethylenediaminetetraacetic acid
EGTA	Ethylene glycol tetraacetic acid
ER	Endoplasmic reticulum
EGFP	Enhanced green fluorescent protein
EtOH	Ethanol

FBS	Foetal bovine serum
FlincG	Fluorescent indicator for cGMP
GC	Guanylyl cyclase
GECI	Genetically encoded Ca2+ indicator
GFP	Green fluorescent protein
GPCR	G-protein-coupled receptor
HBS	HEPES buffered saline
HEK293	Human embryonic kidney 293
HEPES	4-(2-hydroxyethyl)-1-piperazineethanesulfonic acid
hrs	Hours
Ion	Ionomycin
IP_3	Inositol triphosphate
IP_3R	Inositol triphosphate receptor
L-glut	L-glutamine
NAPQI	N-acetyl-4-benzoquinone imine
NO	Nitric oxide
NP	Natriuretic peptide
NPR	Natriuretic peptide receptor
NPRA	A-type natriuretic peptide receptor
NPRB	B-type natriuretic peptide receptor

PBS	Phosphate buffered saline
PDE	Phosphodiesterase
PDI	Protein disulphide isomerase
Pen-Strep	penicillin-streptomycin
PFA	Paraformaldehyde
pGC	Particulate guanylyl cyclase
PHH	Primary human hepatocytes
PIP2	Phosphatidylinositol 4,5-bisphosphate
PKG	cGMP-dependent protein kinase
PMCA	Plasma membrane Ca^{2+} ATPase
RT	Room temperature
S	Second
SERCA	Sarcoplasmic/endoplasmic reticulum Ca^{2+} ATPase
sGC	soluble guanylyl cyclase
SNP	Sodium nitroprusside
Tg	Thapsigargin
Vit C	Vitamin C
VSMC	Vascular smooth muscle cell

Chapter 1

General introduction

1.1 The Liver

1.1.1 Brief Introduction to the Liver

The liver is the largest internal organ in the human body with several important functions that includes metabolism of fats, carbohydrates and proteins, digestion, detoxification, immunity, breakdown of old red blood cells, excretion of bilirubin, cholesterol, hormones and drugs, synthesis of plasma proteins and as an important store for several vitamins (1-3). The human liver weighs about 1500 g and makes up about 2 % of the adult body weight (4, 5). The building block of the liver is the hepatic lobule. It is hexagonal in shape and consist of a portal triad (a branch of the hepatic artery, portal vein and bile ducts), a central vein and hepatocytes.

1.1.2 Cell composition of the liver

The liver is made up of parenchymal and non-parenchymal cells. The parenchymal cells consist of the hepatocytes, while the non-parenchymal cells consist of the stellate fat storing cells, Kupffer, sinusoidal endothelial cells and intrahepatic lymphocytes (3, 6, 7). The cell composition of the liver is diagrammatically represented in Figure 1 below.

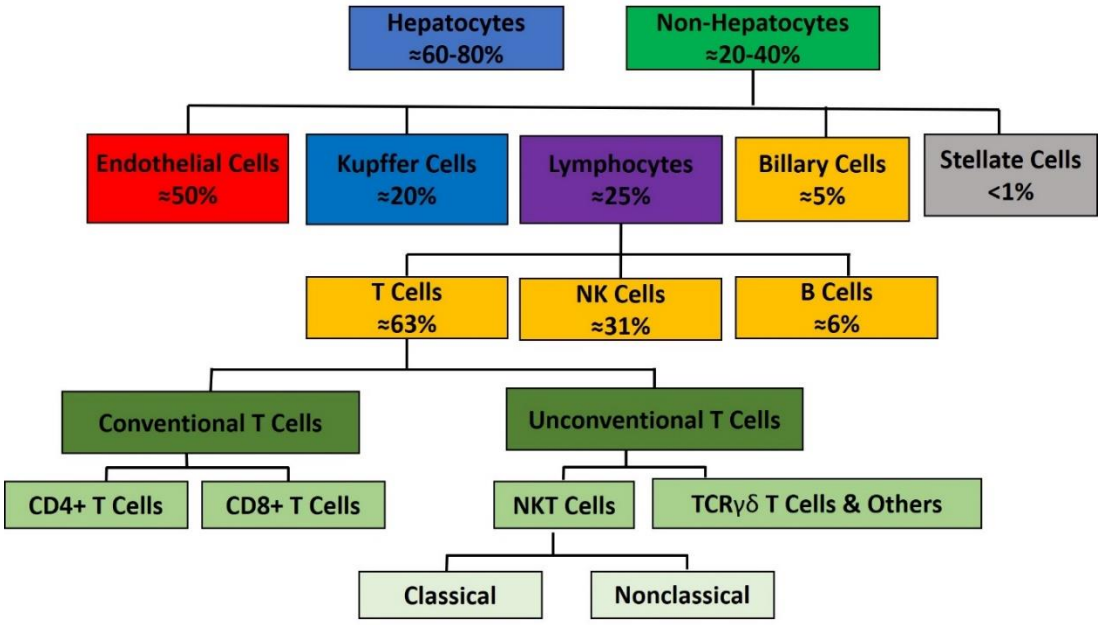

Figure 1.1. Cellular composition of the liver. Adapted from (3).

1.1.2.1 Hepatocytes

Hepatocytes are cells of the main liver parenchyma tissue and they make up 70 to 80 % of the liver cytoplasmic mass (8) and 60-80% of the total cell population (3). Hepatocytes are cuboidal epithelial cells and like other epithelial cells, they have a well organised polarity, with two distinct domains; a basolateral membrane and an apical membrane (9). The basolateral membrane is involved in cell-cell communication and cell-extracellular matrix interaction (10). In hepatocytes, the basal part of the basolateral membrane faces liver sinusoidal endothelial cells, while the apical membrane contributes to the formation of the bile canalicular together with the apical membrane of opposite hepatocytes (9-11) (Figure 1.2). The apical and basolateral domains of hepatocytes separate their internal from external environment and permits a directional absorption and secretion of proteins and other molecules (9). A functional membrane polarity is therefore important for the functions of

hepatocytes such as apical secretion of bile into the bile canaliculi and basal secretion of serum proteins into the sinusoidal blood and this polarity is lost in many liver diseases such as cholestasis (11). Figure 1 below shows the complex anatomy of the liver with the important blood vessels.

A

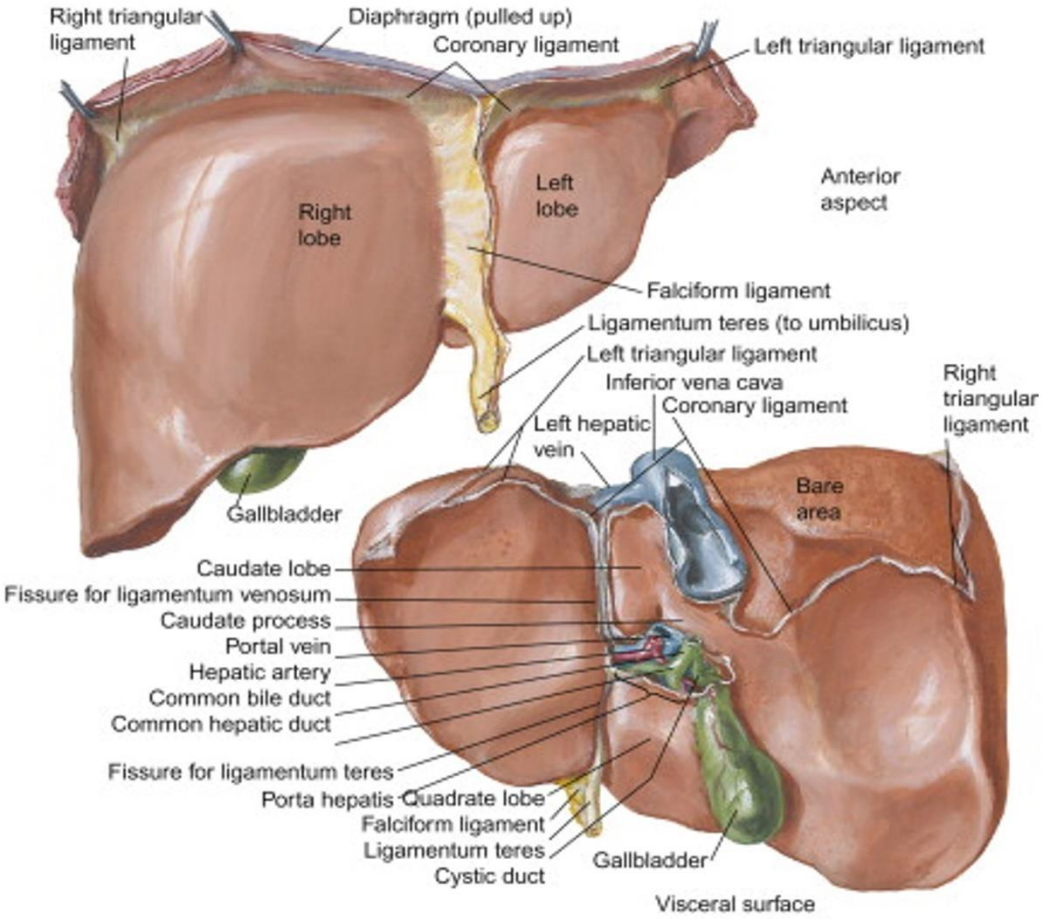
Right triangular ligament
Diaphragm (pulled up)
Coronary ligament
Left triangular ligament
Right lobe
Left lobe
Anterior aspect
Falciform ligament
Ligamentum teres (to umbilicus)
Left triangular ligament
Inferior vena cava
Coronary ligament
Right triangular ligament
Left hepatic vein
Bare area
Gallbladder
Caudate lobe
Fissure for ligamentum venosum
Caudate process
Portal vein
Hepatic artery
Common bile duct
Common hepatic duct
Fissure for ligamentum teres
Porta hepatis
Quadrate lobe
Falciform ligament
Ligamentum teres
Cystic duct
Gallbladder
Visceral surface

B

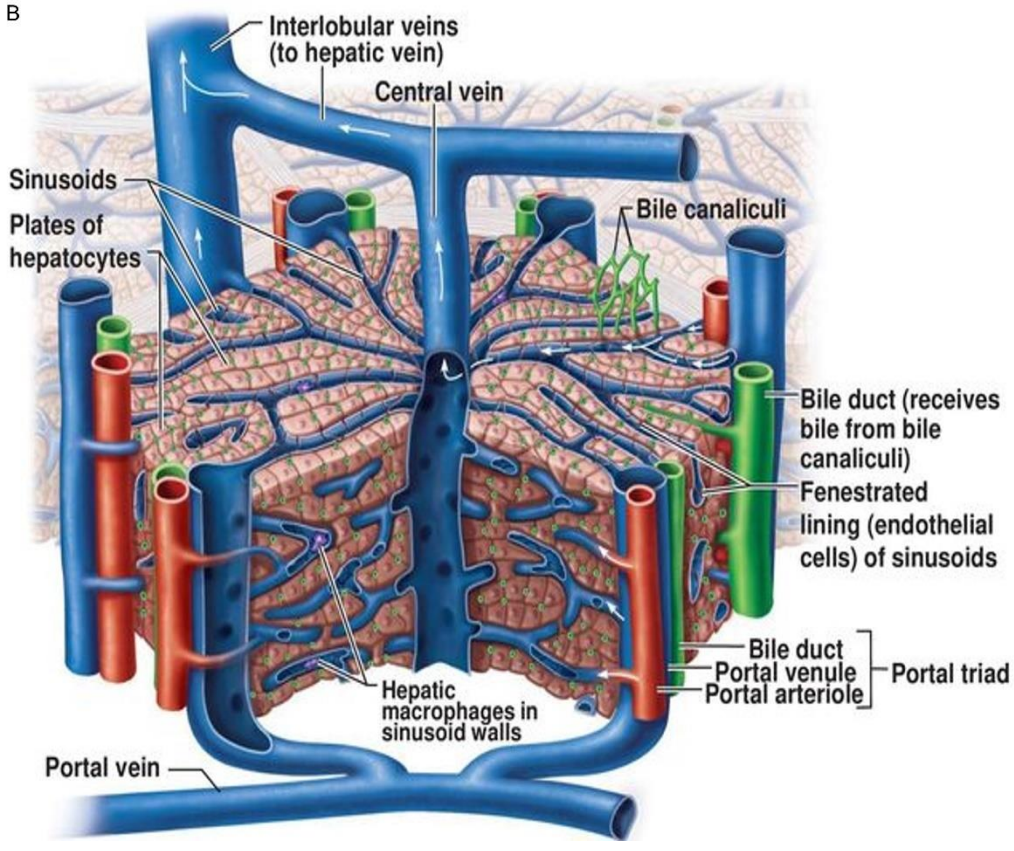
Interlobular veins (to hepatic vein)
Central vein
Sinusoids
Plates of hepatocytes
Bile canaliculi
Bile duct (receives bile from bile canaliculi)
Fenestrated lining (endothelial cells) of sinusoids
Bile duct
Portal venule
Portal arteriole
Portal triad
Hepatic macrophages in sinusoid walls
Portal vein

Figure 1.2. Complex anatomy of the liver. (A) Gross anatomy of the liver showing the lobes and major blood vessels. (B) Pictorial representation of a portion of liver lobule. White arrows indicate direction of blood flow. Image A was taking from (12) and image B was taking from (13).

1.1.2.2 Non-hepatocyte cells of the liver

Lymphocytes: Scattered in the parenchyma and the portal tracts of the liver are lymphocytes. There are about 10 billion (10^{10}) of them in an average human liver, which includes conventional and non-conventional populations of the innate (NK and NKT) and adaptive (B and T) immune systems (14, 15).

Conventional T lymphocytes includes the $CD4^+$ T lymphocytes and $CD8^+$ T lymphocytes expressing the CD4 or CD8 receptors respectively (16). These ($CD4^+$ and $CD8^+$) population of lymphocytes also express αβ T cell receptor (TCR) that recognises antigen in the context of MHC class II and I molecules respectively (16). Typically, there are more $CD8^+$ T cells than $CD4^+$ T cells in the liver.

Unconventional T cells are divided into two subpopulations. First are those that express a γδ TCR whose function include recognition of infections and cancerous cells and regulation of inflammatory responses. They constitute about 15% to 25% of all intrahepatic cells, making the liver one of the most robust sources of γδ T cells in the body (3).

The second subpopulation of unconventional T lymphocytes are the **natural killer T (NKT) cells**. They display the phenotype and function of conventional T cells, as well as the properties of natural killer cells (cytolytic activity); they

express NK cell markers such as CD94 and CD161, as well as T-cell receptor (TCR)-αβ chains, which distinguishes them from typical NK cells that does not display TCR (17). They recognise glycolipid antigens presented in the context of CD1d, a non-classical MHC class I molecule, unlike conventional T lymphocytes which recognises peptide antigens presented in the context of the classical MHC class I and II molecules (3, 18). Because of their ability to generate an array of cytokines upon activation, they not only function in the regulation of innate immunity but also act as a bridging system between innate and adaptive immunity. NKT cells modulates liver inflammation, damage, fibrosis and regeneration, thus, acting as important regulators of the pathogenesis of liver diseases (19). NKT cells account for ≈30% of the intrahepatic lymphocytes (3).

Scattered in the liver are also several forms of **antigen-presenting cells (APCs)** that capture antigens that enters the liver, or those that are released when hepatocytes that are infected with pathogens die. The resident APCs include the Kupffer cells (KCs), liver sinusoidal endothelial cells (LSECs), hepatic stellate cells (HSCs) and hepatic dendritic cells (HDCs).

Kupffer cells are members of the reticuloendothelial system. They were first described as “sternzellen” (stellate or star cells) in 1876 by Karl Wilhelm von Kupffer in 1876 and represent the largest group of resident tissue macrophages in the body; they account for 20% of non-parenchymal cells in the liver (3). KCs were first considered part of the endothelium of the hepatic blood vessels until 1898 when Tadeusz Browiecz identified them as hepatic macrophages (20). Developmentally, KCs are derived from circulating

monocytes that originate from bone marrow precursor cells. These monocytes in peripheral circulation enter the liver and differentiate into hepatic macrophages (KCs). Like other macrophages, the differentiation of KCs is regulated by several growth factors, but predominantly by the macrophage colony stimulating factor. In the liver, the KCs are located within the sinusoidal space where they lie in close contact with the parenchymal and non-parenchymal cells of the liver. This location supports their function to get rid of endotoxins from the sinusoidal blood and phagocytose dead pathogen-infected hepatocyte debris and microorganisms (3).

Liver sinusoidal endothelial cells (LSECs) constitute the most abundant non-parenchymal cells in the liver (≈50%). They form fenestrated endothelium that line the liver sinusoids. Together with KCs, they constitute one of the strongest scavenger systems in the body; an activity that has been attributed to the presence of fenestrae between LSECs, lack of classical basement membrane and their expression of various molecules that promote antigen uptake, including mannose and scavenger receptors, as well as molecules that enhance antigen presentation such as MHC class I and II and other costimulatory molecules such as CD40, CD80 and CD86 (21, 22).

Hepatic dendritic cells are a population of bone marrow-derived antigen-presenting cells that that are involved in antigen presentation to lymphocytes and in the modulation of hepatic immune responses. They are mainly located within the portal tracts and around the central veins (23). In healthy livers, HDCs exist mainly in their immature forms with low ability to endocytose antigens and to stimulate T lymphocytes. These properties of DCs, together

with the constitutive expression of anti-inflammatory cytokines IL-10 and TGF-β by KCs and LSECs which subverts DC maturation and T lymphocyte stimulatory function, significantly contributes to the tolerogenic microenvironment that characterizes healthy liver (24-26). Upon hepatic injury and exposure to inflammatory signals such as microbial products and pro-inflammatory cytokines (including IL-1, GM-CSF and TNF-α), DCs undergo maturation and become efficient antigen presenting cells and migrate via the Space of Disse to the lymphatics in the portal tracts and eventually to the T lymphocyte area of the extrahepatic lymph nodes and spleen (27-29).

1.1.3 Functions of the liver

Hepatocytes being the chief cellular component of the liver are responsible for most of the liver functions including digestion, metabolism, detoxification, storage of nutrients, production of vital plasma proteins.

1.1.3.1 Digestive role of the liver

Hepatocytes play an important role in digestion through the production of bile. They secrete bile from their apical membrane into the bile canaliculi from where the bile is collected into the bile ductules and then into bile ducts. The bile ducts unite to form the right and left hepatic ducts which in turn merge and exit the liver as the common hepatic ducts which eventually channels the bile to the gall bladder for storage. Bile is a mixture of water, bile salts, cholesterol and bilirubin. Mammalian liver synthesizes mainly two primary bile salts: cholic acid (CA), a trihydroxyl acid and chenodeoxycholic acid (CDCA), a dihydroxyl acid (1). The primary bile acids can then be subsequently converted into

secondary bile acids by intestinal bacteria. Cholic acid is converted to deoxycholic acid, a dihydroxyl acid, while CDCA is converted to lithocholic acid, a monohydroxyl acid (1). On arrival of a fatty meal in the duodenum, the cells of the duodenum secret the hormone cholecystokinin (CCK) which stimulates the gall bladder to release bile. The bile in the duodenum helps to emulsify fats, breaking large clumps of fats into smaller fragments with increased surface area that can then be easily digested by the body.

1.1.3.2 Metabolism of digestive products

As all the blood that leaves the digestive system goes directly to the liver through the hepatic portal vein, hepatocytes are tasked with the responsibility of metabolizing all the digestive products of carbohydrates, lipids and proteins into forms that are useful to the body.

1.1.3.2.1 Liver and carbohydrate metabolism

The blood the liver receives from the gastrointestinal tract through the hepatic portal vein is rich in glucose and other nutrients. In the postprandial state, glucose molecules are taken up by hepatocytes via glucose transporter 2 (GLUT2) where they are phosphorylated by the enzyme glucokinase to generate glucose-6-phosphate (G6P) (30). The resulting G6P has several fates including serving as a precursor for glycogen synthesis, undergoing metabolism to generate pyruvate via glycolysis (31). Pyruvate is subsequently transported across the inner mitochondrial membrane into the mitochondrial matrix where it is utilized to generate ATP through the tricarboxylic acid (TCA) cycle and oxidative phosphorylation (31). The G6P can also be channelled through the phosphate pentose pathway to produce NADPH (32). In the fasted

state, glycogen is hydrolysed into glucose by the enzyme glycogen phosphorylase through the process of glycogenolysis with glucose-1-phosphate (G1P) and G6P as intermediate products (30). The G6P can allosterically inhibit glycogen phosphorylase with a concomitant allosteric activation of glycogen synthase, consequently further increasing liver glycogen level (33, 34). In the postprandial state, insulin is secreted by pancreatic β cells in response to raised blood glucose, amino acids and fatty acids. Insulin promotes glucokinase (GK) expression which converts glucose to G6P which in turn promotes glycogenesis and inhibits glycogenolysis (30, 35). Insulin also potentiates glycogenesis and inhibit glycogenolysis by promoting the phosphorylation and inactivation of glycogen synthase kinase 3 (GSK-3) and concomitant dephosphorylation and inhibition of glycogen phosphorylase respectively (36). On the other hand, in the fasted state, the secretion of insulin by the pancreatic β cells is down regulated, also, the secretion of fibroblast growth factor 15/19 (FGF15/19; an activator of glycogen synthesis) is downregulated (30), with a resultant increase in glycogen hydrolysis to release glucose.

Following a prolonged period of fasting, glycogen level depletes, and hepatocytes generates glucose through the process of gluconeogenesis from substrates such as glycerol, certain amino acids (alanine and glutamine), pyruvate and lactate. Gluconeogenesis occurs in the liver and kidneys and is stimulated by diabetogenic hormones such as glucagon, cortisol, epinephrine and growth hormone (37). The process of gluconeogenesis is however an expensive one from an energy standpoint as the complete conversion of two moles of pyruvate to two moles of 1,3-bisphosphoglycerate requires six moles

of ATP. The detailed process is diagrammed in Figure 1.3 below. In brief, cytoplasmic lactate is converted to pyruvate by lactate dehydrogenase. Pyruvate is then transported across the inner mitochondrial membrane to the mitochondrial matrix where it is converted to oxaloacetate by the enzyme pyruvate carboxylase. The mitochondrial oxaloacetate is then acted upon by mitochondrial malate dehydrogenase that reduces it to malate which is then exported to the cytoplasm. In the cytoplasm, the cytoplasmic malate dehydrogenase oxidizes it to regenerate cytoplasmic oxaloacetate which subsequently undergoes series of reactions to give rise to G6P which is then transported to the ER where it is dephosphorylated by glucose-6 phosphatase to yield glucose.

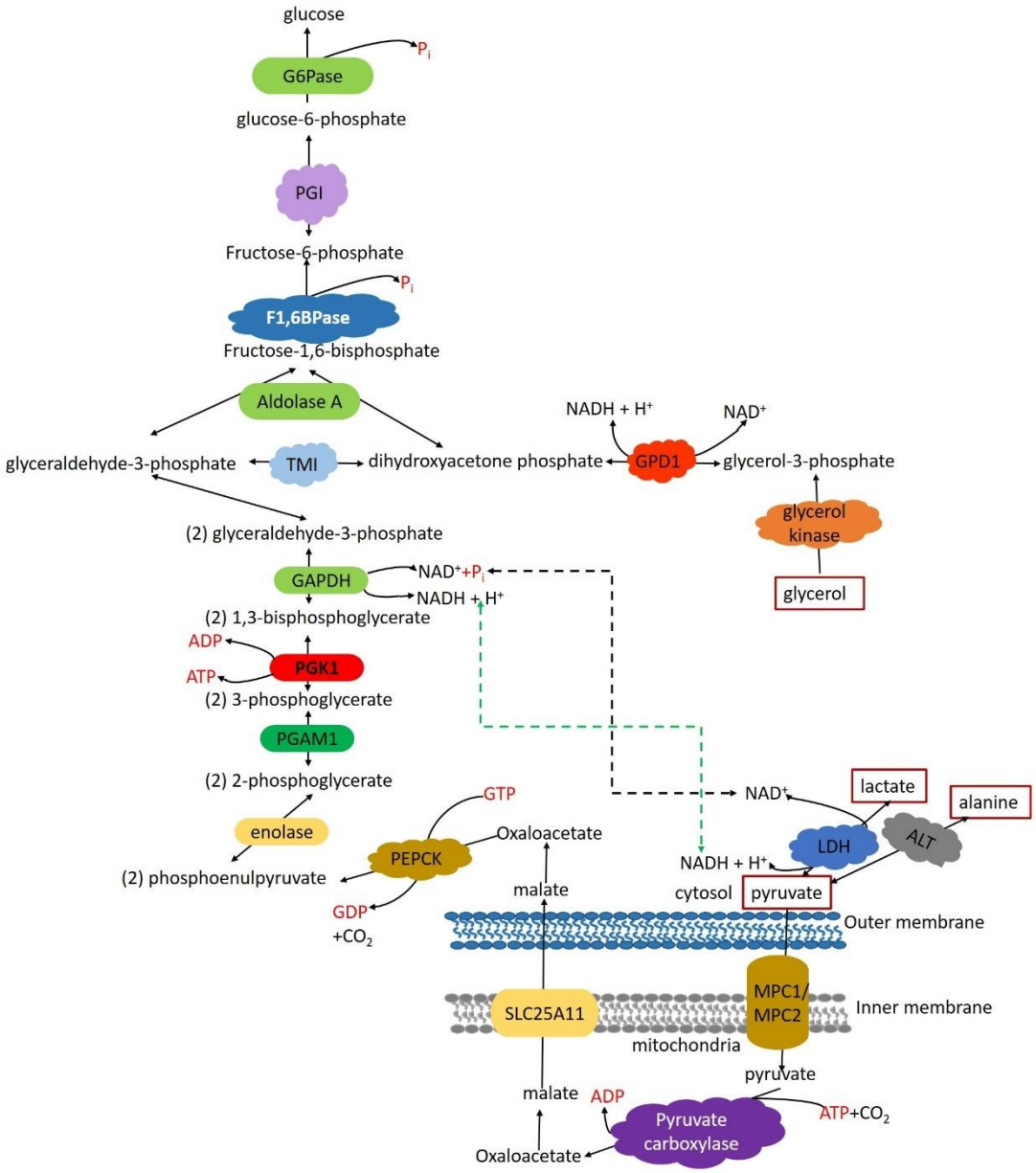

Figure 1.3. Process of gluconeogenesis. Glucose is generated from non-carbohydrate sources such as pyruvate, lactate, glycerol, and certain amino acids. The enzymes of gluconeogenesis are located in the cytosol except the pyruvate carboxylase (present in the mitochondria) and glucose 6-phosphatase (membrane bound in the endoplasmic reticulum).

1.1.3.2.2 Liver and lipid metabolism

Digestion of lipids into fatty acids and glycerol occurs in the small intestine. Fatty acids in the blood that reach the liver enter hepatocytes by two distinct pathways; passive diffusion for short and medium-chain fatty acids and transporter-mediated uptake (by the fatty acid transport protein and fatty acid translocase) for long-chain fatty acid (38, 39). Intracellular fatty acids can be stored as triacylglycerol (TAG) or cholesterol esters in lipid droplets in conditions of excess energy. In conditions of insufficient energy, such as after a long period of fast, TAG stored in adipose tissues are broken down to release fatty acids into circulation, which are subsequently transported to the liver where they undergo oxidation reactions to generate ketone bodies (40, 41). Within the hepatocytes, fatty acids are first activated by the enzyme fatty-acetyl CoA synthetases (ACS) to generate fatty acyl-CoA, which are then carried to intracellular organelles where they are metabolized or to the nucleus where they interact with transcription factors (Figure 1.4). Excess carbohydrates and proteins are also converted into fatty acids and triglyceride which are then exported to and stored in adipocytes (42). Hepatocytes synthesizes large quantities of cholesterol, phospholipids and lipoproteins which are made available to other tissues in the body. Most of the cholesterol produced by hepatocytes are excreted as components of the bile. The pathways for the hepatic metabolism of fatty acids are summarised in Figure 1.4.

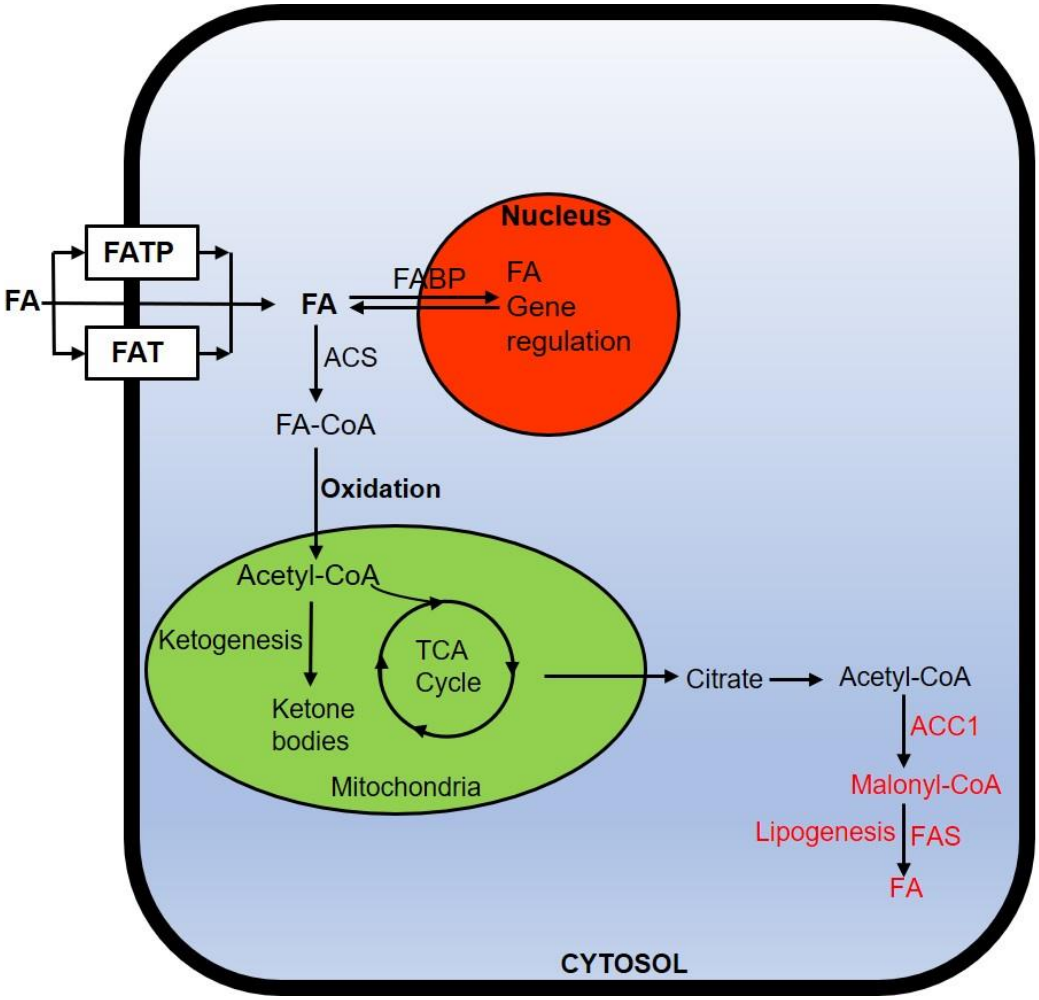

Figure 1.4. Pathways for hepatic fatty acid metabolism. Fatty acids enter the hepatocytes via FATP and FAT and subsequently undergoes a series of chemical reactions. Adapted from (39). FAT: fatty acid translocase. FATP: fatty acid transport protein.

1.1.3.2.3 Liver and protein metabolism

The key roles of the liver in protein metabolism includes synthesis, transamination and deamination of amino acids, as well as synthesis of urea (39). In fact, the liver is the only organ in the body that has the function of removing the nitrogen present in amino acids via urea synthesis. Amino acids that reach the liver via the hepatic portal vein are taken up by hepatocytes via

specialised transporters which are designed for the transport of the various classes of amino acids. Energetically, these transporters can be classified into two groups. The first group are sodium-dependent transporters whose activation depends upon sodium chemical gradient and membrane electrical potential to stimulate hepatocyte uptake of amino acids against a concentration gradient. The second group of transporters are sodium-independent amino acid facilitated diffusion system that depends on concentration gradient to achieve hepatocyte amino acid uptake (39). Once taken up by hepatocytes, amino acids have different fates. They can serve as a precursor for hepatic protein synthesis; including proteins that are required in the liver and those transported to extrahepatic tissues such as albumin. In the liver, amino acids can also undergo transamination, a process catalysed by aminotransferases or transaminases (43). Transamination involves the removal and transfer of an amino group from an amino acid to a 2-oxoacid, resulting in the formation of a new amino acid and a new 2-oxoacid. The resulting 2-oxoacid can be converted to acetyl-CoA which is then subsequently channelled through ketogenesis or lipogenesis to yield ketone bodies and fatty acids respectively or the 2-oxoacid can be converted to pyruvate which can then go through the process of gluconeogenesis to yield glucose (39, 44). Also, the product of transamination such as glutamate (formed by the transfer of an amino group to 2-oxoglutarate) can undergo oxidative deamination, catalysed by glutamate dehydrogenase to yield ammonium ion (NH_4^+) which is subsequently channelled through urea cycle to produce urea which can then be excreted through by the kidney. The process

of hepatic amino acid metabolism is schematically represented in Figure 1.5 below.

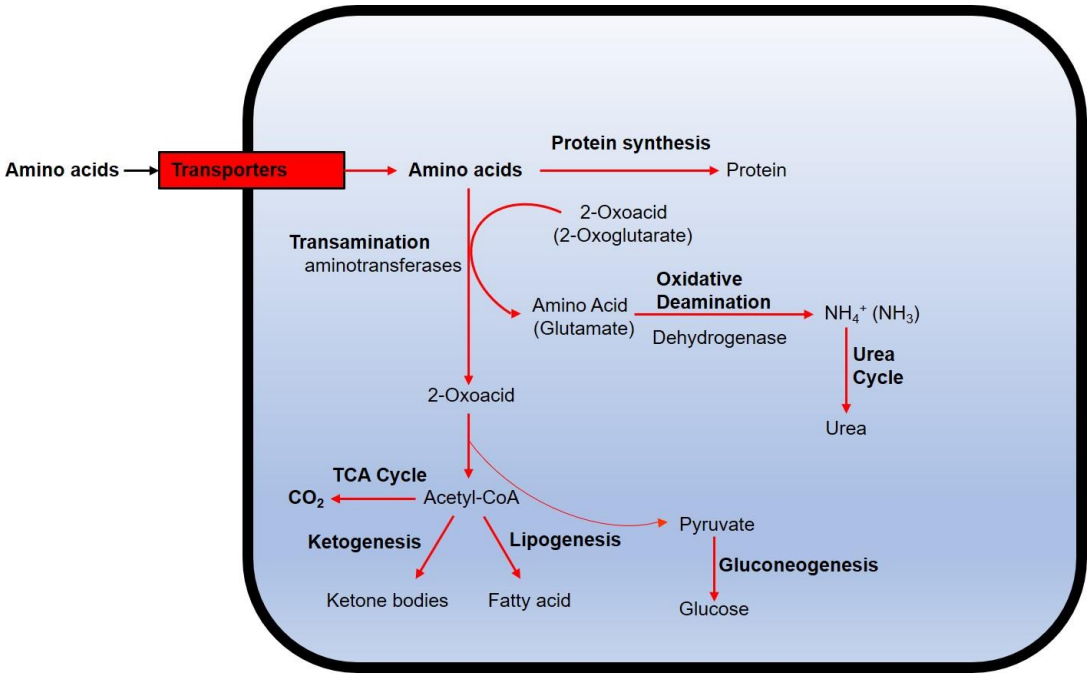

Figure 1.5. Pathways for hepatic amino acid metabolism. Amino acids are taken up by hepatocytes via specialised transporters and subsequently undergoes transamination or are utilized for hepatic protein synthesis. Adapted from (39).

1.1.4 Xenobiotic/drug metabolism and detoxification

Another important role the liver plays in the body is detoxification of xenobiotics. The human body is exposed to millions of foreign compounds that are taken into the body either deliberately in water and food or even in form of chemical compositions such as drugs or unconsciously in the air we breathe. Some of these substances are cytotoxic and are highly lipophilic and therefore have the tendency to stay in the body for long period of times with undesirable effect on the body. Fortunately, the body is equipped with enzymes (most of

which exist in their highest amount in the liver) and mechanisms that converts the lipophilic xenobiotics into hydrophilic forms that can then be easily excreted in the urine, the so-called xenobiotic biotransformation.

Xenobiotic detoxification involves xenobiotic biotransformation and excretion. Xenobiotic biotransformation can be divided into 2 phases of enzymatic reactions, referred to as phase I and phase II reactions. The phase I reactions are generally classed as functionalization reactions that involve interchanging or exposing of already existing polar functional groups or introduce new polar functional groups to the xenobiotic through oxidation, reduction or hydrolytic reactions (45). This consequently increases the hydrophilicity of the substance or prepares it for the phase II reactions. Phase I reactions are mediated by different classes of enzymes including cytochrome P450 (CYP), flavine-containing monooxygenase (FMO), esterases and amidases (45). The phase II reactions are conjugation reactions that include sulfation, glucuronidation and methylation of the xenobiotic metabolites; here, small endogenous polar moieties are conjugated to the functional groups that were introduced/exposed in phase I (45-47). This consequently increases the hydrophilicity and excretability of the xenobiotic metabolite. Phase II reactions are mediated by enzymes such as sulfotransferase, glucuronosyltransferase and N-acetyltransferase.

It is however important to point out that though xenobiotic biotransformation is an integral part of detoxification, the end point of drug/xenobiotic biotransformation is not always detoxification. In fact, the main aim of xenobiotic biotransformation is to convert lipophilic molecules into hydrophiles

that can then easily be excreted in the urine. It is therefore by the excretion of these resultant hydrophiles that detoxification is achieved. At times xenobiotic/drug biotransformation can accidentally lead to an undesirable increase in chemical cytotoxicity by resulting in the formation of electrophilic metabolites which have the potential to bind covalently with cellular macromolecules, consequently, leading to genetic mutation and/or cell death (48, 49).

1.1.5 Liver and immunity

Although the primary functions of the liver are not traditionally considered to be immunological, the liver performs many essential immune tasks; it plays several important functions in both innate and adaptive immunity. For example, 80-90% of the circulating innate immune proteins in the body are produced by the hepatocytes of the liver (50). In addition, there are immune cells resident in the liver, including lymphocytes and Kupffer cells (discussed earlier as part of the cellular composition of the liver). For these reasons, the liver is considered as an immunological and a lymphoid organ.

1.2 Ca^{2+} signalling in normal liver physiology

1.2.1 Mechanisms of Ca^{2+} signalling

Several of the functions of the liver are controlled by Ca^{2+}. These include vesicular trafficking and canalicular contraction that controls the secretion of bile (51, 52), glucose and energy metabolism that occur through the modulatory action of Ca^{2+} on the several enzymatic activities involved (53, 54) and control of cell cycle that involves the modulation of transcription and pro

and anti-apoptotic proteins that regulate cell proliferation. These different functions require different Ca^{2+} signals, so, in order to control these functions simultaneously, intracellular Ca^{2+} signals are highly organised in space, frequency and amplitude.

Just like in other tissues and cell types, in hepatocytes, $[Ca^{2+}]_c$ signal arises from two sources; the internal stores or the extracellular medium (55, 56). The former involves release of Ca^{2+} from internal stores upon the binding of special intracellular messengers to their receptors (56). A typical example of one of such messengers is Inositol-1,4,5-triphosphate (IP_3) which binds to its receptor IP_3 receptor (IP_3R) and causes the release of Ca^{2+} from the endoplasmic reticulum (ER) (57, 58). Other studies have suggested that IP_3 can also stimulate Ca^{2+} release from golgi apparatus into the cytosol (59), nucleus (60-62) and secretory vesicles (63). Also, Ca^{2+} and cyclic ADP ribose (cADPR) can trigger Ca^{2+} signal through their direct interaction with ryanodine receptors (RyRs) (55), so also do nicotinic acid adenine dinucleotide phosphate (NAADP) through their activation of two-pore channels (TPCs) localized in endo-lysosomal compartments (64-68).

IP_3-mediated $[Ca^{2+}]_c$ signal is triggered by the binding of Ca^{2+}-mobilizing hormones and neurotransmitters or growth factors to G-protein coupled receptors (GPCRs) (64, 69, 70) or receptor tyrosine kinases (RTKs) (64, 69, 71) respectively, localized on the plasma membrane. GPCRs are a group of membrane receptors found in eukaryotes. They consist of seven hydrophobic transmembrane α-helical domains separated by alternating extracellular and intracellular loop regions (72). They have an extracellular amino terminus and

an intracellular carboxyl terminus (73), as well as a cytosolic G-protein binding site (55, 74). G proteins are specialised proteins which binds guanosine triphosphate (GTP) and guanosine diphosphate (GDP). GPCR-associated G proteins are heterotrimeric, consisting of three subunits; an α, β and γ subunits (70, 75). The α and γ subunits are attached to the cell membrane by lipid anchors (76). In the inactive state, the α subunit binds a GDP molecule which is replaced with a GTP molecule upon activation. Upon the binding of Ca^{2+}-mobilizing hormones or neurotransmitter to a GPCR, the GPCR undergoes a conformational change, resulting in the exchange of the GDP molecule for a GTP molecule by the α subunit (77). This results in the dissociation of the α subunit from the β-γ dimer (78). The later interacts and activates the membrane bound phospholipase C (PLC). There are different subtypes and isoforms of PLC (79, 80); in particular, PLCβ1 and PLCβ2 are activated by GPCR, while PLCϒ is activated by RTKs (79, 81). Activated PLCβ1 and PLCβ2 in turn catalyses the hydrolysis of membrane bound phosphatidylinositol 4,5-bisphosphate (PIP_2) into IP_3 and diacylglycerol (DAG) (82). IP_3 diffuses through the cytosol to the endoplasmic reticulum (ER) where it binds to and activates the IP_3 receptor (IP_3R), resulting in the release of Ca^{2+} from the ER into the cytosol. DAG remains membrane bound where it interacts with and activates protein kinase C (PKC) which phosphorylates target proteins, thereby mediating several signal transductions (83, 84).

RTKs are another group of specialised membrane receptor that are characterised by an extracellular ligand-binding domain, a single transmembrane domain and an intracellular tyrosine kinase domain. They exist as inactive monomers which then undergoes dimerization upon the

binding of a signalling molecule or as pre-formed inactive dimers prior to ligand binding, which then becomes activated upon ligand binding (85, 86). Switch on of kinase activity requires both receptor dimerization and transphosphorylation of tyrosine residues in the activation loop of the catalytic domain of the receptor (55). The phosphorylated tyrosine residue in activated RTKs then recruits adaptor proteins containing SH2 (Src homology domain 2), SH3 (Src homology domain 3), or PTB (phosphotyrosine binding domain) that in turn triggers signal transduction pathways, leading to cellular responses (55).

Binding of Ca^{2+}-mobilizing growth factors to RTKs is thought to stimulate PLCϒ-mediated breakdown of cell membrane-localized PIP_2 (81). However, other studies suggest that RTK can translocate to the nucleus where it brings about local activation of PLC, hence alternatively resulting in selective breakdown of nuclear PIP_2, with a consequent generation of nuclear IP_3-dependent Ca^{2}+ signals (87, 88).

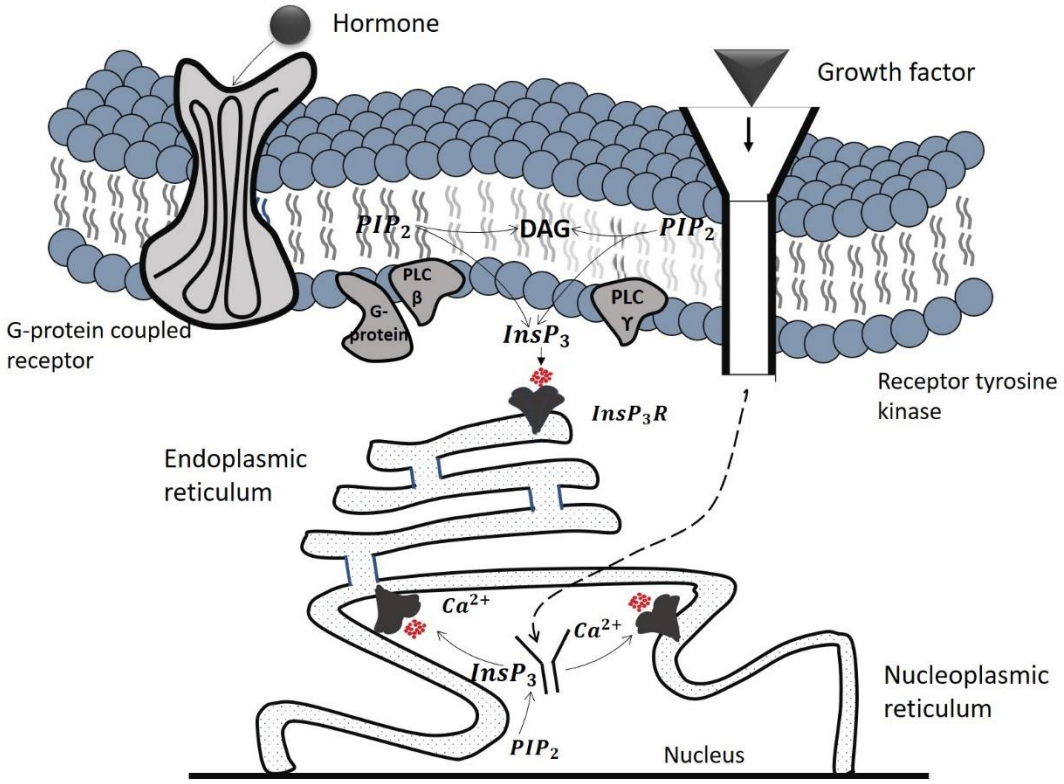

Figure 1.6. Mechanism of Ca^{2+} signal formation in hepatocytes. Recruitment of Ca^{2+} from intracellular stores may arise by the binding of Ca^{2+} mobilizing hormones to GPCRs or growth factors to RTKs which in turn lead to the activation of PLC; PLCβ for GPCRs and PLCY for RTKs. Activated PLC hydrolyzes PIP_2 into IP_3 and DAG. DAG remains in the plasma membrane, while IP_3 diffuses to the ER where it stimulates Ca^{2+} release into the cytosol. RTKs may translocate to the nuclear membrane where it brings about selective activation of nuclear membrane PLC, hydrolysis of nuclear membrane PIP_2 and release of Ca^{2+} from the nucleoplasmic reticulum into the nucleoplasm. Adapted from (55)

1.2.2 Physiological functions of Ca^{2+} signals

1.2.2.1 Ca^{2+} and bile secretion

Bile secretion depends on the regulatory action of Ca^{2+} in hepatocytes which are responsible for the primary formation and initial secretion of bile into the bile canaliculi, and cholangiocytes which line the biliary tree and modify the canalicular bile through a series of secretory and reabsorptive processes as it travels along the biliary tree. In this section, we shall divide bile secretion into two stages which include canalicular secretion (secretion from hepatocytes into bile canaliculi) and ductular secretion (performed by cholangiocytes into the biliary tree), both of which are regulated by Ca^{2+}.

1.2.2.1.1 Canalicular secretion

An important feature of epithelial polarity is the concentration of IP_3R on the apical region, with different isoforms of IP_3R observed in different cell types (89-92). Particularly, IP_3R-2 has been shown to concentrate on the apical or pericanalicular ER of hepatocytes. This pericanalicular localization of IP_3R has been suspected to allow epithelial cells to achieve micromolar apical $[Ca^{2+}]_c$ which is a particularly important for Ca^{2+}-induced exocytosis. Studies suggest that the pericanalicular concentration of IP_3R-2 in hepatocytes and the consequent Ca^{2+} release from these receptors is important for the insertion of the transporter multidrug resistance-associated protein 2 (MRP2) into the hepatocyte apical membrane. MRP2 is the chief transporter of organic anions including bilirubin and GSH from hepatocytes into the canaliculus (93). The apical concentration of IP_3R-2 is also important in maintaining bile acid secretion through the regulation of the bile salt export pump (BSEP) which is

the major transporter of bile acid from hepatocytes into the bile canaliculi. Several lines of evidence support these roles of Ca^{2+} in canalicular secretion. Knockout (KO) of IP_3R-2 in hepatocytes and treatment of wildtype hepatocytes with BAPTA (a selective Ca^{2+} chelator) almost completely abrogated canalicular secretion of the fluorescent organic anion 5-chloromethylfluorescein diacetate, consistent with inhibition of the MRP2 (94). Also, Knockdown (KD) of IP_3R-2 in hepatocytes and treatment of wildtype hepatocytes with BAPTA or with the IP_3R inhibitor xestospongin C inhibited apical secretion of bile acid via the BSEP (95). Together, these studies provide evidence that Ca^{2+} is important for canalicular insertion of MRP2 and BSEP, hence important for hepatocyte organic anions and bile acid secretion. This means that sustained significant variation of $[Ca^{2+}]$ in the liver would result in pathophysiological liver conditions. A typical example is cholestasis which is associated with both elevated $[Ca^{2+}]_c$ in hepatocytes and decreased $[Ca^{2+}]_c$ in cholangiocytes (56).

1.2.2.1.2 Ductular secretion

While hepatocytes secrete the canalicular bile, cholangiocytes are important for modifying the primary bile by hormonal regulated events as they flow along the biliary tree (96, 97). Cholangiocytes perform this function by secreting fluid and bicarbonate (HCO_3^-) into the primary bile (98). In physiological conditions, the most widely studied and most characterised archetypal mechanism of cholangiocyte HCO_3^- secretion is the secretin-stimulated pathway. The binding of secretin to the secretin receptors found on the basolateral membrane of cholangiocytes triggers the synthesis of 3',5'-cyclic adenosine monophosphate (cAMP) by adenylyl cyclase (AC) (99). The synthesized cAMP activates

cAMP-dependent protein kinase (PKA), which in turn activates the cystic fibrosis transmembrane conductance regulator (CFTR). Activation of CFTR leads to the extrusion of chloride ion (Cl^-) into the ductular lumen which is subsequently exchanged with HCO_3^- through the Cl^-/ HCO_3^- exchange, with passive efflux of water (100, 101). This is driven by the Cl^- gradient across the cholangiocyte apical membrane (99) and the HCO_3^- alkalinizes the primary bile and form a protective HCO_3^- layer over the apical membrane of cholangiocytes (102, 103). The intracellular HCO_3^- is generated by the hydration of carbon dioxide; a reaction that is catalysed by carbonic anhydrides, giving rise to HCO_3^- and hydrogen. Besides the secretin-stimulated mechanism, an alternative HCO_3^- secretory mechanism involves the respective acetylcholine (ACh) and ATP stimulation of their receptors; muscarinic acetylcholine receptor M3 and P2Y receptors present on cholangiocyte membrane, resulting in IP_3-dependent $[Ca^{2+}]_c$ elevations and consequent apical Cl^-/HCO_3^- secretion (104, 105). Recent studies show that Ach potentiates secretin stimulation of the Cl^-/HCO_3^- exchanger (106). This suggest a possible interplay between the two HCO_3^- secretory pathways even though they were initially thought to be independent of each other.

Though Ca^{2+} have stimulatory effect on apical organic anion and bile salt secretion, exogenous agonists that elevate $[Ca^{2+}]_c$ either from the extracellular space or from the internal stores in isolated hepatocytes were reported to inhibit net bile secretion (107). The calcium ionophore A23187 which elevates $[Ca^{2+}]_c$ by increasing the influx of extracellular Ca^{2+} (eCa^{2+}) inhibited bile flow in perfused liver (107). Also, vasopressin which elevates $[Ca^{2+}]_c$ through IP_3 release of Ca^{2+} from the ER and through influx of eCa^{2+} also inhibited bile flow

(107). This has been suggested to be as a result of increased paracellular permeability (55) due to compromised tight junctions caused by elevated $[Ca^{2+}]_c$ and reduced extracellular calcium concentration $[Ca^{2+}]_e$ which has been reported by some experimental studies (107, 108). This results in the reflux of bile contents into the sinusoidal blood, thus reduced canalicular bile flow (109). Also, because tight junctions give rise to osmotic gradients within the bile canaliculi that is necessary for bile formation (110, 111), reduced or loss of the tight junction barrier/increased paracellular permeability would dissipate the osmotic gradient and result in net reduced bile formation and flow along the canaliculus. Together, these studies buttress the point that maintaining the right $[Ca^{2+}]$; both intracellular and extracellular concentrations is important for both bile formation and bile flow.

1.2.2.2 Ca^{2+} and glucose homeostasis in the liver

Intracellular Ca^{2+} signal plays a vital role in regulating glucose metabolism in the liver by modulating the phosphorylation and dephosphorylation, hence the activity of the regulatory enzymes of glycogenesis (glycogen synthase) and glycogenolysis (glycogen phosphorylase) (53, 112). Ca^{2+} also regulates the key enzymes of gluconeogenesis (113). Previous studies have shown that Ca^{2+} mobilizing hormones modulate these processes (114) in a Ca^{2+}-dependent manner (115, 116). For example, vasopressin, angiotensin II and α-adrenergic agonists trigger PLC-mediated IP_3 generation, leading to IP_3-mediated Ca^{2+} release from the ER, resulting in the phosphorylation of glycogen phosphorylase, attenuates glycogen synthase activity and glycogenolysis (117, 118). Nucleotides such as ATP and UTP that elevates

$[Ca^{2+}]_i$ via their action on P2Y receptors, stimulate glycogen phosphorylase in human hepatocytes (119). So does another P2Y agonist 2-methylthioadenosine 5'-diphosphate 2-MeSADP in rat hepatocytes (120). Also, the Ca^{2+} ionophore A23187 stimulates the action of glycogen phosphorylase and inhibits that of glycogen synthase (121). These studies provide further evidence that Ca^{2+} plays an important role in the mobilization of glucose from glycogen in the process of glycogenolysis in the liver.

1.2.2.3 Ca^{2+} and hepatocyte proliferation / liver regeneration

Although hepatocytes rarely replicate under physiological condition in adult liver, however, following conditions such as partial hepatectomy, ischaemic liver and acute liver damage due to exposure to certain compounds, hepatocytes are able to re-enter the cell cycle and proliferate (122, 123). Like in other cell types, Ca^{2+} plays a vital role in hepatocyte proliferation (124, 125). Ca^{2+} signal regulates the various stages of cell cycle; from the activation of several immediate-early genes to regulation of the various phases of mitosis (124). The pro-cell proliferative action of Ca^{2+} have been shown to be dependent upon the spatiotemporal dynamics of Ca^{2+} signal, i.e., the ability of Ca^{2+} to mediate the various stages of cell proliferation depends upon the magnitude, amplitude and frequency of Ca^{2+} signal in the subcellular compartments (55). Several lines of evidence show that Ca^{2+} is important for liver regeneration (126). A rise in liver and plasma level of Ca^{2+} mobilizing growth factors have been reported as an early event following partial hepatectomy (PH) (127). For example, the level of hepatocyte growth factor (HGF) and epidermal growth factor (EGF) increases in both the liver and

plasma following partial hepatectomy (PH), and these factors have been shown to stimulate cytosolic Ca^{2+} oscillations in hepatocyte (128), suggesting a possible connection between rise in $[Ca^{2+}]_c$ and liver regeneration. Also, other agonists that elevate $[Ca^{2+}]_c$ such as ATP, noradrenaline and arginine vasopressin have been reported to play important roles in the early stages of liver regeneration (129). Parvalbumin (PV); a calcium-binding protein that is selectively expressed in muscle and neuronal cells, but absent in the liver (130) has been widely used to study the involvement of Ca^{2+} in liver regeneration. Rodrigues and colleagues utilized PV variants targeted selectively to the nucleus and cytoplasm of hepatoma cell lines to determine the relative importance of nuclear and cytoplasmic Ca^{2+} in cell proliferation. It was reported that nuclear Ca^{2+} oscillations was essential for cell proliferation in the hepatoma cell lines and also necessary for cell division to progress through the early stage of prophase (131). In LX-2 immortalized human hepatic stellate cells (HSCs) and primary rat hepatic stellate cells, both nuclear and cytosolic Ca^{2+} were reported to enhance proliferation (132). Lastly, Lagoudakis and colleagues reported that by inducing hepatocytes both *in vitro* and *in vivo* in whole liver, to selectively express PV in the cytosol, they were able to investigate the role of Ca^{2+} in hepatocyte proliferation and liver regeneration. It was reported that agonist-induced cytosolic Ca^{2+} oscillations was attenuated in PV- expressing primary hepatocytes, this was accompanied by reduced proliferation (125). Also, whole liver regeneration post PH was significantly delayed in PV-expressing rats, suggesting that optimum $[Ca^{2+}]_c$ is necessary for hepatocyte proliferation and liver regeneration (125).

From the findings of the studies highlighted above amongst others, it is apparent that in addition to cytosolic Ca^{2+}, nuclear Ca^{2+} is also important for cell (hepatocyte) proliferation and liver regeneration. The importance of nuclear and cytosolic Ca^{2+} for hepatocyte proliferation is dependent upon the action of the various Ca^{2+}-sensitive transcription activators/factors and enzymes which includes cAMP response element binding protein (CREB), ETS Like-1 (Elk1), calcium/calmodulin-dependent protein kinase type 4 (CaMK-IV) and nuclear factor kappa-light-chain-enhancer of activated B cells (NF-κB).

1.2.2.4 Ca^{2+} and cell death

The resting $[Ca^{2+}]_c$ is usually maintained around 100 nM compared to the extracellular concentration that ranges between 1-2 mM (133-136). To maintain this low $[Ca^{2+}]_c$, Ca^{2+} is actively pumped from the cytosol to the extracellular space, or extruded via the Na^+/Ca^{2+} exchangers or sequestered into the ER (136), golgi apparatus (137) and to a certain extent in the lysosome (138). In addition, mitochondria might buffer cytosolic Ca^{2+} (139) as do cytosolic proteins (140). Though coordinated spatiotemporal increases in $[Ca^{2+}]$ in the cytoplasm, nucleus and mitochondria mediates several cellular physiological signals, prolonged elevations in $[Ca^{2+}]_i$ resulting from either the extracellular space or from the intracellular stores triggers a series of cascades that culminate in cell death (136, 141). There are different forms of Ca^{2+}-dependent cell death which includes apoptosis, autophagy, and regulated necrosis (necroptosis).

1.2.2.4.1 Apoptosis

The mechanisms of apoptosis have been classified into two pathways; the intrinsic (mitochondrial) and the extrinsic (death receptor) pathways. There is a third pathway called the perforin/granzyme pathway that is employed by T-cells in eliminating viral-infected or transformed cells (142). The three pathways eventually converge on the same execution pathway (activation of caspases) (142). The intrinsic pathway involves diverse array of stimuli such as biochemical stress, DNA damage and lack of growth factors that result in intracellular stress signals on the mitochondria and consequent formation of mitochondrial permeability transition pore (mPTP) on the inner mitochondrial membrane and eventual release of pro-apoptotic factors from the mitochondria (143, 144). The extrinsic pathway is triggered by the binding of a ligand to a death receptor which are members of the tumour necrosis factor (TNF) receptor gene superfamily such as TNFR1 and FAS receptor (FASR) (142, 145). Previous studies have however reported that Bid mediates the release of cytochrome C from isolated mitochondria. Bid is a proapoptotic protein known to be activated by caspase 8; a protease involved in the extrinsic apoptotic pathway. This suggests that the extrinsic apoptotic pathway could also be mediated by the mitochondria (146).

BCL family of proteins, Ca^{2+} and apoptosis

Members of the BCL family of protein play vital roles in the regulation of apoptosis (147). They mediate pro and anti-apoptotic effects. The pro-apoptotic members of the protein family include the pro-apoptotic pore formers (BAK, BOK and BAX) and the pro-apoptotic BH3-only proteins (BAD, BID, NOXA, HRK, PUMA and BIK). While the anti-apoptotic BCL proteins include

BCL-2, BCL-XL, BCL-W, BFL-1/A1 and MCL-1) (148, 149). The BCL proteins modulates the mitochondrial apoptotic pathway by regulating the release of apoptotic factors from the mitochondria. BCL-2 inhibits apoptosis by lowering ER calcium load (150), while BCL-XL inhibits apoptosis by inhibiting IP_3-R expression on the ER, thereby attenuating IP_3R-mediated Ca^{2}+ release from the ER (151, 152). This way, BCL-2 and BCL-XL collectively reduces that amount of Ca^{2+} released from the ER into the cytosol, consequently reducing the amount of Ca^{2+} that transmits from the cytosol to the mitochondria, thus preventing mitochondrial Ca^{2+} overload, thereby inhibiting the release of pro-apoptotic factors from the mitochondria. On the other hand, pro-apoptotic BCL family members such as BAK and BAX promotes mitochondrial Ca^{2+} uptake by regulating IP_3R phosphorylation and promoting Ca^{2+} release from the ER (153).

1.2.2.4.2 Autophagy

Autophagy is a cellular process that involves the degradation and recycling of cellular materials such as long-lived proteins, lipids, complete organelles and other macromolecules, as well as maintenance of cell function (154). The degradation/recycling processes rely on lysosomal hydrolases and acid lipases. The process of autophagy is activated under stressed conditions such as prolonged fasting (nutrient deprivation), abnormally high temperatures, cytosolic Ca^{2+} overload, oxidative stress and accumulation of damaged organelles, whereas under well-fed conditions, autophagy is maintained at low basal level (155, 156). Activation of autophagy in the former conditions plays a vital role in sustaining cellular homeostasis and maintaining energy requirements and dysregulation of autophagic flux has been implicated in

several diseases such as cancer, cardiovascular and neurodegenerative diseases (157, 158). Autophagy can be classified into three different types, namely macroautophagy, microautophagy and chaperone-dependent autophagy, depending on the mode of material delivery to the lysosomes (159). Of the three, macroautophagy (hereafter called autophagy) is the most common type. It involves the sequestration of the substrates into cytosolic double-membrane vesicles called autophagosomes which subsequently fuses with lysosomes to form autolysosomes, resulting in the degradation and recycling of the enclosed materials (160). The molecular mechanism of autophagy is complex and orthologs of more than 30 autophagy-regulating (ATG) proteins have been implicated in the process. Of these, the mammalian ortholog of ATG6 Beclin 1, which has been suggested to intersect with several calcium signalling pathways, is the key protein involved in the initial formation of autophagosomes (161-163).

Ca^{2+} and autophagy

Ca^{2+} plays a key role in the regulation of autophagy (164). Previous studies have suggested a stimulatory role for Ca^{2+} in the initiation and execution stages of autophagy (165-167). However, other studies have proposed that intracellular Ca^{2+} signalling suppresses autophagy (168-171), suggesting a dual role for Ca^{2+}; as both a positive and negative regulator of the autophagic process. Increased $[Ca^{2+}]_c$ can positively regulate autophagy by various mechanisms. Elevated $[Ca^{2+}]_c$ can activate Calcium/calmodulin-dependent protein kinase beta (CaMKKβ) with a consequent stimulation of 5' adenosine monophosphate-activated protein kinase (AMPK) and inhibition of the

mammalian target of rapamycin (mTOR) signalling (172). mTOR negatively regulates autophagy, hence, its inhibition results in the upregulation of the autophagic process (173, 174). ER-localised Bcl-2 has been suggested to downregulate this process by lowering $[Ca^{2+}]_{ER}$ and attenuating agonist-stimulated intracellular Ca^{2+} signalling (172). On the other hand, other experimental studies have shown that IP_3R-mediated Ca^{2+} release suppresses autophagy. Release of Ca^{2+} from the ER via the IP_3R results in the transfer of Ca^{2+} to the mitochondria which can subsequently result in increased ATP production and downregulation of AMPK with a consequent inhibition of autophagy (172). Experimental evidence showed that abrogation of the IP_3R-mediated Ca^{2+} release in triple knockout (TKO) cells attenuated mitochondrial Ca^{2+} uptake, resulting in reduced oxygen consumption, decreased ATP production and activation of AMPK which consequently promoted autophagy (175).

1.2.2.4.3 Necroptosis

Necroptosis or regulated necrosis is a caspase-8-independent form of programmed cell death. The necroptotic mechanism is thought to be induced by apoptotic stimuli such as members of tumour necrosis factor receptor (TNFR) superfamily, toll-like receptors 3 and 4 (TLR3 and TLR4) and interferon receptors (176, 177). Necroptosis can be grouped into three types based on the nature of the stimuli. They include: TNFα-stimulated extrinsic necroptosis, reactive oxygen species (ROS)-stimulated intrinsic necroptosis and ischemia-stimulated intrinsic necroptosis (177). Although necroptosis can be initiated by various stimuli, the extrinsic necroptosis mediated by TNFα is the most studied and most understood. The binding of the ligand to its receptor

leads to the generation of short-lived high molecular weight membrane signalling complex, known as complex I, consisting of tumour necrosis factor receptor type 1-associated death domain (TRADD) protein, Fas-associated protein with death domain (FADD), Receptor-interacting protein kinase 1 (RIPK1), TNFR-associated factor 2 (TRAF2), TNFR-associated factor 5 (TRAF5), Cellular Inhibitor of Apoptosis Protein 1/2 (cIAP1/cIAP2) and linear ubiquitin chain assembly complex (LUBAC) (178). TRADD is first recruited to the TNFR1, this is followed by the recruitment of TRAF2/5 and RIPK1. The TRAF proteins then recruits the E3 ubiquitin ligases cIAP1/2 and LUBAC to RIPK1.

The transition of complex I to the death-inducing signalling complex II is regulated through the polyubiquitination profile of RIPK1. Removal of ubiquitin from RIPK1 by the deubiquitinating enzymes cylindromatosis (CYLD) and A20 results in the formation of complex II which consists of TRADD, FADD, RIPK1, and caspase-8 (179). Complex II exits in two forms (complex IIa and complex IIb) depending on the protein composition and activity and both forms are capable of inducing apoptosis and necroptosis depending on the cellular environment (180-182). In the absence of active caspase-8, both complexes (IIa and IIb) induce necroptotic cell death by the recruitment of RIPK3 and subsequent formation of microfilament-like complex called the necrosome, consisting of RIPK1 and RIPK3 which subsequently leads to the activation the pseudoprotein mixed lineage kinase domain-like (MLKL) (181, 183). This is followed by the rupture of the plasma membrane and release of cellular materials into the extracellular space.

Experimental evidence has shown that Ca^{2+} modulates the necroptotic process at various stages. For example, in human neuroblastoma cells, elevation of $[Ca^{2+}]_c$ have been shown to trigger the necroptotic process by activating calcium-calmodulin kinase (CaMK) which subsequently mediates RIPK1 phosphorylation (176). Also, in human colon cancer cells, $[Ca^{2+}]_c$ elevation has been reported to mediate necroptosis through the activation of c-Jun N-terminal kinase (JNK) which regulates necroptosis by their kinase activity (184). In both studies, chelation of Ca^{2+} with BAPTA-AM reportedly rescued the cells from necroptosis (176, 184).

1.2.3 Ca^{2+} and liver injury

Ca^{2+} plays an important role in the mediation of most of the functions of the liver, and as a result, long-term dysregulated hepatic Ca^{2+} signal have been implicated in a vast number of abnormal liver conditions such as non-alcohol fatty liver disease (NAFLD) and cholestasis (185). In order to cope with the hepatic injuries that results from the plethora of insults the liver is exposed to, the liver has developed a unique ability to regenerate, an ability which is lacking in most other vital organs of the body. The ability of the liver to regenerate makes it possible for the liver to recover from most acute and non-frequentative insults. However, the liver loses this regenerative ability when exposed to multiple long-term insults. The inability of the liver to regenerate would in turn result in chronic liver damage such as liver cirrhosis.

In this section, we highlight the role of Ca^{2+} in certain liver injury conditions, with focus on drug induced liver injury (DILI).

1.2.3.1 Ca^{2+} and cholestasis

Production and secretion of bile is one of the main functions of the liver (56). The secreted bile contains bile acids which helps in the breakdown of large fat droplets through the process of emulsification (186). Waste products such as bilirubin are also excreted through the bile into the intestine and eventually eliminated in faeces and urine (187). Disruption in the process of bile secretion leads to cholestasis. As discussed earlier, Ca^{2+} plays a crucial role in the process of bile secretion and this is made even more evident by the apical concentration of IP_3Rs in both hepatocytes and cholangiocytes (89, 90) which have been shown to be vital in bile secretion (93, 188). As a result, dysregulation of Ca^{2+} signal and/or decreased IP_3Rs expression, particularly IP_3R2 in hepatocytes and IP_3R3 in cholangiocytes leads to defective bile secretion (cholestasis). For example, IP_3R type III expression is significantly downregulated or completely lacking in patients with cholestasis (189). In line with this, animal studies have also showed a selective loss of IP_3R from biliary epithelia following bile duct ligation or endotoxin treatment, which are both accepted forms of in vitro inducible cholestasis, with a consequent loss of Ca^{2+} signalling and Ca^{2+}-mediated HCO_3^- secretion (189). These findings make clear the importance of tightly controlled Ca^{2+} signalling in bile secretion.

1.2.3.2 Ca^{2+} and hepatic ischaemia-reperfusion injury (IRI)

Hepatic-ischaemia reperfusion injury is an underlying pathophysiological complication that occurs in clinical conditions such as post liver resection or transplantation. In hepatic IRI, the body's metabolic processes shift from aerobic to anaerobic, there is accumulation of products of anaerobic glycolysis

including lactic acid and ketone bodies and there is depletion of intracellular ATP and ATP-dependent cellular processes gradually ceases (190). Also, hepatic IRI results in hepatic hypoxia which would in turn result in mitochondrial dysfunction, decreased ATP production and increased formation of reactive oxygen species (ROS). Increased ROS in turn leads to ER stress (191) which consequently results in increased Ca^{2+} release from the ER into the cytosol, leading to elevated $[Ca^{2+}]_c$ (192). The resulting increased $[Ca^{2+}]_c$ leads to increased mitochondrial Ca^{2+} uptake and perturbation of mitochondrial Ca^{2+}. This in turn leads to opening of mPTP and release of apoptotic factors and eventually results in apoptosis (193, 194).

1.2.3.3 Ca^{2+} and drug induced liver injury

Drug induced liver injury (DILI) is a common consequence of adverse drug reaction that could sometimes lead to drug withdrawal from the market, hospitalization and even in severe cases liver transplantation (195). DILI is responsible for about 5% of all hospital cases and more than half of all cases of acute liver failure (ALF) (196). In fact, more than two-thirds of idiosyncratic adverse drug reactions result in liver transplantation or death (196). Over 900 different drugs and therapeutic agents have been implicated in hepatotoxicity with new cases being reported each month (197) and of all the widely studied hepatotoxic drugs, acetaminophen (APAP) overdose is the most implicated (198).

Sustained perturbation of intracellular Ca^{2+} signal have been implicated in some mechanisms of DILI, however, this is dependent upon certain factors such as the affected hepatic cell type, the molecular target and the

dependency of metabolic activation or the involvement of the immune system (185). Our focus in this project is on Ca^{2+}-mediated drug and other agent-induced hepatotoxicity. However, there are other mechanisms via which drugs can induce liver damage that are independent of disruption of intracellular Ca^{2+} signal which are outside the scope of this study (199-201). Ca^{2+}-mediated liver damage involves perturbation of intracellular Ca^{2+} homeostasis due to drug-induced ER stress and mitochondrial depolarization.

An archetype of DILI is APAP-induced hepatotoxicity. In normal liver physiology, therapeutic doses of APAP are non-toxic as a good percentage is readily converted into non-toxic compounds by glucuronidation and sulphation (202), while only a small amount is converted into the reactive intermediate metabolite N-acetyl-p-benzoquinone imine (NAPQI) by hepatic cytochrome P450 (cyp)-dependent mixed function oxidases (203). The concentration of NAPQI generated by therapeutic doses of APAP is rapidly conjugated with glutathione and subsequently converted to non-toxic forms (202, 204). However, in APAP overdose, a significantly higher concentration of NAPQI is generated and hepatic glutathione is depleted, resulting in the accumulation of toxic amounts of NAPQI in the liver (203). NAPQI induces hepatic necrosis by covalently binding to cellular proteins (205), leading to the formation of reactive oxygen and nitrogen species (ROS and RNS), perturbation of intracellular Ca^{2+} regulation and elevated $[Ca^{2+}]_i$, consequently leading to mitochondrial oxidative stress and formation of mPTP (206, 207). NAPQI also results in ER stress by directly binding to ER proteins such as glutathione-S-transferases, calreticulin, protein disulphide isomerases and sarco/endoplasmic reticulum calcium ATPase (SERCA) (208, 209). Covalent

binding of NAPQI to PDI and calreticulin inhibits protein folding and stimulates ER stress and the unfolded protein response (UPR) (185).

Another widely studied agent that induces Ca^{2+}-mediated cell death which we have extensively investigated in this current study is thapsigargin (Tg). Tg is a sesquiterpene lactone that induces ER stress by irreversibly inhibiting SERCA, thereby preventing sequestration of Ca^{2+} into the ER, depleting ER Ca^{2+} and elevating $[Ca^{2+}]_c$ calcium concentration (210). The resultant ER stress and the consequent downstream events triggers cell death. In addition, prolonged elevated free cytosolic Ca^{2+} leads to mitochondrial Ca^{2+} uptake, which results in mitochondrial Ca^{2+} overload and consequent release of pro-apoptotic agents from the mitochondria.

1.3 Measurement of intracellular Ca^{2+} concentration

To our knowledge, the first reliable measurement of Ca^{2+} was performed by Ridgeway and Ashley where they injected the photoprotein aequorin into the giant muscle fibre of the barnacle (211). Since then, several methods of measuring Ca^{2+} have been developed each with associated advantages and pitfalls. These encompass Ca^{2+} selective microelectrodes, absorbance indicators (212), and the several currently used fluorescent Ca^{2+}-sensitive dyes and genetically encoded fluorescent Ca^{2+} indicators. However, absorbance dyes did not become widely adopted as a tool for measuring Ca^{2+} because of their low sensitivity to $[Ca^{2+}]_c$, hence unable to be used in measuring $[Ca^{2+}]_c$ in monolayers or individual cells (213).

1.3.1 Chemical fluorescent Ca^{2+} indicators

The use of chemical fluorescent Ca^{2+} indicators was introduced by Tsien and colleagues in the 1980s when they synthesized Quin2 and its successors and this was indeed a breakthrough in the measurement of intracellular Ca^{2+} and in the study of intracellular Ca^{2+}-related events (214-216). The fluorescent Ca^{2+} indicators can be classified into various groups based on different criteria. Firstly, they can be classified based on their excitation and emission spectra; those that are excited by near ultraviolet wavelengths (330-380 nm) and those that are excited by visible light (at ≥ 450 nm). Members of the former class include quin-2, fura indicators, indo-1 and their derivatives, while the later class consists of the fluo indicators, calcium green and rhod-2). Secondly, Ca^{2+} indicators can be grouped based on whether they are ratiometric (dual excitation) or nonratiometric (single excitation) indicators. The former includes fura-2, fura-4 and indo-1, while the latter includes quin-2, fluo indicators, calcium green and rhod-2) (213, 217). Just like other indicators, chemical Ca^{2+} indicators have advantages and disadvantages.

One major advantage of chemical Ca^{2+} indicators is their vast commercial availability with a broad range of Ca^{2+} affinities. Another advantage is the ease with which they can be loaded into cells with available well optimised cell loading protocols that does not require cell transfection (217, 218). However, there are also disadvantages associated with chemical indicators. Firstly, their cellular localization cannot be controlled, i.e., they cannot be selectively targeted to a specific subcellular location. Another disadvantage of chemical Ca^{2+} indicators is their Ca^{2+}-buffering effect. Lastly, when loaded into cells, they tend to become compartmentalized and can easily leak out of cells during

experiments. By way of circumventing some of these problems, most commonly used chemical indicators are now available as dextran conjugates. The dextran-conjugated indicators do not become compartmentalized, but remain cytosolic, they also do not leak out of cells, hence can be used for longer recording experiments. Also, dextran indicators do not spontaneously bind to proteins when introduced into cells, but can be selectively linked to peptides, hence allowing specific targeting by peptide signalling motifs (213). The major limitation of dextran indicators is that due to their hydrophilic nature, they do not easily load and would generally need to be directly introduced into cells by injection (218). Most carboxylic acid-based Ca^{2+} dyes are also available as acetoxymethyl (AM) esters. AM dyes are easier to load into cells due to their hydrophobic nature. When inside the cells, the AM moiety is cleaved by endogenous esterases, trapping and concentrating the dye inside the cells.

1.3.2 Bioluminescent Ca^{2+} protein indicators

Bioluminescent Ca^{2+} protein indicators are photoproteins that emits light upon Ca^{2+} binding. Several luminescent Ca^{2+} proteins have been described, they include aequorin, obelin, mitrocomin and clytin, (217, 219), amongst which the most common is aequorin. Bioluminescent indicators have several advantages which include a large signal-to-noise ratio (S/N), selective subcellular distribution, wide dynamic range, low intracellular Ca^{2+}-buffering effect and the simplicity they offer in terms of instrumentation. They emit visible bioluminescence from intramolecular interaction upon Ca^{2+} binding with no exciting light needed (213). The absence of exciting light also means that

photobleaching due to excitation illumination is not an issue and there is no cell and reagent autofluorescence. However, there are also the downsides of these probes, the most serious of which include the methods required to load them into cells; the cells must be amenable to be transfected with the construct (220). Another problem associated with bioluminescent proteins is low light emission (217, 220). For example, one aequorin molecule gives off one photon upon Ca^{2+} binding, in comparison to a molecule of fluorescent dye that can emit up to 10^4 photons (217, 220).

1.3.3 Fluorescent protein-based Ca^{2+} indicators

There now exists several fluorescent protein-based Ca^{2+} indicators generally referred to as genetically encoded Ca^{2+} indicators (GECI). The first step in the development of GECI was the discovery of green fluorescent protein (221) and then the discovery that fluorescence resonance energy transfer (FRET) can take place between two colour-emitting variants of a GFP (222). Genetically encoded indicators (GEIs) have several advantages over the use of dyes as imaging tools. They can be targeted to specific cell types, thus allowing activities to be monitored among a genetically defined subset of cells. They can also be targeted to a specific subcellular location, hence Ca^{2+} dynamics in a defined subcellular compartment can be studied. Lastly, they allow a relatively non-invasive long-term *in vivo* calcium imaging (223). There are two main important classes of GECIs which include the non-FRET-based (GCaMP)-type and the FRET-based GECIs (cameleon). The FRET-based indicators typically consist of a calcium response element flanked on either side by a fluorescent protein, while the GCaMPs consists of a circularly

permuted fluorescent protein (cpFP) fused to calmodulin (CaM) and calmodulin binding region of chicken myosin light chain kinase (M13) (224). One exception of the GCaMP type is the Camgaroo family of indicators which consists of two halves of a green fluorescent protein (GFP), bound to the C and N terminal of a calmodulin fragment.

In this study, we measured real time changes in Ca^{2+} signal using fluo-4, a chemical fluorescent Ca^{2+} indicator and REX-GECO1, a GECI.

1.3.3.1 Fluo-4 is a nonratiometric Ca^{2+} dye with excitation peak at ~490 nm and emission peak at ~520 nm. Fluo-4 is loaded into the cells in its AM ester form (Fluo-4AM) and once inside the cell, it is readily hydrolysed by endogenous esterases to give free, fluorescent Fluo-4 which then binds Ca^{2+}.

1.3.3.2 REX-GECO1 is a GCaMP-type, non-fret-based GECI (Figure 1.7). REX-GECO1 has several advantages. First, it can be used either as an intensiometric (480 nm excitation) or a ratiometric (585 nm excitation/480 nm excitation) Ca^{2+} indicator. Secondly, it can be excited with one photon (480 nm) or with two-photons (910-940 nm). Thirdly, because REX-GECO1 has a Ca^{2+}-bound excitation peak of 480 nm and an emission peak of 585 nm, it can be used for dual-colour imaging with other GFPs as demonstrated by the originator laboratory (224).

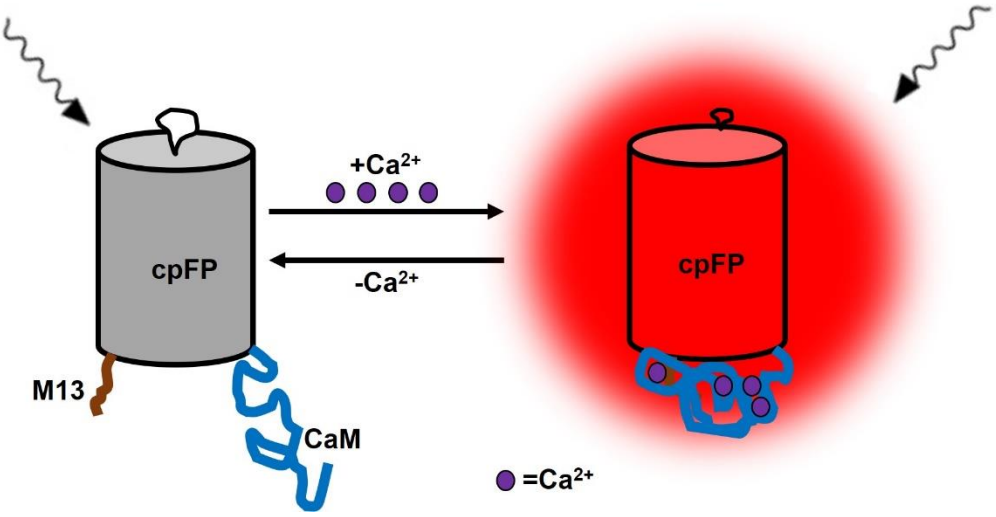

Figure 1.7. Schematic representation of the mechanism of REX-GECO1 function. Binding of Ca^{2+} to CaM induces an interaction of the CaM with M13 which in turn causes a change in the fluorescence emission intensity of the fused cpFP.

1.4 Cyclic guanosine 3',5'-monophosphate (cGMP)

Studies clearly shows that elevated $[Ca^{2+}]_c$ play a major role in liver injuries, including DILI and other chemical/xenobiotic-induced liver injuries, hepatic IRI and metabolic liver diseases (55, 185). One molecule that appears to modulate cytosolic intracellular Ca^{2+} and Ca^{2+}-mediated liver damage is cGMP (225). cGMP is a second messenger molecule that acts as a regulatory agent in several cellular processes such as regulation of ion channel conductance, vision and vascular tone, modulation of cell growth and differentiation and inhibition of mitochondrial permeability transition pore.

1.4.1 cGMP generation

cGMP is synthesized from cytoplasmic guanosine triphosphate (GTP) by the action of two classes of guanylyl cyclases (GCs); particulate GC (pGC) and soluble GC (sGC). Mammals express seven isoforms of the pGC which include guanylyl cyclase A (GC-A), guanylyl cyclase B (GC-B), guanylyl cyclase C (GC-C), guanylyl cyclase D (GC-D), guanylyl cyclase E (GC-E), guanylyl cyclase F (GC-F) and guanylyl cyclase G (GC-G), however, GC-D and GC-G are only pseudogenes in humans (226). The isoforms expressed in the liver include GC-A also called natriuretic peptide receptor type A (NPRA), GC-B also called natriuretic peptide receptor B (NPR-B) and GC-C also known as natriuretic peptide receptor type C (NPR-C) (226-228). GC-A is activated by atrial natriuretic peptide (ANP) and brain natriuretic peptide (BNP), GC-B is activated by type C natriuretic peptide (CNP), while GC-C is activated by guanylin, uroguanylin and bacterial heat stable enterotoxin (226).

There are two subunits of the sGC in mammals; soluble guanylyl cyclase alpha (sGC-α) and soluble guanylyl cyclase beta (sGC-β) with two isoforms of the different subunits (226). The isoforms include soluble guanylyl cyclase alpha 1 (sGC-α1), soluble guanylyl cyclase alpha 2 (sGC-α2), soluble guanylyl cyclase beta 1 (sGC-β1) and soluble guanylyl cyclase beta 2 (sGC-β2) (226). The expression of the different isoforms is tissue specific, with the α1 and β1 isoforms being the dominant isoforms in most tissues (229). In particular, the β1 isoform have been reported in rat liver (226, 230). In the basal state, sGC exits as a heterodimer consisting of different combinations of the α and β subunits (229) and is activated mainly by nitric oxide (NO) and to a certain degree by carbon monoxide (CO) (231, 232).

1.4.2 cGMP downstream effector components

Once synthesized, cGMP mediates cellular processes via its downstream effector components which include cGMP-dependent protein kinase (PKG), cyclic nucleotide gated (CNG) channels and cGMP-hydrolysing PDEs and (233) (Figure 1.7).

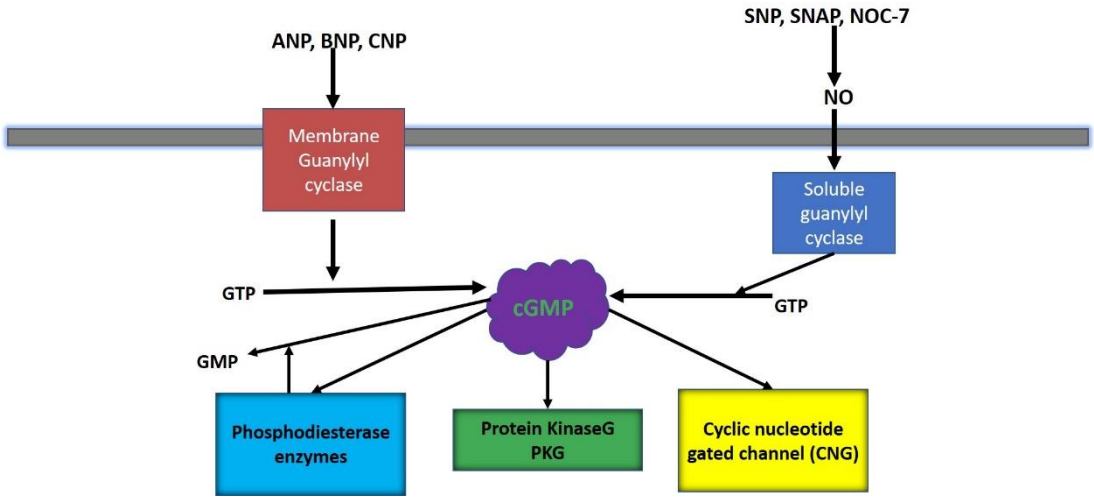

Figure 1.8. cGMP generation and its downstream components. Natriuretic peptides and NO activates pGC and sGC respectively, which in turn converts GTP to cGMP. cGMP mediates several downstream signalling events including regulation of cyclic nucleotide gated channels, phosphorylation of PKG and act on cGMP-dependent phosphodiesterases.

1.4.2.1 cGMP-dependent protein kinase G (PKG)

The principal cGMP downstream effector is PKG; a serine/threonine protein kinase (234). There are two families of PKG encoded by two separate genes prkg1 and prkg2 (235). The cytosolic protein kinase G I (PKGI) consisting of two isoforms (PKGIα and PKGIβ) and the membrane bound protein kinase G II (PKGII) respectively. The three PKGs all exists as homodimers (236). The

expression of PKGI and/or PKGII appear to be cell type-dependent. Over a decade ago, our group reported the expression of PKGIα and PKGIβ with no detectable PKGII in primary rat hepatocytes (225). Since then, to our knowledge, the presence of PKGII has not been reported in any species' hepatocytes, whereas, it is expressed in other cell/tissue types such as epithelial cells of mice intestine (237), different regions of rat brain such as the olfactory bulb and thalamus (238), juxtaglomerular (JG) cells, the ascending thin limb (ATL), and the brush border of proximal tubules of rat kidney (239) and rat chondrocytes (240). A typical PKG (both PkGI and II) consists of three different domains: an amino terminus, a regulatory domain containing cGMP binding site and a C-terminal catalytic domain for ATP binding which is responsible for catalysing the transfer of phosphate residues to serine/threonine motif (234). Upon binding of cGMP to the cGMP binding site in the regulatory domain, the inhibition of the catalytic domain induced by the N-terminal autoinhibitory domain is released, resulting in PKG activation (241). Full activation of one PKG monomer requires binding of two molecules of cGMP. Once activated, the protein then brings about the phosphorylation of downstream target proteins.

1.4.2.2 Cyclic nucleotide gated channels (CNGCs)

CNGCs are members of the voltage-gated ion channels superfamily, although their activity shows minimal voltage-dependence (242). They are non-selective cation channels that were first identified in the photoreceptor cells of the retina and olfactory sensory neurons (OSNs), but since then, CNGCs have been reportedly detected in non-neuronal tissues such as the heart, adrenal

gland, pancreas, kidney, liver, testis, skeletal muscle and colon (242, 243). Though CNGCs pass both monovalent (Na^+ and K^+) and divalent (Ca^{2+}) cations, and are said to be non-selective, they select divalent over monovalent cations (244, 245). They are directly activated by cyclic nucleotides (cAMP and cGMP) upon the binding of the latter to the cyclic nucleotide binding site present on the channel protein (246, 247). In general, a functional CNG channel is made up of four subunits, with each subunit consisting of six transmembrane segments (248). The binding of a single ligand to one of the subunits increases the chances of CNG channel opening, but to cause the channel to open, at least three of the four subunits must be occupied and to achieve full activation, four ligands are required (249, 250). Once activated, CNGCs allow the influx of Na^+ and Ca^{2+}. Unlike ligand-gated ion channels (LGCs), prolonged or repetitive binding of CNs to CNGCs does not cause any desensitization of the channel. However, their activity is regulated by two physiological mechanisms; by direct binding of Ca^{2+}-calmodulin (Ca^{2+}-CaM) complex to the channel and by phosphorylation (242). Although CNG channels respond to both cAMP and cGMP, they are generally more sensitive to cGMP than cAMP (244, 251), but with some degree of variability. For example, the CNG channels in rods and cones discriminate between cAMP and cGMP and are more sensitive to cGMP, whereas those of OSNs have almost equal sensitivity to both ligands (242, 252).

1.4.2.3 cGMP-hydrolysing phosphodiesterases (PDEs)

The cellular level of the cyclic nucleotide (CN) second messengers; cGMP and cAMP is regulated by members of the PDE superfamily of enzymes (253). PDE catalyses the hydrolysis of the phosphate bonds in the CNs to yield 5'-AMP and 5'-GMP (254). The mammalian PDE superfamily consists of eleven enzymes denoted as PDE1 – PDE11. PDE4, PDE7 and PDE8 are specific to cAMP, PDE5, PDE6 and PDE9 are specific to cGMP, while PDE1, PDE2, PDE3, PDE10 and PDE11 are dual substrate specific to both cAMP and cGMP (255, 256). The most characterised of the cGMP-specific PDEs is PDE5, but to our knowledge, till date, no study has investigated its expression in the liver, however, some in vitro studies suggest functional evidence of its presence in rat liver (257). cGMP-specific PDE that are reportedly expressed in the liver includes PDE9 (258) as well as some of the dual-specific PDEs: PDE2 (259), PDE3 (260) and PDE11 (261, 262).

The PDE9 family catalyses the hydrolysis of cGMP with the highest affinity for cGMP amongst all the members of the PDE superfamily and is resistant to majority of the PDE inhibitors including 1-methyl-3-isobutylxanthine (IBMX) (258, 263). Azevedo and colleagues (264) proposed that the insensitivity of PDE9 family to most of the reference PDE inhibitors could be due to the low amino acid sequence homology between their catalytic domain and that of other PDEs (258, 263, 265).

PDE 2, 3 and 5 are particularly relevant in the regulation of cGMP degradation because of their propensity to be activated or inhibited by cGMP and they alter cGMP or cAMP levels (241).

PDE2 degrades both cAMP and cGMP, however, this is cell-type dependent (264). It has a higher binding affinity for cGMP than cAMP (266). PDE2 family members are also called cGMP-stimulated cAMP PDEs (241, 264). Upon the binding of cGMP to the GAF-B domain present in their N-terminal regulatory region, their catalytic activities are allosterically stimulated, resulting in increased cAMP hydrolysis, thus reduction of cellular cAMP level (253, 267). Hence, PDE2 is said to induce a negative cross talk between cGMP and cAMP-dependent processes (253).

PDE3 catalyses the hydrolysis of both cGMP and cAMP with about 10-fold greater rate of cAMP hydrolysis over cGMP hydrolysis, however, the binding affinity for cGMP is higher than that of cAMP, hence cGMP is said to competitively inhibit PDE3 hydrolysis of cAMP (268). cGMP competitively inhibit the cAMP hydrolysing effect of PDE3, thereby maintaining an increased cAMP level (268). Hence PDE3 can also be referred to as cGMP-inhibited cAMP PDEs. In addition to the direct inhibitory action of cGMP on the cAMP hydrolysing ability of PDE3, there are evidence of a putative PKG phosphorylation site in the N-terminal regulatory region of PDE3 family members which can become phosphorylated by PKG, suggestive of an indirect modulation of PDE3 catalytic activity by cGMP (241, 269). Hence, PDE3 provides an additional crosstalk between cAMP and cGMP signalling pathways.

PDE5 is another cGMP-specific PDE. It catalyses the hydrolysis of cGMP and is also referred to as cGMP-stimulated cGMP PDE. PDE5 contain two N-terminal tandem GAF domains: GAFA and GAFB. Allosteric binding of cGMP

to the GAF-A domain enhances the phosphorylation of the enzyme, increasing its binding affinity for cGMP as well as promoting its catalytic activity for cGMP hydrolysis (270, 271).

PDE11 is the most recently discovered member of the PDE superfamily (261) and hydrolyses both cAMP and cGMP with varying affinities depending on the isoform (264). In humans, there are four isoforms of PDE11 that are encoded by the same PDE11A gene, they include PDE11A1, PDE11A2, PDE11A3 and PDE11A4 (264). Of all the isoforms, only PDE11A4 has two complete GAF domains, although the exact function of PDE11's GAF domain is still unestablished (272). PDE11 is said to have a catalytic domain similar to that of PDE5 than that of its immediate predecessor PDE10 (261) which provides a possible explanation for the reported inhibition of PDE11 activity by tadalafil, a PDE5 specific inhibitor.

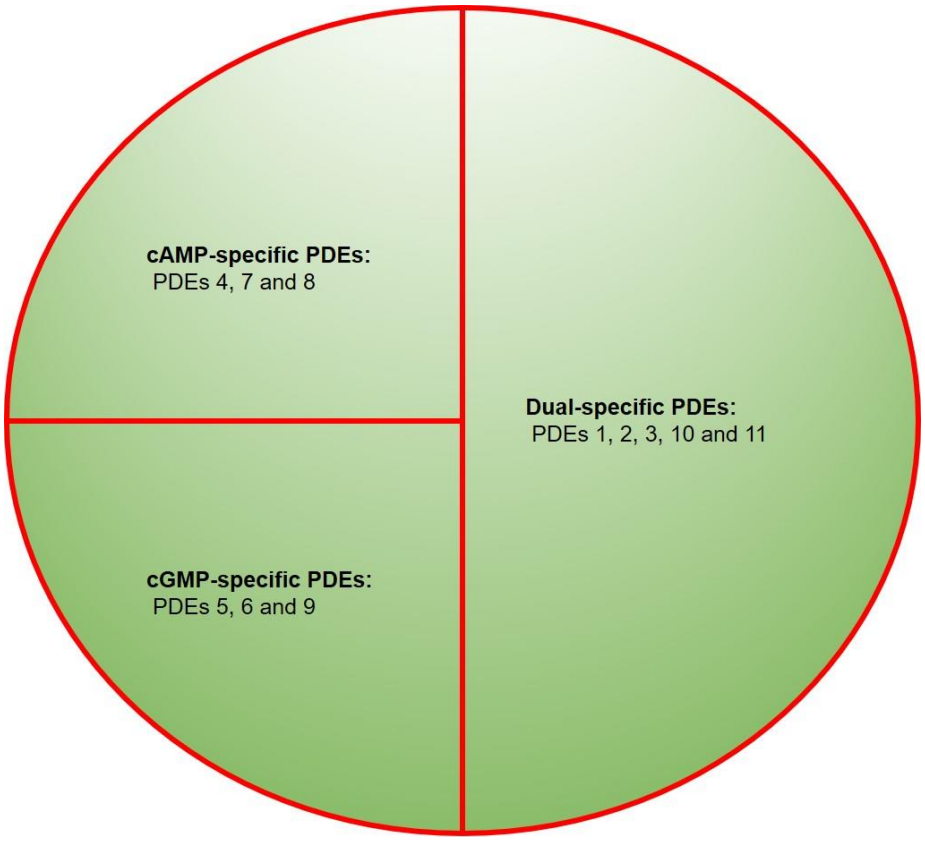

Figure 1.9. Mammalian PDEs according to substrate specificity. PDEs 4, 7 and 8 are cAMP-specific, PDEs 5, 6 and 9 are cGMP-specific, and PDEs 1, 2, 3, 10 and 11 are dual substrate-specific.

1.4.3 cGMP and modulation of intracellular Ca^{2+}

Studies clearly show that cGMP modulates intracellular Ca^{2+} signal in several cell types (273-281), including guinea-pig hepatocytes (282) and rat hepatocytes (225, 283-285). As discussed earlier, cells generate cGMP via two known pathways; the NO/sGC pathway and the NP/pGC pathway. Different studies have in the past reported conflicting observations on the effect of cGMP (applied directly as cGMP analogues or stimulated by NO and ANP) on hepatocyte Ca^{2+} signalling. In these studies, cGMP was reported to attenuate (225, 283, 285, 286), potentiate (284, 287) or unalter (288) Ca^{2+} signalling in rat hepatocytes. The reason for these contradicting observations remains unclear, they however point to one thing; that the mechanism of cGMP modulation of hepatocyte Ca^{2+} signal remains an area that requires further studies. Milbourne and Bygrave (275) proposed that the mechanism is cGMP concentration-dependent; at low concentrations, cGMP stimulate Ca^{2+} ion influx, thus resulting in elevations in $[Ca^{2+}]_c$, while at high concentrations, it inhibits Ca^{2+} influx (275).

The mechanism of cGMP modulation of intracellular Ca^{2+} signalling is a complex system that goes beyond just stimulation and inhibition of Ca^{2+} influx, but a multifaceted process, involving both direct and indirect actions of cGMP. In this thesis, we will classify the mechanism of cGMP modulation of intracellular Ca^{2+} into three pathways: one direct pathway and two indirect

pathways. The direct pathway involves the stimulation of cyclic nucleotide gated ion channels (CNGCs) by the direct binding of cGMP to the channel protein and consequently resulting in the influx of extracellular Ca^{2+} (refer to the section cGMP downstream effector components) (246, 247, 289). The second pathway (the first indirect pathway) is mediated by two classes of PDEs: cGMP-stimulated and cGMP-inhibited cAMP PDEs. Binding of cGMP to the GAF domain of cGMP-stimulated cAMP PDE (PDE2), results in increased degradation of cAMP, with a consequent reduction of cellular cAMP and inhibition Ca^{2+} influx via the cAMP-stimulated L-type Ca^{2+} channels (253, 267, 290). On the other hand, binding of cGMP to cGMP-inhibited cAMP PDE (PDE3) inhibits the hydrolysis of cAMP, resulting in an increased cAMP level, which can activate cAMP-stimulated L-type Ca^{2+} channels and consequent influx of Ca^{2+}. The third pathway (the second indirect pathway) involves the activation of endogenous PKG which in turn phosphorylates target proteins and channels (291) that eventually culminate in reduction in $[Ca^{2+}]_c$. The PKG pathway appears to be the main pathway via which cGMP modulates intracellular Ca^{2+}.

Activated PKG can modulate intracellular Ca^{2+} via multiple possible ways that includes:

1) Phosphorylation of G-protein activated phospholipase C-β3 (PLC-β3) at two phosphorylation sites (Ser^{26} and Ser^{1105}), thereby inhibiting the hydrolysis of PIP_2 and subsequent IP_3 generation and consequent IP_3-mediated Ca^{2+} release (292). Mutation at the two PKG phosphorylation

sites abolishes the PKG-induced phosphorylation, thereby blocking the ability of PKG to phosphorylate the protein (292).

2) Direct phosphorylation of IP_3R at two possible sites (Ser^{1589} and Ser^{1756}) (293), thereby inhibiting IP_3-mediated Ca^{2+} release from internal stores.
3) Phosphorylation/activation of plasma membrane Ca^{2+} ATPase which in turn results in Ca^{2+} efflux (294). This has been particularly reported in primary rat hepatocytes and was shown to be mediated by ANP and not SNP-induced cGMP elevations (225, 283).
4) Phosphorylation/activation of large conductance Ca^{2+}-activated potassium ion (K^+) channels (BK channels) which results in efflux of intracellular K^+, thereby causing hyperpolarization of the plasma membrane and consequent inhibition of Ca^{2+} via the L-type Ca^{2+} channels (295-299).
5) Phosphorylation of phospholamban (PLN), thereby relieving its inhibitory action on SERCA pump and allowing sequestration of cytosolic Ca^{2+} into the ER/SR with a net decrease of $[Ca^{2+}]_c$. However, this is only applicable to cells that express phospholamban (PLN) such as smooth and cardiac muscle cells.

1.4.4 cGMP and hepatoprotection

Several studies have shown that cGMP protects hepatocytes against cell damage. In isolated rat hepatocytes, it was reported that ANP through PKG attenuates ATP-induced elevation in $[Ca^{2+}]_c$ and protects hepatocytes from ATP and TLC-induced cell death (225). Also, data from another group revealed that ANP and cGMP analogue 8-Br-cGMP through protein kinase G

protects rat hepatocytes against hypoxic injury (300). 8-Br-cGMP through PKG and NO through the stimulation of sGC have also been shown to protect rat hepatocytes against TNFα-induced apoptosis and caspase 3-like activity (301). The endogenous precursor of NO, L-arginine (302, 303) and 8-Br-cGMP (303) were also reported to protect against hepatic ischaemia reperfusion injury in rat liver.

1.5 Measurement of cellular cGMP

Several methods have been used in the past to measure cGMP in cells. Firstly, the cellular cGMP level has been measured by radioimmunoassays (RIAs). This involves generation of cGMP antibodies and radioactively labelling cGMP. cGMP has also been measured by cGMP enzyme-linked immunoassays (ELISAs). Though the above-mentioned techniques are quite sensitive and specific, they involve homogenization of cells or tissues, hence, only mean cGMP content of all cells can be measured, not cGMP content of individual cells. Similarly, with these methods of cGMP measurement, real-time spatiotemporal dynamics of cGMP cannot be monitored (304). To overcome the limitations of antibody-based cGMP measurement assays, researchers designed cGMP indicators that allow for continuous monitoring of cGMP signal in living cells. In recent years, several FRET-based cGMP indicators have been developed and used to monitor spatiotemporal dynamics of intracellular cGMP and have significantly advanced our understanding of cGMP dynamics in various cell types (305-310). However, FRET-based cGMP biosensors have limitations. For example, they require a technically laborious dual emission detection system and generally express minimal cyan/yellow

emission ratio changes in whole cells (311). Also, FRET-based cGMP indicators are limited in their sensitivity to cGMP, hence have limited ability to measure small cGMP signal induced by low (nanomolar) physiological NO concentrations (305). However, recent studies have revealed that NO concentrations in the low nanomolar range (≤10 nM) are enough to activate soluble guanylyl cyclase (312, 313). To get around these disadvantages, non-FRET-based cGMP biosensors called Fluorescent indicators of cGMP (FlincG) were developed to allow for monitoring intracellular cGMP spatiotemporal dynamics induced by low concentrations of guanylyl cyclase stimulators.

Three variants of FlincG indicators, namely α-, β-, and δ-FlincG were first generated by the originator laboratory (311). α-, β-, and δ-FlincGs respectively consist of the regulatory domains of PKG I α, PKG Iβ and N-terminal deletion mutant of PKG I α fused to the N terminus of circularly permuted enhanced green fluorescent protein (cpEGFP) (311) (Figure 1.). It was reported that δ-FlincG has dual excitation maxima at 410 nm and 491 nm, while α- and β-FlincGs have single excitation maximum at 491 nm (311). Unlike FRET-based cGMP biosensors, FlincG indicators were engineered to have minimal interactions with endogenous proteins and to give high fluorescent intensity changes in living cells. Particularly, δ-FlincG was reported to have no interaction with wildtype PKG due to the absence of the N-terminal dimerization domain and maintained maximal fluorescence intensity change in living cells when compared to that observed under cell-free conditions (311). On the other hand, α- and β-FlincGs displayed some interactions with wildtype PKG and showed reduced change in fluorescence intensity in living cells

compared to observations made in cell-free conditions, thus, reportedly making δ-FlincG the best choice of the variants for studying cellular cGMP dynamics (311). Also, according to the originator laboratory δ-FlincG is resistant to small changes in pH because of its low pKa value of 6.1 (311). However, subsequent studies by another group refuted this report, and rather submitted that δ-FlincG has a pKa of 7.5 and is pH sensitive (314). Also the authors stated that the C-terminal tail present in δ-FlincG have a major impact on its cGMP biosensing (314), contrary to the submission of the originator laboratory that the c-terminal tail have no impact on the change in fluorescence intensity of the indicator (311).

Further optimizations lead to the generation of improved versions of δ-FlincG (FlincG2 and FlincG3). FlincG2 retained the sequence of the original δ-FlincG, but with a divergent C-terminal tail and gave moderate basal fluorescence and cGMP response amplitude. FlincG3 (also called H6-FGA^{M}) on the other hand has the same C-terminal tail as δ-FlincG, but contains an M335K substitution in the cpEGFP region and an N-terminal enzyme-cleavable hexahistidine (His) tag and was reportedly superior to FlincG2 and δ-FlincG in terms of basal fluorescence intensity and cGMP biosensing, but with a loss of the ratiometric response characteristic of δ-FlincG (314).

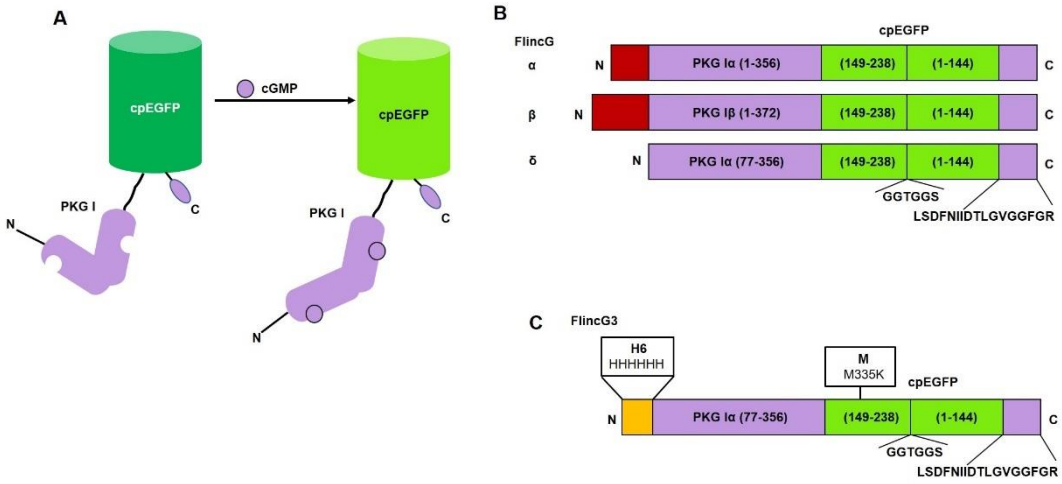

Figure1.10. Illustration of FlincG variants. (A) Schematic diagram illustrating the general formation and mechanism of FlincG function: binding of cGMP to the cGMP binding sites of PKG1 fragments induces change in fluorescence emission intensity of fused cpEGFP. (B) Schematic illustration of α-, β-, and δ-FlincG domain structures designed from the fusion of cpEGFP to PKG1 fragments. (C) Domain architecture of FlincG3 with N-terminal His tag and M335K substitution in the cpEGFP domain. Adapted from (311, 314).

1.6 Vitamin C (Vit C)

Vitamin C (referred to in this thesis as Vit C), also known as L-ascorbic acid (L-AA) or ascorbic acid (AA) or L-ascorbate or just ascorbate, is a six carbon lactone which is synthesized from glucose in the liver of some mammals but not by some mammalian species including humans, non-human primates and guinea pigs. This is due to the lack of the L-gulonolactone oxidase (L which is the terminal enzyme involved in the biosynthesis of Vit C. Hence, humans and the other species lacking the L-gulonolactone oxidase must ingest the necessary amount of Vit C they need either in diets or by other forms. *In vivo*, Vit C is important for normal growth and development and serves as an

enzyme co-factor for several enzymes such as those involved in carnitine biosynthesis, post-translational hydroxylation of collagen, amidation of peptides and tyrosine metabolism (315).

1.6.1 Vit C as an antioxidant

Free radicals and oxidants when released in excess leads to the generation of the deleterious process of oxidative stress, that can cause severe damage to the cell plasma membrane and other cellular structures including proteins, lipids and deoxyribonucleic acid (DNA). Oxidative stress is simply a result of an imbalance between formation of free radicals and the protection against them, which can consequently lead to cellular damage and even chronic and degenerative diseases such as cancer, autoimmune diseases, cardiovascular diseases, neurodegenerative diseases, liver diseases and hepatic fibrosis. The deleterious effects of free radicals and oxidants are prevented by enzymatic and non-enzymatic antioxidants by their ability to scavenge these free radicals and ROS. Enzymatic antioxidants include glutathione peroxidase, glutathione reductase, catalase, superoxide dismutase, while examples of non-enzymatic antioxidants include glutathione, and Vit C and vitamin E (315). Chemically, Vit C is a potent antioxidant because of its ability to donate electrons to oxidised species/free radicals, resulting in the reduction of these species and consequently quenching their reactivity and concomitantly forming a relatively stable ascorbyl-free radical (316). It forms part of the first line antioxidant defence, protecting lipid membranes and proteins against the effect of oxidative stress (315). Vitamin C is a potent scavenger against reactive oxygen and nitrogen species (ROS and RNS) including H_2O_2, singlet

oxygen, superoxides and hydroxyl radical, sulphur radicals, hypochlorous acid, nitrosamines, and other nitrosating compounds, nitrous acid related compounds and ozone. This way, Vit C protects cells against free radical-mediated toxicity.

1.6.2 Vit C as a pro-oxidant

Though by donating electrons to oxidised species, Vit C brings about the reduction of these species, however, referring to Vit C as antioxidant can be misleading in certain instances as Vit C can also lead to the formation of reactive oxygen species (ROS). This is however outside the scope of this study. In brief, Vit C can interact and reduce redox active transition metallic ions such as copper (II) ion to Copper (I) ion (Cu^{2+} to Cu^{+}) and iron (III) to iron (II) ion (Fe^{3+} to Fe^{2+}). The reduced metallic ions then interact with oxygen (O_2) to form superoxides which can in turn undergo dismutation to form hydrogen peroxides (H_2O_2). The resulting H_2O_2 can then interact with another transition metal to give rise to reactive oxygen species (ROS). This however occurs mainly in the extracellular fluid, but not in the blood, because in the latter, the H_2O_2 is readily acted upon by catalase and glutathione peroxidase (GPx) and is converted to water and oxygen.

1.6.3 Vit C generation of cGMP and hepatoprotection

Studies suggest that Vit C is hepatoprotective. Vit C protects rat liver against hepatic injury induced by various drugs such as acetaminophen (317), artemether (318) and 5-fluorouracil-induced hepatotoxicity (319). Vit C also protects liver against various toxin-induced hepatotoxicity such as ethanol-

induced liver injury (320, 321), cypermethrin-induced hepatotoxicity in rat (322), styrene-induced rat liver damage (at organ level) (323) and triptolide-induced mice liver injury (324). In human chronic hepatitis C (CHC) patients, plasma Vit C level negatively correlates with hepatic portal/periportal inflammation and fibrosis (325) and aspartate aminotransferase (326). These hepatoprotective effect of Vit C have traditionally been attributed to its direct antioxidant property and ability to scavenge free radicals and prevent cellular oxidative stress, however, acetaminophen and ethanol-induced liver damage is not entirely free-radical mediated. Studies have reportedly implicated perturbed $[Ca^{2}+]_i$ in acetaminophen (327) and ethanol (328) induced hepatotoxicity. This suggests that in addition to its direct free radical scavenging ability, Vit C could be mediating hepatoprotection via other molecular pathways involving regulation of intracellular Ca^{2+} homeostasis.

Interestingly, evidence show that Vit C modulates cellular cGMP in certain cell types such as pheochromocytoma 12 (PC 12) cells (329) and human umbilical vein endothelial cells (HUVECs) (330). Also, in humans, Vit C have been shown to modulate cGMP *in vivo* (331). We have discussed earlier about the different ways via which cGMP can modulate intracellular Ca^{2+} including experimental evidences that show that cGMP added directly to cells as cGMP analogue 8-Br-cGMP or stimulated by cGMP elevators such as ANP and SNP/NO modulates intracellular Ca^{2+} and protects rat hepatocytes against Ca^{2+}-mediated toxicity. Similar to the actions of cGMP and cGMP elevating agents (SNP/NO and ANP), Vit C has been reported to decrease $[Ca^{2+}]_i$ in human lymphoid cells (332) and bovine aortic endothelial cells (331), but the studies did not investigate whether the action of the vitamin was cGMP-

mediated. Our group have also recently observed that Vit C elevates cGMP in primary rat hepatocytes (PRH) and via PKG, reduces $[Ca^{2+}]_c$, consequently protecting PRH against Ca^{2+}-mediated hepatotoxicity (unpublished data). The cGMP elevation action of Vit C has also been demonstrated in PC12 cells (329). Taken together, these studies demonstrate that Vit C elevates cGMP in various cell types and has the potential to reduce $[Ca^{2+}]_c$ and protect rat hepatocytes from Ca^{2+}-mediated injury. However, the exact mechanism via which the vitamin is mediating the cGMP elevating action is still not clear and whether this cGMP stimulation action of Vit C and consequent $[Ca^{2+}]_c$ reduction and hepatoprotection can be achieved in human hepatocytes remain unelucidated. Chen and colleagues proposed that the vitamin mediates the cGMP generation action via the ANP/pGC route in PC12 cells (329). We agree with their submission, but in addition, we speculate a possible involvement of cell surface protein disulphide isomerase (csPDI) in the mechanism.

1.6.4 Protein disulphide isomerase (PDI) and modulation of cGMP generation

PDI is a multifunctional protein that functions as a molecular chaperone. It is a dithiol-disulphide oxidoreductase, having the ability to reduce, oxidize or isomerize disulphide bonds (333). PDI was traditionally considered to be an ER-resident protein due to the presence of the C-terminal KDEL (lysine, aspartic acid, glutamic acid and leucine) sequence. However, recent studies show that the isomerase also exists as membrane-bound enzyme in certain cell types including vascular smooth muscle cells (VSMCs), endothelial cells (ECs), human mesangial cells (HMCs) and rat hepatocytes (333-336). When present on the membrane, PDI is generally referred to as cell surface PDI

(csPDI) because it is believed to be attached to the extracellular surface of the cell membrane by lipid, glycan and integral membrane protein anchors (336, 337). csPDI has been shown to colocalize and modulate the action of neighbouring membrane proteins. It catalyzes thiol-disulfide exchange on cell surface proteins and mediates integrin-dependent cell migration and adhesion (338). PDI has also been implicated in the entry of viruses into host cells by altering the arrangement of the disulphide bonds on the viral envelop, thereby causing fusion of the viral envelop to the membrane of the host cell and consequent viral entry into the host cell (339, 340). PDI therefore has been shown to be highly involved in the alteration of disulphide bond arrangement on membrane proteins, including cell surface receptors, thereby, modulating downstream peptide signalling. Particularly, csPDI was shown to colocalize with and modulate the cGMP generation action of membrane-bound guanylyl cyclase-linked receptors type A (GCA/NPRA) and B (GCB/NPRAB) in response to natriuretic peptides (NPs) in HUVECs and HMCs (333). The authors suggested that membrane PDI physically interacts with both natriuretic peptides (NPs) and their receptors (NPRs), consequently functioning as an allosteric modulator of NPs-induced pGC generation of cGMP (333). Considering that Chen and colleagues (329) had earlier suggested that Vit C mediates its cGMP generation action, like ANP, by activating the membrane-bound guanylyl cyclase, we therefore speculate that csPDI would modulate Vit C generation of cGMP similar to the observation reported for ANP-induced generation of cGMP by Pan and group (333).

1.7 Aims of the study

We aim to test the following hypotheses in this study:

1. Vit C elevates cGMP in human liver cells, using HepG2 cells as our model hepatocyte cell line.
2. csPDI modulates Vit C elevation of cGMP in HepG2 cells
3. Vit C reduces $[Ca^{2+}]_i$ in HepG2 cells and this is modulated by csPDI
4. The cGMP elevation and $[Ca^{2+}]_i$ reduction actions of Vit C can be achieved in other cell types, using HEK293 cells as non-hepatocyte model.
5. Human hepatocytes (HepG2 cells and PHHs) express membrane PDI and the isomerase colocalizes with membrane-bound guanylyl cyclase-linked receptor (NPRA)
6. Vit C protects hepatocytes against Ca^{2+}-mediated damage, and this protection is mediated by cGMP/PKG
7. csPDI modulates the hepatoprotective effect of Vit C against Ca^{2+}-mediated damage

To test these hypotheses, we utilized a recombinant real-time reporter of cGMP (FlincG3) to measure Vit C-induced cGMP signal in HepG2 cells and in HEK293 cells which served as our non-hepatocyte model. We also investigated the involvement of csPDI in the mechanism by inhibiting it using bacitracin (Bac), a hydrophilic, poorly cell permeant polypeptide that is widely used as an inhibitor of PDI and other thiol isomerases of the PDI family (333, 341) and RL90, an anti-PDI monoclonal antibody. We utilized the monoclonal antibody in this study to inhibit csPDI since the intact membrane of living cells

are generally impermeable to large polypeptides including antibodies (342, 343). To investigate whether Vit C reduces $[Ca^{2+}]_i$, we utilized Fluo-4 AM and REX-GECO1 (a genetically encoded Ca^{2+} reporter) to measure real-time changes in Ca^{2+} signal in HepG2 and HEK293 cells upon thapsigargin (Tg) treatment, in the presence and absence of Vit C. The involvement of csPDI in the Vit C modulation of intracellular Ca^{2+} was also investigated using Bac and RL90.

We then investigated the expression of csPDI and its colocalization with NPRA in hepatocytes (HepG2 cells and PHHs) by immunofluorescence. The membrane expression of these proteins was also investigated in HEK293 cells by immunofluorescence. Finally, we investigated whether Vit C would protect hepatocytes against Ca^{2+}-mediated hepatocyte damage via a cGMP/PKG-dependent pathway. To do this, Tg was used as hepatotoxin and Rp-8-Br-cGMP was used to inhibit PKG.

Chapter 2

Materials and Methods

2.1 Materials

2.1.1 Reagents, drugs and chemicals

Ethylenediaminetetraacetic acid (EDTA, 8741092) used to chelate calcium during cell culture was purchased from sigma-Aldrich (Dorset, UK) Trypsin/EDTA (15400-054) used for dissociation and disaggregation of adherent cells was purchased from Thermo Scientific (Loughborough, UK). Dulbecco's Modified Eagles Media (DMEM, 31966-021) was purchased from Thermo Scientific (Loughborough, UK). Fetal bovine serum (FBS, 10270-106) was purchased from Thermo Scientific (Loughborough, UK). Dulbecco's Phosphate Buffered Saline (DPBS, 14190-144) was purchased and Penicillin-streptomycin (Pen-strep, 15140-122) were purchased from Thermo Scientific (Loughborough, UK). L-glutamine (L-glut, G3126) was purchased from Sigma-Aldrich (Dorset, UK). Insulin transferrin selenium (ITS, 41400045) was purchased from Thermo Scientific (Loughborough, UK) and dexamethasone (Dex, D4902) was purchased from Sigma-Aldrich (Dorset, UK).

Startub reagent reservoir (E2310-1010) was purchased from Starlab (Milton Keynes, UK). Corning T75 flask (BC301) was purchased from Sigma-Aldrich (Dorset, UK). 12 well plates (665180) were purchased from Greiner Bio-one (Stonehouse, UK). Corning 48 well plates (BC014) were purchased from Appleton woods Ltd (Birmingham, UK). Corning black clear bottom 96 well plates (CLS3603-48EA) were purchased from Sigma Aldrich (Dorset, UK), Corning collagen I-coated 96 well plates (354407) were purchased from Thermo Scientific (Loughborough, UK). 13 mm cover slips (0111530) were

purchased from Paul Marienfeld GmbH & Co.KG (Lauda-Königshofen, Germany).

2.1.2 Buffers and solutions

Tris-Borate-EDTA (TBE): 45 mM Tris-Borate (54 g Tris Base and 27.5 g Boric acid), 1 mM EDTA (4.6875 g disodium EDTA)

Tris base, boric acid and EDTA were dissolved in 800 mL of deionised water. Once dissolved, solution was adjusted to pH 8.3 before addition of more deionised water to a total volume of 1 L. TBE was used at 1 X concentration

Hepes buffered saline (HBS)

10 mM Hepes (2.383 g), 145 mM NaCl (8.474 g), 5 mM KCl (0.373 g), 1 mM $MgSO_4$ (0.246 g), 1 mM Na_2HPO_4 (0.138 g).

Hepes, NaCl, KCl, $MgSO_4$ and Na_2HPO_4 were dissolved in 800 mL of deionised water. Once dissolved, the pH was adjusted to 7.4 at room temperature (RT) and the final volume was made up to 1 L with deionised water.

Paraformaldehyde (PFA) for fixation

4 % PFA (20 g), PBS (500 mL)

PFA powder was heated to 37 °C and regularly stirred and the pH was raised by the addition of NaOH dropwise until the solution turned clear. The pH was adjusted to 7.4 at RT and aliquotted into 50 mL falcons and stored at -20^{o}C.

2.1.3 Cells used in the study

HepG2 cells were obtained from Chris Goldring's team (pharmacology department, Institute of Translational Medicine, University of Liverpool), at passage 12 (P12) and was expanded and frozen down at P14.

HEK293 cells were obtained from John Quayle's team (physiology department, Institute of Translational Medicine, University of Liverpool) at passage 6.

Primary human hepatocytes were isolated from liver specimen obtained from the Aintree university teaching hospital. Details of isolation procedure is detailed in the section ''primary human hepatocyte isolation''.

2.1.4 Plasmid DNAs and biosensors

pTriEx4-H6-FGAm (FlincG3, 49202) and CMV-REX-GECO1 (REX-GECO1, 61246) were purchased from Addgene (Teddington, UK).

2.1.5 FlincG3 and REX-GECO1 preparation reagents

LB Broth (L322-250G) and LB Agar (52062) were purchased from Sigma-Aldrich (Dorset, UK). Soc medium (15544-034) and Ultrapure agarose gel (16500-500) were purchased from Thermo Scientific (Loughborough, UK). Qiagen miniprep Kit (27104) and maxiprep kit were purchased from Qiagen (Manchester, UK). Ampicillin (A9518) and Glycerol (200-289-5) were purchased from Sigma-Aldrich (Dorset, UK). NeBuffer 2.1 (B7202S) was purchased from New England Biolabs (Hitchin, UK). Ethidium bromide (A25645) was purchased from Thermo Scientific (Loughborough, UK).

Cutsmart buffer (B72045) was purchased from New England Biolabs (Hitchin, UK). Bovine Serum albumin (BSA, R396D) was purchased from Promega (Southhampton, UK). G418 (04727878001) was purchased from Roche (Burgess Hill, UK). Gel loading dye (B7025S) was purchased from New England Biolabs (Hitchin, UK). 1Kb DNA ladder (N0552S) was purchased from New England Biolabs (Hitchin, UK). T4 DNA Ligase (B0202S) was purchased from New England Biolabs (Hitchin, UK). Nhe1HF (RS131S) was purchased from New England Biolabs (Hitchin, UK). BamH1HF was purchased from New England Biolabs (Hitchin, UK).

Table 2.1. Summary of Restriction Enzymes used in the Study

Enzyme	Supplier
Xba1 (R618A)	Promega (Southampton, UK)
Xho1 (899194)	Roche (Burgess Hill, UK)
PVUII (ER0631)	Thermo Scientific (Loughborough UK)
Nhe1HF (RS131S)	New England Biolabs (Hitchin, UK)
BamH1HF (R3136S)	New England Biolabs (Hitchin, UK)
EcoR1 (R0101S)	New England Biolabs (Hitchin, UK)

Table 2.2. Summary of transfection reagents used in the study

Reagent	Supplier
Turbofect	Thermo Scientific (Loughborough, UK)
Lipofectamine™ 2000 (LF2000)	Thermo Scientific (Loughborough, UK)
Lipofectamine™ 3000 (LF3000)	Thermo Scientific (Loughborough, UK)
Happfect (THFP-500)	Tecrea (London, UK)
Jetprime 114-07	Polyplus (Reading, UK)

2.1.6 Drugs and reagents for real time cGMP and Ca^{2+} measurement experiments

Sodium nitroprusside (SNP, S0501), atrial natriuretic peptide (ANP, A1663-.1MG), +(-)Sodium L-ascorbate (Vit C, A7631-25G), Adenosine triphosphate (ATP, A9272-100MG), ionomycin (10634-1MG), pluronic F-127 (P2443), Bacitracin (Bac, 11702-5G) and Bovine serum albumin (BSA, A2153-50G) were purchased from Sigma Aldrich (Dorset, UK), Thapsigargin (Tg, 1138) was purchased from Tocris Bioscience (Bristol, UK), Fluo-4 AM (F14201) was purchased from Thermo Scientific. Sulfinpyrazone (SPzn; S2159000) was purchased from Sigma-Aldrich (Dorset, UK).

2.1.7 Immunofluorescence reagents

Paraformaldehayde (PFA, P6148) for the fixation of cells was purchased from sigma Aldrich (Dorset, UK). Ammonium chloride (NH_4Cl, 27149) for quenching of fixation was purchased from BDH chemicals (Poole, UK). Triton X-100 for cell permeabilization was purchased from Sigma Aldrich (Dorset, UK). Chick

serum (C5405) used for blocking of non-specific antibody binding was also purchased from Sigma Aldrich (Dorset, UK). Anti-NPRA antibody (NBP1-31333) and anti-PDI antibody (RL90, NB300-519) used to tag both the cytoplasmic and cell surface NPRA and PDI respectively were purchased from Novus Biologicals (Cambridge, UK). Alexa Fluor 488 and 594 fluorescent conjugated secondary antibodies used for the detection of NPRA and PDI in immunofluorescence were purchased from Thermo Scientific (Loughborough, UK). 4′,6-diamidino-2-phenylindole (DAPI, D1306) used from staining cell nuclei was purchased from Thermo Scientific (Loughborough, UK). Prolong Gold (P36930) used to mount coverslips and prevent photobleaching was purchased from Thermo Scientific (Loughborough, UK). Nail varnish (113794) was purchased from Poundland (Liverpool, UK).

2.2 Methods

2.2.1 Preparation of ampicillin stock

Stock of 100 mg/mL of ampicillin was dissolved in autoclaved deionised water (dH_2O) and sterile-filtered using a 0.22 µm filter and stored at -20^{o}C in 1 mL aliquots.

2.2.2 Preparation of LB media solution

20 g of LB broth was suspended in 1 L dH_2O and autoclaved for 15 minutes at 121 ^{o}C. The LB media solution was then retrieved from the autoclave and allowed to cool down to RT and then stored at 4 ^{o}C till when needed.

2.2.3 Preparation of LB agar plates

40 g of LB agar was dissolved in 1 L of dH_2O and autoclaved for 15 minutes at 121 ^oC. The prepared LB agar was retrieved from the autoclave and allowed to cool to about 50^oC in a water bath and ampicillin was added at a final concentration of 75 µg/mL. The solution was thoroughly mixed by vigorous shaking and immediately poured into petri dishes at 20 mL of agar per dish and allowed to set at RT. The dishes were stored at 4^oC till when needed.

2.2.4 Streaking bacterial on LB agar plate

Using a sterile wire loop, an LB agar plate was inoculated as follows. First, the metal loop was flamed and held in the air around a Bunsen burner to cool down, then the loop was used to gently touch the bacterial growing in the stab culture. The loop with the bacteria was then used to make the first streak by drawing a set of three lines (#1 streak) over an area of the plate. The loop was then flamed again and held in the air to cool down and from the first set of streaks/lines, another set of three lines (#2 streak) were drawn across another area of the plate, the flaming of the loop was repeated and loop help in the air and another set of streak (#3 streak) by dragging #2 streak over another area of the plate. Loop was flamed again and held in the air to cool down and from #3 streak, a single zigzag line representing the 4th streak was drawn across the centre of the plate. The streaking pattern of the plate is diagrammatically represented in figure 2.1 below.

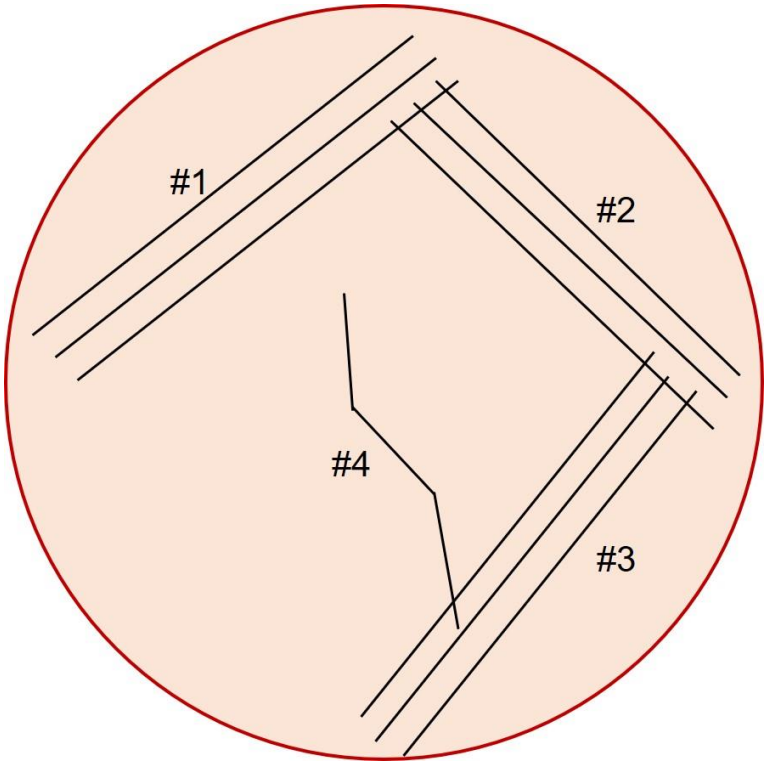

Figure 2.1. Schematic representation of the bacterial streaking pattern. Four sets of successive streaks were made in order to dilute the bacterial culture and allow for the selection of a single colony post incubation. The first streak to third streaks consists of three lines, while the last streak consists of one single zigzag line drawn to the centre of the plate.

2.2.5 Plasmid DNA (FlincG3 and REX-GECO1) extraction (Miniprep)

FlincG3 and REX-GECO1 plasmid DNAs were extracted using Qiagen plasmid miniprep kit, following the procedure provided by the supplier. In brief, using a sterile pipette tip, colonies were picked from freshly streaked LB agar plates. The pipette tips containing the colonies were dropped in 30 mL universal containers containing 5 mL LB medium supplemented with 75 µg/mL of ampicillin and incubated for 12 hrs at 37^{o}C with shaking (225 rpm). 1.5 mL

of the culture was then transferred onto a 1.5 mL Eppendorf tube and spun at 13,000 rpm for 3 minutes at RT. Pelleted bacterial was then resuspended in 250 µL buffer P1, followed by the addition of 250 µL of buffer P2 and thoroughly mixed by 4-6 times inversion and incubated for 5 minutes. 350 µL buffer N3 was added and the resultant mixture was thoroughly mixed by inversion (4-6 times) and centrifuged for 10 minutes at 13,000 rpm. The supernatant was applied to a QIAprep 2.0 spin column by pipetting and was centrifuged for 60 seconds (S) at 13,000 rpm and the flow through was discarded. The QIAprep 2.0 spin column was then washed with 500 µL buffer PB and centrifuged for 60 S and the flow through was discarded. The QIAprep 2.0 spin column was then washed again with 750 µL buffer PE and centrifuged for 60 S and the flow through was discarded. The QIAprep 2.0 spin column was then transferred to the collecting tube and spun for 1 minute to remove residual wash buffer. The QIAprep 2.0 spin column was placed in a clean 1.5 mL Eppendorf tube. To elute DNA, 50 µL buffer EB was added and allowed to stand for 1 minute and then spun for 1 minute at 13,000 rpm.

2.2.6 Restriction digest of FlincG3 and agarose gel electrophoresis

The extracted FlincG3 DNA was then verified by restriction digest and agarose gel electrophoresis. The digest was performed with PVUII restriction enzyme (illustrated in Figure 2.2) and the typical digestion reaction set up was as shown in Table 2.1 below. Following the digest, the digest product was run on a 0.8 % agarose gel electrophoresis as described below.

Table 2.3. Restriction digest reaction of FlincG3 DNA

Reagent	Amount/Volume
dH_2O	10 µL
NEBuffer 2.1	2 µL
BSA	2 µL
PVUII	1 µL
FlincG3 DNA	1 µg (5 µL)
Total Reaction Volume	20 µL

Schematic representation of restriction enzyme digest of FlincG3 plasmid DNA

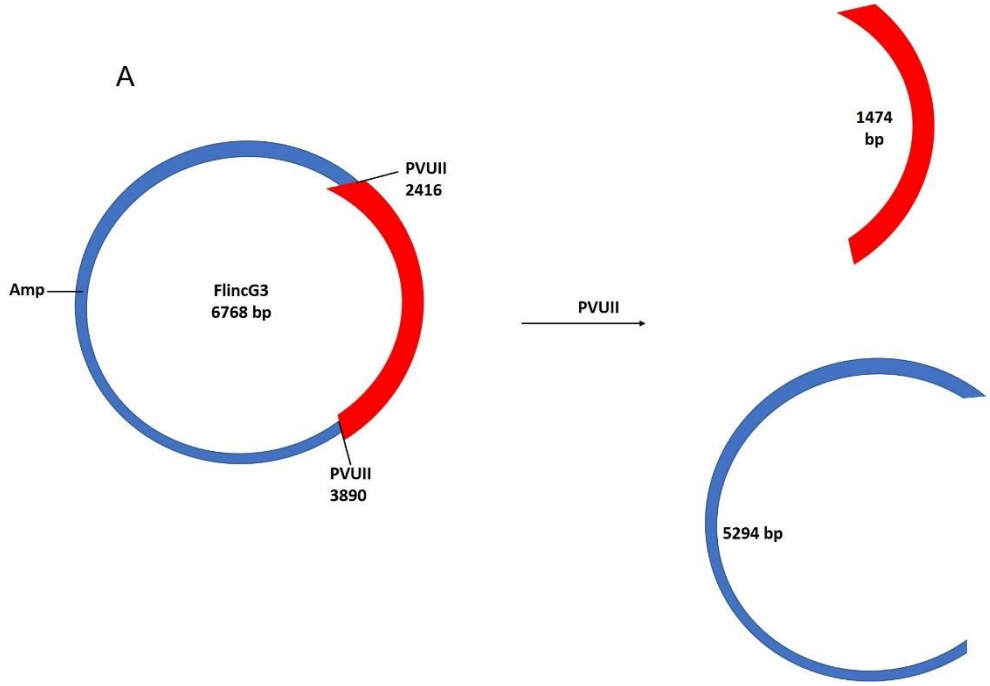

Figure 2.2 Schematic representation of restriction enzyme digest of FlincG3 plasmid DNA. (A) The restriction digest was carried out using PVUII enzyme.

2.2.7 Preparation of 0.8% agarose gel

To prepare a 0.8% agarose gel, 0.4 g of agarose was dissolved in 50 mL of 1x TBE buffer and the mixture was heated in a microwave for 90 S in order to achieve a complete dissolution of the agarose. The mixture was allowed to cool to about 50^{o}C and 0.2 µg/mL of ethidium bromide (EB) was added, and the agarose was poured into a gel tray with the comb in place. Gel was then kept at RT for 40 minutes until it has completely solidified.

2.2.8 Loading samples and running agarose gel electrophoresis

Once the gel had completely solidified, it was placed in a gel box (electrophoresis unit) and was covered with 1x TBE containing 0.2 µg/mL EB. To load the samples, the digest product was supplemented with 1x DNA loading dye and mixed by pipetting. The samples and 1 kb DNA ladder were then loaded into the wells and the gel was run at 100 V for 1.5 hrs or until the dye line has migrated approximately 75% down the gel. The gel was then retrieved from the gel box, with the power turned off and the electrodes disconnected from the power source. The DNA fragments were then visualized using a gel documentation system and images were captured and saved.

2.2.9 Restriction digest of REX-GECO1 and agarose gel electrophoresis

Like in the case of FlincG3, the purified REX-GECO1 DNA was also verified by restriction digest and agarose gel electrophoresis. The digest was performed with BamHI and EcoRI restriction enzyme and the reaction components are shown in Table 2.2 below. Following the digest, the digest product was run on a 0.8 % agarose gel electrophoresis.

Table 2.4. Restriction digest reaction of REX-GECO1 plasmid DNA

Reagent	Amount/Volume
dH_2O	10.3 µL
NEBuffer 2.1	3.5 µL
BSA	3.5 µL
BamHI	1 µL
EcoRI	1 µL
REX-GECO1	500 ng (15.7 µL)
Total Reaction Volume	35 µL

Schematic representation of restriction enzyme digest of REX-GECO1 plasmid DNA

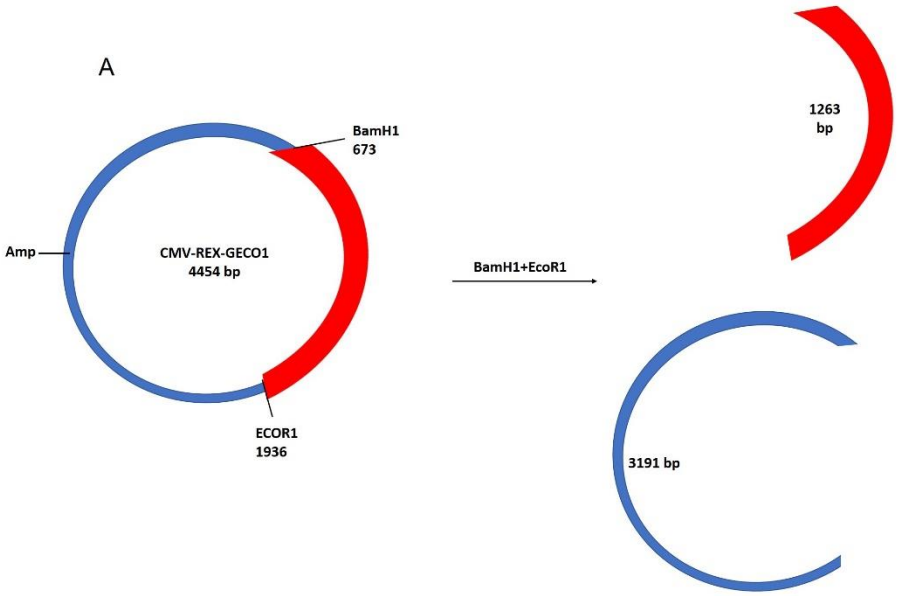

Figure 2.3. Schematic representation of restriction digest of REX-GECO1 plasmid DNA. (A) The Restriction digest was carried out using BamHI and EcoRI.

2.2.10 Plasmid DNA (FlincG3 and REX-GECO1) extraction (Maxiprep)

After verification of the plasmid DNAs (FlincG3 and REX-GECO1) that were extracted using miniprep kit, a maxiprep was then performed in order to obtain a higher amount (concentration and volume) of the DNAs. The extraction was performed using the Maxiprep protocol described in Qiagen handbook. In brief, A starter culture was inoculated as described previously. The starter culture was then diluted 1/500 in LB broth supplemented with 75 µg/mL of ampicillin and grown overnight at 37^{o}C with shaking (225 rpm). The bacteria were then harvested by centrifugation at 6000 xg for 15 minutes at 4^{o}C and

the supernatant was discarded, and the pellet was resuspended in 10 mL buffer P1. This was followed by the addition of 10 mL buffer P2 and thorough mixing. The resultant mixture was incubated at RT for 5 minutes. After the 5 minutes incubation, 10 mL of pre-chilled buffer P3 was added and the mixture was thoroughly mixed by vigorous inversion (4-6 times) and incubated on ice for 20 minutes. The lysate was then centrifuged at 16,000 xg for 45 minutes at 4^{o}C, the DNA-containing supernatant was removed and centrifuged again at 16,000 g for 30 minutes at 4^{o}C. Finally, the DNA-containing supernatant was collected. The supernatant was applied to a QIAGEN tip and allowed to enter a 50 mL falcon tube by gravity flow. The QIAGEN-tip was then washed with 10 mL buffer QC and DNA was eluted with 15 mL buffer QF. DNA was then precipitated by adding 10.5 mL RT molecular grade isopropanol and centrifuged at 16,000 xg for 30 minutes at 4^{o}C and the supernatant was decanted. The DNA pellet was then washed with 5 mL RT 70 % molecular grade ethanol and centrifuged at 16,000 xg for 10 minutes at 4^{o}C. The supernatant was decanted, and the DNA pellet was air dried for 10 minutes and re-dissolved in TE buffer. The concentration was determined using NanoDrop UV visible spectrophotometer. The average yield was 1 µg/µL in 750 µL.

2.2.11 Cell culture

HepG2 and HEK293 cells were cultured in Dulbecco's Modified Eagles Media (DMEM) supplemented with 10 % FBS and 1 % pen-strep.

Primary human hepatocytes (PHHs) were cultured in complete hepatocyte culture medium. The complete culture medium consisted of William's E

medium supplemented with 1% L-glutamine (L-glut), 1% pen-strep, 1 % insulin transferrin selenium (ITS), and 0.1 % dexamethasone (Dex).

2.2.11.1 Routine passage of HepG2 cells

All HepG2 cells used in this study were between passage numbers 12 to 25. HepG2 cells were grown in T75 cm^2 flasks containing 20 mL complete culture medium (DMEM growth medium supplemented with 10 % FBS and 1 % pen-strep) in a 5 % CO_2 humidified incubator maintained at a temperature of 37^0C. Cells were routinely passaged every 3-4 days when reaching about 80-90% confluency. Old cell culture medium was aspirated, and cells were washed with 3 mL of DPBS thrice. Cells were then incubated in 0.05 mM EDTA for 5 minutes in 5 % humidified incubator at temperature of 37^0C. EDTA was aspirated and cells were then trypsinised with 3 mL 0.05 % trypsin/EDTA solution for 5 minutes. This was followed by neutralization of trypsin/EDTA with 10 mL of complete culture medium. Cells were then spun at 800 rpm for 5 minutes. The supernatant was aspirated, and the cell pellets were re-suspended in complete culture medium. Cells were counted and cultured in T75 cm^2 flasks at $2.5X10^6$ cells/flask in a final volume of 20 mL.

2.2.11.2 Freezing of HepG2 cells

Cells were grown to approximately 80-90 % confluency and then harvested following passaging procedure described above. Cells were then counted and resuspended in a freezing medium (complete culture medium supplemented with 5% (v/v) DMSO) at $1X10^6$ cells/mL. 1 mL cell suspension was then aliquoted into a cryovial. Cryovials were then placed in a freezing container

(Mr. Frosty) containing isopropanol and stored in a freezer at -80^{0}C overnight. Next day cells were retrieved from the freezer and transferred to liquid nitrogen where they were kept for long-term storage.

2.2.11.3 Resuscitation of HepG2 cells from liquid nitrogen

20 mL of pre-warmed complete culture medium was added to a T75 cm^2 flask. A cryovial containing the HepG2 cells was removed from the liquid nitrogen container and transported in dry ice. Cells were thawed in a 37^o C water bath with gentle swirling for about 1.5 minutes or until ~95 % thawed. Cryovials were then cleaned with 70 % ethanol and transferred to the hood where cells were gently pipetted into the T75 cm^2 flask containing the pre-warmed complete culture medium. Cells were incubated in a 5 % CO_2 humidified incubator at a temperature of 37^{o}C for 6 hrs after which the medium was replaced with fresh complete culture medium after cells had adhered to the flask.

2.2.11.4 Passage of HEK293 cells

All HEK293 cells used in this study were between passage numbers 6 and 15. HEK293 cells were grown in T75 cm^2 flasks containing 15 mL complete culture medium (DMEM growth medium supplemented with 10 % FBS and 1 % pen-strep) in a 5 % CO_2 humidified incubator maintained at a temperature of 37^{0}C. Cells were routinely passaged every 2-3 days when reaching about 80-90% confluency. Old cell culture media was aspirated, and cells were washed with 3 mL of DPBS thrice. Cells were then trypsinised with 1.5 mL 0.05 % trypsin/EDTA solution for 3 minutes. This was followed by neutralization of

trypsin/EDTA with 5 mL of complete culture medium. Cells were re-suspended in complete culture medium, counted and cultured in T75 cm^2 flasks at $2.0X10^6$ cells/flask in a final volume of 15 mL.

2.2.11.5 Freezing of HEK293 cells

HEK293 Cells were grown to approximately 80-90 % confluency and then harvested following passaging procedure described above. Cells were then frozen following exactly the same protocol as that used in freezing down HepG2 cells.

2.2.11.6 Resuscitation of HEK293 cells from liquid nitrogen

HEK293 cells were resuscitated following the same protocol as that of the HepG2 cells.

2.2.11.7 Primary human hepatocytes (PHHs) culture

Human Liver specimens were obtained from Aintree University Teaching Hospital, Liverpool and the primary human hepatocytes were isolated from the specimen as described below.

2.2.11.8 Isolation and culturing of PHHs

With the aid of a peristaltic pump, human liver tissues were perfused intravenously with 1X Hepes Buffered Saline (HBS) maintained at 37^oC, at flow rates between 15 and 30 mls/min for an average tissue size of 20 g to 50 g depending on the size and capsule integrity, until the red coloured tissue turned blanched, indicating near complete removal of blood. The tissue was

then perfused with collagenase and $CaCl_2$-containing HBS at the same flow rate as above for about 20/30 minutes or until tissue began to sag or change in colour/appearance. The perfused buffer was then removed and discarded, and tissue was covered in ice cold Williams E medium and cut apart using forceps and blunt ended scissors. As much tissue as possible were dissociated to ensure maximum cell release. The cell and Williams E medium mixture was then filtered through a mesh into a sterile beaker and transferred into 50 mL non-skirted falcon tubes and centrifuge at 80xg for 5 minutes at 4^{o}C. The supernatant was then carefully discarded without dislodging the pellet, with small amount of the supernatant left to aid in resuspension. This was followed by gentle rocking of the pellet back and forth to resuspend the pellet in the remaining medium. This was followed by the addition of ice-cold Williams medium E to the Falcon tube containing the cells up to the 50 mL mark. Cells were then recentrifuged at the same conditions (g, temp and time). Again, supernatant was discarded, and cells were resuspended in the complete culture medium (Williams E medium supplemented with 1% L-glut, 1% pen-strep, 1 % ITS, and 0.1 % Dex). Where multiple tubes were used, cell suspensions in the various tubes were then added together in one falcon tube. Cells were then counted and plated on collagen-coated plates at the appropriate density required for the specific experiment. Cells were washed three hrs post seeding and incubated for subsequent treatment or experiments. Figure 2.1 below shows the diagrammatic representation of the process of PHH isolation.

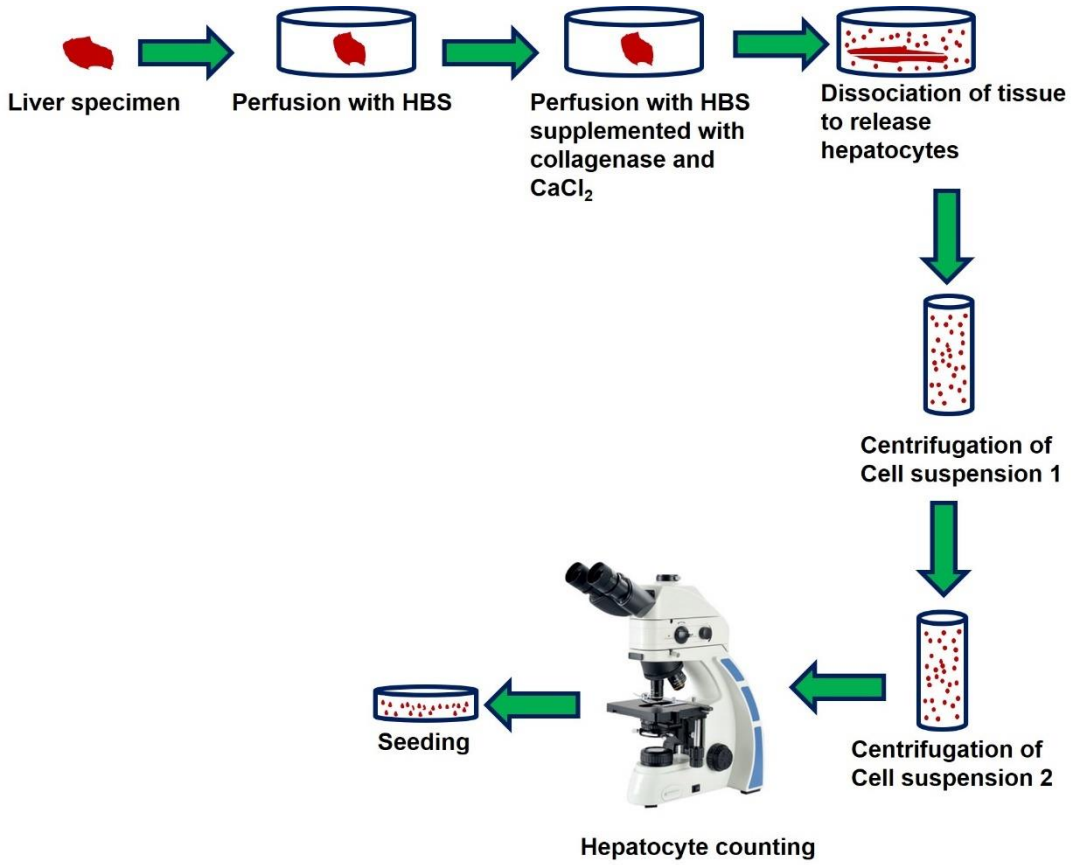

Figure 2.4. Schematic representation of complete PHH isolation process from Liver specimen.

2.2.12 Coating of cell culture plates and coverslips with collagen

As HEK293 cells and PHHs are not very adherent cells and as such easily detach during experimental procedures, in order to enhance their adherence to plates and coverslips, culture plates and coverslips were coated with rat tail collagen type I using the manufacturers protocol. In brief, the rat tail type 1 collagen was diluted to a final concentration of 50 µg/mL in 20 mM acetic acid and added to well plates with or without coverslips at 5 µg/cm^2. The collagen-containing plates were then incubated for 1 hour at RT. Following the 1-hour incubation, the collagen solution (in acetic acid) was aspirated and the wells

were washed three times with equal volumes of sterile 1X PBS in order to remove excess acetic acid. Coated plates were either used immediately or allowed to air dry, sealed with parafilm and stored at 4^{o}C for not more than 2 weeks.

2.2.13 Transient HEK293 and HEPG2 cell transfection

Transient transfection of HEK293 and HepG2 cells with FlincG3 and REX-GECO1 was carried out using the different transfection reagents listed in Table 2.2**.** Cells were seeded 24 hrs prior to transfection at 5.0X10^{4} cells per well of 48 well plate for HEK293 cells and 7.5X10^{4} cells per well of a 48 well plate for HepG2 cells. Prior to seeding, the plates in which HEK293 cells were cultured were first coated with rat tail type 1 collagen as described above. On the day of transfection, cells were transfected following the protocols provided by the manufacturers. In cases where the transfection conditions were optimized, the optimizations carried out are detailed in the specific experimental chapters (chapters 3 and 4).

2.2.14 Cloning of FlincG3 into pcDNA3.1+ vector

We sought to attempt generation of HepG2 cells stably expressing the FlincG3 protein. The FlincG3 insert was cloned into a pcDNA3.1+ vector containing a neomycin resistant gene. In brief, 5 µg of pcDNA3.1+ was digested with NheI enzyme for 4hrs at 37^{o}C. Following the 4 hrs digestion, the digest product was purified using QIAquick® Gel PCR and Cleanup Kit following the protocol provided by the manufacturer. The cleaned-up product was then digested with XhoI and the product of XhoI digest was also cleaned up using the QIAquick®

PCR and Gel Cleanup Kit and the purified product was stored at -20ºC until needed. 4 µg of FlincG3 was simultaneously digested with XbaI and XhoI for 4 hrs at 37ºC. The product of FlincG3 enzyme digest was then run on an agarose gel electrophoresis and the gel containing FlincG3 insert was excised using a sterile disposable scalpel. A small amount of the purified product of pcDNA3.1+ enzyme digest was also run on an agarose gel electrophoresis in order to confirm digestion (Figure 2.5). The FlincG3 insert was then extracted from the agarose gel using QIAquick® Gel PCR and Clean-up Kit. The FlincG3 insert was then ligated to the pcDNA3.1+ vector at the ratio of 1:3 (vector to insert) using T4 DNA ligase. The restriction enzyme digest and the ligation reactions were set up as shown in Tables 2.3 to 2.6 below. Next, the ligation product was transformed into Thermo Scientific competent DH5α cells using the protocol provided by the manufacturer. In brief, DH5alpha cells were thawed on ice. 5 µL of the ligation product was applied to 50 µL of competent DH5alpha cells and incubated on ice for 30 minutes. The mixture was then heat shocked in a 42ºC water bath for 45 S and incubated on ice for 2 minutes. This was followed by the addition of 250 µL of SOC medium and the resultant mixture was incubated at 37ºC for 1.5 hrs in a shaking incubator at 250 rpm. Following the 1.5 hr incubation, cells were then spread on a pre-warmed LB Agar plate and incubated overnight at 37ºC. The following morning, several colonies were picked and 5 mL LB broth containing 75 µg/mL of ampicillin was inoculated and incubated for 12 hrs hrs at 37ºC with shaking (225 rpm). After the 12 hrs incubation, the cloned plasmid DNAs were miniprepped using Qiagen plasmid miniprep kit with the protocol described previously. Restriction digest and agarose gel electrophoresis of the cloned DNA was performed

using XmaI restriction enzyme in order to confirm the size of the clone DNA. The reaction set up was as shown in Table 2.7. The cloned DNA (FlincG3 in pcDNA3.1+ vector) was subsequently sequenced for confirmation.

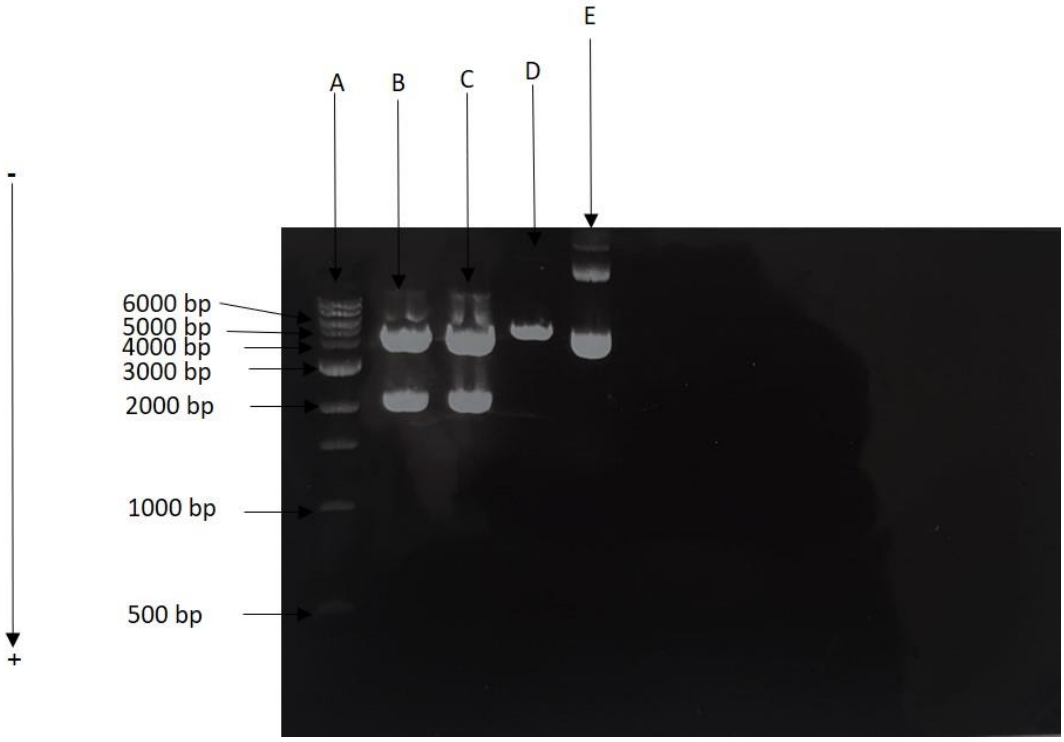

Figure 2.5. Agarose gel electrophoresis of FlincG3 digested with XbaI and XhoI and pcDNA3.1+ digested with NheI and XhoI. (Lane A) DNA size marker which is the commercial 1 Kb DNA ladder. **(**Lanes B and C) FlincG3 DNA digested with XbaI and XhoI. (Lane D) pcDNA3.1+ digested with NheI and XhoI. (Lane E) undigested pcDNA3.1+. The direction of DNA migration is indicated by the direction of the arrowed line.

Table 2.5. Restriction enzyme digest of pcDNA3.1+ with NheI

Reagent	Amount/Volume
dH_2O	6.9 µL
CutSmart Buffer	2 µL
BSA	2 µL
NheI	2 µL
pcDNA3.1+	5 µg (7.1 µL)
Total Reaction Volume	20 µL

Table 2.6. Second restriction digest of pcDNA3.1+ (purified from the reaction above) with XhoI

Reagent	Amount/Volume
dH_2O	2 µL
CutSmart Buffer	6 µL
BSA	6 µL
XhoI	2 µL
pcDNA3.1+	44 µL
Total Reaction Volume	60 µL

Table 2.7. Restriction enzyme digest of FlincG3 DNA with XbaI and XhoI

Reagent	Amount/Volume
dH_2O	6.88 µL
CutSmart Buffer	2 µL
BSA	2 µL
XbaI	2 µL
XhoI	2 µL
FlincG3 DNA	4 µg (5.12 µL)
Total Reaction Volume	20 µL

Table 2.8. Ligation of Purified FlincG3 Insert with pcDNA3.1+ Vector

The ligation was set up at the ratio of 1:3 (vector to insert) as shown in the table below.

Reagent	Amount/Volume
dH_2O	5.32 µL
Vector (pcDNA3.1+)	100 ng (1.53 µL)
Insert (FlincG3)	119.65 ng (5.65 µL)
Ligase buffer	1.5 µL
T4 DNA Ligase	1 µL
Total Reaction Volume	15 µL

pcDNA3.1+ and pTriEx4-H6-FGAm (FlincG3) Plasmid Maps

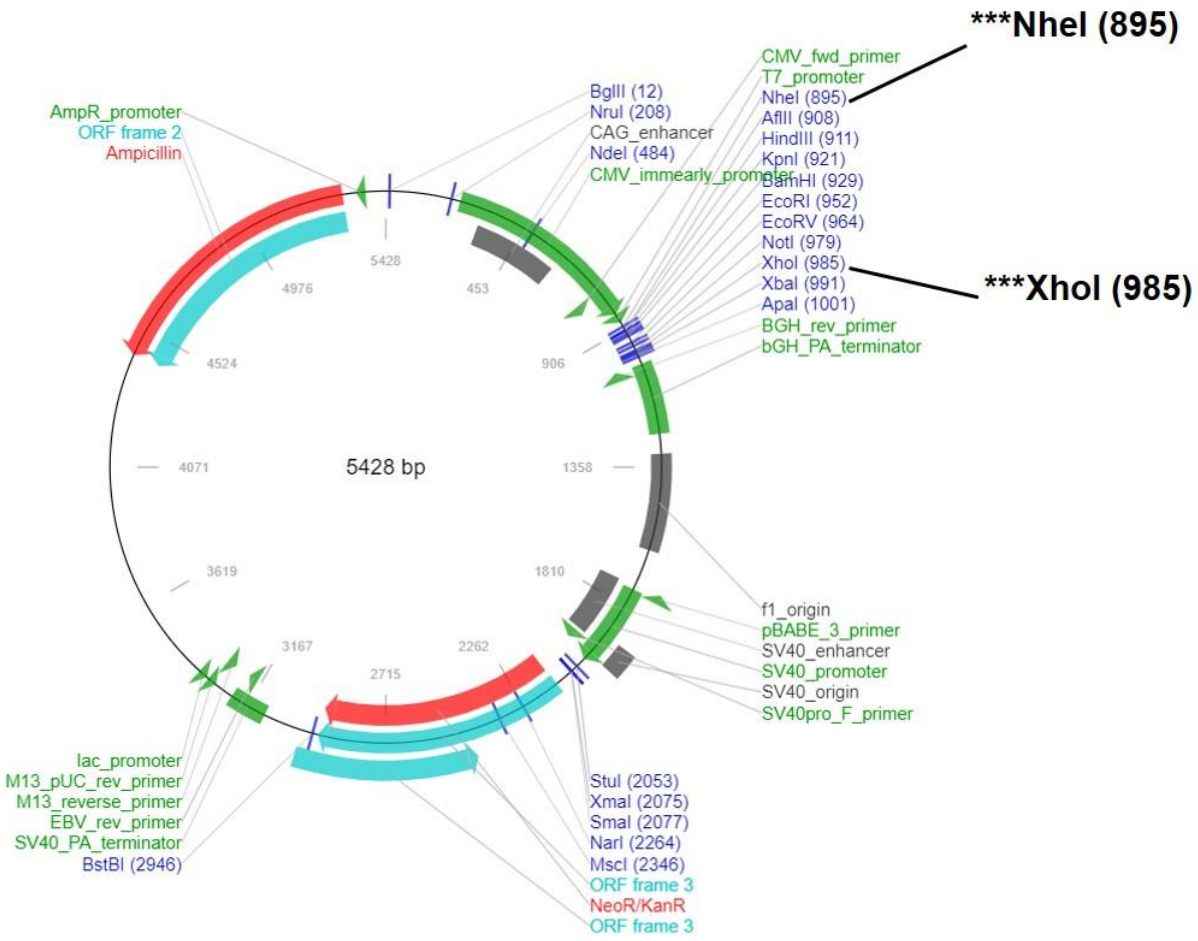

Figure 2.6. Circular plasmid map of pcDNA3.1+, highlighting the restriction site for NheI and XhoI which were used for cloning the FlincG3 insert into pcDNA3.1+ vector. Diagram was copied from Addgene website.

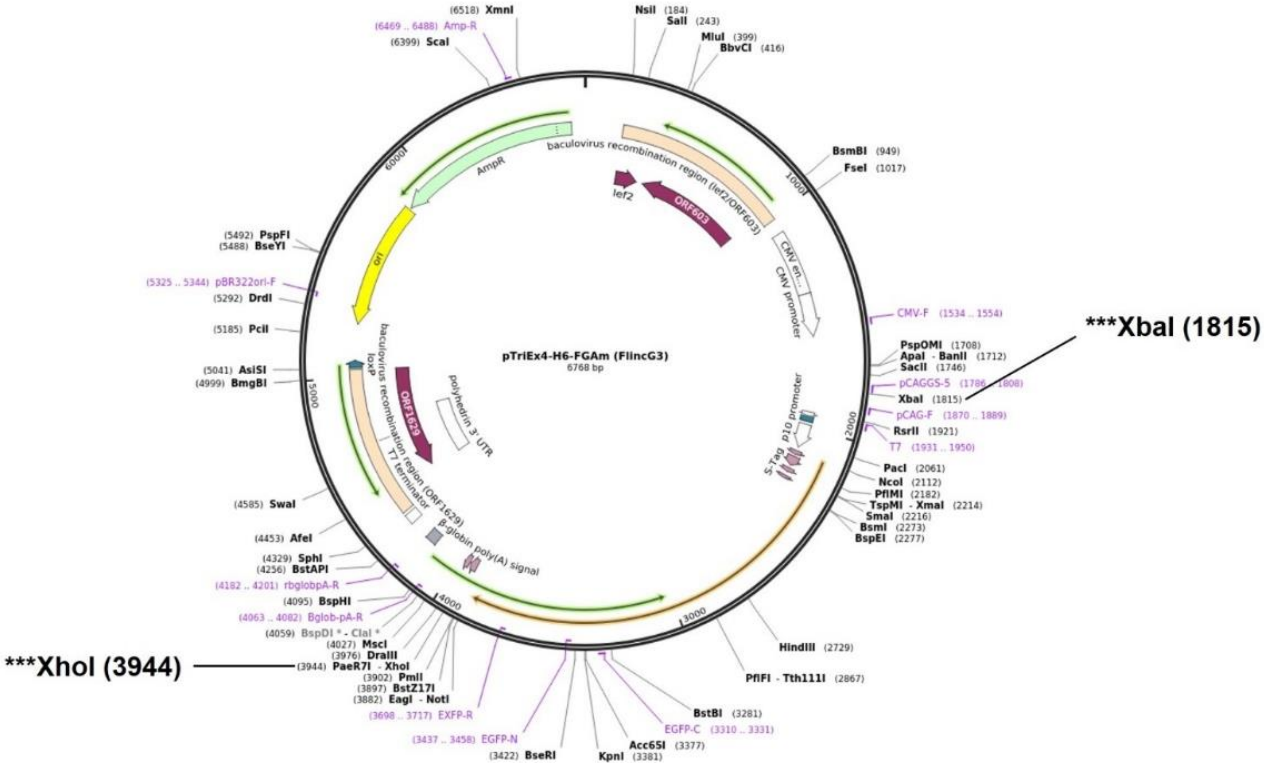

Figure 2.7. Circular plasmid map of FlincG3, highlighting the restriction site for XbaI and XhoI which were used for cloning the FlincG3 insert into pcDNA3.1+ vector. Diagram was copied from Addgene website.

Diagrammatic representation of the process of cloning FlincG3 insert into pcDNA3.1+ vector

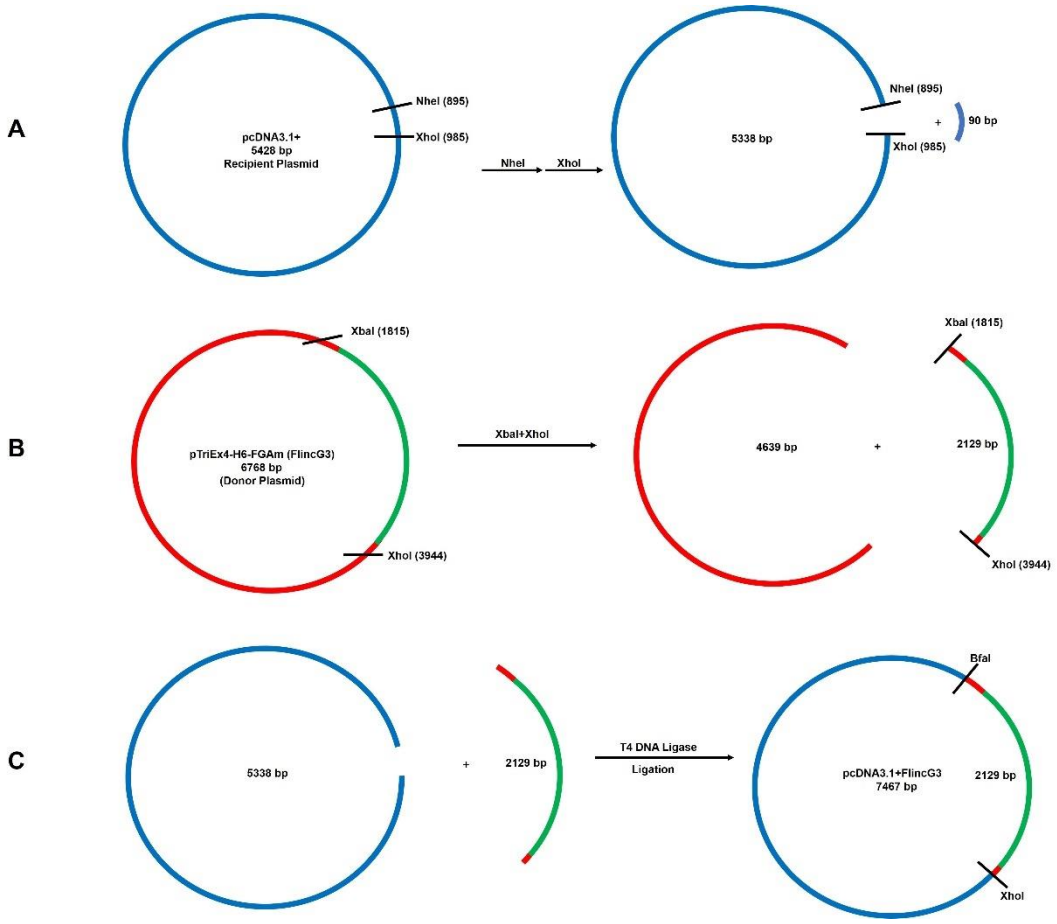

Figure 2.8. Diagrammatic representation of pcDNA3.1+ and FlincG3 digestion and ligation. (A) Digestion of pcDNA3.1+ with NheI and XhoI. (B) Digestion of FlincG3 with XbaI and XhoI. (C) Ligation of FlincG3 insert to the pcDNA3.1+ Vector using T4 DNA ligase. NheI and XhoI give rise to compatible cohesive ends that upon ligation generates a new restriction site cleavable by BfaI.

Diagnostic digest of cloned FlincG3 in pcDNA3.1+ backbone (pcDNA3.1+FlincG3)

Reagent	Amount/Volume
dH_2O	14.68 µL
CutSmart Buffer	2 µL
BSA	2 µL
XmaI	2 µL
pcDNA3.1+FincG3	250 ng (0.32 µL)
Total Reaction Volume	20 µL

2.2.15 Real time cGMP measurement

Cellular cGMP was measured using FlincG3. Cells (HepG2 and HEK293) were seeded and transfected as described in the section ‘’transient cell transfection’’. The FlincG3 reporter protein expression and live cell imaging were performed 72 hrs post transfection using a Zeiss LSM 800 Airyscan confocal microscope. FlincG3-transfected cells were excited at 488 nm and emission collected at 509 nm. On the day of real time cGMP measurement experiments, old cell culture medium was aspirated from the FlincG3-trasnfected cells and cells were washed with $CaCl_2$ and glucose-supplemented HBS and cells were left in 200 mL $CaCl_2$ and glucose-supplemented HBS and transferred to the confocal imaging stage and experiments were performed under 10 x dry objective at room temperature (RT). First, the experiment was allowed to run for 180 S (3 minutes) in order

to obtain a stable baseline. To induce cGMP signal, cells were stimulated by adding fresh HBS containing the agonist(s) and experiment run for a total of 600 S. The agonists used in this study to induce cGMP signal were SNP and ANP which are established cGMP elevating agents. To investigate whether Vit C has the ability to elevate cGMP, like in the case of SNP and ANP, fresh HBS containing the appropriate concentration of Vit C was added at 180 S and the experiment was run for a total of 600 S. The HBS used in the experiments was supplemented with 1 mM $CaCl_2$ and 10 mM glucose. To investigate the involvement of cell surface PDI in Vit C, ANP and SNP-induced cGMP elevation, cells were incubated in bacitracin (Bac; a widely used, PDI inhibitor) and RL90 (an anti-PDI monoclonal antibody) for 45 minutes at RT prior to addition of Vit C, ANP and SNP.

2.2.16 Real time Ca^{2+} measurement with REX-GECO1

Real time Ca^{2+} Imaging was carried out using the Ca^{2+}-sensitive dye Fluo-4 AM and the recombinant Ca^{2+} reporter REX-GECO1. When REX-GECO1 was used, the cells were transiently transfected with the REX-GECO1 DNA as described in the section ‘’transient cell transfection’’ above. Visualization of REX-GECO1 reporter protein expression was carried out using a Zeiss LSM 800 Airyscan confocal microscope. REX-GECO1-transfected cells were excited at 488 nm and emission collected at 609 nm.

For the real time Ca^{2+} measurement experiments, REX-GECO1-transfected cells were washed with $CaCl_2$ and glucose-supplemented HBS and cells were left in 200 mL $CaCl_2$ and glucose-supplemented HBS and transferred to the confocal imaging stage and experiments were performed under 10 x dry

objective at room temperature (RT). First, the experiment was allowed to run for 180 S (3 minutes) in order to obtain a stable baseline. To induce intracellular Ca^{2+} signal, REX-GECO1-transfected cells were stimulated with ionomycin or ATP, or Tg. To investigate the ability of cGMP elevating agents (Vit C, SNP and ANP) to reduce $[Ca^{2+}]_i$, cells were treated with Tg in combination with or without Vit C or ANP or SNP. The possible involvement of csPDI in the Vit C, ANP and SNP-mediated reduction of $[Ca^{2+}]_i$ was investigated using Bac and RL90. The cells were pre-incubated in RL90 and Bac for 45 minutes at RT prior to Tg ± Vit/ANP/SNP addition.

2.2.17 Loading of HEK293 and HepG2 Cells with Fluo-4 AM and measurement of Ca^{2+} with Fluo-4 AM

HEK293 cells were seeded 24 hrs prior to Ca^{2+} imaging experiments at $5.0X10^4$ cells per well of a collagen-coated 48 well plate for HEK293 cells and $7.5X10^4$ cells per well of a 48 well plate for HepG2 cells. On the day of experiment, cells were washed 3 times with 1x HBS supplemented with 1 mM $CaCl_2$ and 10 mM glucose, then loaded with 4 µM fluo-4 AM (dissolved in DMSO containing 10 % pluronic F127 and diluted in Fluo-4 AM loading buffer) and incubated in a 5 % CO_2 humidified incubator maintained at a temperature of 37^{o}C for 45 minutes. The Fluo-4 AM loading buffer consisted of 1x HBS supplemented with 1 mM $CaCl_2$, 10 mM glucose, 0.01 % BSA and 200 µM sulfinpyrazone (SPzn). Cells were then retrieved from the incubator and the loading buffer was aspirated. Cells were then washed twice with HBS supplemented with $CaCl_2$, glucose, BSA and SPzn to remove excess dye. Cells were left in 200 µL of HBS supplemented with $CaCl_2$, glucose, BSA and SPzn and incubated at 37^{o}C for 20 minutes for de-esterification. Cells were

imaged using a Zeiss LSM 800 Airyscan confocal microscope. For the real time Ca^{2+} experiments, cells were treated with different agonists and antagonists as detailed above (in the section '' Real time Ca^{2+} Imaging with REX-GECO1'').

2.2.18 Confocal immunofluorescence microscopy

Cellular presence and colocalization of PDI and NPRA in HepG2 cells, PHHs and HEK293 cells was investigated by immunofluorescence. HEK393 cells, HepG2 cells and PHHs were respectively seeded at $2.0X10^5$ cells/well, $3.0X10^5$ cells/well and $1.0X10^6$ cells/well of a 12 well plate and grown overnight in a 5 % CO_2 humidified incubator maintained at a temperature of 37^0C. Both HEK293 cells and PHHs were grown on collagen-coated 13 mm coverslips, while HepG2 cells were grown on uncoated coverslips. On the day of the experiment, cells were washed three times with 1x PBS and fixed with 4 % PFA at RT for 10 minutes, followed by incubation in 50 mM ammonium chloride (NH_4Cl) chloride to quench fixation. Cells were then either permeabilized or Non-permeabilized with 0.1% triton X and blocked with 10 % chick serum for 30 minutes before incubation in primary antibodies. PDI was labelled with mouse anti-PDI monoclonal antibody (RL90; 1/100) and visualized with chicken anti-mouse antibody (1/500), while NPRA was labelled with rabbit anti-NPRA polyclonal antibody (1/100) and visualized with chicken anti-rabbit antibody (1/500). All primary antibody incubation was performed at 4^oC overnight, while secondary antibody incubation was performed at RT for 1.5 hrs in the dark. Cell nuclei was stained with 5 µg/mL DAPI for 10 minutes at RT and then DAPI was washed off. Cells were then mounted on prolong

gold on microscope slides and visualized using a Zeiss LSM 800 Airyscan confocal microscope.

The involvement of golgi-dependent route in the externalization of PDI in hepatocytes (HepG2 and PHHs) was investigated using brefeldin A (BFA). Cells were seeded and grown at the same density and conditions as described for normal immunofluorescence above. On the day of the experiment, cells were washed and treated with 5 µg/mL BFA for 4.5 hrs in a 5 % CO_2 humidified incubator maintained at a temperature of 37^{o}C. Controlled cells were only treated with 0.1% DMSO vector. Cells were then washed, and normal immunofluorescence was performed using the protocol highlighted above.

2.2.19 CellTitre Glo luminescent cell viability assay

HepG2 cells and freshly isolated PHHs were seeded at 4.0x10^{4} cells/well and 1.0x10^{5} cells/well of a flat bottom 96 well plate (X2) and incubated overnight in a 5 % CO_2 humidified incubator maintained at a temperature of 37^{o}C. The following morning, cells were treated with appropriate concentration of drugs and incubated in 37^{o}C 5% CO_2 incubator for 24 and 48 hrs. On the day of the assay, CellTiter-Glo® Buffer and CellTiter-Glo® were thawed and equilibrated to room temperature. The CellTiter-Glo® Buffer was then transferred to the CellTiter-Glo® substrate bottle and the mixture was thoroughly mixed by gentle vortexing. Treated cells were then retrieved from the incubator and washed gently with PBS and 100 µL of fresh complete culture medium was added, followed by the addition of 20 µL CellTiter-Glo® reagent and shaken on a shaker at 700 RPM for 1 minute to lyse cells and then incubated for 5 minutes

in the dark. Plates were read using Varioskan microplate reader and data was expressed as percentage of control.

2.2.20 Image, data and statistical analyses

All immunofluorescence and live cell imaging were conducted with a Zeiss LSM 800 Airyscan confocal microscope. Image J was subsequently used for quantification of fluorescence and Excel software was used to generate all figures. Calculation of area under curves and statistical analyses were carried out using OriginLab software. Data are expressed as mean±standard error of mean (SEM). N numbers of all the experiments are given in the figure legends. Statistical significance was determined with a Student's t-test (paired and un-paired) or by using ANOVA with Tukey's test for post hoc analysis, and for all data, significance level was set at $p \leq 0.05$. Where necessary, differing significance level are indicated by varying number of asterisks as follows: $*p \leq 0.05$, $**p \leq 0.01$, $***p < 0.001$.

Chapter 3

Investigating the ability of vitamin C to elevate cGMP in human hepatocyte cell line and HEK293 cells

3.1 Introduction

cGMP is known to modulate intracellular Ca^{2+} signal in hepatocytes and indeed other cell types such as cultured human hepatic stellate cells (HSCs), pancreatic acinar cells, rat megakaryocytes and smooth muscle cells (279, 280, 285, 344-347). In particular, ANP, an agent that elevates cellular cGMP by activating membrane-bound guanylyl cyclase, reduces intracellular Ca^{2+} concentration in primary rat hepatocytes by activating protein kinase G (PKG), consequently stimulating plasma membrane Ca^{2+} efflux and inhibiting Ca^{2+} influx (225, 283). Also, ANP blunts endothelin-induced elevations in intracellular Ca^{2+} concentration $[Ca^{2+}]_i$ in cultured human HSCs (345). SNP, another agent which elevates cGMP via the soluble guanylyl cyclase (sGC) pathway has been shown to lower $[Ca^{2+}]_i$ in isolated pillar cells of the guinea pig cochlea (348).

There is evidence of vitamin C (Vit C) modulating cGMP in certain cell types, including primary rat hepatocytes (preliminary data from our group). Chen and his team also showed that Vit C elevates cellular cGMP level in pheochromocytoma 12 (PC12) cells (329). Also, in human umbilical vein endothelial cells (HUVECs), Vit C was shown to modulate cGMP (330). Though these studies clearly show that Vit C elevates cellular cGMP level in certain cell types, however, whether this can be achieved in human hepatocytes has never been investigated. In addition, the exact mechanism remains unclear, but there are some indications of the involvement of cell surface protein disulphide isomerase (csPDI).

Protein disulphide isomerase (PDI) was traditionally thought to be an ER-resident protein, however, there is evidence to suggest that the protein is expressed on the surface of certain cell types where it colocalizes with and modulates the action of membrane associated particulate guanylyl cyclase. Pan and colleagues (333) reported that csPDI colocalizes with membrane associated guanylyl cyclase-linked receptors (GC-A and GC-B) in human umbilical vein endothelial cells (HUVECs) and human mesangial cells (HMCs) and modulates the cGMP generation action of their corresponding guanylyl cyclase (GCs) in response to natriuretic peptides (NPs). (333). Also, in pig kidney epithelial cells (LLC-PK1) which lack detectable PDI, it was reported that the addition of purified PDI to LLC-PK1 cells significantly enhanced the cGMP elevation action of NPs (333), consistent with PDI modulation of the cGMP generation action of membrane associated particulate guanylyl cyclase (pGC).

Interestingly, in PC12 cells, Chen and colleagues proposed that Vit C mediates its cGMP-elevating action via the ANP/pGC pathway and not via the Nitric oxide/soluble guanylyl cyclase (NO/sGC) pathway (329). Preliminary data from our group also suggest that Vit C elevation of cGMP in primary rat hepatocytes is mediated via the pGC pathway, in line with the submission of Chen and colleagues. Taking together with the observation that csPDI modulates NP elevation of cGMP (333), we therefore hypothesized that csPDI would likely also play a role in Vit C-induced generation of cGMP.

3.2 Chapter aims

1) Since it is well established that ANP and SNP elevates cGMP in various cell types, we first aimed to confirm, using these agents, that the liver cell line (HepG2 cells) used in this study is able to generate cGMP upon stimuli.
2) To determine whether Vit C elevates cGMP in human hepatocytes using HepG2 as a hepatocyte cell line model
3) To investigate possible modulatory action of csPDI on Vit C-induced generation of cGMP in HepG2 cells.
4) To investigate possible involvement of csPDI in SNP and ANP-mediated generation of cGMP in order to confirm which pathway Vit C is mediating its action.
5) To use non-hepatocyte cell line to examine if Vit C-induced elevation of cGMP is more generalised. This was carried out using HEK293 which is a well established cell line.

The development of recombinant reporter system based on GFP and other fluorescent proteins has enabled the measurement of second messenger molecules such as Ca^{2+}, cAMP and cGMP in real time. To achieve our objectives for this part of the study, we utilized a type of genetically encoded cGMP indicator based on recombinant fluorescent protein; FlincG3 (fluorescent indicator of cGMP 3) to measure real time changes in cGMP in HepG2 and HEK293 cells upon stimulation.

3.3 Method and preliminary results

3.3.1 Restriction enzyme digest of FlincG3 DNA with PVUII revealed the right expected band sizes

To measure cellular cGMP in real time, we utilized FlincG3. First, we extracted the FlincG3 plasmid DNA using Qiagen DNA extraction kit and a diagnostic restriction digest was subsequently performed using PVUII as detailed in general methodology section. The agarose gel electrophoresis result revealed the two correct band sizes (1474 bp and 5294 bp) as expected with the PVUII restriction digest (Figure 3.1), indicating successful expansion of the plasmid.

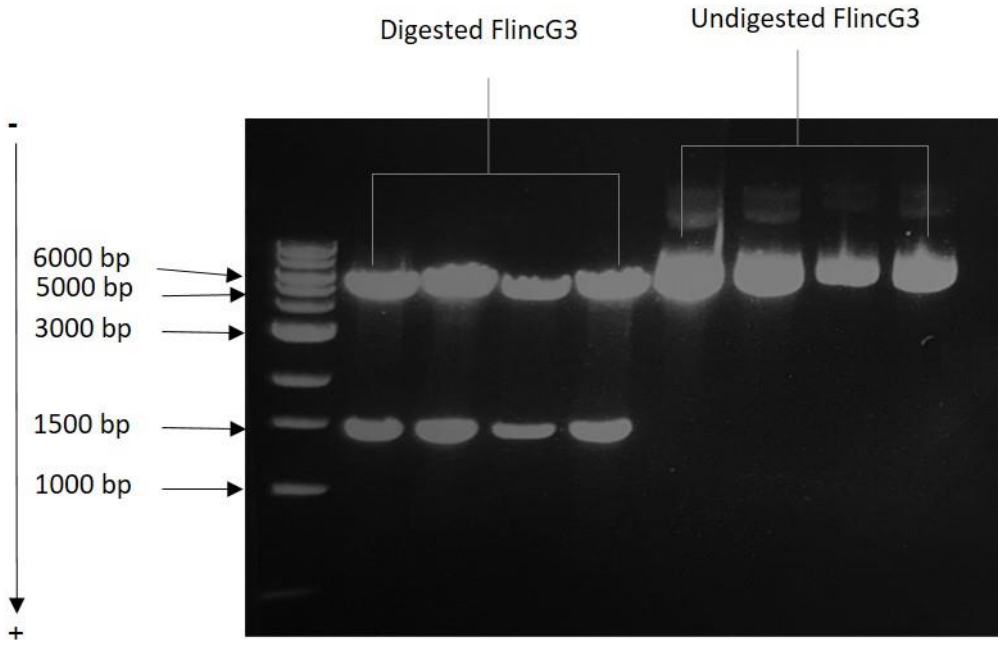

Figure 3.1. Agarose gel verification of FlincG3. Product of FlincG3 DNA digested with PVUII was run on a 0.8 % agarose gel. The DNA size marker is the commercial 1 Kb DNA ladder. Digested and undigested FlincG3 respectively represents the FlincG3 digested with PVUII and the undigested DNA. The direction of DNA migration is indicated by the direction of the arrowed line.

3.3.2 Cell Transfection with FlincG3

FlincG3 was first tested in HEK293 cells in order to validate the expression of the probe. HEK293 Cells were transiently transfected with the FlincG3 DNA using different transfection reagents (Turbofect, Lipofectamine 2000 and Lipofectamine 3000) and the GFP reporter expression was visualized using a Zeiss LSM 800 Airyscan confocal microscope at 24 hrs, 48 hrs and 72 hrs post transfection and images captured. The results revealed that the optimal maturation time for the FlincG3 protein was 72 hrs (Figure 4.2). Also, for the different transfection reagents used, the protein expression was about the same at 24 hrs and 72 hrs post transfection. However, cells transfected with Lipofectamine 3000 showed a better FlincG3 protein expression at 48 hrs post transfection (Figure 3.2).

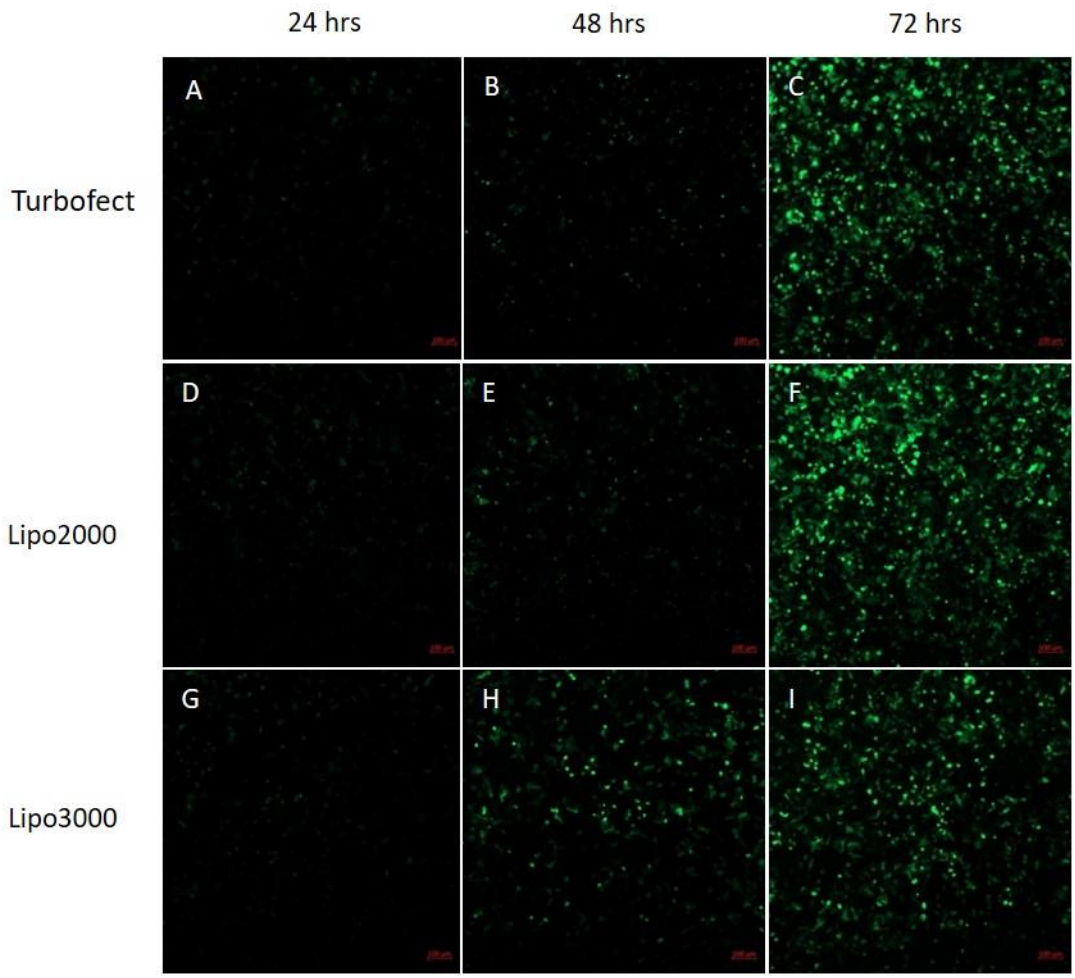

Figure 3.2. HEK293 cells expressing FlincG3 protein. (ABC) FlincG3 expression in HEK293 cells transfected with Turbofect reagent (DNA amount = 0.5 µg, DNA to reagent ratio = 1:2) at 24 hrs, 48 hrs and 72 hrs post transfection, respectively. (DEF) FlincG3 expression in HEK293 cells transfected with Lipofectamine 2000 reagent (DNA amount = 0.4 µg, DNA to reagent ratio = 1:2.5) at 24 hrs, 48 hrs and 72 hrs post transfection, respectively. (GHI) FlincG3 expression in HEK293 cells transfected with Lipofectamine 3000 reagent (DNA amount = 0.3125 µg, DNA to reagent ratio = 1:2.4) at 24 hrs, 48 hrs and 72 hrs post transfection, respectively. Cells were excited at 488 nm and emission collected at 509. Data are representative of 3 experiments. Scale bar = 100 µm.

3.3.3 Validation of the functionality of the FlincG3 probe

We then sought to validate the functionality of the FlincG3 probe. As before, HEK293 which is a well-established cell line was used to validate the functionality of the probe. HEK293 cells were transiently transfected with the FlincG3 DNA using Turbofect transfection reagent and at 72 hrs post transfection, real time cGMP signal was measured upon atrial natriuretic peptide (ANP) stimuli. 200 nM ANP rapidly elevated the fluorescence signal at 488 nm by 30 % above basal level as measured by the FlincG3 probe, indicative of cGMP elevation (Figure 3.3).

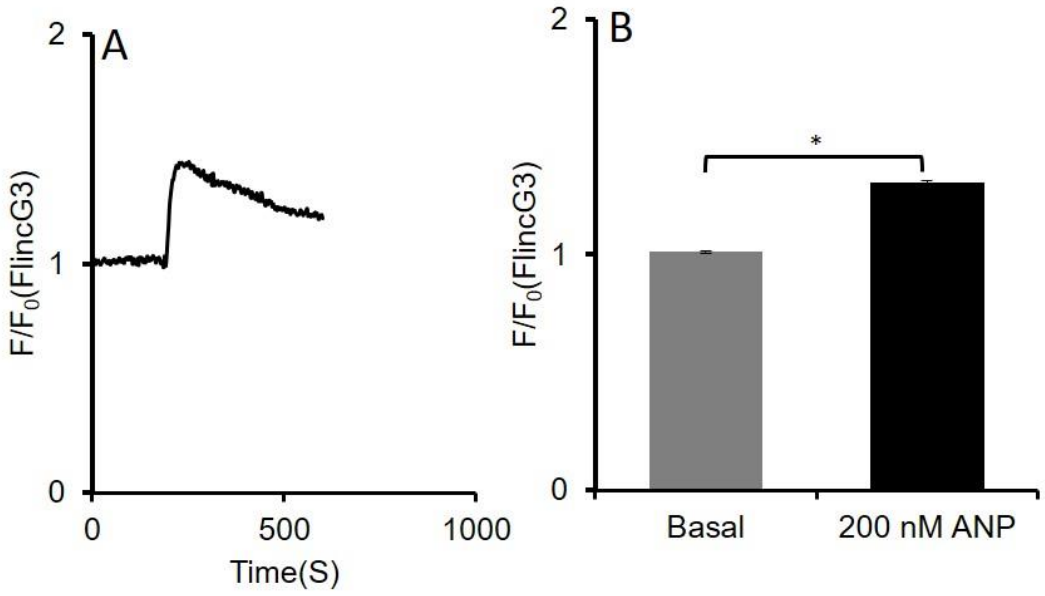

Figure 3.3. 200 nM ANP rapidly elevates cGMP in HEK293 cells. (A) Time course of average fluorescence change of HEK293 cells transfected with FlincG3. (B) Mean±SEM of FlincG3 fluorescence at basal level (just before ANP addition) and peak level (after ANP addition). (n=25 cells from 3 experiments). Experiment was performed at RT in HBS supplemented with 10 mM glucose and 1 mM $CaCl_2$. Cells were excited at 488 nm and emission was collected at 509 nm.

3.3.4 Cloning of the FlincG3 construct into a pcDNA3.1+ vector

As the original vector backbone (pTriEx4) did not have a mammalian antibiotic resistance gene, we sought to clone the FlincG3 construct into a vector containing a mammalian resistance gene in order to attempt to generate single HepG2 cell clones. We utilized pcDNA3.1+ which contains the neomycin resistance gene (NeoR). To do this, the FlincG3 construct was excised from the original pTriEx4 vector backbone into a pcDNA3.1+ as detailed in the general methodology section. A restriction enzyme digest was subsequently performed on the cloned DNA using XmaI and the digest product was run on an agarose gel to confirm band size of the cloned FlincG3 in pcDNA3.1+ vector (pcDNA3.1+FlincG3). The agarose gel electrophoresis revealed that the FlincG3 insert was successfully cloned into the pcDNA3.1+ vector as revealed by the observed band sizes (2820 bp and 4647 bp) which corresponds to the expected band sizes for the Xmal enzyme used (Figure 3.4). The cloned DNA was subsequently sent for sequencing and the result revealed the right expected sequence.

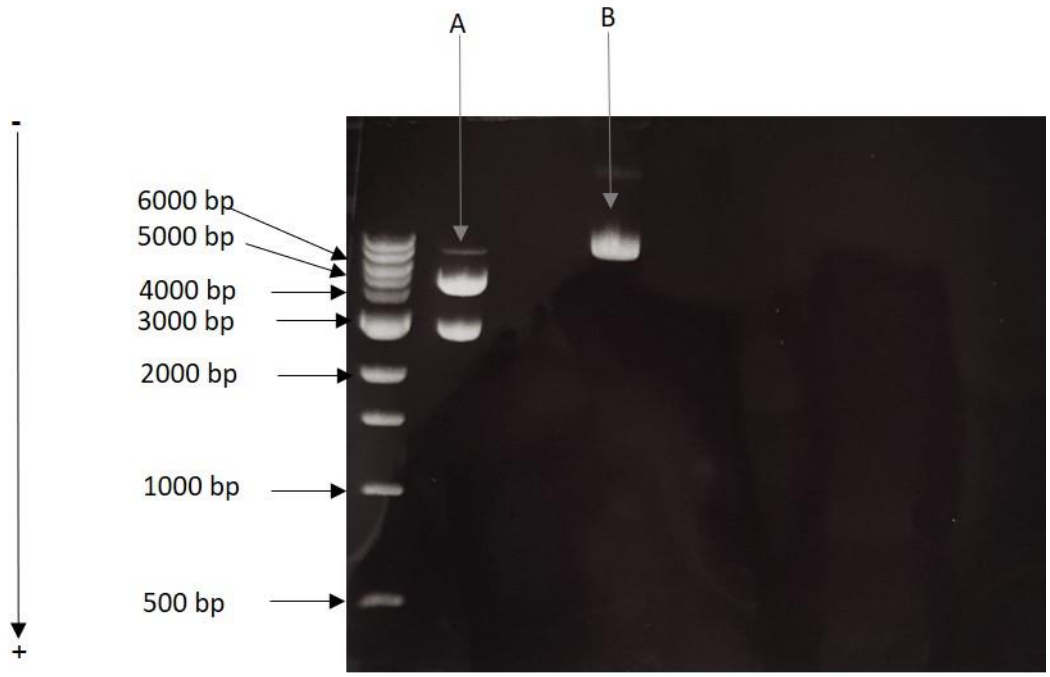

Figure 3.4. Agarose gel electrophoresis of the FlincG3 cloned into pcDNA3.1+ vector. The DNA size marker is the commercial 1 Kb DNA ladder. A and B represents the digested and undigested pcDNA3.1+FlincG3 cloned DNA, respectively. The direction of DNA migration is indicated by the direction of the arrowed line.

3.3.5 Verifying the expression of the cloned DNA (pcDNA3.1+FlincG3)

We then went on to verify the expression of the cloned pcDNA3.1+FlincG3 DNA in HEK293 cells. We transfected the original FlincG3 DNA and the cloned pcDNA3.1+FlincG3 DNA into HEK293 cells in order to compare the transfection efficiency of the cloned DNA to that of the original DNA. The result revealed a much lower transfection efficiency with the cloned pcDNA3.1+FlincG3 DNA (Figure 3.5B) compared to the original FlincG3 (Figure 3.5A), possibly due to the difference in the size of the DNAs; 6768 bp for the original DNA as compared to 7467 bp for the cloned DNA.

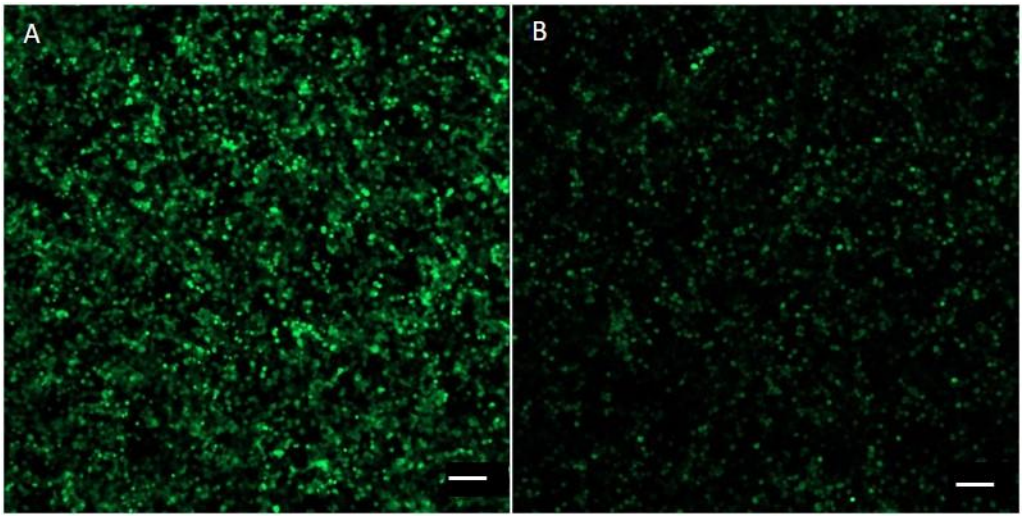

Figure 3.5. HEK293 cells expressing the original FlincG3 protein and the cloned (pcDNA3.1+FlincG3) protein. (A) HEK293 cells transfected with the original FlincG3 DNA. (B) HEK293 cells transfected with the cloned (pcDNA3.1+FlincG3) DNA. Cells were transfected with Turbofect reagent (DNA amount = 0.5 µg, DNA to reagent ratio = 1:2) and images were captured 72 hrs post transfection. Cells were excited at 488 nm and emission was collected at 509 nm. Scale bar = 100 µm. Data are representative of 3 experiments.

3.3.6 Optimization of FlincG3 transfection in HepG2

Having validated the expression and functionality of the FlincG3 protein in HEK293 cells, we then sought to measure real time cGMP signal in HepG2 cells using the probe. First, we optimized the transient transfection of the FlincG3 DNA in HepG2 cells using different transfection reagents (Happyfect, Turbofect, Jetprime and Lipofectamine 3000). For all transfection reagent used, cells were incubated overnight in the medium containing the transfection reagent and DNA. The next day, the medium was aspirated and replaced with fresh medium. The reporter protein expression was observed 72 hrs post transfection and images were captured using a Zeiss LSM 800 Airyscan confocal microscope. The images collected shows that Lipofectamine 3000 gave the optimal transfection (Figure 3.6). It was observed that Turbofect was toxic to the HepG2 cells when the cells were incubated in the medium containing the Turbofect reagent overnight (brightfield image not shown).

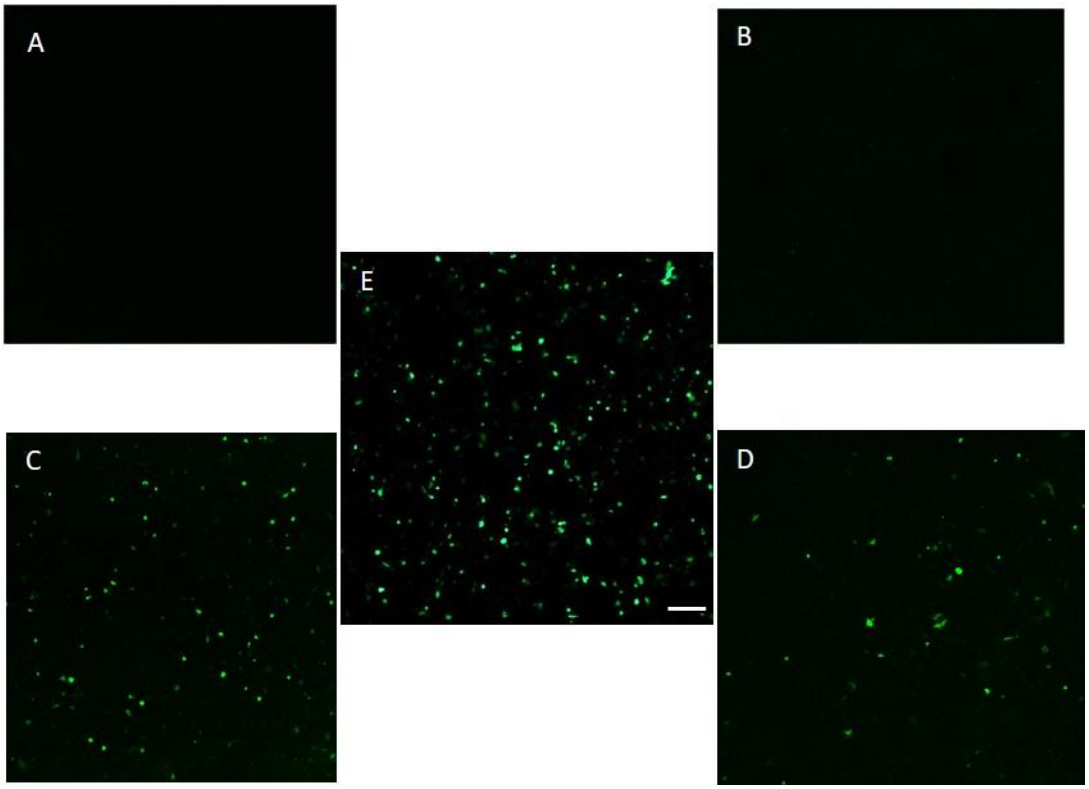

Figure 3.6. HepG2 cells expressing FlincG3 protein 72 hrs post-transfection. The original FlincG3 DNA (in pTriEx4 backbone) was transfected into HepG2 cells using different transfection reagents. (A) Control (no DNA, no reagent). (B) HepG2 cells transfected with Happyfect reagent (DNA amount = 0.5 µg, DNA to reagent ratio = 1:2.5). (C) HepG2 cells transfected with Turbofect reagent (DNA amount = 0.5 µg, DNA to reagent ratio = 1:2). (D) HepG2 cells transfected with Jetprime reagent (DNA amount = 0.4 µg, DNA to reagent ratio = 1:2). (E) HepG2 cells transfected with Lipofectamine 3000 (DNA amount = 0.3125 µg, DNA to reagent ratio = 1:2.4). Images were captured 72 hrs post transfection. Cells were excited at 488 nm and emission collected at 509 nm. Scale bar= 100 µm. Data are representative of 3 experiments.

We then sought to investigate whether withdrawing the Turbofect-containing medium at an earlier time post transfection would confer any advantage over overnight incubation in terms of cell viability and possibly enhancing the transfection efficiency. The result revealed that replacing the Turbofect-containing medium with fresh medium at 4 hrs post transfection prevented the Turbofect-induced cytotoxicity observed with overnight incubation (brightfield image not shown) and enhanced the FlincG3 reporter protein expression (Figure 3.7).

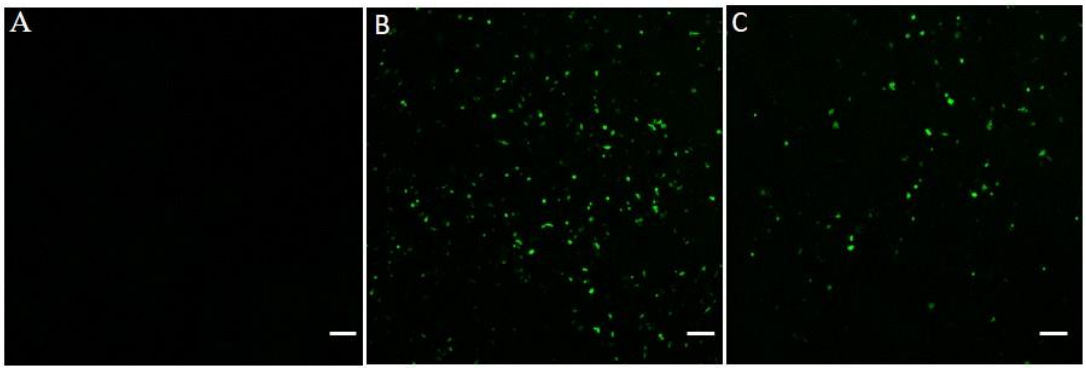

Figure 3.7. Shortening the incubation time of HepG2 cells in Turbofect-containing medium slightly improved the transfection. (A) Negative control (no DNA, no Turbofect reagent) (B) HepG2 cells transfected with FlincG3 DNA and Turbofect-containing medium withdrawn and fresh medium added at 4 hrs post transfection. (C) FlincG3-transfected HepG2 cells and incubated overnight in Turbofect-containing medium. DNA amount = 0.5 µg, DNA to reagent ratio = 1:2. Images were captured at 72 hrs post transfection and cells were excited at 488 nm and emission was collected at 509 nm. Data are representative of 3 experiments.

3.3.7 Attempt to Transfect cloned pcDNA3.1+FlincG3 DNA into HepG2 cells was Unsuccessful

As the purpose of cloning the FlincG3 DNA into pcDNA3.1+ vector was to enable us to generate stable HepG2 cell clones expressing the FlincG3 protein, We then went on to transfect the cloned FlincG3 DNA (FlincG3 in pcDNA3.1+ vector) into HepG2 cells using the same transfection reagents that were earlier used to transfect the original FlincG3 DNA into the cells (Happyfect, Turbofect, Jetprime and Lipofectamine 3000). Unfortunately, the transfection was unsuccessful with almost no single cell expressing the FlincG3 protein even at 72 hrs post transfection (data not shown). Hence, we could not generate FlincG3-stably expressing HepG2 cells even though that was our initial purpose for cloning the construct into the pcDNA3.1+ vector. Hence, subsequent cGMP measurement experiments were carried out with transiently transfected cells using Lipofectamine 3000 reagent at the same DNA amount (0.3125 µg) and DNA to reagent ratio (1:2.4) used earlier.

3.4 Results

3.4.1 SNP, ANP and Vit C elevates cGMP in HepG2 cells

Here we sought to investigate whether vitamin C will elevate cGMP in human hepatocytes similar to the preliminary observation our group made in rat hepatocytes. To do this, we first sought to confirm the cGMP-generation ability of the liver cell line used (HepG2 cells) by treating FlincG3-transfected HepG2 cells with varying concentrations of established cGMP elevators; SNP (which dissociates in solution to yield NO; an activator of sGC) and ANP (an NP that activates pGC) before we then proceeded with the Vit C experiments.

We show here that stimulating FlincG3-transfected HepG2 cells with different concentrations of SNP (100 µM and 200 µM) and ANP (25 nM, 50 nM and 100 nM) rapidly elevated the FlincG3 fluorescent signal, indicative of cGMP elevation (Figure 3.8 and 3.9 respectively). Both the SNP and ANP-induced cGMP elevations were concentration-dependent. These results confirm that HepG2 cells can generate cGMP via both the SNP/sGC and ANP/pGC route.

Our data also revealed that Vit C elevates cGMP in HepG2 cells. Upon stimulation of FlincG3-transfected HepG2 cells with Vit C, a concentration-dependent, rapid increase in the FlincG3 fluorescence signal was observed, consistent with cGMP elevations (Figure 3.10).

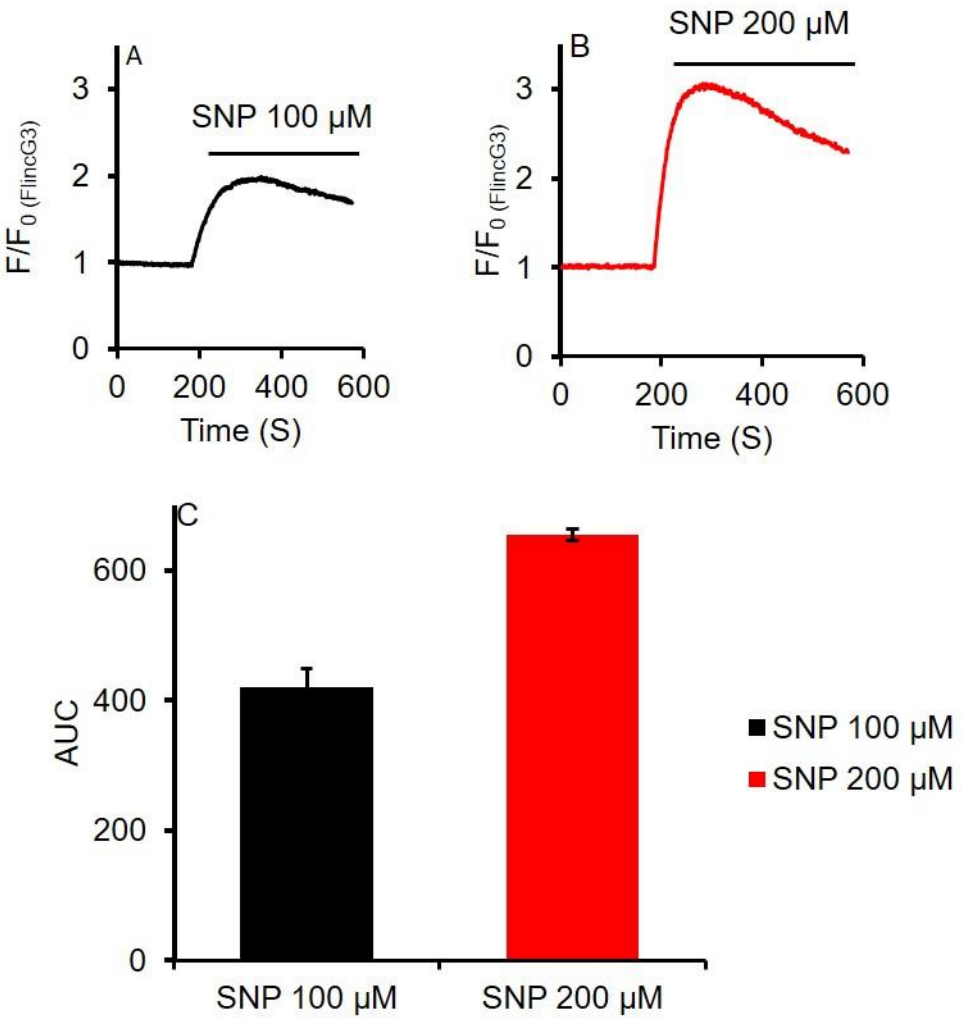

Figure 3.8. SNP elevates cGMP in HepG2 cells. (A) Mean fractional fluorescence change of FlincG3-transfected HepG2 cells induced by 100 µM SNP (n=15 cells from 3 experiments). (B) Mean fractional fluorescence change of FlincG3-transfected HepG2 cells induced by 200 µM SNP (n=15 cells from 3 experiments). (C) Area under curves A and B (AUCA and AUCB) presented as Mean±SEM (Black bar = AUCA, n= 15 cells from 3 experiments. Red bar = AUCB, n= 15 cells from 3 experiments). Experiments were performed at RT in HBS supplemented with 10 mM glucose and 1 mM $CaCl_2$.

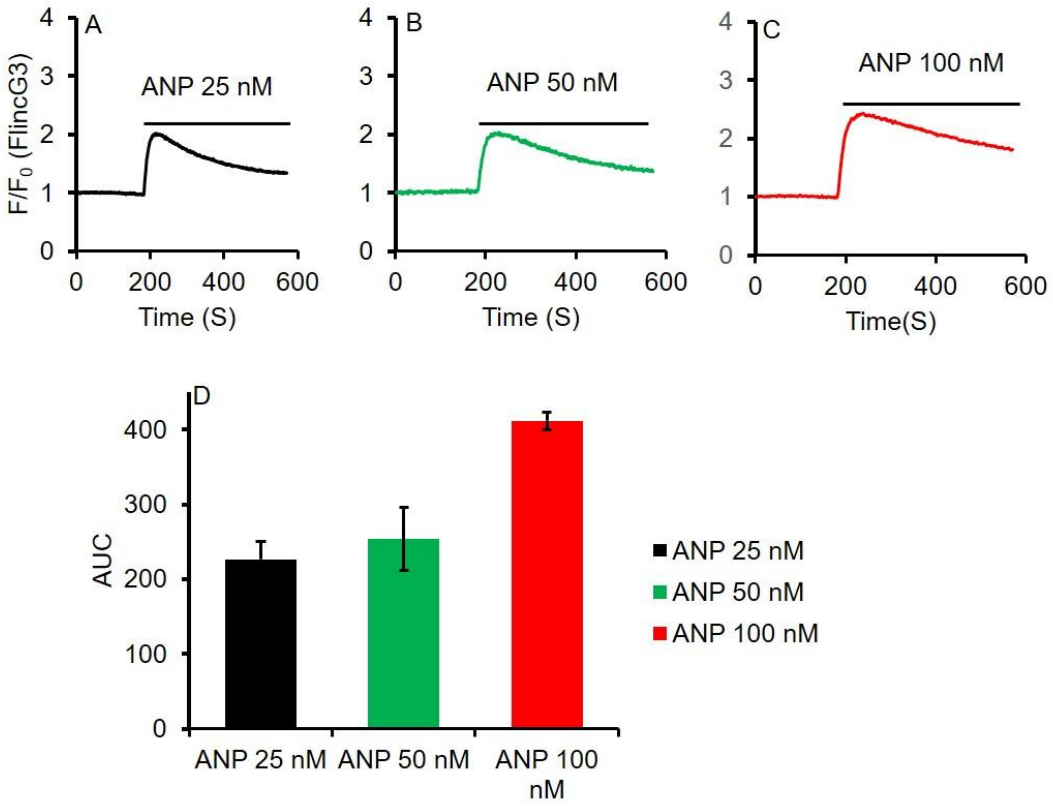

Figure 3.9. ANP elevates cGMP in HepG2 cells. (A) Mean fractional fluorescence change of FlincG3-transfected HepG2 cells induced by 25 nM ANP (n=15 cells from 3 experiments). (B) Mean fractional fluorescence change of FlincG3-transfected HepG2 cells induced by 50 nM ANP (n=12 cells from 2 experiments). Mean fractional fluorescence change of FlincG3-transfected HepG2 cells induced by 100 nM ANP (n=13 cells from 2 experiments). (D) Area under curves A, B and C (AUCA, AUCB and AUCC) presented as Mean±SEM (Black bar = AUCA, n= 15 cells from 3 experiments. Green bar = AUCB, n= 12 cells from 2 experiments, Red bar= AUCC. N= 13 cells 2 experiments). Experiments were performed at RT in HBS supplemented with 10 mM glucose and 1 mM $CaCl_2$.

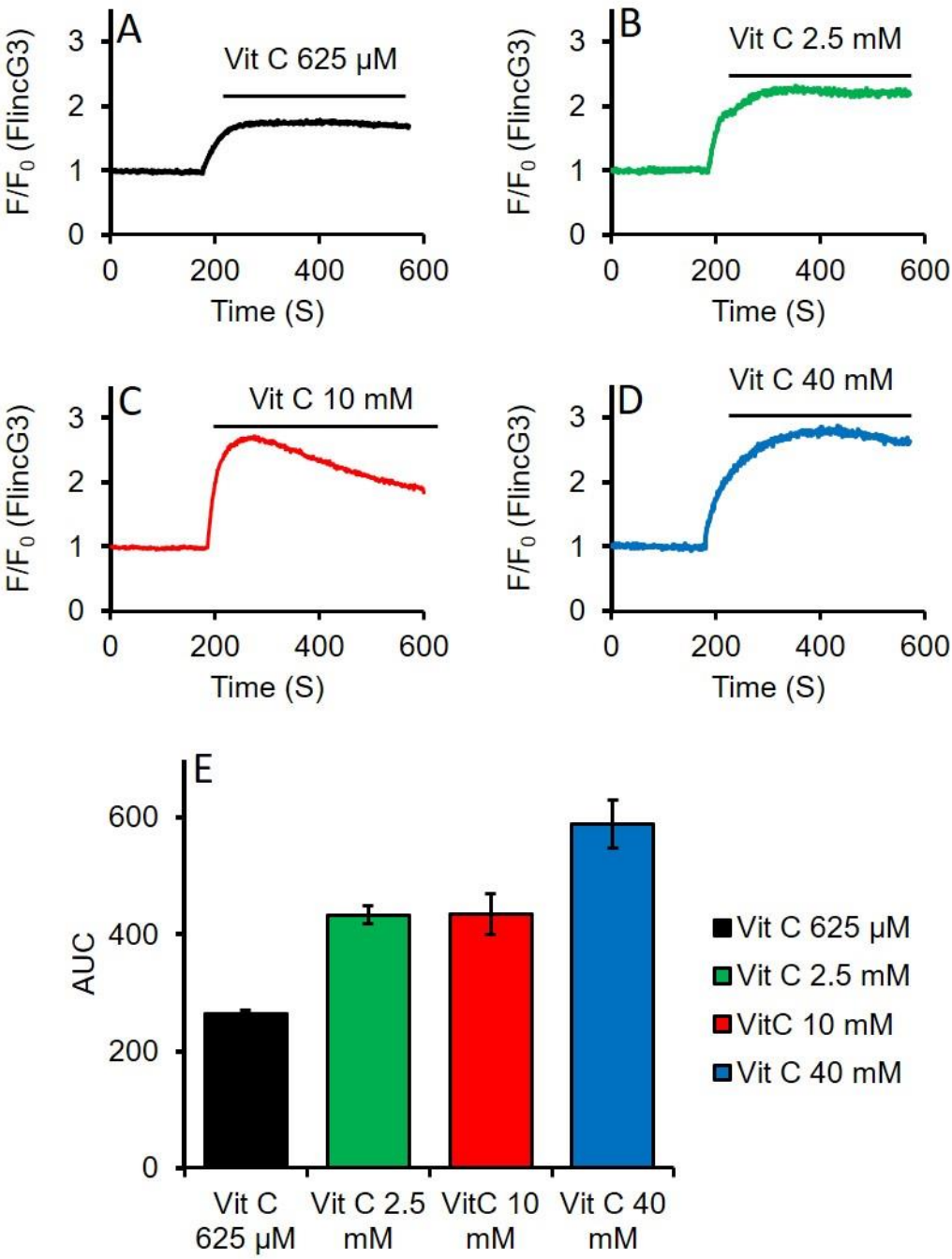

Figure 3.10. Vit C generation of cGMP in HepG2 cells is concentration dependent. (A) Mean fractional fluorescence change of FlincG3-transfected HepG2 cells induced by 625 µM Vit C (n=16 cells from 3 experiments). (B) Mean fractional fluorescence change of FlincG3-transfected HepG2 cells induced by 2.5 mM Vit C (n=10 cells from 2 experiments). (C) Mean fractional fluorescence change of FlincG3-transfected HepG2 cells induced by 10 mM

Vit C (n=14 cells from 3 experiments). (D) Mean fractional fluorescence change of FlincG3-transfected HepG2 cells induced by 40 mM Vit C (n=10 cells from 2 experiments) (E) Area under curves A (black bar) (n=16 cells from 3 experiments), B (green bar) (n=10 cells from 2 experiments), C (red bar) (n=14 cells from 3 experiments) and D (blue bar) (n=10 cells from 2 experiments). Data represent Mean±SEM. Experiments were performed at RT in HBS supplemented with 10 mM glucose and 1 mM $CaCl_2$.

3.4.2 The observed increase in FlincG3 fluorescence signal is not due to intracellular pH change induced by the weak acidic property of Vit C.

To rule out the possibility that the observed change in FlincG3 fluorescent signal could be as a result of the intracellular pH changes induced by the weak acidic property of Vit C, we utilized sodium butyrate (NaB), a weak acid that have been widely used to induce intracellular pH changes (349). Addition of 2.5 mM of NaB to FlincG3-transfected HepG2 cells produced no observable change in the FlincG3 fluorescence signal (Figure 3.11).

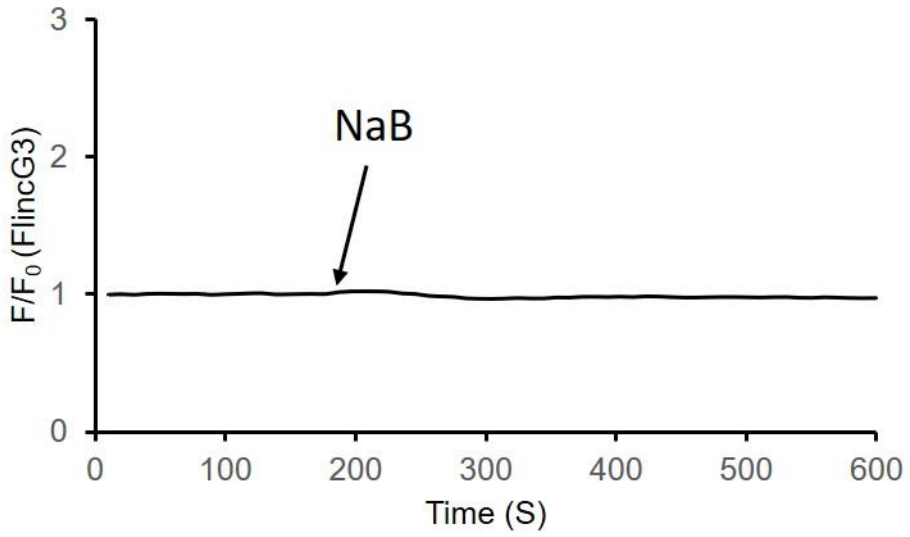

Figure 3.11. Sodium Butyrate (NaB) does not cause any change on the Fluorescence signal of FlincG3. Addition of 2.5 mM NaB to FlincG3-transfected HepG2 cells had no effect on the FlincG3 fluorescence signal. (n= 10 cells from 2 experiments). Experiments were performed at RT in HBS supplemented with 10 mM glucose and 1 mM $CaCl_2$.

3.4.3 Cell surface PDI (csPDI) modulates Vit C generation of cGMP

Previous studies carried out on pheochromocytoma 12 (PC12) cells suggested that Vit C elevation of cGMP is via the ANP/pGC route (329). In line with this, preliminary data from our group also suggested that Vit C elevation of cGMP in primary rat hepatocytes is via the same ANP/pGC route. A separate study on HUVECs and HMCs had earlier demonstrated that ANP elevation of cGMP is modulated by csPDI (333). Having established that Vit C has the ability to elevate cGMP in HepG2 cells (Figure 3.10), we then sought to investigate whether csPDI would play any role in the mechanism. To do this, we used bacitracin (Bac; a widely used inhibitor of PDI and other thiol isomerases of the PDI superfamily) and RL90 (an anti-PDI monoclonal antibody) to inhibit the function of csPDI. Pre-incubation of HepG2 cells with 20 µg/mL RL90 (Figure 3.12B) and Bac (0.5 mg/mL and 2.5 mg/mL) (Figures 3.12C and D respectively) significantly attenuated Vit C-induced cGMP elevations as compared to the control (Figure 4.12A). The effect of bacitracin was concentration-dependent.

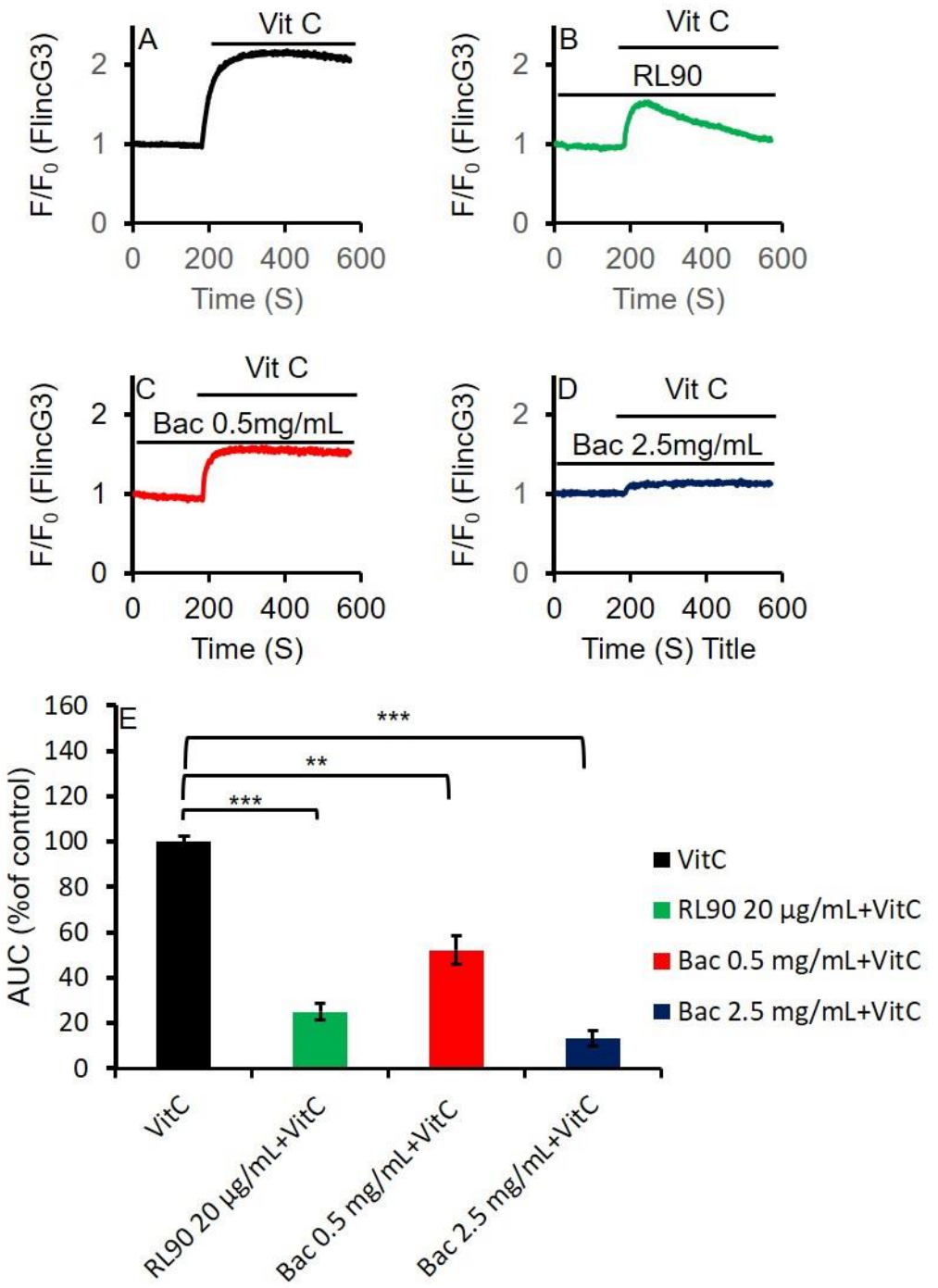

Figure 3.12. Cell surface protein disulphide isomerase inhibition attenuates Vit C-mediated generation of cGMP in HepG2 cells. (A) Vit C 1.25 mM elevates cGMP in HepG2 cells (n=20 cells from 4 experiments). (B) RL90 20 µg/mL attenuates Vit C elevation of cGMP (n=20 cells from 4 experiments). (C) Bac 0.5 mg/mL attenuates Vit C elevation of cGMP (n=15

cells from 3 experiments) (D) Bac 2.5 mg/mL attenuates Vit C elevation of cGMP (n=20 cells from 4 experiments). (E) Area under curves A, B, C and D. Data are presented as Mean±SEM. Experiments were performed at RT in HBS supplemented with 10 mM glucose and 1 mM $CaCl_2$.

3.4.4 csPDI modulates ANP, but not SNP-induced cGMP generation

As vitamin C generation of cGMP has been reported to be mediated via the particulate guanylyl cyclase pathway but not the soluble guanylyl cyclase pathway in pheochromocytoma 12 (PC 12) cells (329) and in rat hepatocytes (our unpublished data). Similarly, csPDI was shown to modulate NPs activation of particulate guanylyl cyclase and consequent cGMP generation in human umbilical vein endothelial cells (HUVECS), human aortic smooth muscle cells (HASMCs) and human glomerular mesangial cells (HMCs) (333). We sought to investigate the involvement of csPDI in the two established cGMP elevation routes; NPs activation of particulate guanylyl cyclase and NO activation of soluble guanylyl cyclase. To do this, we treated FlincG3-transfected HepG2 cells with ANP and SNP in the presence and absence PDI inhibitors (bacitracin and RL90). Our data showed that both PDI inhibitors significantly attenuated ANP stimulated cGMP generation (Figure 3.13) but had no effect on SNP-induced cGMP elevations (Figure 3.14).

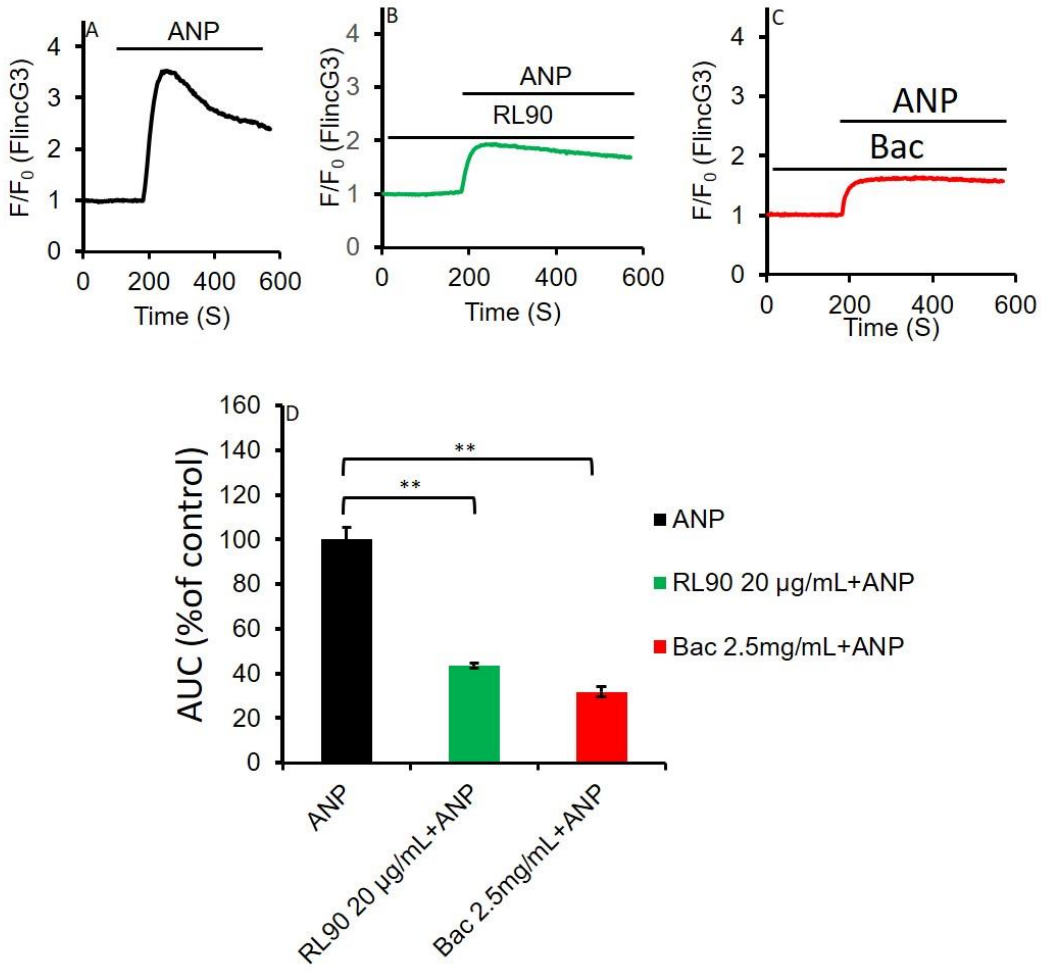

Figure 3.13. PDI inhibition attenuates ANP-mediated particulate guanylyl cyclase generation of cGMP in HepG2 cells. (A) ANP 200 nM elevates cGMP in HepG2 cells (n=20 cells from 4 experiments). (B) RL90 20 µg/mL attenuates ANP-mediated cGMP synthesis in HepG2 cells (n=20 cells from 4 experiments). (C) Bac 2.5 mg/mL attenuates ANP-mediated cGMP elevations in HepG2 cells (n=20 cells from 4 experiments). (D) Area under curves A, B and C. Data are presented as Mean±SEM. Experiments were performed at RT in HBS supplemented with 10 mM glucose and 1 mM $CaCl_2$.

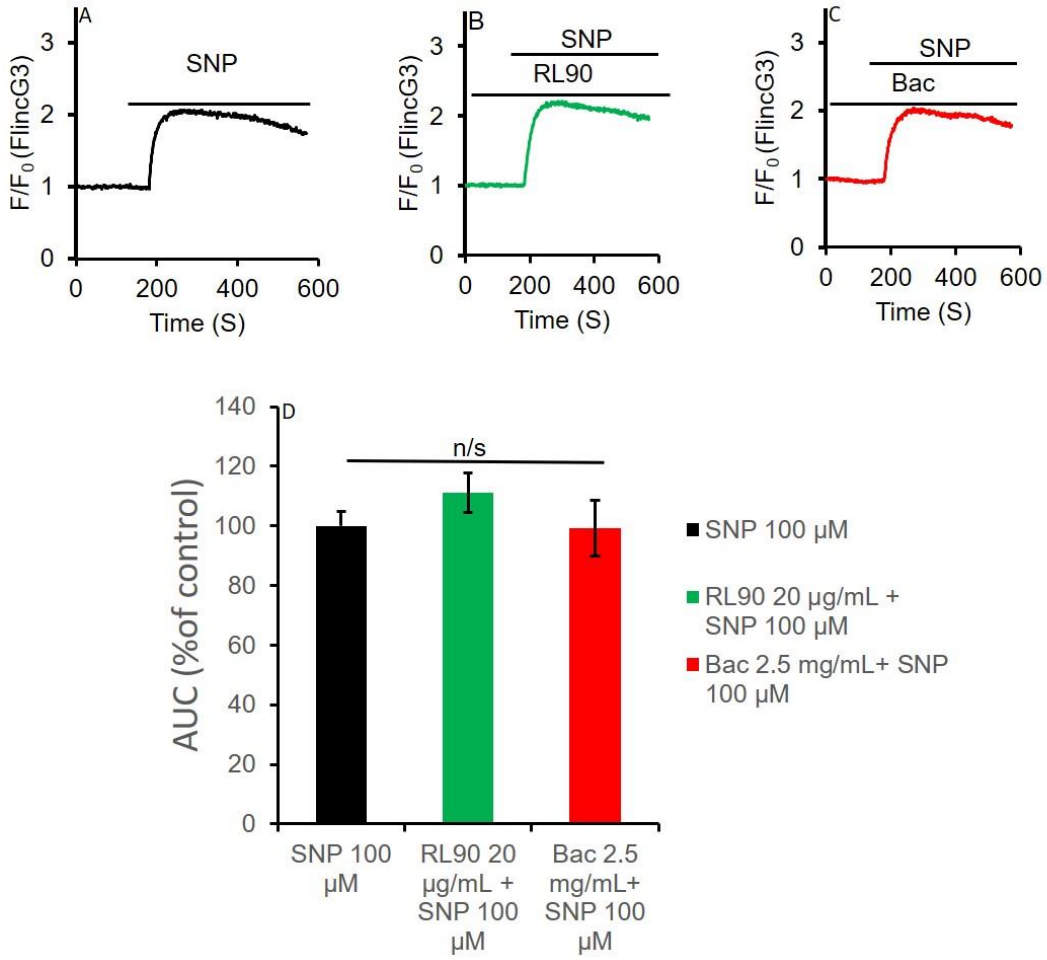

Figure 3.14. PDI inhibition has no effect on SNP-mediated soluble guanylyl cyclase generation of cGMP in HepG2 cells. (A) SNP 100 µM elevates cGMP in HepG2 cells (n=20 cells from 4 experiments). (B) RL90 20 µg/mL had no effect on SNP-induced cGMP elevation in HepG2 cells (n=20 cells from 4 experiments). (C) Bac 2.5 mg/mL had no effect on SNP-induced cGMP elevation in HepG2 cells (n=20 cells from 4 experiments). (D) Area under curves A, B and C. Data represent Mean±SEM. Experiments were performed at RT in HBS supplemented with 10 mM glucose and 1 mM $CaCl_2$.

3.4.5 Vitamin C elevates cGMP in HEK293 cells

It has been shown that Vit C activates particulate guanylyl cyclase and consequently elevates cGMP in PC12 cell (329). Preliminary data from our group also revealed that Vit C elevates cGMP in primary rat hepatocytes and in this chapter, we have shown that Vit C elevates cGMP in HepG2 cells (Figure 4.10). Our current data also suggest that csPDI modulates the Vit C-induced generation of cGMP in HepG2 cells. We then sought to investigate whether the PDI-modulation of Vit C-induced cGMP elevation is hepatocyte-specific. This was investigated using HEK293 cells. We first investigated whether Vit C elevates cGMP in HEK293 cells by treating FlincG3-transfected HEK293 cells with three different concentrations of Vit C (625 µM, 2.5 mM and 10 mM). Our result showed that stimulating HEK293 cells with Vit C elevates cGMP in the cells (Figures 3.15A-D). We then went on to investigate whether csPDI modulates the Vit C-mediated elevation of cGMP. Here, we used Bac and RL90 to inhibit the function of csPDI. Our data showed that inhibiting PDI with RL90 and Bac significantly attenuated Vit C-induced cGMP elevations (Figures 3.16A-D), in line with our observation in HepG2 cells. This data is consistent with the notion that csPDI-modulation of Vit C-induced cGMP generation is not hepatocyte-specific.

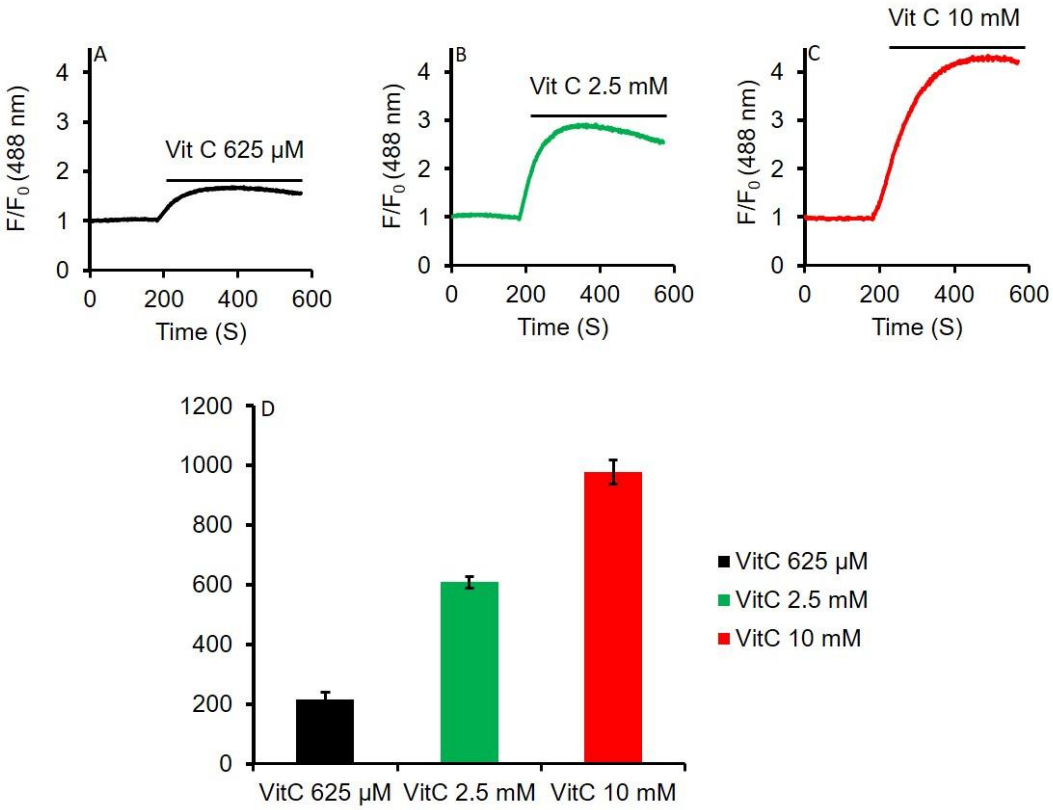

Figure 3.15. Vit C elevates cGMP in HEK293 cells in a concentration-dependent manner. (A) Mean fractional fluorescence change of FlincG3-transfected HEK293 cells induced by 625 µM Vit C (n=20 cells from 4 experiments). (B) Mean fractional fluorescence change of FlincG3-transfected HEK293 cells induced by 2.5 mM Vit C (n=15 cells from 3 experiments). (C) Mean fractional fluorescence change of FlincG3-transfected HEK293 cells induced by 10 mM Vit C (n=15 cells from 3 experiments). (D) Area under curves A (black bar), B (green bar) and C (red bar). Data represent Mean±SEM. Experiments were performed at RT in HBS supplemented with 10 mM glucose and 1 mM $CaCl_2$.

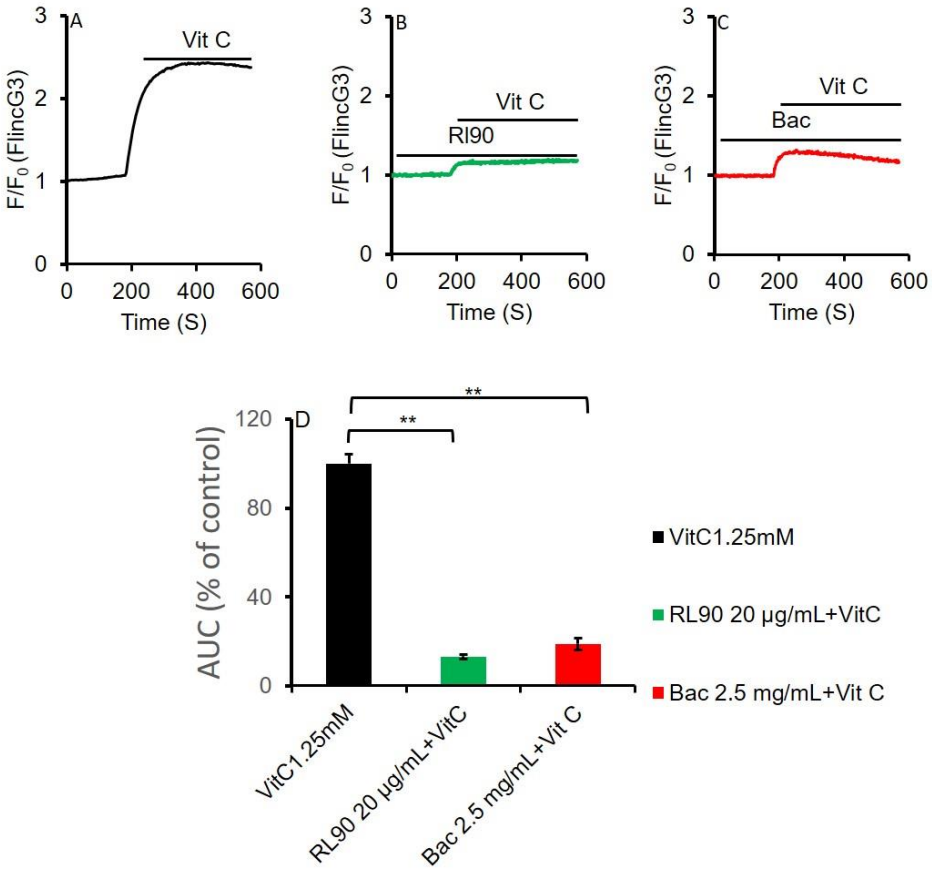

Figure 3.16. PDI inhibition attenuates Vit C-mediated cGMP generation in HEK293 cells. (A) Vit C 1.25 mM elevates cGMP in HEK293 cells (n=20 cells from 4 experiments). (B) RL90 20 µg/mL attenuates Vit C-mediated cGMP generation in HEK293 cells (n=20 cells from 4 experiments). (C) Bac 2.5 mg/mL attenuates ANP-mediated cGMP elevations in HEK293 cells (n=20 cells from 4 experiments). (D) Area under curves A, B and C. Data represent Mean±SEM. Experiments were performed at RT in HBS supplemented with 10 mM glucose and 1 mM $CaCl_2$.

3.5 Discussion

We show here for the first time that Vit C elevates cGMP in human hepatocytes using HepG2 cells as our hepatocyte model. We also show that ANP and Vit C, but not SNP-induced generation of cGMP in HepG2 cells was attenuated by RL90 (anti-PDI monoclonal antibody) and Bac (a widely used PDI inhibitor). This is consistent with csPDI-modulation of Vit C and ANP activation of particulate guanylyl cyclase (pGC), but not SNP activation of soluble guanylyl cyclase (sGC). The Vit C-induced elevation of cGMP and the inhibitory action of the PDI inhibitors (RL90 and Bac) were also observed in HEK293 cells.

To assess whether vitamin C has the potential to elevate cGMP in human hepatocytes, we used HepG2 cells as our model hepatocyte cell line. We transfected HepG2 cells with the FlincG3 DNA to measure real time changes in cGMP signal. First, we confirmed the ability of HepG2 cells to generate cGMP via both the pGC and sGC-dependent route by treating the cells with established activators of these enzymes; ANP and SNP, respectively. In line with previous studies carried out in other cell types (350, 351), treatment of FlincG3-transfected HepG2 cells with 100 µM and 200 µM SNP rapidly increased the fluorescence signal of FlincG3 at 488 nm by about 2-fold and 3-fold respectively (Figures 3.8 A and B), indicative of cGMP elevation. Similarly, Stimulating the cells with different concentrations of ANP (25 nM, 50 nM and 100 nM) rapidly elevated the cellular cGMP level (Figure 3.9). Together, these data suggest the presence of functional sGC and pGC in the HepG2 cells and the ability of the cells to synthesize cGMP via the NO/sGC and ANP/pGC routes.

To establish whether Vit C elevates cGMP in HepG2 cells, we transfected HepG2 cells with FlincG3 DNA and then measured real time changes in cGMP signal upon treatment with different concentrations of Vit C. In agreement with previous studies on PC 12 cells (329) and primary rat hepatocytes (unpublished data from our group), the data revealed that Vit C elevates cellular cGMP level in HepG2 cells in a concentration-dependent manner (Figure 3.10). In stark comparison, treating the cells with the weak acid sodium butyrate did not cause any change in the FlincG3 fluorescent signal (Figure 3.11). Together, these data militate against any assumption that the observed change in florescent signal induced by Vit C could be a result of intracellular pH changes induced by the weak acidic property of the vitamin. The data also support that the change in fluorescence signal of the probe observed upon Vit C stimuli represents an increase in cGMP signal.

Previous studies have shown that Vit C stimulates cGMP generation by the activation of the pGC pathway (329). Also, ANP and other NPs-induced cGMP generation have been shown to be modulated by csPDI (333), but whether PDI modulates Vit C and SNP-mediated generation of cGMP has yet to be defined. Using RL90 and Bac, we investigated the involvement of csPDI in Vit C, ANP and SNP-induced generation of cGMP in HepG2 cells. Inhibition of csPDI with RL90 and Bac significantly attenuated Vit C (Figure 3.12) and ANP (Figure 3.13) induced generation of cGMP, but not the SNP-induced generation (Figure 3.14). RL90 like other antibodies is a large polypeptide and the intact membrane of living cells are generally impermeable to large proteins including antibodies (342, 343). Bac is a hydrophilic, poorly cell-permeant mixture of polypeptides that has been used in previous studies to demonstrate

the modulatory effect of csPDI on NP-mediated generation of cGMP (333, 341). Our observation that RL90 and Bac inhibited the cGMP elevation action of Vit C and ANP, but not that of SNP is therefore consistent with csPDI-modulation of Vit C and ANP activation of pGC, but not csPDI modulation of SNP/NO activation of sGC. The modulatory action of csPDI on the cGMP elevation action of ANP and other NPs has been suggested to be due to the colocalization of the isomerase with natriuretic peptide receptors (NPRs) on the cell membrane (333). Pan and colleagues suggested that the colocalization of PDI with NPRs on the cell membrane permits PDI to physically interact with the NPRs and NP ligands, allowing for modulation of their effects by the isomerase (333). Taking together with the submission of Chen and colleagues that Vit C mediates its cGMP generation action in PC12 cells by activating pGC (329) and our observation that inhibition of csPDI attenuates Vit C and ANP-mediated elevation of cGMP in HepG2 cells, we propose that like ANP, Vit C elevates cGMP in HepG2 cells by activating pGC, and this effect is modulated by csPDI.

Although the ability of Vit C to modulate cGMP has been investigated in a few cell types, there is still less data to on whether this action of Vit C is cell type specific. Therefore, using HEK293 cells as our non-hepatocyte model, we explored the ability of the vitamin to modulate cGMP in another cell type in addition to the already reported cell types such as PC12 cells (329), HUVECs (330) and hepatocytes (Figure 4.10 and unpublished data from our group). Consistent with what was observed in PC12 cells (329), HUVECs (330), HepG2 cells (Figure 3.10) and primary rat hepatocytes (preliminary data from our group), Vit C elevated cGMP in HEK293 cells in a concentration-

dependent manner (Figure 3.15). Taking together, these data suggest that the Vit C-induced elevations of cellular cGMP is obtainable in a variety of cell types.

We then sought to investigate the involvement of csPDI in the Vit C elevation of cGMP in HEK293 cells. In line with our observation in HepG2 cells, inhibition of PDI with RL90 and Bac significantly attenuated the ability of Vit C to elevate cGMP in HEK293 cells (Figure 3.16). This data is suggestive that the Vit C-induced cGMP generation in HEK293 cells is also modulated by csPDI.

One major limitation of this chapter was that the transfection efficiency of the FlincG3 DNA in HepG2 cells was low and attempts to generate a FlincG3-stably expressing HepG2 cell line proved unsuccessful as the FlincG3 construct which was successfully cloned into a pcDNA3.1+ backbone could not be transfected into HepG2 cells (nearly zero protein expression even at 72 hrs post transfection). This could partly be due to the fact that the HepG2 is generally a difficult-to-transfect cell line and partly due to the larger size of the cloned pcDNA3.1+FlincG3 DNA (7464 bp) as compared to that of the original FlincG3 in pTriEx4 backbone (6768 bp). In order to improve FlincG3 expression in HepG2 cells, it may be necessary to use a different plasmid backbone or switch to viral expressing vector or use a retro transposon system such as Sleeping Beauty.

In summary, our study shows that like SNP and ANP, Vit C elevates cGMP in HepG2 cells. Inhibition of PDI with RL90 and Bac attenuated Vit C and ANP-induced cGMP elevations, but not SNP-induced elevation. This is consistent with csPDI modulating both the ANP and Vit C-induced cGMP generation, but

not SNP-induced generation. The results of this study also show that the cGMP generation action of Vit C is also achievable in HEK293 cells. Together with the findings from previous studies, it could be asserted that Vit C elevation of cGMP can be achieved in a variety of cell types.

Chapter 4

Investigating the ability of vitamin C to decrease intracellular Ca^{2+} concentration in human hepatocyte cell line and HEK293

4.1 Introduction

Elevated $[Ca^{2+}]_i$ and consequent activation of Ca^{2+} dependent enzymes is a prerequisite event in hepatocyte damage (352-355). Previous studies have implicated a sustained raised $[Ca^{2+}]_i$ in several liver pathologies such as in ischemic reperfusion liver injury (IRI) (356), drug induced liver injury (DILI) by acetaminophen (357), bile salts-induced liver damage (358) and damage by other agents such as extracellular ATP(353) and tetrachloromethane (359).

One molecule that appears to interfere with the Ca^{2+}-mediated cell damage is cGMP. Studies show that cGMP added directly as cGMP analogues or stimulated by cGMP elevators such as NO and ANP, modulates intracellular Ca^{2+} signal in various cell types such as supporting cells of the guinea pig cochlea, vascular smooth muscle cells and primary rat hepatocytes (283, 360-362). However, there seem to be conflicting submissions from different groups on the effect of cGMP on intracellular Ca^{2+} signalling even in the same cell type of the same species. For example, in rat hepatocytes, different groups have reported different observations of cGMP either attenuating, potentiating or having no effect on Ca^{2+} signals (225, 283-285, 288). So, our first aim in this chapter was to investigate the effect of cGMP on intracellular Ca^{2+} signals in the cell lines used in this study.

In chapter 3, we showed that like ANP and SNP, Vit C elevates cGMP in HepG2 cells and in HEK293 cells which was our non-hepatocyte control, in line with previous observations in PC12 cells (329) and in primary rat hepatocytes (unpublished data from our group). Interestingly, like ANP and SNP, Vit C has been reported to modulate $[Ca^{2+}]_i$ in certain cell types. For

example, in human lymphoid cells, Vit C was shown to decrease A23187-induced $[Ca^{2+}]_i$ elevations (332). Also, unpublished data from our group revealed that Vit C attenuates ATP and TLC-induced Ca^{2+} oscillations in primary rat hepatocytes. However, whether the Vit C modulation of $[Ca^{2+}]_i$ can be achieved in human hepatocytes remains unelucidated.

Another important observation we made in chapter 3 was that Vit C and ANP, but not SNP-induced cGMP generation was downregulated by the inhibition of PDI with RL90 and Bac, consistent with csPDI modulation of the ability of Vit C and ANP, but not SNP to elevate cellular cGMP. Since evidence have shown that cGMP modulates intracellular Ca^{2+} signal and our data from this study have revealed that csPDI modulates Vit C and ANP-induced cGMP elevation in HepG2 and HEK293 cells, we therefore predicted that csPDI would modulate the effect of Vit C and ANP on intracellular Ca^{2+} signal.

4.2 Aims

4.2.1 Main aims

In this chapter, we aimed to investigate whether elevating cellular cGMP with Vit C would lower $[Ca^{2+}]_i$ in hepatocytes, using HepG2 cells as our model hepatocyte cell line, which can then be a potential therapeutic intervention against drug-induced Ca^{2+}-mediated damage. As our data in chapter 3 showed that inhibition of PDI with RL90 and Bac modulates the Vit C-induced generation of cGMP, consistent with csPDI modulation of the ability of the vitamin to elevate cGMP. In this chapter, we also aimed to investigate whether csPDI would modulate Vit C lowering of $[Ca^{2+}]_i$.

4.2.2 Other aims

We showed in chapter 3 that ANP and SNP elevates cGMP in HepG2 cells, in this chapter, we aimed to investigate the effect of these agents (ANP and SNP) on $[Ca^{2+}]_i$. Also, as our data in chapter 3 showed that inhibition of PDI with Bac and RL90 attenuated the ability of ANP to elevate cGMP, but not that of SNP, consistent with csPDI modulation of ANP-induced cGMP generation, in this chapter we sought to investigate the involvement of csPDI in the ANP and SNP-attenuated elevations in $[Ca^{2+}]_i$.

In the experiments reported here, we used the fluorescent Ca^{2+} dye Fluo-4 AM and a genetically encoded Ca^{2+} indicator CMV-REX-GECO1 to measure the change in $[Ca^{2+}]_i$ in HepG2 and HEK293 cells upon stimulation.

4.3 Results

4.3.1 Measurement of $[Ca^{2+}]_i$ with Fluo-4 AM.

We first tried to measure real time changes Ca^{2+} signals in HepG2 and HEK293 cells using Fluo-4 AM. The initial experiments were first performed in HEK293 cells which we used all through this study as our non-hepatocyte control and for experimental optimizations. We first sought to confirm the fluorescence of the Fluo 4. To do this, HEK293 cells were loaded with Fluo-4 AM using the protocol detailed in the general methodology section and visualized using a Zeiss LSM 800 Airyscan confocal microscope. Figure 4.1 shows brightly fluorescent HEK293 cells loaded with Fluo-4 AM.

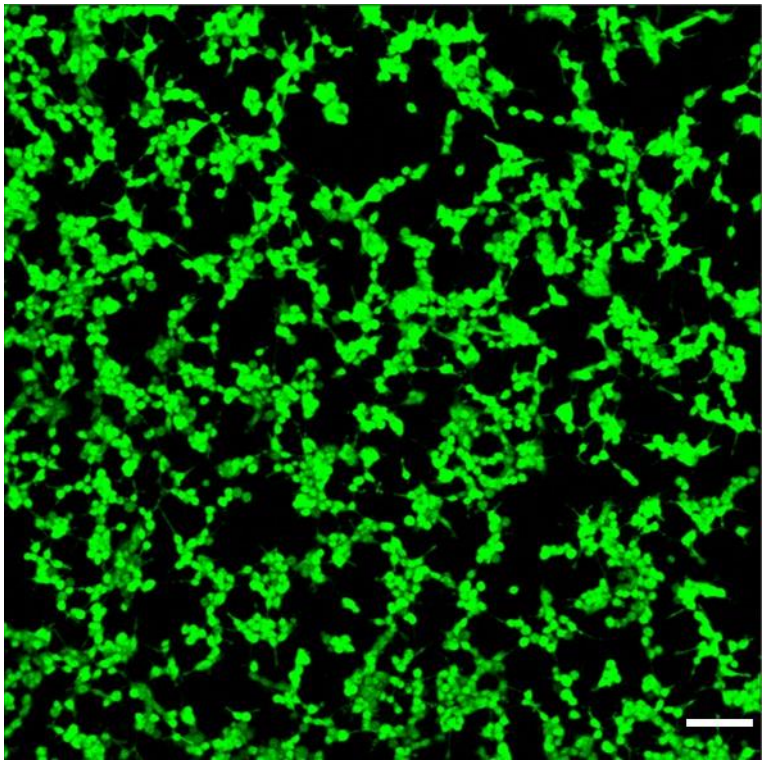

Figure 4.1: HEK293 cells loaded with Fluo-4 AM. Picture of HEK293 cells loaded with 4 μM Fluo-4 AM. Cells were excited at 488 nm and emission was collected at 509 nm. Scale bar = 100 μm. Data is a representative of at least 3 experiments.

4.3.2 Confirming the Ability of Fluo-4 AM to measure Changes in $[Ca^{2+}]_i$

Although, Fluo-4 AM is a widely used Ca^{2+} sensing dye, however, in this study, we still first sought to confirm its ability to detect and measure real time changes in $[Ca^{2+}]_i$ before using it for our experiments. To do this, HEK293 cells loaded with Fluo-4 AM were treated with thapsigargin (Tg) and change in fluorescence signal was measured. The result shows that 500 nM Tg rapidly elevated the fluorescence signal by approximately 4-fold, an indication of the change in $[Ca^{2+}]_i$ (Figure 4.2).

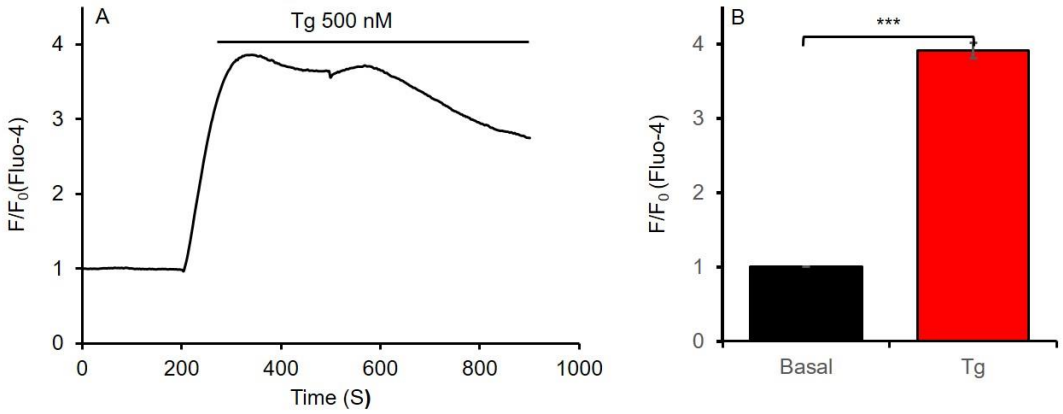

Figure 4.2. Measurement of real time changes in $[Ca^{2+}]_i$ with Fluo-4 AM. HEK293 cells loaded with Fluo-4 AM were stimulated with 500 nM Tg. (A) Time course of fractional fluorescence change of HEK293 cells treated with 500 nM Tg. (B) Mean±SEM of Fluo-4 fluorescence at basal level (just before Tg addition) and peak level (after Tg addition) (n=30 cells from 3 experiments). Experiment was performed at RT in HBS supplemented with 10 mM glucose and 1 mM $CaCl_2$.

4.3.3 Vit C attenuates Tg-induced elevations in $[Ca^{2+}]_i$ in HEK293 cells

Our data from chapter 3 revealed that Vit C elevates cellular cGMP in both HepG2 and HEK293 cells, and from previous studies, it has been reported that agents that elevate cGMP (ANP and NO) attenuates elevations in $[Ca^{2+}]_i$ signal (225, 360, 363). Also, like ANP and NO donors, Vit C have been shown to reduce agonist (A23187)-induced elevations in $[Ca^{2+}]_i$ in human T-lymphoid cell line (Molt-3 cells) (332). We therefore sought to investigate whether Vit C would attenuate agonist (Tg and ATP)-induced elevations in $[Ca^{2+}]_i$. As in previous experiments, these experiments were first performed in HEK293 cells. As described initially, cells were loaded with Fluo-4 AM and subsequently stimulated with Tg or ATP in the presence and absence of Vit C (10 mM). The data revealed that 10 mM vitamin C significantly attenuated both Tg and ATP-induced elevations in $[Ca^{2+}]_i$ (Figure 4.3 and 4.4 respectively).

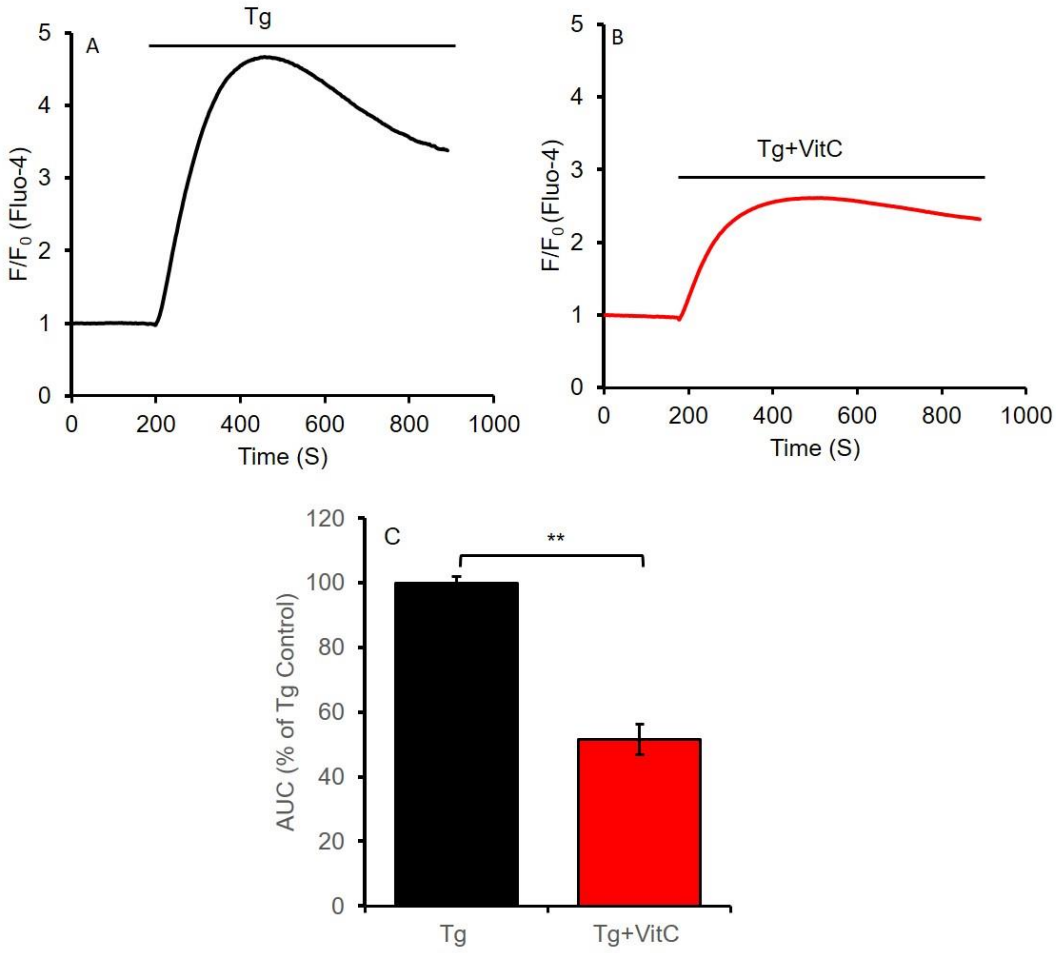

Figure 4.3. Vit C attenuates Tg induced elevations in $[Ca^{2+}]_i$ in HEK293 cells. Curves show mean time course of fractional fluorescence change of HEK293 cells loaded with Fluo-4 AM, indicative of changes in $[Ca^{2+}]_i$. (A) 1 µM Tg elevates $[Ca^{2+}]_i$ in HEK293 cells (n=25 cells from 3 experiments). (B) 10 mM Vit C attenuates Tg-induced elevations in $[Ca^{2+}]_i$ in HEK293 cells (n=25 cells from 3 experiments). (C) Area under curves (AUC) A and B expressed as percentage of the Tg control. Data are presented as mean AUC±SEM. (**p value ≤0.01). Experiments were performed at RT in HBS supplemented with 10 mM glucose and 1 mM $CaCl_2$.

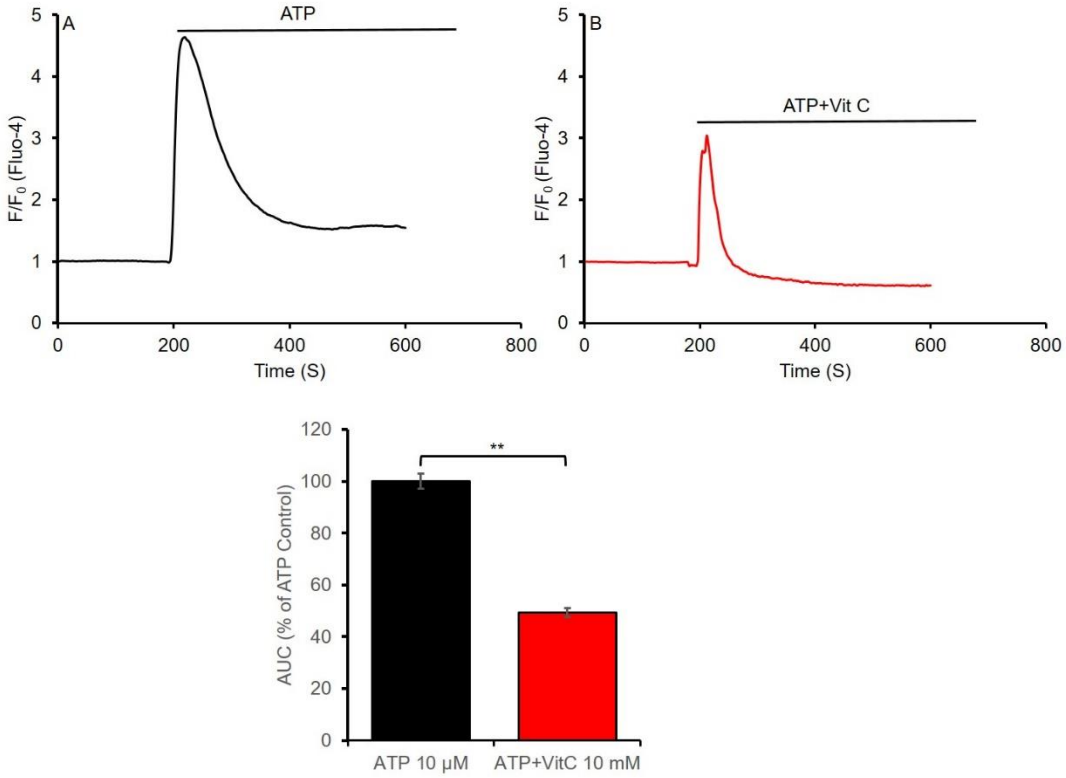

Figure 4.4. Vit C attenuates ATP induced elevations in $[Ca^{2+}]_i$ in HEK293 cells. Curves show mean time course of fractional fluorescence change of HEK293 cells loaded with Fluo-4 AM, indicative of changes in $[Ca^{2+}]_i$ (A) ATP 10 µM elevates $[Ca^{2+}]_i$ (n=25 cells from 3 experiments). (B) Vit C 10 mM attenuates ATP-induced elevations in $[Ca^{2+}]_i$ (n=25 cells from 3 experiments). (C) Mean± SEM of area under curves (AUC) A and B expressed as % of ATP control. (**p value ≤0.01). Experiments were carried out at RT in HBS supplemented with 10 mM glucose and 1 mM $CaCl_2$.

4.3.4 Vit C attenuates elevations in $[Ca^{2+}]_i$ post-Tg treatment in HEK293 cells

As we have established that Vit C added together with Tg and ATP attenuates both Tg and ATP-induced $[Ca^{2+}]_i$ elevations, we sought to investigate whether Vit C added post Tg-treatment would lower the already raised $[Ca^{2+}]_i$. To do this, we first treated Fluo-4 AM-loaded HEK293 cells with 1 µM Tg, this was followed by the addition of 10 mM Vit C. The data revealed that addition of Vit C post-Tg treatment decreased the Tg-induced elevations in $[Ca^{2+}]_i$ (Figure 4.5).

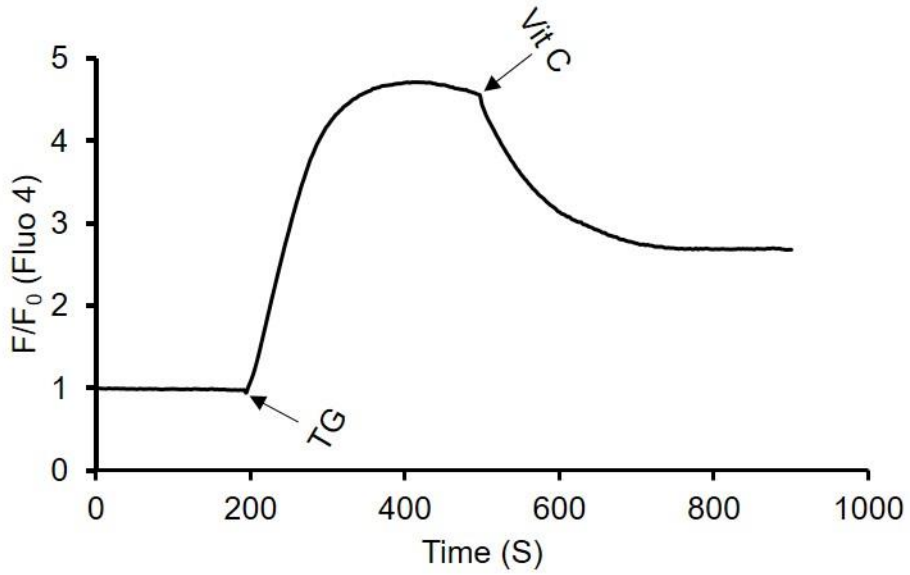

Figure 4.5 Vit C attenuates elevations in $[Ca^{2+}]_i$ post-Tg treatment in HEK293 cells. Addition of 10 mM Vit C post-Tg treatment decreases Tg-induced elevations in $[Ca^{2+}]_i$. Trace shows mean time course of fractional fluorescence change of HEK293 cells loaded with Fluo-4 AM (n=25 cells from 3 experiments). Experiments were performed at RT in HBS supplemented with 10 mM glucose and 1 mM $CaCl_2$.

4.3.5 Loading Fluo-4 AM into HepG2 cells

Having optimised the experimental conditions and performed the first set of experiments in HEK293 cells (our non-hepatocyte model), we then sought to carry out these experiments in hepatocytes which is our main interest. As in the previous chapter, HepG2 cells was used in this chapter as our model hepatocyte cell line. First, HepG2 cells were loaded with Fluo-4 AM and visualized under a a Zeiss LSM 800 Airyscan confocal microscope to confirm the uptake of the dye by the HepG2 cells. Figure 4.6 shows a brightly fluorescent Fluo4 AM-loaded HepG2 cells.

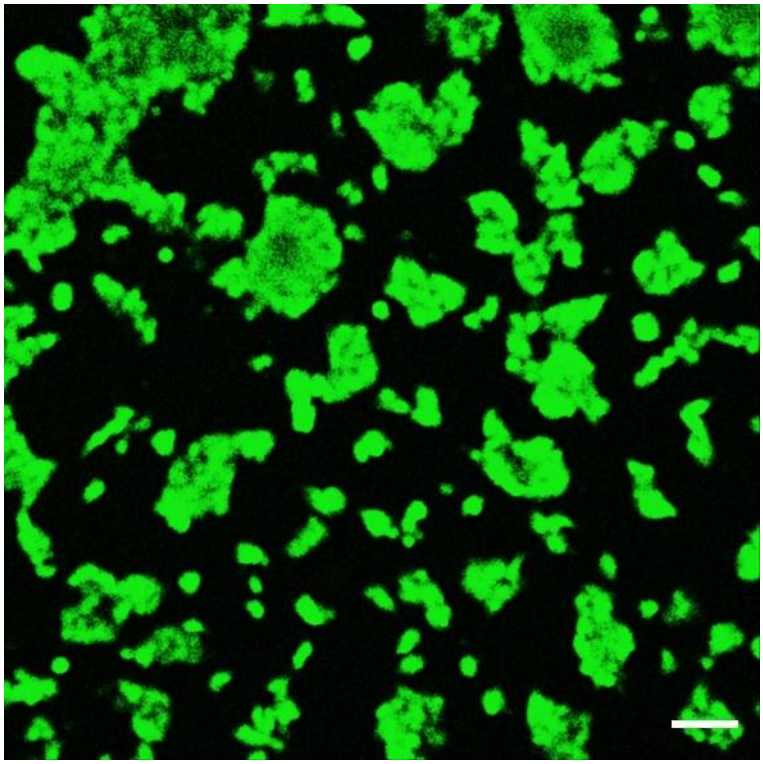

Figure 4.6: HepG2 cells loaded with Fluo-4 AM. Cells were imaged using a Zeiss LSM 800 Airyscan confocal microscope. Cells were excited at 488 nm and emission was collected at 509 nm. Scale bar = 100 µm. Data is a representative of at least 3 experiments.

4.3.6 Vit C attenuates Tg-Induced $[Ca^{2+}]_i$ elevations in HepG2 cells

The ability of Vit C to attenuate agonist induced elevations in $[Ca^{2+}]_i$ in HepG2 cells was then investigated using Tg as the agonist. To do this, HepG2 cells loaded with Fluo-4 AM were treated with 1 µM Tg in combination with or without 10 mM Vit C. Addition of Tg alone rapidly elevated $[Ca^{2+}]_i$ (Figure 4.7A) by approximately 3 folds. Preincubation of the cells in 10 mM Vit C significantly attenuated the Tg-induced $[Ca^{2+}]_i$ elevations (Figure 4.7B).

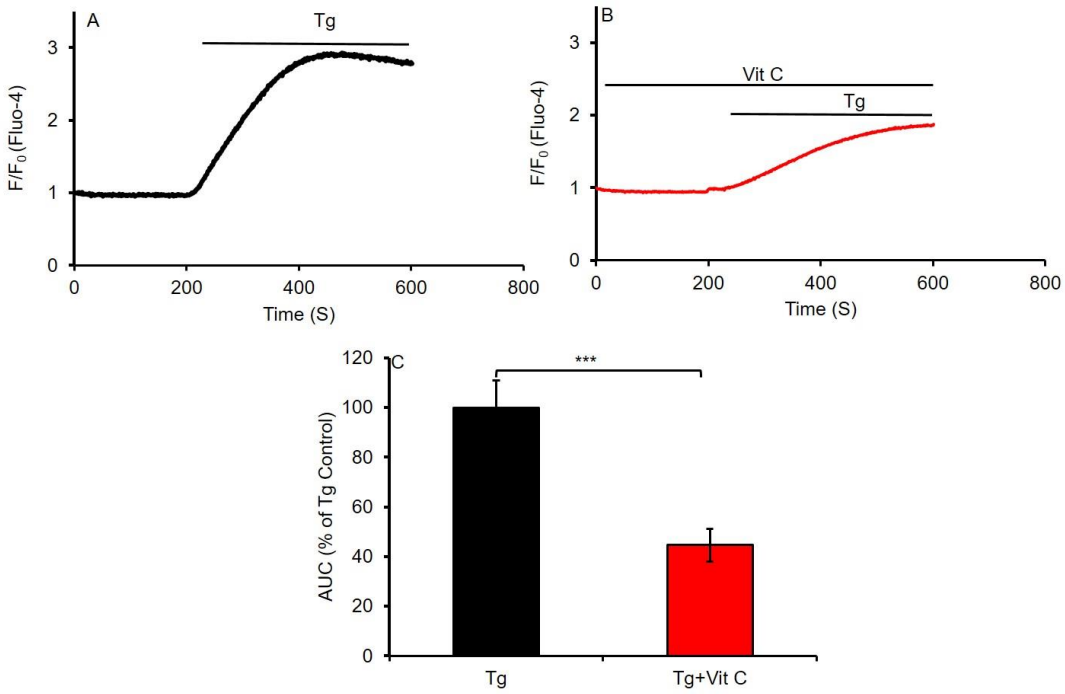

Figure 4.7. Vit C attenuates Tg-induced elevations in $[Ca^{2+}]_i$ in HepG2 cells. Curves show mean time course of fractional fluorescence change of HepG2 cells loaded with Fluo-4 AM, indicative of changes in $[Ca^{2+}]_i$ (A) 1 µM Tg elevates $[Ca^{2+}]_i$ (n=25 cells from 3 experiments). (B) Vit C 10 mM attenuates Tg-induced $[Ca^{2+}]_i$ elevations (n= 25 cells from 3 experiments). (C) mean area under the curves (AUC) from which A and C were averaged. Bars represent mean AUC± SEM (***p value ≤0.001). Experiments were performed at RT in HBS supplemented with 10 mM glucose and 1 mM $CaCl_2$.

4.3.7 Measuring changes in $[Ca^{2+}]_i$ using REX-GECO1.

Having established that Vit C attenuates agonist-induced elevations in $[Ca^{2+}]_i$ in HepG2 and HEK293 cells using Fluo-4 AM, we then sought to carry out these experiments using fluorescent recombinant Ca^{2+} reporter in order to further validate the findings we made with Fluo-4 AM. To do this we purchased 4 different Ca^{2+} biosensor plasmids in form of bacterial stabs from Addgene, namely; CMV-GEM-GECO1 (GEM-GECO1), CMV-GEX-GECO1 (GEX-GECO1), CMV-CAR-GECO1 (CAR-GECO1) and CMV-REX-GECO1 (REX-GECO1). First, we purified the plasmid DNAs from the stab cultures as detailed in the methodology section and a diagnostic restriction digest was performed using ECORI and BamHI as detailed in the methodology section. The agarose gel electrophoresis result revealed the two correct band sizes for all four DNAs; 1254 bp (insert) and 3200 bp (backbone) as expected for the enzymes used (Figure 4.8). The subsequent Ca^{2+} measurement experiments were carried out with REX-GECO1.

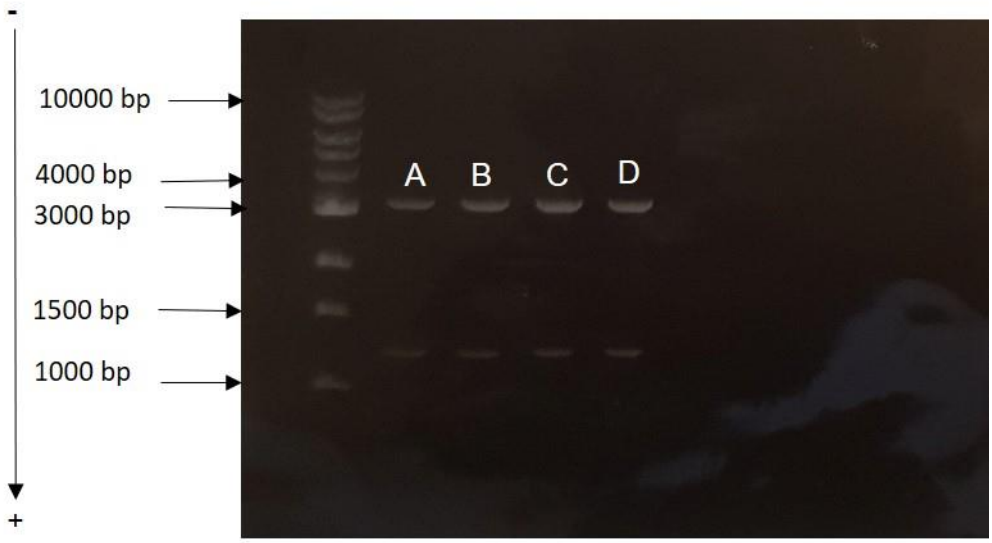

Figure 4.8. Agarose gel verification of REX-GECO1 DNAs. Product of the four CMV-GECO1 DNAs (GEM, GEX, CAR and REX-GECO1) digested with ECORI and BamHI was run on a 0.8 % agarose gel. (A) CMV-GEM-GECO1. (B) CMV-GEX-GECO1. (C) CMV-CAR-GECO1. (D) CMV-REX-GECO1. The DNA size marker is the commercial 1 Kb DNA ladder. The direction of DNA migration is indicated by the direction of the arrowed line.

4.3.8 Transient cell transfection with REX-GECO1

REX-GECO1 was first tested in HEK 293 cells in order to validate the mammalian expression of the probe and to optimize the transfection conditions. To do this, HEK 293 cells were transiently transfected with the REX-GECO1 DNA using different transfection reagents (Turbofect, Lipofectamine 2000 and Lipofectamine 3000) and the reporter protein expression was visualized using a Zeiss LSM 800 Airyscan confocal microscope at 24, 48 and 72 hrs post transfection and images were captured. The data revealed that in general, Lipofectamine 3000 produced the best REX-GECO1 protein expression, followed by Lipofectamine 2000, while Turbofect gave the lowest protein expression (Figure 4.9). The optimal maturation time for the REX-GECO1 protein was 48/72 hrs (Figure 4.9). As mentioned above, the subsequent Ca^{2+} measurement experiments were performed with cells that were transiently transfected with REX-GECO1 using Lipofectamine 3000 reagent.

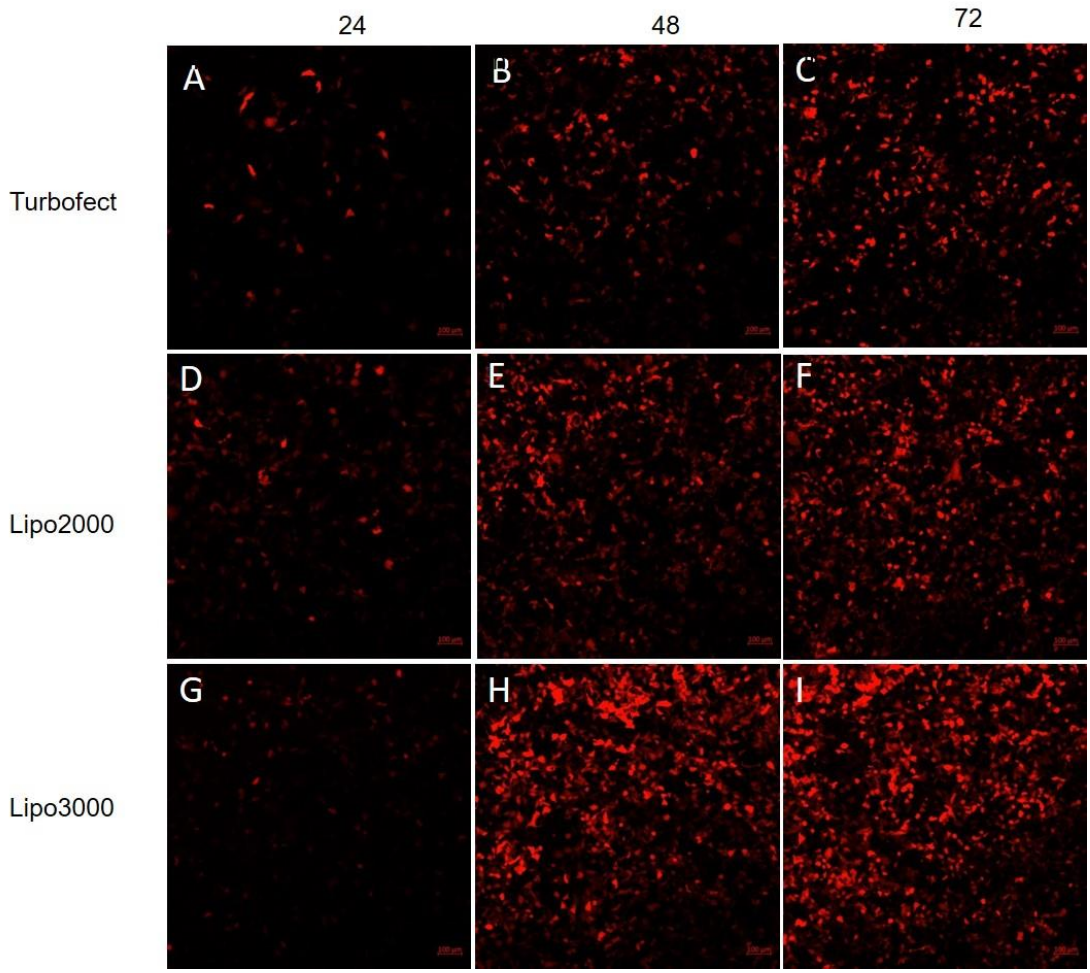

Figure 4.9. REX-GECO1 transfection optimization in HEK293 cells. (ABC) REX-GECO1 protein expression in HEK293 cells transfected with Turbofect reagent (DNA amount = 0.5 µg, DNA to reagent ratio = 1:2) at 24 hrs, 48 hrs and 72 hrs post transfection, respectively. (DEF) REX-GECO1 protein expression in HEK293 cells transfected with Lipofectamine 2000 reagent (DNA amount = 0.4 µg, DNA to reagent ratio = 1:2.5) at 24 hrs, 48 hrs and 72 hrs post transfection, respectively. (GHI) REX-GECO1 protein expression in HEK293 cells transfected with Lipofectamine 3000 reagent (DNA amount = 0.3125 µg, DNA to reagent ratio = 1:2.4) at 24 hrs, 48 hrs and 72 hrs post transfection, respectively. Cells were excited at 488 nm and emission collected at 609 nm. Scale bar = 100 µm. Data are representative of 3 experiments.

4.3.9 Validation of the functionality of the REX-GECO1 Probe

We then sought to validate the functionality of the REX-GECO1 probe. This was first done in HEK293 cells. HEK293 cells were transiently transfected with the REX-GECO1 DNA using Lipofectamine 3000 transfection reagent and at 72 hrs post transfection, real time changes in $[Ca^{2+}]_i$ was measured upon stimulating the cells with 250 nM ionomycin. Addition of ionomycin rapidly elevated the fluorescent signal by 3-fold over basal level, indicative of elevation in $[Ca^{2+}]_i$ (Figure 4.10).

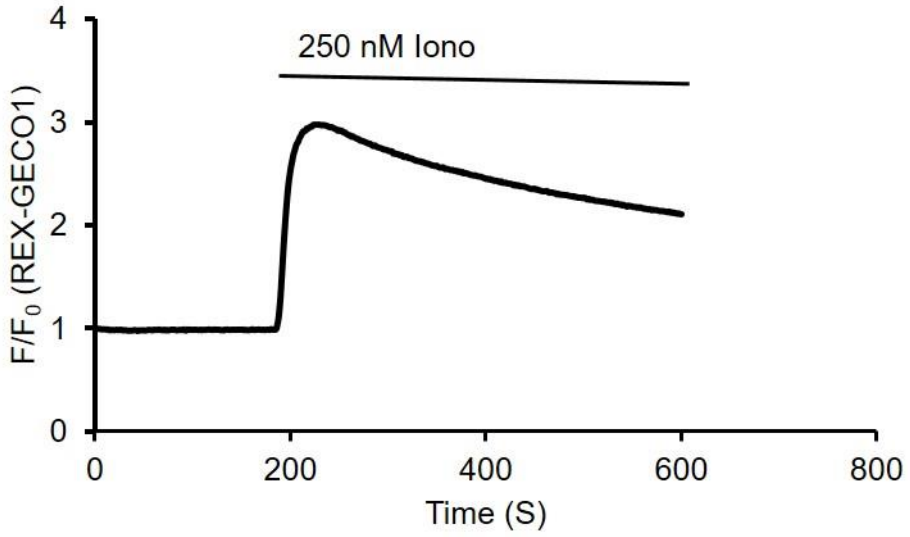

Figure 4.10. Validating functionality of REX-GECO1 in HEK293 cells. Trace shows mean time course of ionomycin-induced fractional fluorescence change of HEK293 cells transfected with REX-GECO1, indicative of changes in $[Ca^{2+}]_i$. (n=25 cells from 3 experiments). Cells were excited at 488 nm and emission collected at 609 nm. Experiment was performed at RT in HBS supplemented with 10 mM glucose and 1 mM $CaCl_2$.

4.3.10 Transfection of HepG2 cells with REX-GECO1

Having validated the functionality of the REX-GECO1 probe in HEK293 cells, we then sort to measure real time changes in $[Ca^{2+}]_i$ in HepG2 cells using the probe. To do this, we first sought to confirm the expression of the REX-GECO1 protein in HepG2 cells. HepG2 cells were transiently transfected with the REX-GECO1 DNA using Lipofectamine 3000 transfection reagent. The REX-GECO1 reporter protein expression was visualized 72 hrs post transfection, and image was captured with a Zeiss LSM 800 Airyscan confocal microscope. The data revealed good, but not excellent REX-GECO1 protein expression by the HepG2 cells (Figure 4.11).

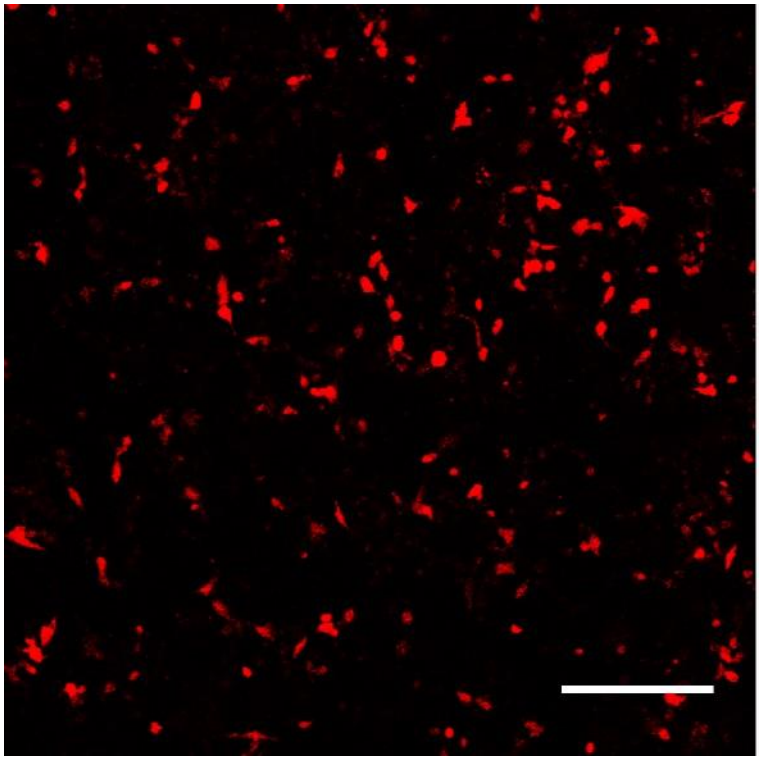

Figure 4.11. HepG2 cells transfected with REX-GECO1 DNA using Lipofectamine 3000 transfection reagent. Cells were excited at 488 nm and emission was collect at 605 nm. (DNA amount = 0.3125 µg, DNA to reagent ratio = 1:2.4. Scale bar = 200 µm. Data are representative of 3 experiments.

4.3.11 Measuring changes in $[Ca^{2+}]_i$ in HepG2 cells using REX-GECO1

Next we sought to measure real time changes in $[Ca^{2+}]_i$ using REX-GECO1. This was done partly in order to confirm the results we obtained using Fluo-4 AM and secondly because we were interested in measuring real time Ca^{2+} changes using a genetically encoded indicator due to the advantages they confer over the chemical indicators as discussed in the general introduction.

Though we have established that the probe is able to measure real time changes in $[Ca^{2+}]_i$ in HEK293 cells, here we sought to also confirm that the probe is able to measure real time changes in $[Ca^{2+}]_i$ in HepG2 cells by treating HepG2 cells with ionomycin, ATP and Tg after transfecting them with the REX-GECO1 DNA.

Our data showed that 250 nM ionomycin (Figure 4.12), 5 µM ATP (Figure 4.13 A) and 10 µM ATP (Figure 4.13 B), 500 nM Tg (Figure 4.14 A) and 2 µM Tg (figure 4.14 B) rapidly elevated the REX-GECO1 fluorescent signal by 2.7 fold, 4.7 fold, 7.8 fold, 3.3 fold and 5 fold respectively above basal level, indicative of elevations in $[Ca^{2+}]_i$.

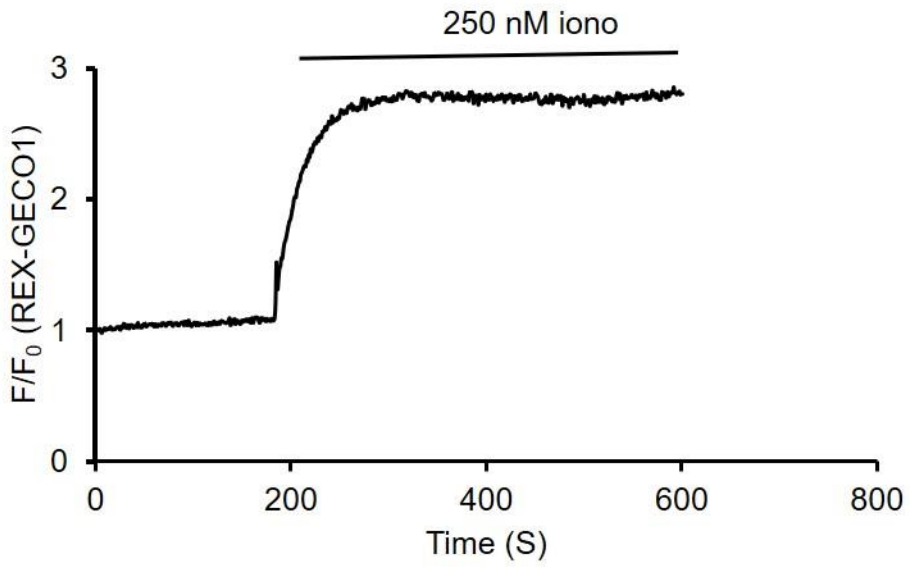

Figure 4.12. Measuring real time changes in $[Ca^{2+}]_i$ in HepG2 cells upon ionomycin stimuli using REX-GECO1. Trace shows mean time course of ionomycin-induced fractional fluorescence change of HepG2 cells transfected with REX-GECO1, indicative of changes in $[Ca^{2+}]_i$. (n=20 cells from 2 experiments). Experiment was performed at RT in HBS supplemented with 10 mM glucose and 1 mM $CaCl_2$.

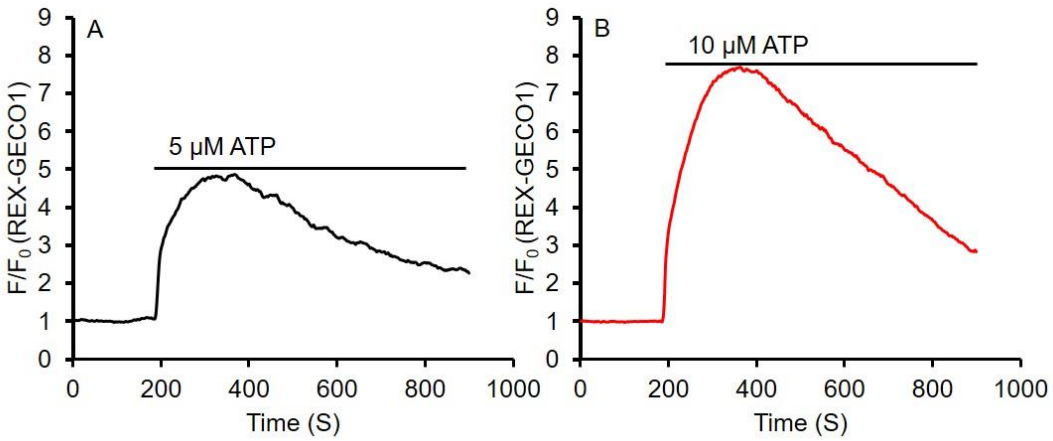

Figure 4.13. Measuring ATP-induced changes in $[Ca^{2+}]_i$ in HepG2 cells using REX-GECO1. (A) Mean time course of 5 μM ATP-induced fractional fluorescence change of HepG2 cells transfected with REX-GECO1 (n=20 cells from 2 experiments). (B) Mean time course of 10 μM ATP-induced fractional fluorescence change of HepG2 cells transfected with REX-GECO1 (n=20 cells from 2 experiments). Experiments were performed at RT in HBS supplemented with 10 mM glucose and 1 mM $CaCl_2$.

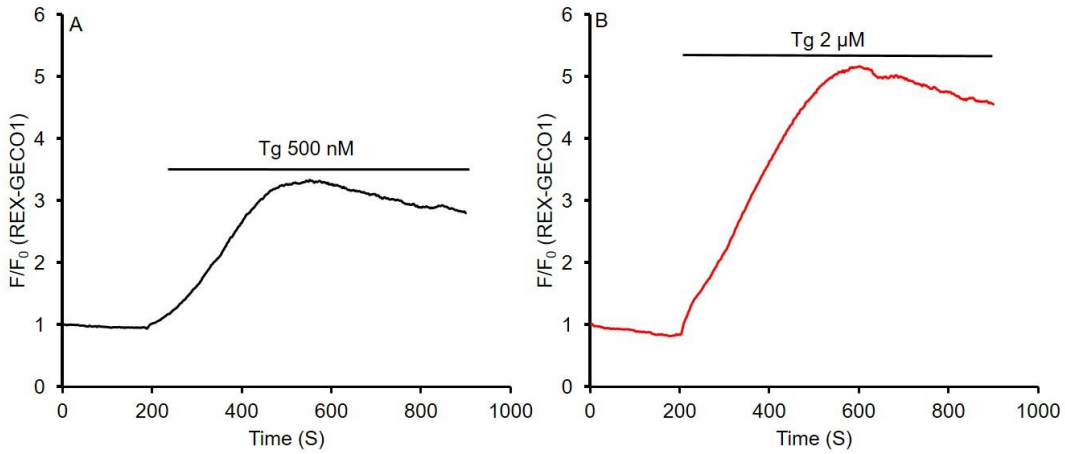

Figure 4.14. Measuring Tg-induced changes in $[Ca^{2+}]_i$ in HepG2 cells using REX-GECO1. (A) Mean time course of 500 nM Tg-induced fractional fluorescence change of HepG2 cells transfected with REX-GECO1 (n=20 cells from 2 experiments). (B) Mean time course of 2 µM Tg-induced fractional fluorescence change of HepG2 cells transfected with REX-GECO1 (n=20 cells from 2 experiments). Experiments were performed at RT in HBS supplemented with 10 mM glucose and 1 mM $CaCl_2$.

4.3.12 Inhibition of PDI modulates Vit C attenuation of Tg-induced $[Ca^{2+}]_i$ elevations in HepG2 cells

In chapter 3, we showed that inhibition of PDI with Bac and RL90 modulates the cGMP elevation effect of Vit C and ANP but not that of SNP, consistent with csPDI regulation of the ability of Vit C and ANP to elevate cGMP, but not that of SNP. Here we sought to investigate whether the inhibition of csPDI with Bac and RL90 would have a corresponding modulatory action on the effect of these cGMP-elevating agents (Vit C, ANP and SNP) on Ca^{2+} signal. To do this, we transfected HepG2 cells with REX-GECO1 and subsequently treated the transfected cells with Tg in combination with or without Vit C, ANP and SNP and inhibitors of PDI (RL90 and Bac). Bac is mixture of cyclic peptides that has been widely used to inhibit PDI function, while RL90 is an anti-PDI monoclonal antibody that has also been widely used to inhibit PDI function (333, 364, 365). The data revealed that 1.25 mM Vit C (Figure 4.15), 200 nM ANP (Figure 4.16) and 100 µM SNP (Figure 4.17) attenuated the $[Ca^{2+}]_i$-elevating action of Tg. Importantly, the data revealed that pre-incubation of the cells with RL90 and Bac antagonised the attenuation effect of Vit C and ANP, but not that of SNP on the Tg-induced elevations in $[Ca^{2+}]_i$ (Figure 4.15, 4.16 and 4.17 respectively). By calculating and comparing the area under the curves (AUCs), the percentage attenuation effect of Vit C, ANP and SNP, as well as the effect of inhibiting PDI with RL90 and Bac on the Tg-induced $[Ca^{2+}]_i$ elevations was quantified (expressed as percentage of Tg control). Figure 4.15 shows that Vit C significantly reduced the Tg-induced $[Ca^{2+}]_i$ elevations as revealed by the AUCs, and this effect of Vit C was significantly blunted when PDI was inhibited with RL90 and Bac (Figure 4.15 E). A similar trend was also

observed for the ANP attenuation of Tg-induced $[Ca^{2+}]_i$ elevations (Figure 4.16E), while figure 4.17D which represents the area under curves 4.17A to C shows that inhibiting PDI with Bac had no significant effect on the SNP attenuation of Tg-induced $[Ca^{2+}]_i$ elevations in HepG2 cells.

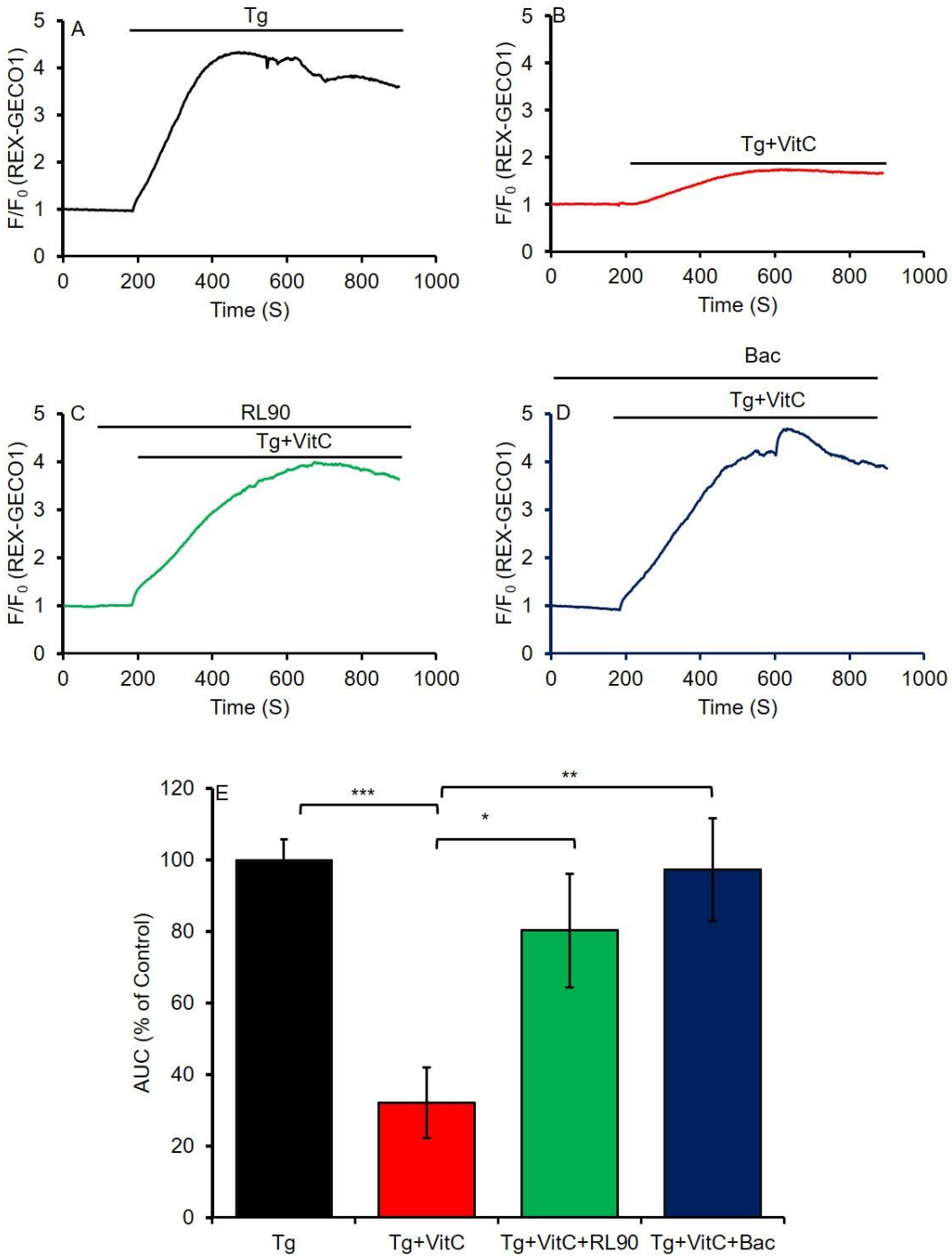

Figure 4.15. Vit C attenuation of Tg-induced elevations in $[Ca^{2+}]_i$ in HepG2 cells is downregulated by Bac and RL90. Curves show mean time course of fractional fluorescence change of HepG2 cells transfected with REX-GECO1, indicative of changes in $[Ca^{2+}]_i$ (A) 1 µM Tg elevates $[Ca^{2+}]_i$ in HepG2 cells (n=25 cells from 3 experiments). (B) 1.25 mM Vit C attenuates Tg-

induced elevations of $[Ca^{2+}]_i$ in HepG2 cells (n=20 cells from 3 experiments). (C) Inhibition of csPDI with RL90 20 µg/mL downregulates Vit C attenuation of Tg-induced $[Ca^{2+}]_i$ elevations (n=20 cells from 3 experiments). (D) Inhibition of csPDI with Bac 2.5 mg/mL downregulates Vit C attenuation of Tg-induced $[Ca^{2+}]_i$ elevations (n=20 cells from 3 experiments). (E) Mean±SEM of area under the curves from which A to D was averaged (expressed as % of Tg control). (*p value ≤0.05, **p value ≤0.01, ***p value ≤0.001).

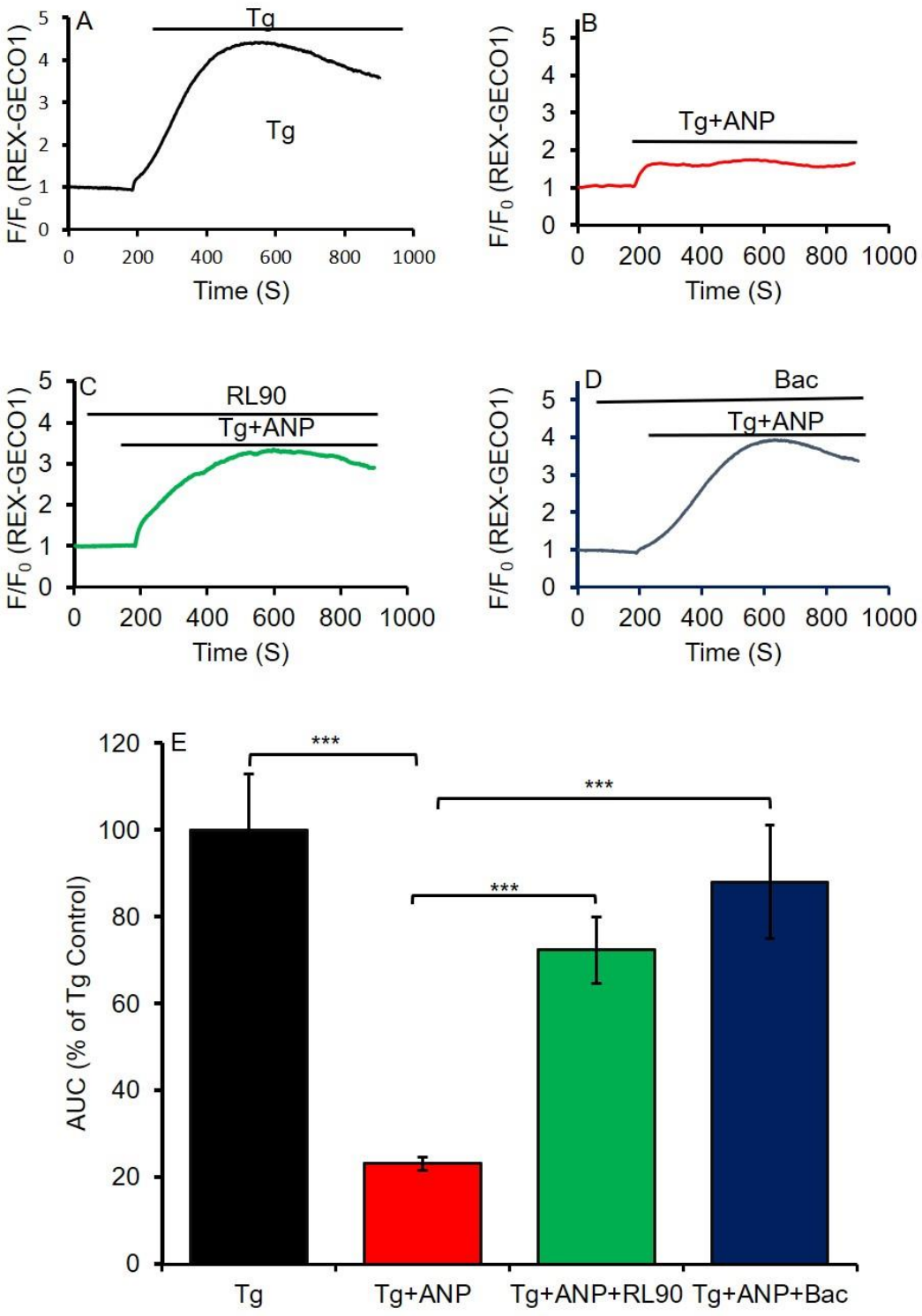

Figure 4.16. ANP attenuation of Tg-induced elevations in $[Ca^{2+}]_i$ in HepG2 cells is downregulated by Bac and RL90. Curves show mean time course of fractional fluorescence change of HepG2 cells transfected with REX-GECO1, indicative of changes in $[Ca^{2+}]_i$ (A) 1 µM Tg elevates $[Ca^{2+}]_i$ in HepG2

cells (n=24 cells from 3 experiments). (B) 200 nM ANP attenuates Tg-induced elevations in $[Ca^{2+}]_i$ in HepG2 cells (n=31 cells from 4 experiments). (C) Inhibition of csPDI with RL90 20 µg/mL downregulates ANP attenuation of Tg-induced $[Ca^{2+}]_i$ elevations (n=30 cells from 4 experiments). (D) Inhibition of csPDI with Bac 2.5 mg/mL downregulates ANP attenuation of Tg-induced $[Ca^{2+}]_i$ elevations (n=25 cells from 3 experiments). (E) Mean±SEM of area under the curves from which A to D was averaged (expressed as % of Tg control). (***p value ≤0.001).

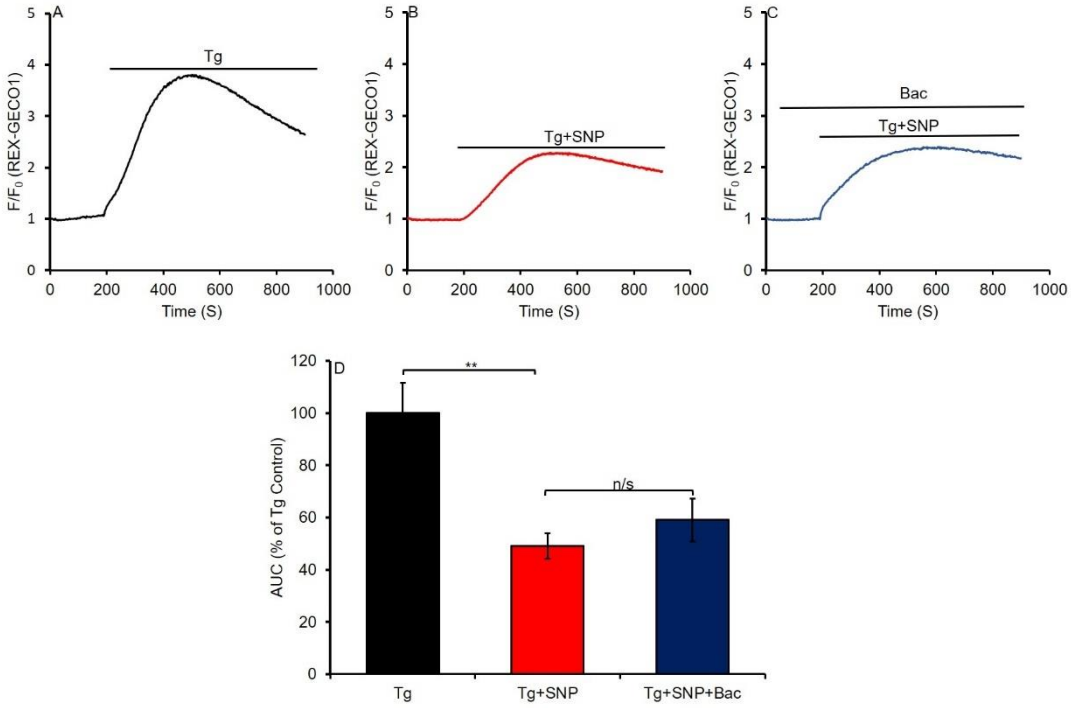

Figure 4.17. SNP attenuation of Tg-induced elevations in $[Ca^{2+}]_i$ in HepG2 cells is not affected by the inhibition of PDI. Curves show mean time course of fractional fluorescence change of HepG2 cells transfected with REX-GECO1, indicative of changes in $[Ca^{2+}]_i$ (A) 1 µM Tg elevates $[Ca^{2+}]_i$ in HepG2 cells (n=20 cells from 3 experiments). (B) 100 µM SNP attenuates Tg-induced elevations in $[Ca^{2+}]_i$ in HepG2 cells (n=20 cells from 3 experiments). (C) PDI inhibition by Bac 2.5 mg/mL does not significantly affect SNP attenuation of Tg-induced $[Ca^{2+}]_i$ elevations (n=20 cells from 3 experiments). (D) Mean±SEM of area under the curves from which A to C was averaged (expressed as % of Tg control). (**p value ≤0.01).

4.3.13 Vit C decreases $[Ca^{2+}]_i$ elevations post-Tg stimulation

As we have established that Vit C attenuates Tg -induced $[Ca^{2+}]_i$ elevations (Figures 4.7 and 4.15) in HepG2 cells when the cells were co-stimulated with Tg and Vit C, we sought to investigate whether Vit C added post Tg-addition would decrease an already raised $[Ca^{2+}]_i$. The data revealed that 1.25 mM Vit C had only marginal effect on the already raised $[Ca^{2+}]_i$ induced by Tg (Figure 4.18B), whereas, 10 mM Vit C added post-Tg treatment rapidly decreased the Tg-induced elevations in $[Ca^{2+}]_i$ (Figure 4.18C). Upon PDI inhibition with Bac, this Vit C attenuation of Tg-induced $[Ca^{2+}]_i$ elevation was downregulated (Figure 4.18D). Figure 4.18E compares the rates of decline (ROD).

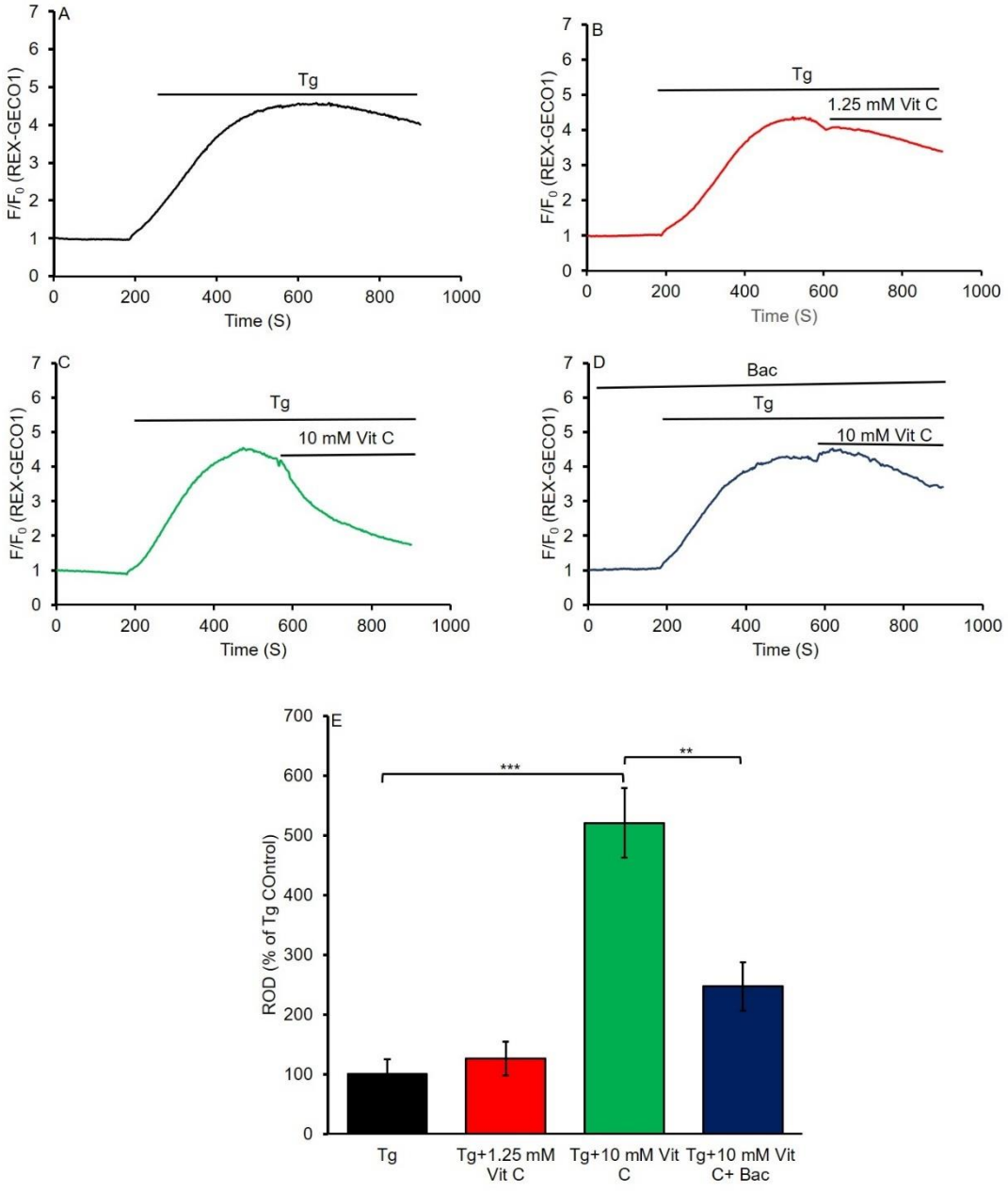

Figure 4.18. Vit C attenuation of $[Ca^{2+}]_i$ post-Tg treatment in HepG2 cells is concentration-dependent and is partly downregulated by PDI inhibition by Bac. Curves show mean time course of fractional fluorescence change of HepG2 cells transfected with REX-GECO1, indicative of changes in $[Ca^{2+}]_i$. (A) 1 µM Tg elevates $[Ca^{2+}]_i$ in HepG2 cells (n=22 cells from 3 experiments). (B) addition of 1.25 mM Vit C post-Tg treatment had marginal effect on Tg-induced elevations in $[Ca^{2+}]$i (n=22 cells from 3 experiments). (C)

Addition of 10 mM Vit C post-Tg treatment decreases Tg-induced elevations in $[Ca^{2+}]_i$ (n=23 cells from 3 experiments). (D) PDI inhibition by Bac 2.5 mg/mL downregulates Vit C attenuation of Tg-induced $[Ca^{2+}]_i$ elevations (n=20 cells from 3 experiments). (E) Mean±SEM of Vit C-induced rate of decline of elevated $[Ca^{2+}]_i$ (expressed as % of Tg control). (**p value ≤0.01, ***p value ≤0.001).

.

4.3.14 Inhibition of PDI modulates Vit C attenuation of Tg-induced $[Ca^{2+}]_i$ elevations in HEK293 cells.

We have shown that Vit C like other agents that elevates cellular cGMP (ANP and SNP) attenuates Tg-induced elevations in $[Ca^{2+}]_i$ in HepG2 cells (Figures 4.7 and 4.15B). We have also shown that this effect of Vit C was downregulated when csPDI was inhibited with RL90 and Bac (Figures 4.15C and D). The data from our preliminary experiments performed with Fluo-4 AM also revealed that 10 mM Vit C attenuated agonist (Tg and ATP)-induced elevations in $[Ca^{2+}]_i$ in HEK293 cells (Figure 4.3 and 4.4 respectively), indicative that this effect of Vit C is not hepatocyte-specific. With the REX-GECO1 recombinant probe, we then sought to repeat these experiments in HEK293 cells (even with lower concentration of Vit C; 1.25 mM) and to also determine whether inhibition of csPDI in HEK293 cells would have a similar inhibitory effect on the action of Vit C as was observed in HepG2 cells. To do this, we transfected HEK293 cells with the REX-GECO1 DNA and subsequently treated the transfected cells with Tg in combination with or without Vit C, and inhibitors of PDI (RL90 and Bac). The data showed that 1.25 mM Vit C attenuated Tg-induced $[Ca^{2+}]_i$ elevations (Figures 4.19B and E). Importantly, the data revealed that inhibition of csPDI with Bac and RL90 downregulated the ability of Vit C to attenuate Tg-induced elevations in $[Ca^{2+}]_i$ (Figure 4.19C, D and E), in line with what we observed in HepG2 cells. This suggests that the ability of Vit C to attenuate agonist-induced elevations in $[Ca^{2+}]_i$ and the modulation of this mechanism by csPDI is not hepatocyte-specific, but can be achieved in other cell types.

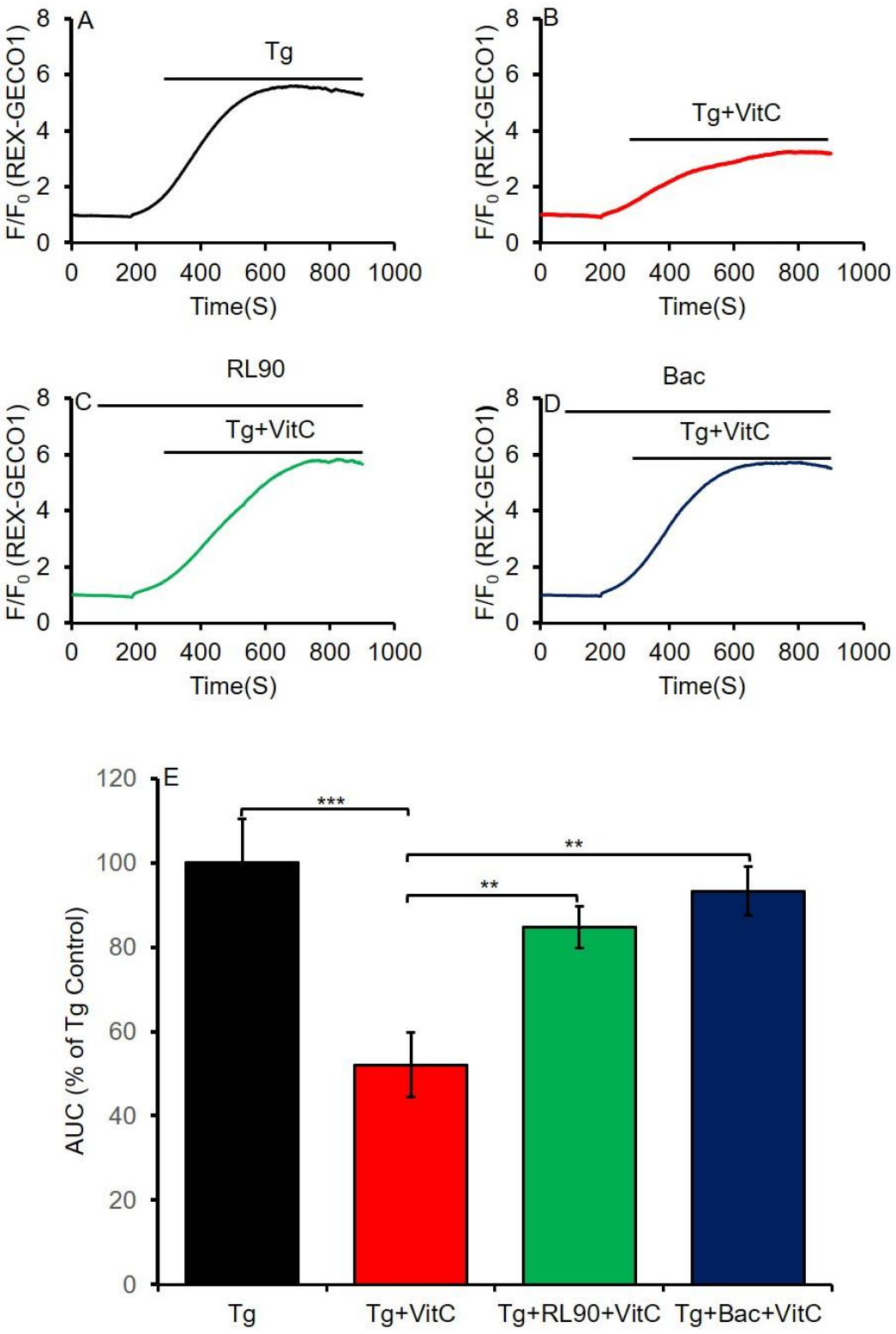

Figure 4.19. Vit C attenuation of Tg-induced elevations in $[Ca^{2+}]_i$ in HEK293 cells is modulated by the inhibition of PDI with RL90 and Bac. Curves show mean time course of fractional fluorescence change of HEK293

cells transfected with REX-GECO1, indicative of changes in $[Ca^{2+}]_i$ (A) 1 µM Tg elevates $[Ca^{2+}]_i$ in HEK293 cells (n=25 cells from 3 experiments). (B) 1.25 mM Vit C attenuates Tg-induced elevations of $[Ca^{2+}]_i$ (n=25 cells from 3 experiments). (C) Inhibition of csPDI with RL90 20 µg/mL downregulates Vit C attenuation of Tg-induced $[Ca^{2+}]_i$ elevations (n=25 cells from 3 experiments). (D) Inhibition of csPDI with Bac 2.5 mg/mL downregulates Vit C attenuation of Tg-induced $[Ca^{2+}]_i$ elevations (n=25 cells from 3 experiments). (E) Mean±SEM of area under the curves (AUC) from which A to D were averaged (expressed as % of Tg control). (**p value ≤0.01, ***p value ≤0.001).

4.4 Discussion

The data from this part of the study demonstrate that Vit C like other agents that elevates cellular cGMP (ANP and SNP) attenuates agonist-induced $[Ca^{2+}]_i$ elevations in HepG2 cells. The data also reveal that Vit C and ANP, but not SNP-mediated attenuation of Tg-induced $[Ca^{2+}]_i$ elevations in HepG2 cells is downregulated by the inhibition of PDI with RL90 and Bac. This is consistent with csPDI modulation of Vit C and ANP-mediated attenuation of Tg-induced elevations in $[Ca^{2+}]_i$, but not csPDI modulation of SNP-mediated attenuation. When we investigated whether the Vit C attenuation of agonist-induced $[Ca^{2+}]_i$ elevations can be achieved in HEK293 cells, we observed that the vitamin attenuated Tg and ATP-induced $[Ca^{2+}]_i$ elevations in the cells. The ability of Vit C to attenuate Tg-induced elevations in $[Ca^{2+}]_i$ was also observed to be downregulated by Bac and RL90, in line with the observation in HepG2 cells. Importantly, the data rule out any non-specific effect of Vit C since both RL90 and Bac opposed its effect.

To access whether Vit C has the potential to attenuate $[Ca^{2+}]_i$ elevations in human hepatocytes and other cell types, we utilized HepG2 cells as our model hepatocyte cell line and HEK293 cells as our non-hepatocyte comparator. As mentioned in the introduction, we performed these experiments with two different Ca^{2+} indicators; Fluo-4 AM (a green fluorescent calcium sensing dye) and REX-GECO1 (a genetically encoded fluorescent calcium probe) in order to improve the validity of the findings. Our results revealed that either of the two concentrations of Vit C used (10 mM; Figures 4.3 and 1.25 mM; Figures 4.19B and E) when added in combination with Tg, attenuated Tg-induced

$[Ca^{2+}]_i$ elevations in HEK293 cells. 10 mM Vit C also attenuated ATP-induced elevations in $[Ca^{2+}]_i$ in HEK293 cells (Figure 4.4). On the HepG2 cells, our data showed that Vit C (10 mM; Figure 4.7 and 1.25 mM; Figure 4.15B and E), like ANP (Figure 4.16B and E) and SNP (Figure 4.17B and D) attenuated Tg-induced elevations in $[Ca^{2+}]_i$. This is in line with previous studies from another group that reported that Vit C attenuates A23187-induced elevations in $[Ca^{2+}]_i$ in Molt-3 human lymphoblastoid cells (332), and unpublished data from our group on primary rat hepatocytes where it was observed that Vit C attenuates ATP-induced elevations in $[Ca^{2+}]_i$. Together, these data suggest that Vit C attenuates agonist-induced $[Ca^{2+}]_i$ elevations and this effect of the vitamin is not hepatocyte-specific.

The effects of sGC and pGC activation on Ca^{2+} signalling have been previously investigated by Green and colleagues in rat hepatocytes (225, 283). It was reported that ANP (an activator of pGC), but not SNP (NO donor/activator of sGC) through PKG stimulates plasma membrane Ca^{2+} efflux and inhibits Ca^{2+} influx (225, 283). However, ANP was found to have no effect on the release of Ca^{2+} from or re-uptake into intracellular stores (225). The authors attributed the differing abilities of these agents to stimulate net plasma membrane Ca^{2+} efflux to the differing subcellular localization of their target guanylyl cyclases (GCs) and consequent cGMP compartmentation. They proposed that ANP through the activation of plasma membrane bound pGC could be mediating localized cGMP elevation, activation of membrane localized PKG and consequent stimulation of hepatocyte plasma membrane calcium ATPase (PMCA), thus resulting in Ca^{2+} efflux (225). According to the authors, SNP which mediates mainly cytosolic cGMP elevation may be

ineffective in stimulating PMCA (225). In this current study, we have not exclusively investigated the effect of the cGMP elevators (ANP, SNP and Vit C) on Ca^{2+} efflux, influx or release and re-uptake from intracellular stores, but our data clearly shows that all three agents; SNP, ANP and Vit C attenuated Tg-induced $[Ca^{2+}]_i$ elevations in both HepG2 and HEK293 cells. In agreement with our findings, previous studies have reported that SNP, through PKG, attenuates ATP-induced $[Ca^{2+}]_i$ elevations in supporting cells of the guinea pig cochlea (348, 363). Taking into account the submission by Green and colleagues that SNP neither stimulate Ca^{2+} efflux via PMCA nor inhibit Ca^{2+} influx (225, 283), it is therefore likely that SNP modulates $[Ca^{2+}]_i$ signals via other pathways that does not involve plasma membrane Ca^{2+} fluxes. In addition to the stimulation of net plasma membrane Ca^{2+} efflux via the activation of PMCA and inhibition of Ca^{2+} influx via membrane Ca^{2+} channels, cGMP can modulate $[Ca^{2+}]_i$ via other mechanisms. For example, cGMP through PKG, can modulate $[Ca^{2+}]_i$ signals by the inhibition of Ca^{2+} release from intracellular stores. Interestingly, previous studies have inferred that SNP downregulates Ca^{2+} signal by cGMP dependent IP_3R inhibition. For example, Dufour and colleagues suggested that SNP through cGMP elevation interferes with bile canalicular contraction by inhibiting IP_3-dependent Ca^{2+} release (285). Also, Tertyshnikova and colleagues reported that SNP through PKG inhibits IP_3-induced Ca^{2+} release but has no effect on Ca^{2+} extrusion in rat megarkaryocytes (280). Taking together, these data from previous studies and our findings from this study suggest that ANP and Vit C modulation of $[Ca^{2+}]_i$ signals are mediated via same pathway, distinct from the SNP-mediated route. This notion is supported by our observation that Vit C and ANP, but not SNP-

induced cGMP elevation (chapter 3) and reduction in $[Ca^{2+}]_i$ appears to be mediated via the same pathway as the ANP and Vit C, but not SNP effects were observed to be attenuated by the inhibition of PDI with RL90 and Bac. Preliminary data from our group also further support this notion. The data revealed that Vit C through PKG attenuates ATP-induced $[Ca^{2+}]_c$ elevations by stimulating net plasma membrane Ca^{2+} efflux, in line with the initial submission by Green and colleagues that ANP attenuates elevations in $[Ca^{2+}]_c$ in rat hepatocytes via the same mechanism (225).

In addition, our data from this current study suggest a possible involvement of the store-operated Ca^{2+} entry (SOCE) or capacitative Ca^{2+} entry (CCE) in the Vit C reduction of $[Ca^{2+}]_i$. Tg raises $[Ca^{2+}]_i$ by inhibiting SERCA, thereby causing ER Ca^{2+} depletion. The store depletion activates the SOCE, a mechanism which involves Ca^{2+} influx from the extracellular fluid following intracellular depletion (366). After the initial release of Ca^{2+} from intracellular stores, SOCE plays a key role in maintaining $[Ca^{2+}]_i$ plateau and in replenishing the stores (367). Upon stimulation of the HEK293 and HepG2 cells with Tg, our data revealed a typical Tg-induced biphasic Ca^{2+} response consisting of the initial increase in $[Ca^{2+}]_i$, followed by a sustained plateau which was abruptly reduced by the addition of Vit C (Figure 4.5 and 4.18E). This is consistent with Vit C inhibition of the SOCE pathway.

An important observation made on the Vit C attenuation of Tg-induced elevations in $[Ca^{2+}]_i$ in HepG2 cells was that though 1.25 mM Vit C when added together with Tg, attenuated the Tg-induced $[Ca^{2+}]_i$ elevations, addition of this same concentration of Vit C (1.25 mM) to the cells post-Tg treatment had no

apparent effect on the already raised $[Ca^{2+}]_i$ induced by Tg (Figures 4.18A and B). However, 10 mM Vit C added post-Tg treatment rapidly decreased the Tg-induced elevated $[Ca^{2+}]_i$ (Figure 4.18C). This is in line with our observation in HEK293 cells where 10 mM Vit C rapidly decreased Tg-induced elevated $[Ca^{2+}]_i$ (Figure 4.5). Together, these data suggest that though co-treatment of Tg with 1.25 mM Vit C attenuates Tg-induced elevations in $[Ca^{2+}]_i$, a higher concentration of Vit C (10 mM in this case) is required to lower an already raised $[Ca^{2+}]_i$.

PDI has been shown to colocalize with membrane guanylyl cyclase in HUVEC and HMC where it was also reported to modulate the cGMP-elevating action of Natriuretic peptides (ANP, BNP and CNP) (333). In chapter 3 we showed that Inhibition of PDI with RL90 and Bac downregulates the cGMP-elevating action of Vit C and ANP in HepG2 cells, but not that of SNP. Whether this PDI modulating action on the cGMP-elevating agents would result in a corresponding modulation of their effect on $[Ca^{2+}]_i$ was yet to be defined. Therefore, utilizing the PDI inhibitors RL90 and Bac, we investigated the possible involvement of PDI in Vit C, ANP and SNP attenuation of $[Ca^{2+}]_i$ elevations. Vit C (Figures 4.15 and 4.18) and ANP (Figure 4.16) attenuation of Tg-induced $[Ca^{2+}]_i$ elevations in HepG2 cells was significantly downregulated upon PDI inhibition with RL90 and Bac, but SNP-mediated attenuation was unaffected (Figure 4.17). This is consistent with csPDI modulation of the cGMP elevating action of Vit C and ANP, and consequent modulation of their effect on Ca^{2+} signal, but not that of SNP. Importantly, a similar trend on the effect of RL90 and Bac on Vit C attenuation of $[Ca^{2+}]_i$ elevations was observed in HEK293 cells. In these cells, inhibition of PDI with these agents (RL90 and

Bac) downregulated the ability of Vit C to attenuate Tg-induced $[Ca^{2+}]_i$ elevations (Figure 4.19). Together, these data suggest that csPDI modulation of Vit C effect on $[Ca^{2+}]_i$ is not hepatocyte specific.

In conclusion, we have been able to show that Vit C attenuates Tg-induced elevations in $[Ca^{2+}]_i$ in HepG2 cells. In HEK293 cells which we used as our non-hepatocyte model cell line to investigate whether the ability of Vit C to attenuate $[Ca^{2+}]_i$ elevations is more general, we observed that Vit C attenuated Tg and ATP-induced $[Ca^{2+}]_i$ elevations, in line with the observation in HepG2 cells. Taking together with the previous study by Ozturk and colleagues that revealed that Vit C decreases A23187-induced $[Ca^{2+}]_i$ elevations in Molt-3 lymphoblastoid cells (332), it is therefore conceivable that the Vit C attenuation of agonist-induced $[Ca^{2+}]_i$ elevations can be achieved in a variety of cell types. Upon inhibition of csPDI with Bac and RL90 in HepG2 and HEK293 cells, we observed that the Vit C-mediated attenuation of Tg-induced $[Ca^{2+}]_i$ elevations was downregulated. A similar effect of the PDI inhibitors was also observed for ANP, but not SNP-mediated attenuation of Tg-induced $[Ca^{2+}]_i$ elevations in HepG2 cells. Taking together, we propose that Vit C and ANP attenuation of $[Ca^{2+}]_i$ elevations are likely via the same pathway, distinct from the SNP-mediated pathway.

Chapter 5

Presence and cellular localization of protein disulphide isomerase and natriuretic peptide receptor-A in human hepatocytes and HEK293 cells

5.1 Introduction

Protein disulphide isomerase (PDI) has been reported to modulate the function of plasma membrane proteins in certain cell types, including the cGMP generation action of the guanylyl cyclase-linked receptors (natriuretic peptide receptors). For example, in human umbilical vein endothelial cells (HUVECs), human mesangial cells (HMCs), human aortic smooth muscle cells (HASMCs) and pig kidney epithelial cells (LLC-PK1), PDI was reported to regulate particulate guanylyl cyclase (pGC) generation of cGMP in response to natriuretic peptides (NPs) (333). In chapter 3 of this study, we showed that PDI inhibition by RL90 and Bac attenuates ANP and Vit C-induced cGMP generation in HepG2 cells. Also, in chapter 4, our data revealed that inhibition of PDI with RL90 and Bac downregulates ANP and Vit C-mediated reduction of $[Ca^{2+}]_i$ in HepG2 cells. These inhibitory effects of RL90 and Bac were also observed in HEK293 cells. This is consistent with PDI modulation of the ability of Vit C and ANP to stimulate pGC and consequent cGMP elevation and reduction of $[Ca^{2+}]_i$. Pan and colleagues suggested that the PDI modulation of the pGC generation of cGMP is due to its colocalization with the guanylyl cyclase-linked receptors (natriuretic peptide receptors; NPR-A and NPR-B) on the plasma membrane of the various cell types (333).

Though PDI has widely been thought to be an ER-resident protein due to the presence of the ER-retention signal; the C-terminal KDEL sequence, studies have identified it on the plasma membrane of certain cell types such as endothelial cells (ECs), lymphocytes, platelets, vascular smooth muscle cells (VSMCs), hepatocytes, exocrine pancreatic cells and some cancer cells

(335, 336, 368-371). In the cells where PDI has been identified on the plasma membrane, it is referred to as cell surface PDI (csPDI) as it is thought to be attached to the extracellular surface of the plasma membrane by lipid, glycan and integral membrane protein anchors (336, 337).

The externalization route of PDI across distinct cell types including hepatocytes remains elusive, but it is well clear from previous studies on other cell types that it is cell type dependent. For example, csPDI externalization in VSMCs occurs entirely via an unconventional golgi-independent route, while in ECs, its externalization is partly via the classical golgi-dependent route and partly via an unconventional route (334, 335). Moreover, a clear characterization of the extracellular PDI pool and the mode of externalization in human hepatocytes remain unelucidated.

5.2 Aims

As our data in chapters 3 and 4 suggested that PDI modulates cGMP elevating action of ANP (in HepG2 cells) and Vit C (in HepG2 and HEK293 cells) and their consequent ability to attenuate $[Ca^{2+}]_i$ signal in these cells, our aims in this chapter were to verify whether these cells (HepG2 and HEK293 cells) express PDI on their plasma membrane (csPDI). And if so, we aimed to investigate whether the csPDI colocalizes with the membrane NPRs. Also, if we verify the above on the HepG2 cells which we have used in this study as our model hepatocyte cell line, our next aim was to investigate the possible expression and colocalization of these proteins on the membrane of primary human hepatocytes (PHH) as this would then inform us whether csPDI can be a possible therapeutic target in Ca^{2+}-mediated hepatocyte injury. Lastly, as

PDI externalization route in hepatocytes remain unelucidated, we aimed to investigate the involvement of the conventional golgi-dependent route in the externalization of the protein in human hepatocytes.

5.3 Results

5.3.1 Investigating the presence and cellular localization of PDI and NPRA in HepG2 cells

In order to distinguish membrane and cytoplasmic PDI and NPRA in HepG2 cells, cells were labelled with anti-PDI antibody and anti-NPRA antibody either with or without triton permeabilization post fixation. The data from the permeabilized cells revealed a distribution of both the PDI (Figure 5.1) and NPRA (Figure 5.2) throughout the intracellular space, most likely the ER. Whereas, in the Non-permeabilized cells, both PDI (Figure 5.1) and NPRA (Figure 5.2) expression were restricted to the cell margin, consistent with plasma membrane localized PDI and NPRA.

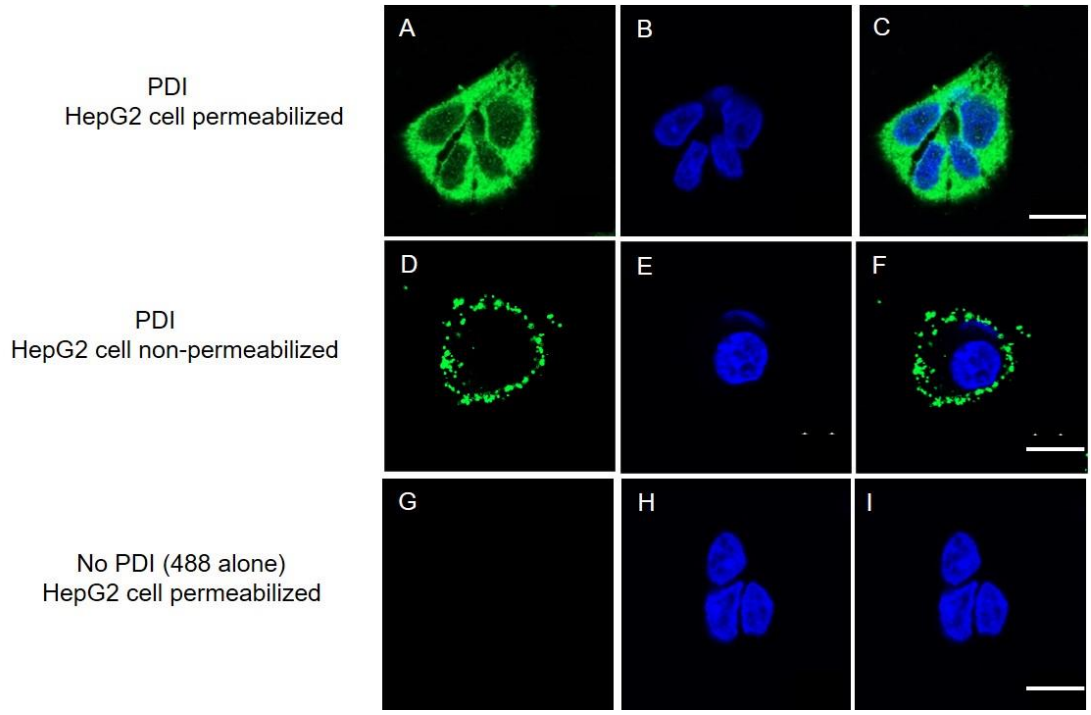

Figure 5.1. HepG2 cells express both cytoplasmic and plasma membrane PDI. (A, B and C) Permeabilized HepG2 cell; cytoplasmic PDI was labelled with anti-PDI antibody (RL90) and detected with Alexa Fluor 488 secondary antibody and the nucleus was stained with DAPI. (D, E and F) Non-permeabilized HepG2 cell; membrane PDI was labelled with anti-PDI antibody (RL90) and detected with Alexa Fluor 488. (G, H and I) Control IF (No anti-PDI antibody, only Alexa Fluor 488). Data is a representative of four independent experiments. Scale bar = 10 µm.

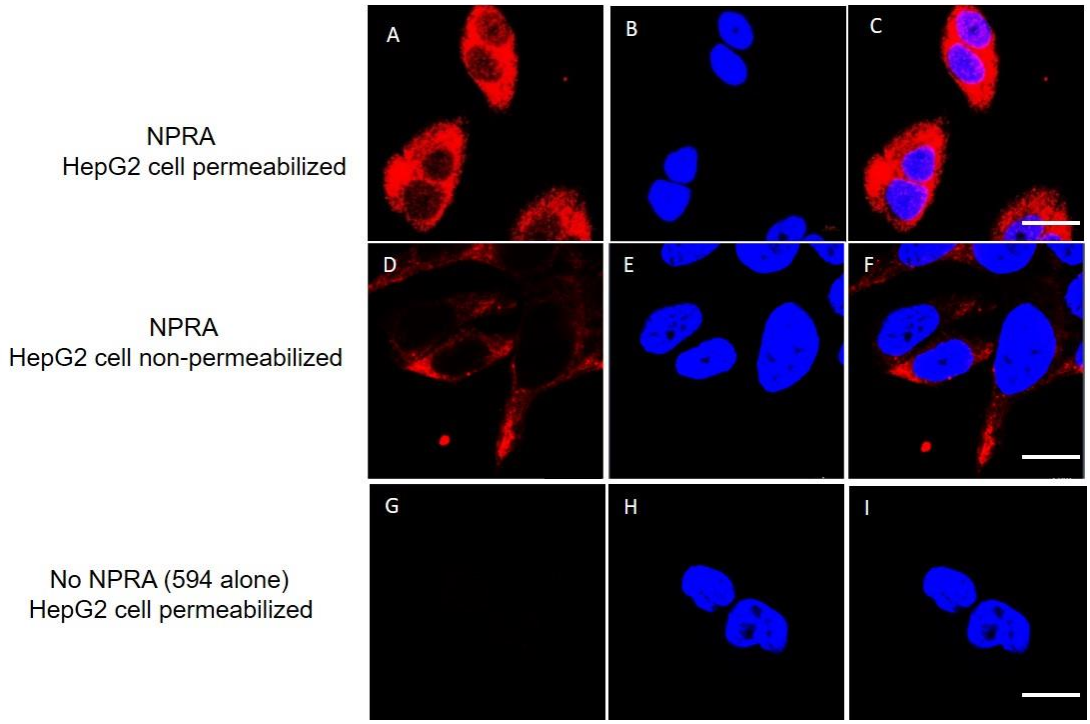

Figure 5.2. HepG2 cells express both cytoplasmic and plasma membrane NPRA. (A, B and C) Permeabilized HepG2 cells; cytoplasmic NPRA was labelled with anti-NPRA antibody and detected with Alexa Fluor 594 secondary antibody and the nucleus was stained with DAPI. (D, E and F) Non-permeabilized HepG2 cells; membrane NPRA was labelled with anti-NPRA antibody and detected with Alexa Fluor 594 secondary antibody. (G, H and I) Control IF (No anti-NPRA antibody, only Alexa Fluor 594). Data is a representative of three independent experiments. Scale bar = 10 µm.

5.3.2 Plasma membrane PDI colocalizes with membrane NPRA in HepG2 cells

To determine whether the plasma membrane PDI colocalizes with NPRA in HepG2 cells, we co-labelled the membrane PDI and NPRA with mouse anti-PDI antibody (RL90) and rabbit anti-NPRA antibody in non-permeabilized HepG2 cells. The confocal microscopy images (Figures 5.3A-E) showed that NPRA colocalizes with membrane PDI in HepG2 cells with a Pearson's correlation coefficient of 0.743 (74.3%). This data is consistent with the notion that membrane PDI and NPRA can interact.

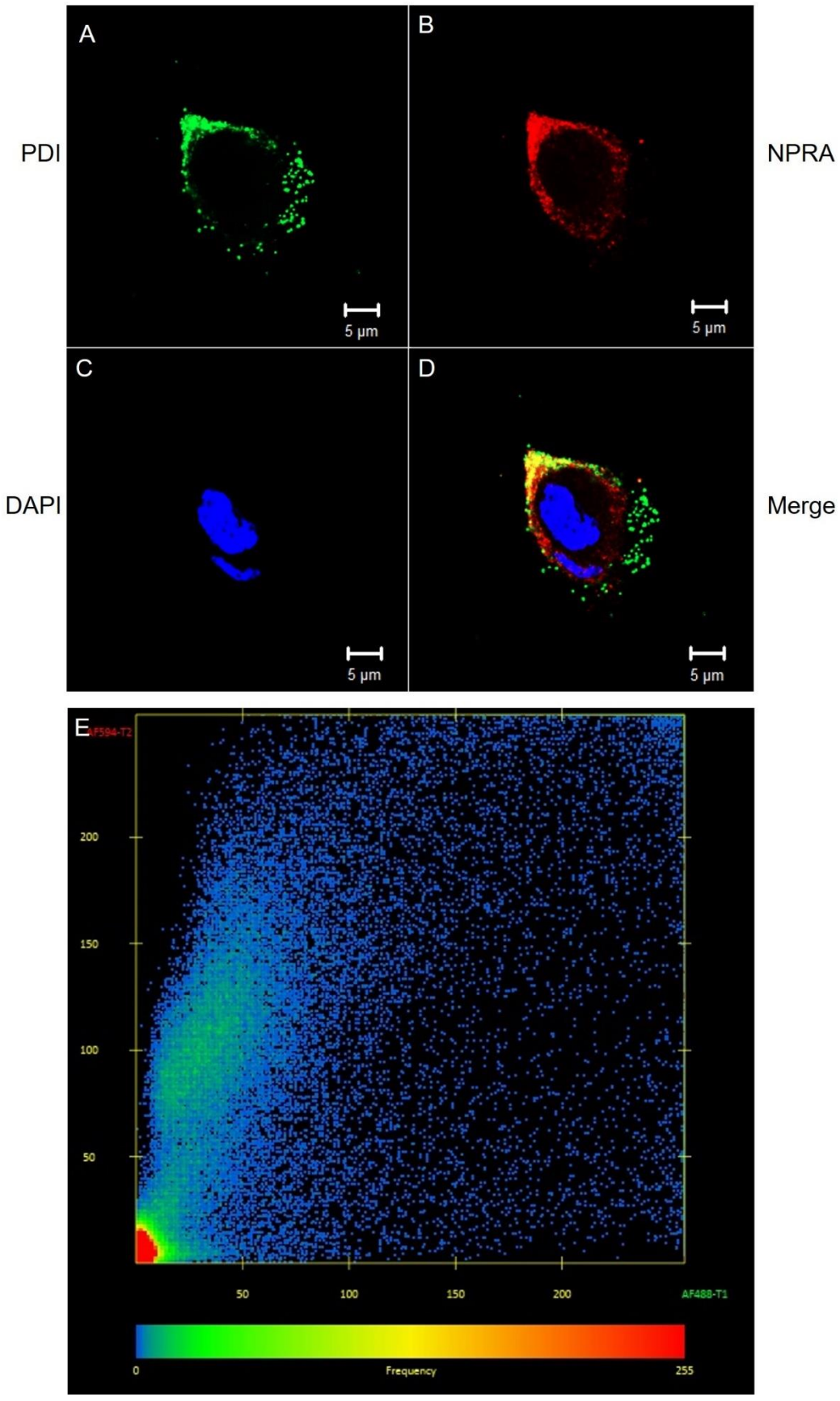
A
B
C
D
PDI
NPRA
DAPI
Merge
5 µm
5 µm
5 µm
5 µm
E
AF594-T2
200
150
100
50
50
100
150
200
AF488-T1
0
Frequency
255

Figure 5.3. Plasma membrane PDI colocalized with NPRA in HepG2 cell. (A). PDI (green) in non-permeabilized HepG2 cell detected with Alexa Fluor 488. (B) NPRA (red) in non-permeabilized HepG2 cell detected with Alexa Fluor 594. (C) nucleus (blue) stained with DAPI. (D) overlay of A, B and C. (E) Colocalization analysis of membrane PDI and NPRA (Pearson's correlation coefficient =0.743). Data is a representative of three independent experiments. Scale bar= 5 µm.

5.3.3 Brefeldin A (BFA) Inhibits PDI Externalization in HepG2 Cells

As PDI externalization route has been reported to be cell type specific (334) and till date the externalization route in hepatocytes remain unclear, we sought to investigate whether PDI externalization in hepatocytes occurs via the classical ER-Golgi-dependent route. To do this, we used BFA, a fungal macrocyclic lactone that disrupts ER-to-golgi protein translocation, thereby inhibiting golgi-dependent protein externalization. The data revealed that incubation of HepG2 cells with 5 µg/mL BFA for 4.5 hrs inhibited PDI externalization as compared to the control (Figure 5.4), consistent with PDI externalization occurring partly via the golgi-dependent route in HepG2 cells.

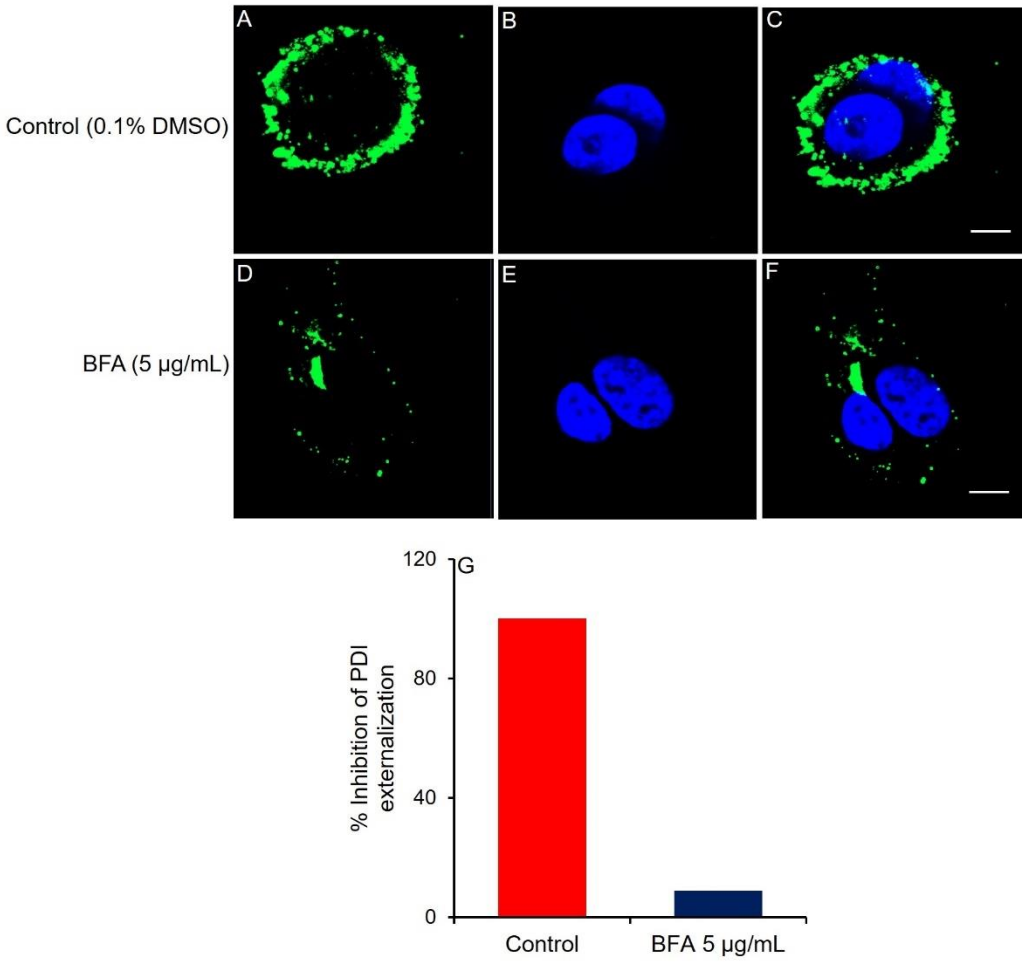

Figure 5.4. BFA inhibits PDI externalization in HepG2 cells. (A, B and C) membrane PDI in non-permeabilized HepG2 cell labelled with anti-PDI antibody (RL90). (D, E and F) Similar experiment post BFA (5 µg/mL) treatment. (G) membrane PDI expression level in both basal and BFA-treated conditions (expressed as percentage of the control). Control = 0.1 % DMSO vehicle. Data is a representative of three independent experiments. Scale bar = 5 µm.

5.3.4 HEK293 Cells Express Cytoplasmic and Membrane PDI and NPRA

We have shown that HepG2 cells express plasma membrane PDI and NPRA and we have also shown that these proteins colocalize on the membrane of these cells, consistent with the notion that these proteins interact. This colocalization provides an explanation for our observation of PDI modulating natriuretic peptide (NP) and Vitamin C (Vit C) elevation of cGMP and reduction of $[Ca^{2+}]_i$ in HepG2 cells in chapters 3 and 4. Since a similar observation of PDI modulating Vit C-mediated cGMP generation and $[Ca^{2+}]_i$ reduction was also made in HEK293 cells, in this part of the study we sought to investigate whether HEK293 cells also express PDI and NPRA on their membrane. HEK293 cells were labelled with anti-PDI (RL90) and anti-NPRA antibodies either with or without triton permeabilization. The data reveal that PDI (Figure 5.5) and NPRA (Figure 5.6) are expressed in both permeabilized and non-permeabilized HEK293 cells. The data clearly shows PDI (Figures 5.5D, E and F) and NPRA (Figures 5.6D, E and F) expression on the margin of the cell and the cellular projections in the non-permeabilized HEK293 cells, consistent with plasma membrane PDI and NPRA.

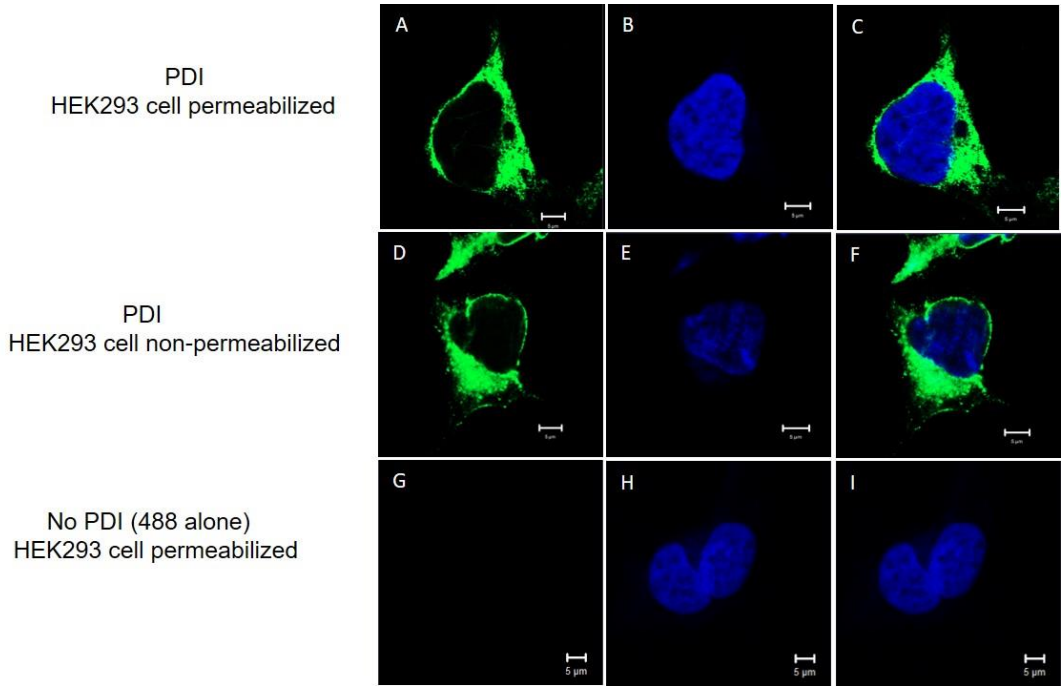

Figure 5.5. HEK 293 cells express cytoplasmic and membrane PDI. (A, B and C) Permeabilized HEK293 cell; cytoplasmic PDI was labelled with anti-PDI antibody (RL90) and detected with Alexa Fluor 488 secondary antibody and the nucleus was stained with DAPI. (D, E and F) Non-permeabilized HEK293 cell; membrane PDI was labelled with anti-PDI antibody (RL90) and detected with Alexa Fluor 488. (G, H and I) Control IF (No anti-PDI antibody, only Alexa Fluor 488). Data is a representative of two independent experiments. Scale bar = 5 µm.

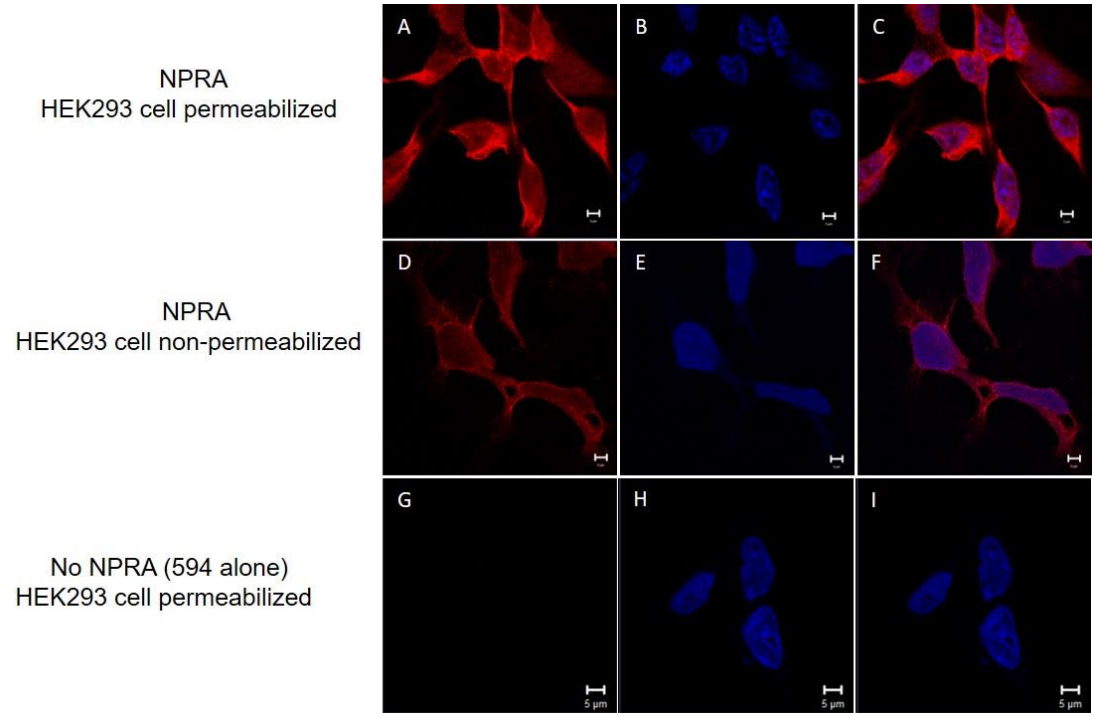

Figure 5.6. HEK 293 cells express cytoplasmic and membrane NPRA. (A, B and C) Permeabilized HEK293 cells; cytoplasmic NPRA was labelled with anti-NPRA antibody and detected with Alexa Fluor 594 secondary antibody and the nucleus was stained with DAPI. (D, E and F) Non-permeabilized HEK293 cells; membrane NPRA was labelled with anti-NPRA antibody and detected with Alexa Fluor 594 secondary antibody. (G, H and I) Control IF (No anti-NPRA antibody, only Alexa Fluor 594). Data is a representative of two independent experiments. Scale bar = 5 µm.

5.3.5 Primary human hepatocytes express cytoplasmic and Membrane PDI and NPRA

As our data revealed that HepG2 cells express cytoplasmic and membrane PDI and NPRA, we then sought to determine whether these proteins are also expressed in primary human hepatocytes (PHHs). PHHs were labelled with anti-PDI antibody (RL90) either with or without triton permeabilization. The data from the permeabilized PHHs revealed a distribution of both the PDI (Figure 5.7) and NPRA (Figure 5.8) throughout the intracellular space, most likely the ER. Whereas, in the Non-permeabilized cells, both PDI (Figure 5.7) and NPRA (Figure 5.8) expression were restricted to the cell margin, consistent with plasma membrane localized PDI and NPRA.

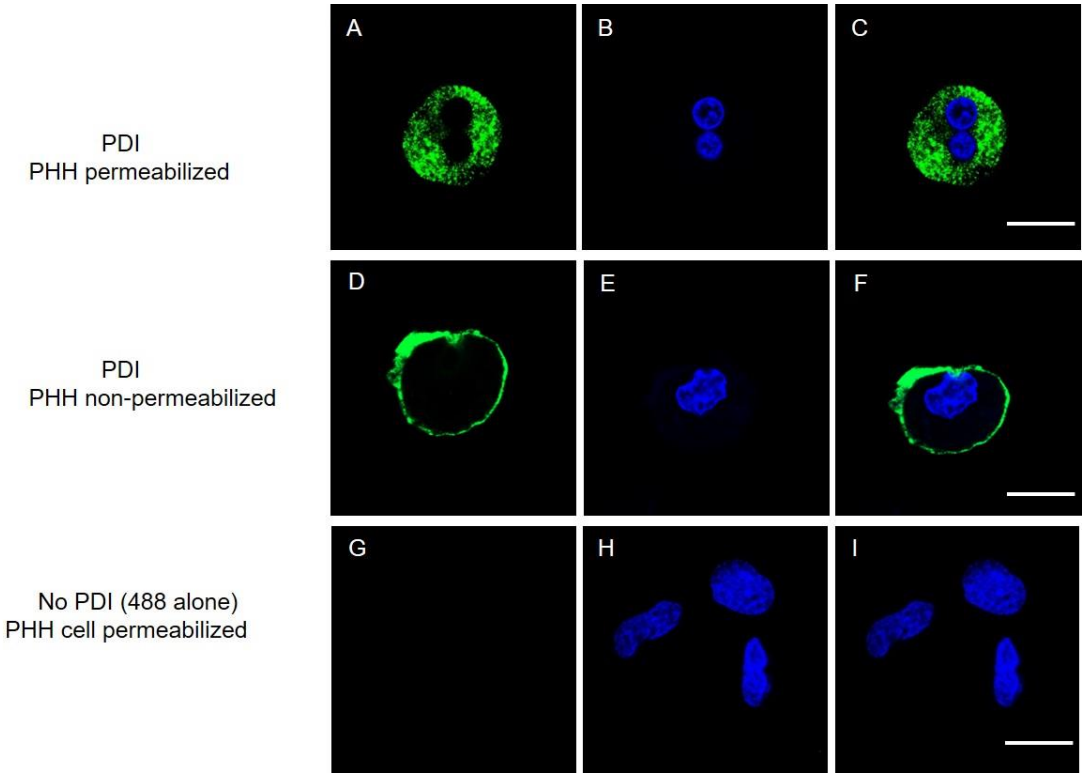

Figure 5.7. PHHs express cytoplasmic and membrane PDI. (A, B and C) Permeabilized PHH; cytoplasmic PDI was labelled with anti-PDI antibody (RL90) and detected with Alexa Fluor 488 secondary antibody and the nucleus was stained with DAPI. (D, E and F) Non-permeabilized PHH; membrane PDI was labelled with anti-PDI antibody (RL90) and detected with Alexa Fluor 488. (G, H and I) Control IF (No anti-PDI antibody, only Alexa Fluor 488). Data is a representative of four independent experiments. Scale bar = 10 µm.

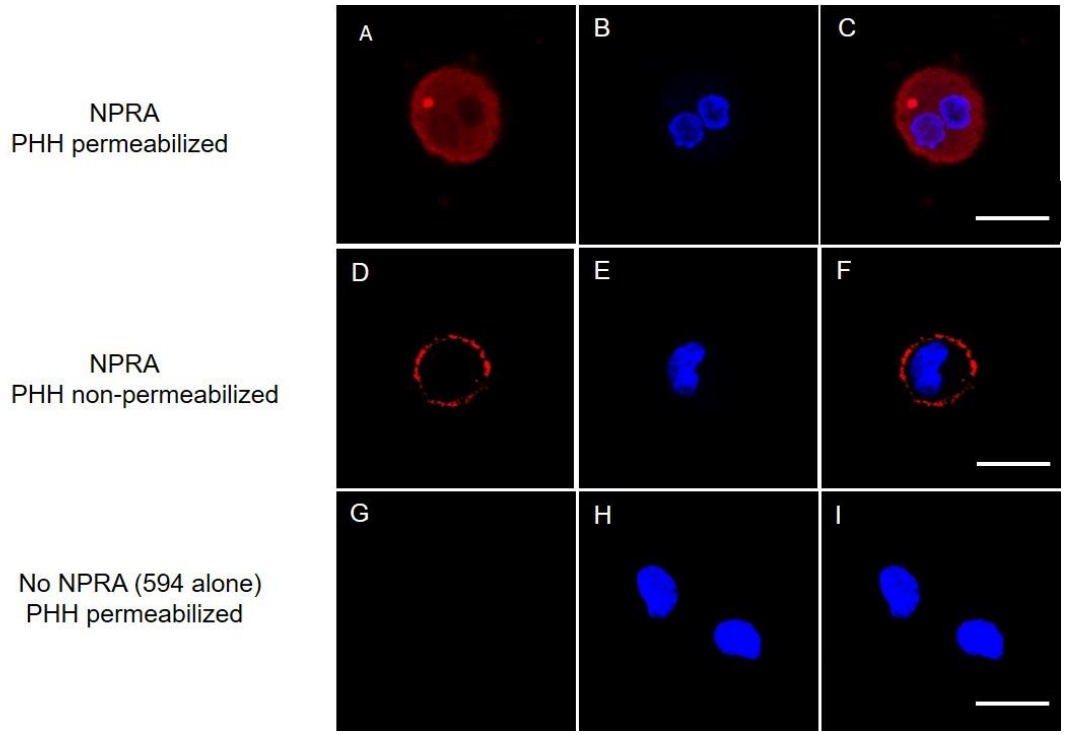

Figure 5.8. PHHs express both cytoplasmic and plasma membrane NPRA. (A, B and C) Permeabilized PHH; cytoplasmic NPRA was labelled with anti-NPRA antibody and detected with Alexa Fluor 594 secondary antibody and the nucleus was stained with DAPI. (D, E and F) Non-permeabilized PHH; membrane NPRA was labelled with anti-NPRA antibody and detected with Alexa Fluor 594 secondary antibody. (G, H and I) Control IF (No anti-NPRA antibody, only Alexa Fluor 594). Data is a representative of three independent experiments. Scale bar = 10 µm.

5.3.6 Plasma membrane PDI colocalizes with NPRA in PHHs

As primary cells represent more what is happening *in vivo* compared to cell lines, having confirmed that membrane PDI colocalizes with NPRA in HepG2 cells, we sought to determine whether this is consistent in PHHs. We double-labelled PHHs with mouse anti-PDI antibody (RL90) and rabbit anti-NPRA antibody. The data revealed that membrane PDI colocalizes with membrane NPRA in PHHs (Figure 5.9) with a Pearson's correlation coefficient of 0.952 (95.2%), in line with our observation in HepG2 cells. This data is consistent with the notion that membrane PDI and NPRA can interact in PHHs.

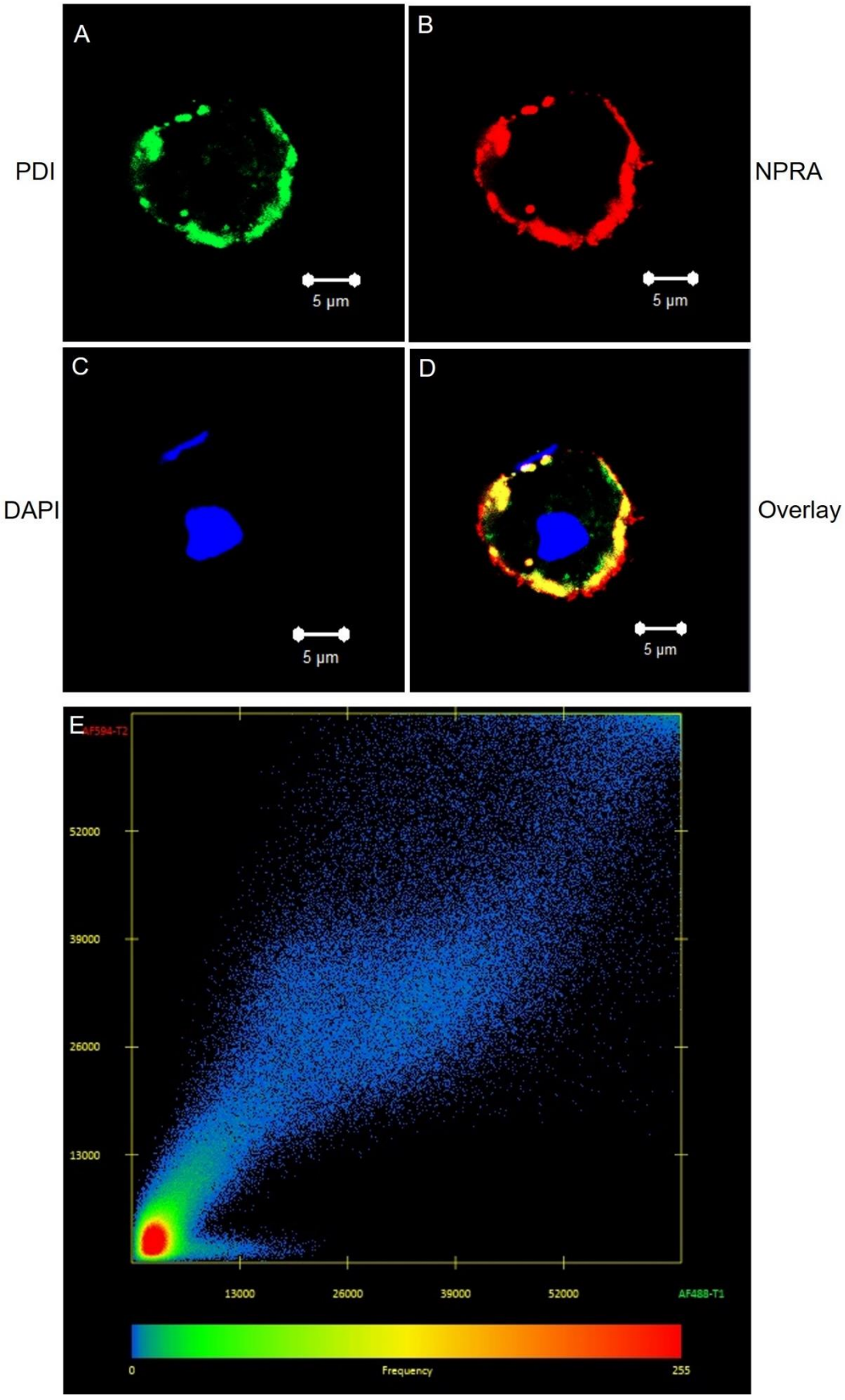
A
B
PDI
NPRA
5 µm
5 µm
C
D
DAPI
Overlay
5 µm
5 µm
E
AF594-T2
52000
39000
26000
13000
13000
26000
39000
52000
AF488-T1
0
Frequency
255

Figure 5.9. Membrane PDI colocalized with membrane NPRA in PHHs. (A) PDI (green) in non-permeabilized PHH detected with Alexa Fluor 488. (B) NPRA (red) in non-permeabilized PHH detected with Alexa Fluor 594. (C) nucleus (blue) detected with DAPI. (D) overlay of A, B and C. (E) Colocalization analysis of membrane PDI and NPRA (Pearson's correlation coefficient =0.952). Data is a representative of three independent experiments. Scale bar = 5 µm.

5.3.7 BFA inhibits PDI externalization in PHHs

As our data suggests that PDI externalization in HepG2 cells was inhibited by BFA, we then sought to investigate whether BFA treatment would have any effect on PDI externalization in PHHs. PHHs were incubated in BFA (5 µg/mL for 4.5 hrs) prior to membrane PDI labelling. The data revealed that BFA inhibited PDI externalization as compared to the control (Figures 5.10), consistent with the notion that ER-golgi protein translocation route is involved in PDI externalization in PHHs.

.

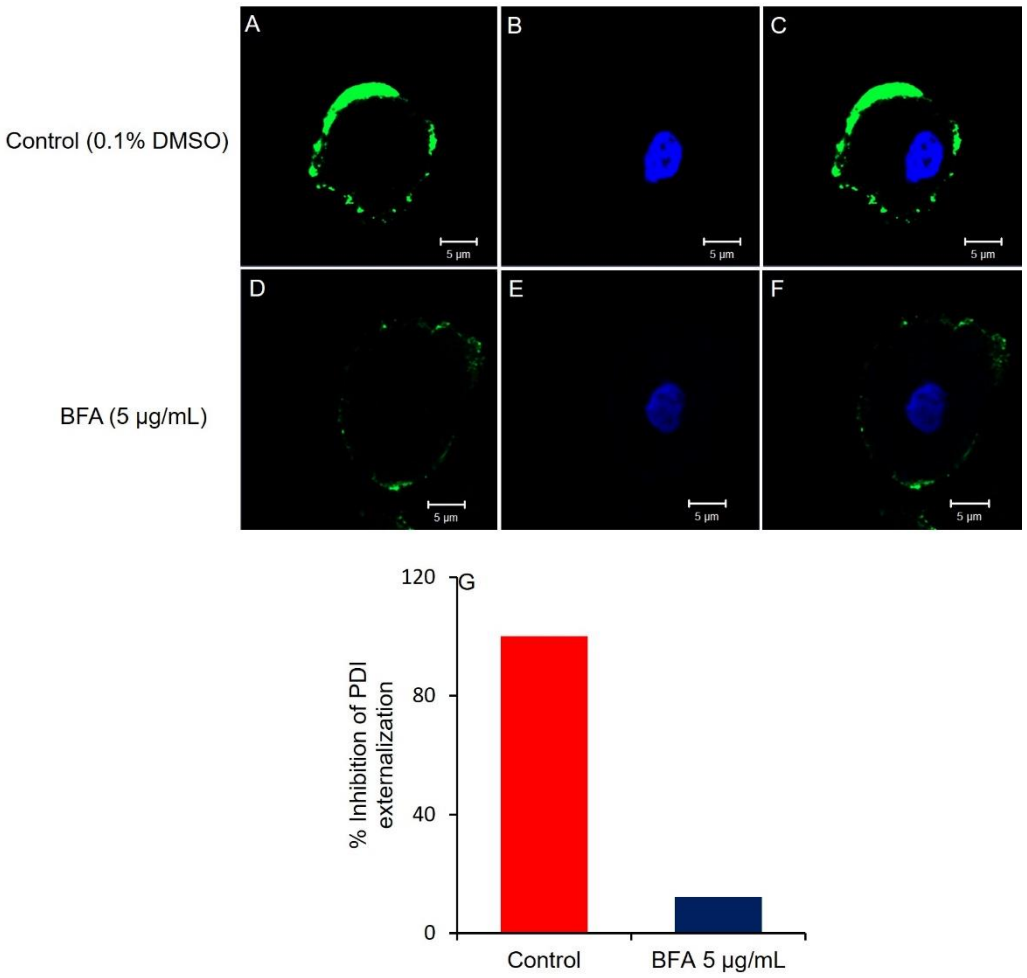

Figure 5.10. BFA Inhibits PDI Externalization in PHHs. (A, B and C) membrane PDI in Non-permeabilized HepG2 cells labelled with anti-PDI antibody (RL90). (D, E and F) Similar experiment post BFA (5 µg/mL) treatment. (G) membrane PDI expression level in both basal and BFA-treated conditions. Control = 0.1 % DMSO vehicle. Data is a representative of three independent experiments. Scale bar = 5 µm.

5.4 Discussion

We show here that human hepatocytes; the human liver cancer cell line HepG2 cells and primary human hepatocytes (PHHs), as well as HEK293 cells express cytoplasmic and plasma membrane PDI and NPRA. We also show that the plasma membrane PDI colocalizes with membrane NPRA in HepG2 cells and PHHs, consistent with the notion that the two proteins interact at the cell membrane. Using BFA, a widely used inhibitor of ER-golgi protein translocation, we have demonstrated the involvement of the golgi-dependent route in PDI externalization in both HepG2 cells and PHHs.

PDI expression on the plasma membrane of various cell types including rat hepatocytes is becoming increasingly evident even though the protein had widely been thought to be ER-resident due to the presence of the C terminal ER retention KDEL sequence (333, 334, 336). Importantly, the membrane PDI is revealing vital roles in cGMP signalling in some of the cell types where it is expressed, including HUVECs, HASMCs and HMCs where plasma membrane localized PDI was reported to modulate natriuretic peptide (NP)-mediated generation of cGMP (333). In line with this, the data in chapters 3 and 4 respectively were consistent with membrane PDI modulating ANP and Vit C elevation of cGMP and reduction of $[Ca^{2+}]_i$ in HepG2 and HEK293 cells. Pan and colleagues had suggested that membrane PDI mediates this important role in cGMP signalling by colocalizing with the natriuretic peptide receptors type A and B (NPRA and NPRB) and by directly interacting with the NPRs and their ligands, consequently modulating their effects (333). Other studies have also demonstrated that PDI catalyses the isomerization of the disulphide bonds on cell surface proteins (372-375), and this interaction is thought to alter

the conformation of the proteins, consequently altering their functions (333). Taking together, we therefore hypothesized that our observation in chapters 3 and 4 of PDI modulating ANP and Vit C effect on cGMP and Ca^{2+} signalling in HepG2 and HEK293 cells could be due to a possible expression and colocalization of PDI and NPRs on the membrane of these cells. We therefore sought to confirm the involvement of PDI in the ANP and Vit C-mediated generation of cGMP and attenuation of $[Ca^{2+}]_i$ by investigating its presence and cellular localization/colocalization with NPRA (NPR type A) on the membrane of these cells. We also sought to investigate whether this applies to PHHs as this would then enable us to predict whether the PDI modulation of cellular cGMP and $[Ca^{2+}]_i$ signal observed in HepG2 and HEK293 cells can be relevant to PHHs.

Immunofluorescence was used to investigate the presence and cellular localization of PDI and NPRA in HepG2 cells, HEK293 cells and PHHs. The data revealed the expression of both cytoplasmic (in permeabilized cells) and membrane (in non-permeabilized cells) PDI and NPRA in HepG2 cells (Figures 5.1 and 5.2), HEK293 cells (Figures 5.5 and 5.6) and PHHs (Figures 5.7 and 5.8). One important feature of the membrane PDI distribution pattern in HepG2 cells is its vesicular/patch-like appearance (Figure 5.1) compared to the majorly smooth ring-like distribution pattern of that of PHHs (Figure 5.7).

In addition to the confirmation of the presence and cellular localization of PDI and NPRA in the three different cell types used in this study, immunofluorescence analysis also revealed that the two proteins colocalizes on the plasma membrane of HepG2 cells and PHHs (Figures 5.3 and 5.9 respectively) with a Pearson correlation coefficient of 0.743 and 0.952 for

HepG2 and PHH respectively. This is in line with the previous studies mentioned earlier that reported a colocalization of membrane PDI and NPRA in HUVECs and PDI and NPRB in HMCs (333). However, we did not investigate the colocalization of the two proteins in HEK293 cells. The data confirms the PDI modulation of ANP and Vit C mediated cGMP elevation and $[Ca^{2+}]_i$ reduction in HepG2 cells observed in chapters 3 and 4 respectively, in line with the submission of Pan and colleagues that the colocalization of membrane PDI and NPRs in HUVECs and HMCs allows the isomerase to physically interact with the NPRs and their NP ligands and thus to modulate their effects. One key observation made on the colocalization of these two proteins in HepG2 cells and PHHs was that the immunofluorescence data revealed a higher level of colocalization between the two proteins on PHH membrane compared to their colocalization on the HepG2 cell membrane as revealed by both the immunofluorescence image and the Zen colocalization analysis (Figure 5.3 Vs Figure 5.9). These data may suggest a higher degree of interaction between the membrane PDI and NPRA in PHHs compared to HepG2 cells.

Despite the increasing evidence of membrane PDI expression in several cell types, its route of externalization is still not clear. Previous studies in other cell types, however, suggest that the externalization route is cell type dependent. In VSMCs, PDI externalization was shown to follow a non-classical golgi-independent route, while in ECs, the externalization was reported to be partly via the golgi-dependent route and partly via a non-classical route (334, 335). Curiously, we sought to investigate whether PDI externalization in hepatocytes is supported by the classical ER-golgi translocation path using BFA. In line

with the observation in ECs (335), our data showed that incubation of HepG2 cells and PHHs in BFA inhibited membrane PDI expression level in these cells. This is consistent with the notion that the ER-golgi protein translocation route is involved in PDI externalization in HepG2 cells and PHHs. However, we cannot ascertain how good a tool BFA alone is to make this distinction, hence, a further study with other agents that disrupts the ER-golgi protein translocation route such as monensin would help provide more information on the externalization route of PDI in hepatocytes. Unfortunately, resources did not let us explore this.

In conclusion, we have been able to establish that HepG2 cells, HEK293 cells and PHHs express cytoplasmic and plasma membrane localized PDI and NPRA. We have also shown that membrane PDI at the level of immunofluorescence colocalizes with NPRA in HepG2 cells and PHHs, however, it would be useful to confirm the colocalization by co-immunoprecipitation. PDI by colocalizing with NPRs, may physically interact with the receptors and their NP ligands, consequently modulating their cGMP generation effects (333). We believe that the PDI modulation of ANP effects in chapters 3 and 4 is due to its interaction with NPRA and ANP owing to its colocalization with NPRA in HepG2 cells. Since Vit C has been shown to elevate cGMP via the same pathway as ANP (329), we propose that the PDI modulation of Vit C effect on cGMP and Ca^{2+} signal observed in chapters 3 and 4 respectively is likely due to its interaction with Vit C and with NPRA present on the HepG2 cell membrane. Investigation of the effect of BFA on PDI externalization revealed that BFA inhibits PDI externalization in HepG2

cells and PHHs, consistent with the notion that the ER-golgi protein translocation route is involved in PDI externalization in human hepatocytes.

Chapter 6

Exploring the hepatoprotective effect of vitamin C against Ca^{2+}-mediated damage and the role of protein disulphide isomerase

6.1 Introduction

Vitamin C (Vit C) is a potent antioxidant due to its ability to donate an electron to a substrate while itself becomes oxidised to a relatively stable ascorbyl radical. This way, Vit C reduces or scavenges physiologically/pathophysiologically relevant free radicals and reactive oxygen species (ROS). Studies have shown that Vit C protects liver and hepatocytes against heavy metals, drugs, insecticides, and other chemical-induced hepatotoxicity. Vit C protects rat hepatocytes against acetaminophen (317) and alcohol (320) induced toxicity, as well as rat liver against gasoline vapour-induced damage (376). Vit C also protects mice liver against 5-fluorouracil-induced hepatotoxicity (319). Traditionally, these hepatoprotective effects of Vit C have been attributed to its direct antioxidant power/free-radical scavenging ability, however, ER stress and perturbation of $[Ca^{2+}]_i$ have emerged as important events in drug-induced liver injury (DILI) (203, 206, 377). Acetaminophen induces liver damage through its reactive metabolite NAPQI which depletes glutathione present in cells and binds covalently to proteins, consequently leading to mitochondrial dysfunction, oxidative stress and hepatocyte death by necrosis (378). Diclofenac (DCLF) metabolism produces its reactive metabolite *p*-benzoquinoneimines, which can bind to ER proteins, resulting in ER stress and consequent elevation of $[Ca^{2+}]_c$ (379-381). Interestingly, chelation of intracellular Ca^{2+} and inhibition of IP_3R ameliorates DCLF-induced cytotoxicity in HepG2 cells (382). The points above suggest that, in addition to release of free radicals, Ca^{2+} perturbations are key events in drug-induced liver damage, suggesting that Vit C-mediated

hepatoprotection might not entirely be via its free radical-scavenging ability, but also by other mechanism(s) that involve attenuation of Ca^{2+} perturbations.

Interestingly, evidence show that Vit C modulates cellular cGMP (329, 383) and Ca^{2+} (332) in a variety of cells and tissues and previous studies from our group have shown that elevated cellular cGMP protects rat hepatocytes against Ca^{2+}-mediated damage (225). Unpublished data from our group also revealed that Vit C elevates cGMP, and through PKG, stimulates plasma membrane Ca^{2+} efflux, thereby decreasing $[Ca^{2+}]_i$ and protecting rat hepatocytes against Ca^{2+}-mediated cell death. In chapters 3 and 4 of this study, we showed that Vit C elevates cGMP in HepG2 cells and attenuates Tg-induced $[Ca^{2+}]_i$ elevations.

In addition to Vit C modulation of cellular cGMP and Ca^{2+} signal in HepG2 cells, our data in chapters 3 and 4 also revealed that the mechanism was regulated by csPDI. Inhibition of PDI with Bac and RL90, which have previously been used to examine the function of csPDI (333), attenuated Vit C-induced elevations in cGMP (chapter 3) and reduction in $[Ca^{2+}]_i$ (chapter 4). In confirmation of the above findings, our data in chapter 5 showed that PDI colocalizes with NPRA on the membrane of HepG2 cells and PHHs

6.2 Aims

Since elevated cellular cGMP has been reported to protect rat hepatocytes against Ca^{2+}-mediated cell death (225), in this chapter, we aimed to investigate whether the Vit C-induced elevations in cellular cGMP and reductions in $[Ca^{2+}]_i$ observed in HepG2 cells (chapters 3 and 4) would result in the protection of the cells against the hepatotoxic actions of Ca^{2+} elevators. Also, our data in chapters 3, 4 and 5 were consistent with csPDI modulation of the cGMP elevation and $[Ca^{2+}]_i$ reduction action of Vit C, demonstrated with the PDI inhibitors Bac and RL90. Therefore, in this chapter we aimed to investigate whether inhibiting PDI with these agents (Bac and RL90) would affect the cGMP-mediated hepatoprotective action of Vit C. In addition, we sought to see If the hepatoprotective actions of Vit C observed in HepG2 cells could be achieved in PHHs.

6.3 Results

6.3.1 Determination of Tg Working Concentration on HepG2 Cells

To investigate whether Vit C protects hepatocytes against Ca^{2+}-mediated cell death, we sought to treat HepG2 cells (our model hepatocyte cell line) with an agonist that elevates $[Ca^{2+}]_c$. We utilized Tg which elevates $[Ca^{2+}]_c$ by irreversibly inhibiting the Sarco/endoplasmic reticulum Ca^{2+} ATPase (SERCA), thus inhibiting the sequestration of cytosolic Ca^{2+} into the ER. We first performed a concentration response experiment for Tg on the HepG2 cells in order to establish a concentration of Tg that would reduce the viability of HepG2 cells to less than 50% which we would then use as our working concentration. In order to do this, HepG2 cells were treated with different concentrations of Tg and incubated in a 5 % CO_2 humidified incubator maintained at a temperature of 37^{o}C for 24 hrs and 48 hrs. Following the 24 and 48 hrs incubation, CellTitre Glo luminescent cell viability assay was performed on the Tg-treated cells. The assay determines the number of active viable cells based on quantitation of the ATP present, an indication of metabolically active cells. The data revealed that 4 µM Tg reduced the viability of HepG2 cells to 55.24 and 40.72 % at 24 hrs and 48 hrs respectively post Tg-treatment (Figure 6.1) which we then used as our Tg working concentration in the subsequent Tg-induced hepatotoxicity experiments.

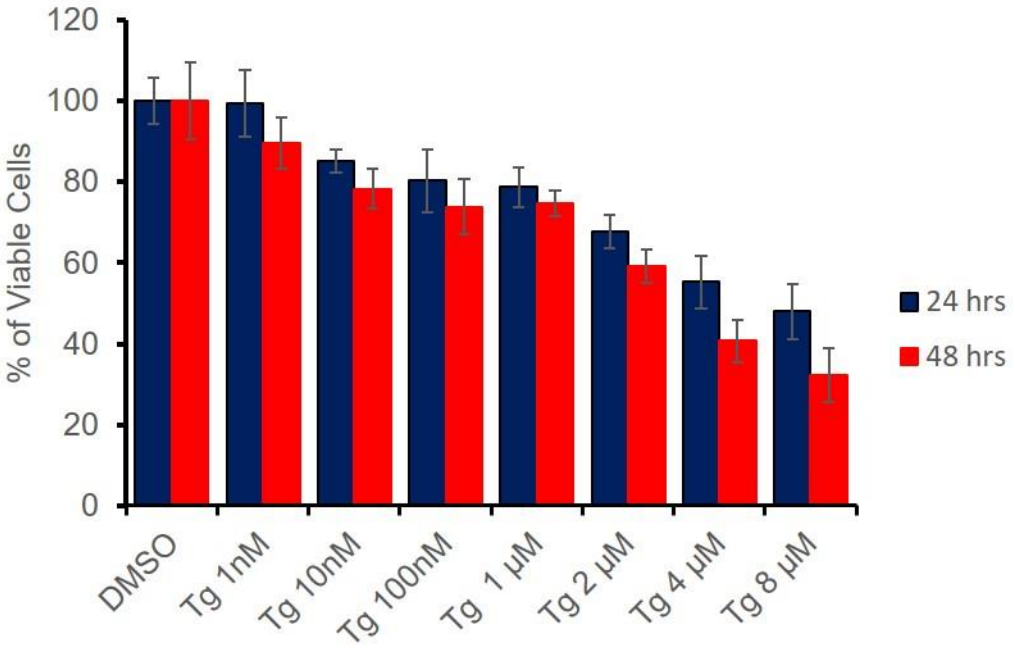

Figure 6.1 Concentration-response of Tg on HepG2 cells. The bar graph summarises cell death induced by different concentrations of Tg on HepG2 cells at 24 hrs (blue bars) and 48 hrs (red bars) post Tg-treatment. Data represent mean±SEM. n= 3 wells from one experiment performed in triplicate.

6.3.2 cGMP elevators (Vit C, ANP and SNP) abrogates Tg-induced hepatotoxicity in HepG2 cells

To determine whether Vit C protects hepatocytes from Tg-induced cell death, HepG2 cells were treated with 4 µM Tg in combination with or without Vit C (1.25 mM and 10 mM). Known cGMP elevators; ANP (200 nM and 600 nM) and SNP (100 µM and 200 µM) were used as positive controls. Following a 24 hr and 48 hr incubation, a CellTitre-Glo luminescent cell viability assay was performed on the treated cells. The data revealed that 1.25 mM Vit C protected HepG2 cells against Tg-induced damage at the two different time points (24 and 48 hrs), whereas 10 mM Vit C enhanced the hepatotoxic effect of Tg. SNP (100 µM and 200 µM) did not confer any protection on the HepG2 cells at the 24-hr end point, but protection was observed at the 48-hr end point. ANP (200 nM and 600 nM) protected HepG2 cells from Tg-induced damage at the 24 hr end point, however, this protection was not observed at the 48 hr end point (Figure 6.2).

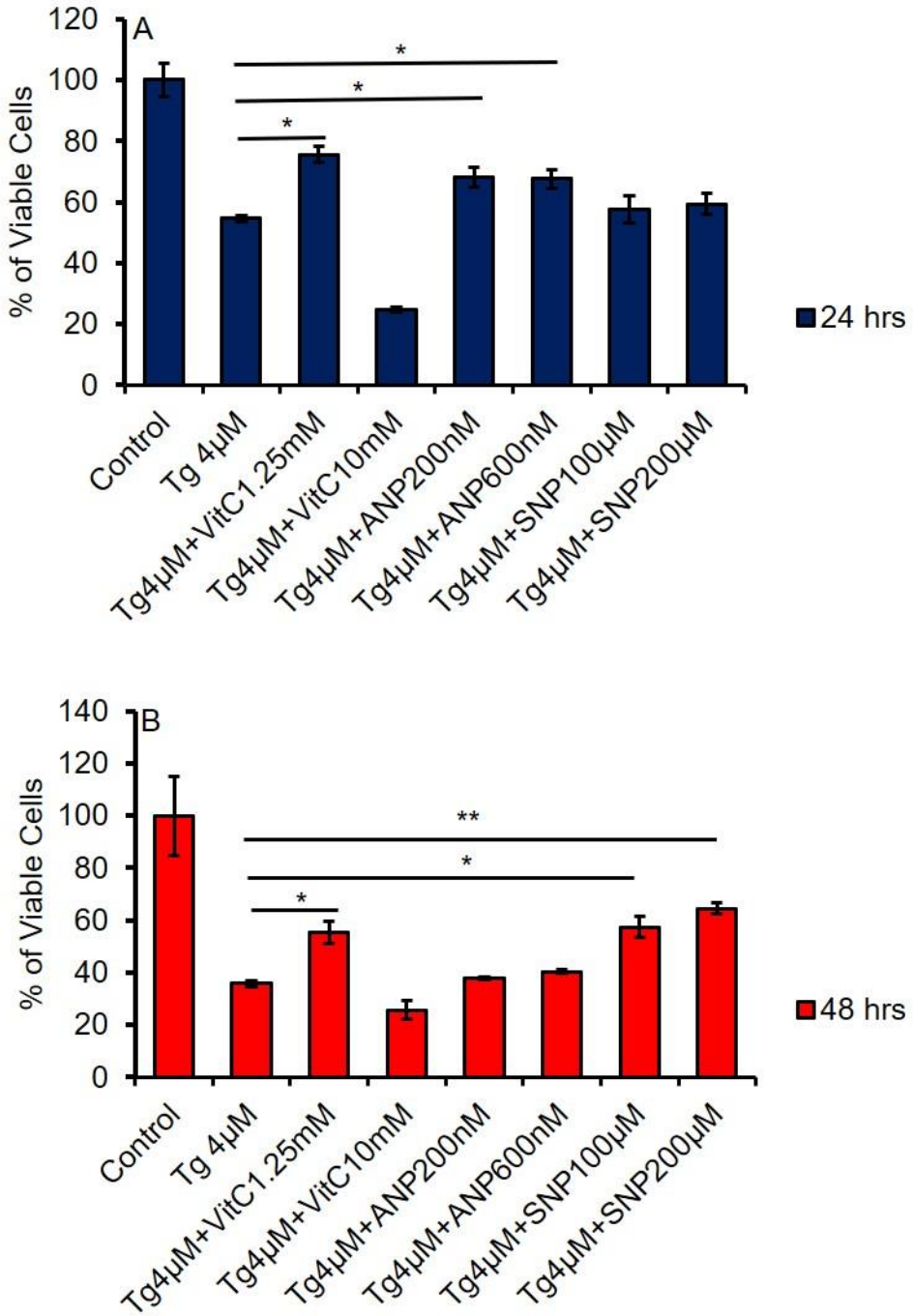

Figure 6.2. Vit C, ANP and SNP protects against Tg-induced HepG2 cell damage. (A) The bar graph summarises the hepatoprotective effect of different concentrations of Vit C, ANP and SNP against Tg-induced HepG2 cell death at 24 hrs post treatment. (B) The bar graph summarises the hepatoprotective effect of different concentrations of Vit C, ANP and SNP against Tg-induced HepG2 cell death at 48 hrs post treatment. Control = 0.1

% DMSO vehicle. Data represent mean±SEM (n= 6 wells from 3 experiments performed in duplicate). (*p value ≤0.05, **p value ≤0.01).

6.3.3 Investigating the effect of Vit C, ANP and SNP on the viability of HepG2 cells

Since we observed that 10 mM Vit C had additive hepatotoxic effect with Tg on HepG2 cells, we sought to investigate what the effect of treating the cells with Vit C, SNP and ANP alone (without Tg) would be. To do this, we treated HepG2 cells with the different concentrations of Vit C (1.25 mM and 10 mM), SNP (100 µM and 200 µM) and ANP (200 nM and 600 nM) that was used in the previous experiment. The data revealed that only 10 mM Vit C had a significant damaging effect on the HepG2 cells at the two endpoints, while the other agents had no significant effect on the cell viability (Figure 6.3).

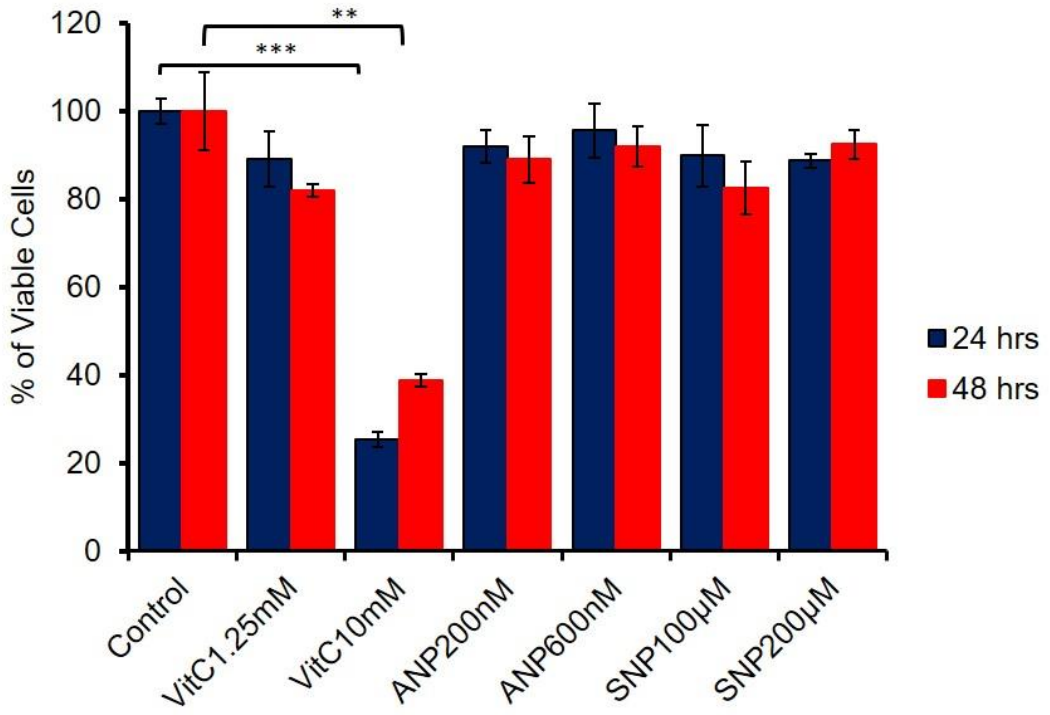

Figure 6.3. The effect of Vit C, ANP and SNP on HepG2 cell viability. The bar graph summarises the effects of Vit C, ANP and SNP on HepG2 cell viability at 24 hrs (blue bars) and 48 hrs (red bars) post treatment. Data represent mean±SEM (n=6 wells from 3 experiments performed in duplicate). (**p value ≤0.01, ***p value ≤0.001).

6.3.4 Investigating the effect of lower concentrations of Vit C on the viability of HepG2 cells

As we were keen on determining the lowest concentration of Vit C (as closest to the plasma Vit C concentration as possible) that would protect hepatocytes from Ca^{2+}-mediated damage, we sought to investigate what effect lower concentrations of the vitamin would have on HepG2 cells and subsequently investigated whether these concentrations would confer any protection on the cells. We treated HepG2 cells with different concentrations of Vit C (from 0 nM to 1 mM) and then performed a CellTitre Glo luminescent cell viability assay at 24-hr and 48-hr endpoint. The data revealed that these concentrations of Vit C had no cytotoxic effect on HepG2 cells. Surprisingly, a higher viability was observed with the 250 µM Vit C-treated cells as compared to the control (Figure 6.4A).

We then treated the HepG2 cells with Tg in combination with or without these lower Vit C concentrations. The data revealed that concentrations of Vit C from 100 µM and above significantly protected HepG2 cells against the cytotoxic effect of Tg (Figure 6.4B).

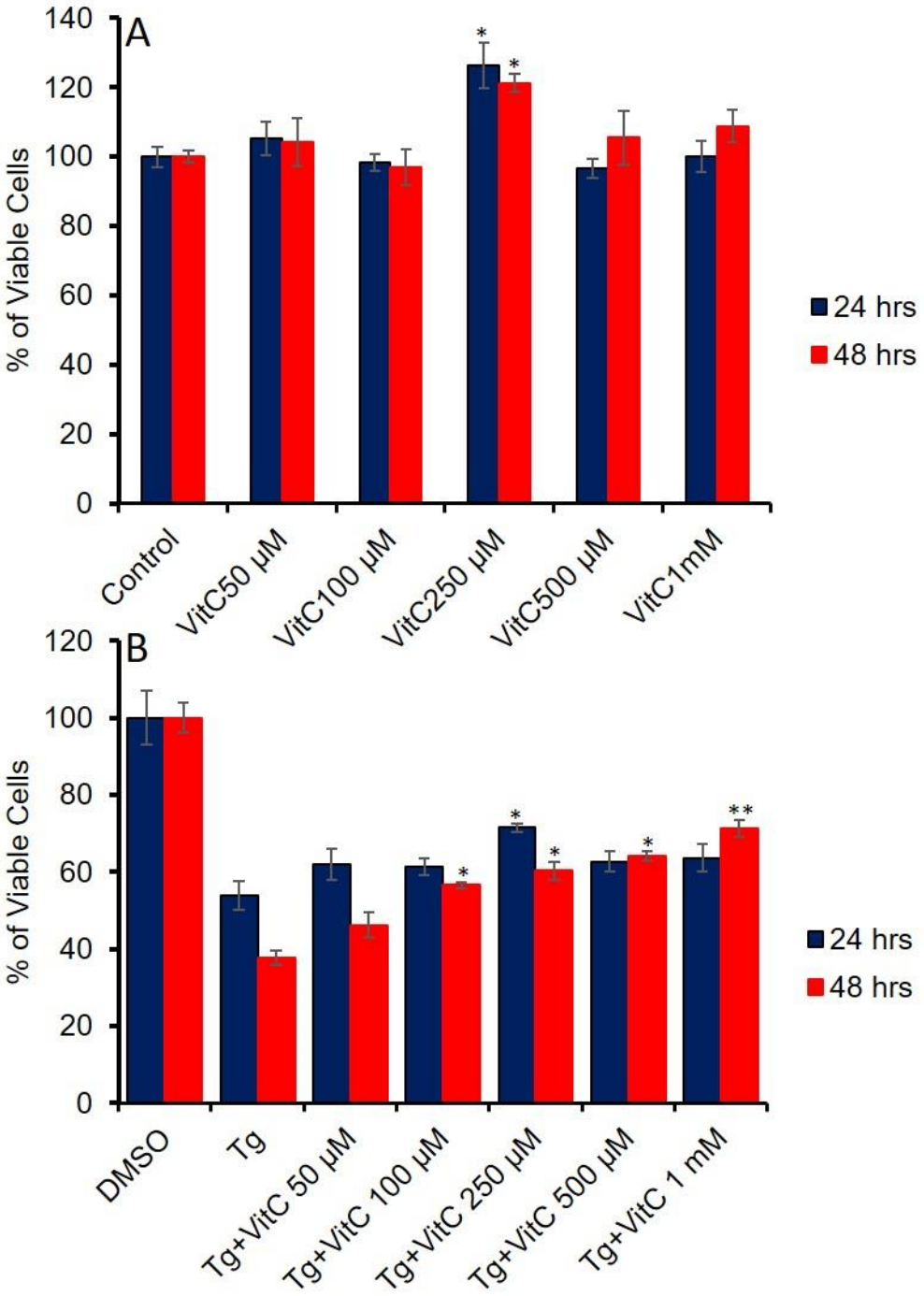

Figure 6.4. The effect of various concentrations of Vit C on HepG2 cell viability (A) The bar graph summarises the effect of different concentrations of Vit C (50 µM to 1 mM) on basal HepG2 cell viability at 24 hrs (blue bars) and 48 hrs (red bars) post treatment. (B) The bar graph summarises the effect of the different concentrations of Vit C used in A (50 µM to 1 mM) on Tg-

induced HepG2 cell damage at 24 hrs (blue bars) and 48 hrs (red bars) post treatment. DMSO control = 0.1 % DMSO vehicle. Data represent mean±SEM (n=6 wells from 3 experiments performed in duplicate). (*p value ≤0.05, **p value ≤0.01).

6.3.5 Vit C protection of HepG2 cell is cGMP-mediated

We then sought to determine whether the Vit C-mediated protection against Tg-induced HepG2 cell damage was cGMP-mediated. To do this, we utilized Rp-8-br-cGMP; a cell permeant cGMP analogue that binds to cGMP-dependent protein kinase (PKG) without activating it, thereby resulting in competitive inhibition of PKG and abrogating the PKG-dependent downstream effects of cGMP. The data revealed that Rp-8-Br-cGMP (50 µM) attenuated the cytoprotective effect of Vit C (1 mM) against Tg (4 µM)-induced HepG2 cell damage (Figure 6.5), consistent with the notion that the Vit C-mediated hepatoprotection against Tg-induced HepG2 cell damage is cGMP-mediated.

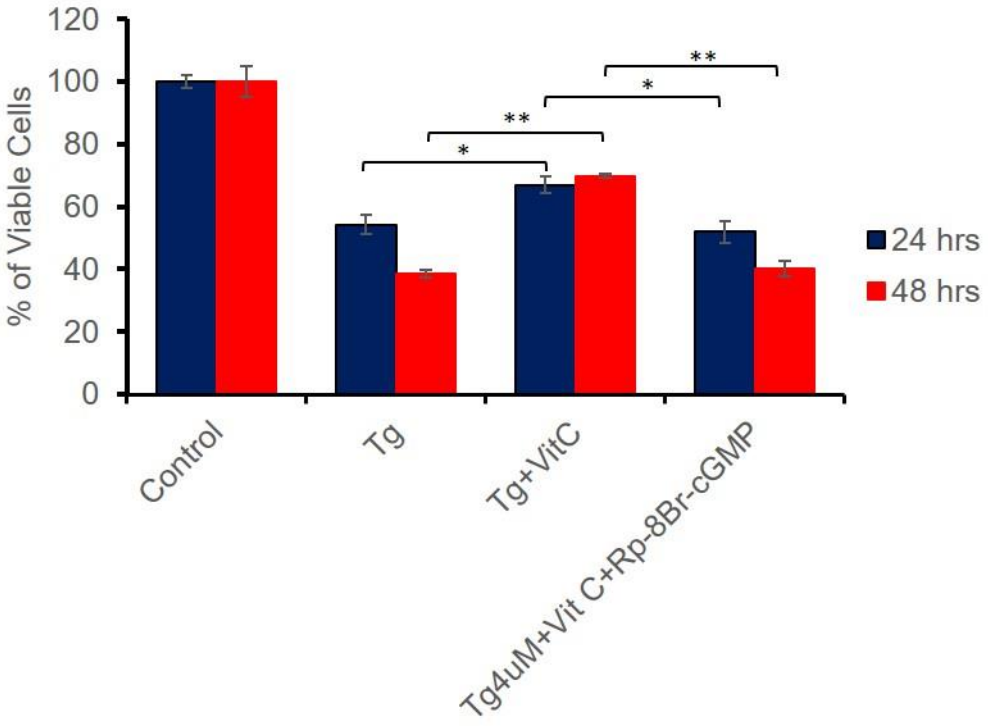

Figure 6.5. Vit C protection of HepG2 cells against Tg-induced cell damage is downregulated by the PKG inhibitor Rp-8-Br-cGMP. The bar graph summarises the effect of Rp-8-Br-cGMP (50 µM) on Vit C-mediated protection of HepG2 cells against Tg-induced cell damage at 24 hrs (blue bars) and 48 hrs (red bars) post treatment. DMSO control = 0.1 % DMSO vehicle. Data represent mean±SEM (n=9 wells from 3 experiments performed in triplicate). (*p value ≤0.05, **p value ≤0.01).

6.3.6 Investigating the involvement of csPDI in the Vit C-mediated HepG2 cell protection

As our data in chapters 3 and 4 revealed that inhibition of PDI with RL90 and Bac attenuated Vit C-induced cGMP generation and reduction of $[Ca^{2+}]_i$, we sought to investigate the effect of PDI inhibition on Vit C-mediated HepG2 cell protection against Tg-induced cell death. We treated HepG2 cells with Tg in combination with or without Vit C ± Bac or RL90. In line with our hypothesis, Vit C-mediated HepG2 cell protection against Tg-induced hepatotoxicity was significantly inhibited with 20 µg/mL RL90. This data is consistent with the notion that inhibition of csPDI downregulates the hepatoprotective effect of Vit C against Tg-induced HepG2 cell damage. Surprisingly, Bac (2.5 mg/mL and 5 mg/mL) enhanced Vit C-mediated HepG2 cell protection (Figure 6.6), contrary to our expectation. The effect of Bac was concentration-dependent.

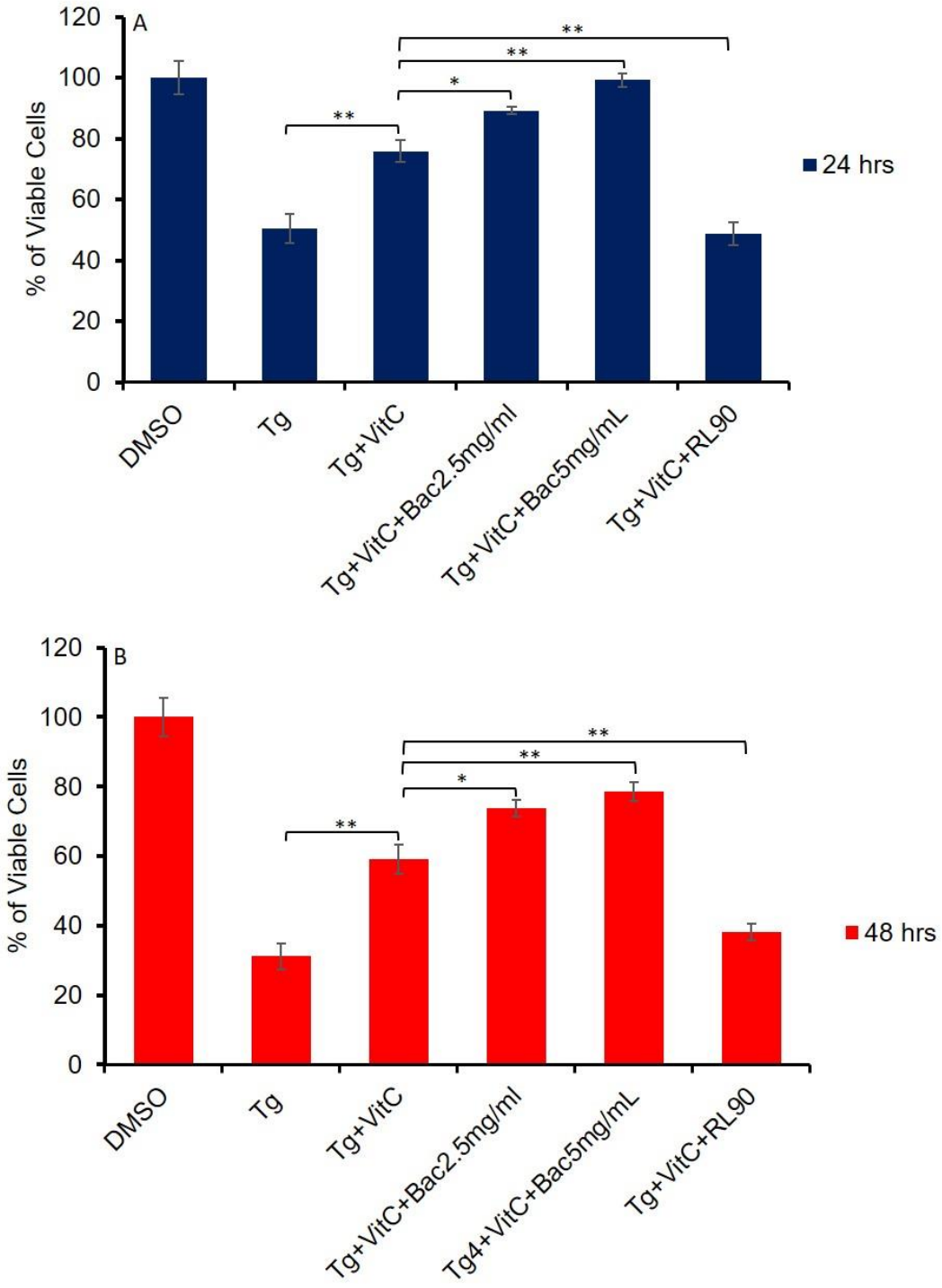

Figure 6.6. Vit C protection of HepG2 cells is attenuated by RL90 but potentiated by Bac. (A) The bar graph summarises the effect of Bac (2.5 mg/mL and 5 mg/mL) and RL90 (20 µg/mL) on the hepatoprotective action of

Vit C against Tg-induced HepG2 cell damage at 24 hrs post treatment. (B) The bar graph summarises the effect of Bac (2.5 mg/mL and 5 mg/mL) and RL90 (20 µg/mL) on the hepatoprotective action of Vit C against Tg-induced HepG2 cell damage at 48 hrs post treatment. Control = 0.1 % DMSO vehicle. Data represent mean±SEM (n=6 wells from 3 experiments performed in duplicate). (*p value ≤0.05, **p value ≤0.01).

6.3.7 Bac, but not RL90 protects HepG2 cells against Tg-induced cell death

Following our surprising observation that Bac potentiated the hepatoprotective effect of Vit C against Tg-induced HepG2 cell damage, while RL90 attenuated the protection, it became necessary to investigate the effect of these agents (Bac and RL90) alone on Tg-induced HepG2 cell damage. Interestingly, the data revealed that Bac (2.5 mg/mL and 5 mg/mL) protects HepG2 cells against Tg-induced cell damage, while RL90 (20 µg/mL) was of no apparent effect (Figure 6.7)

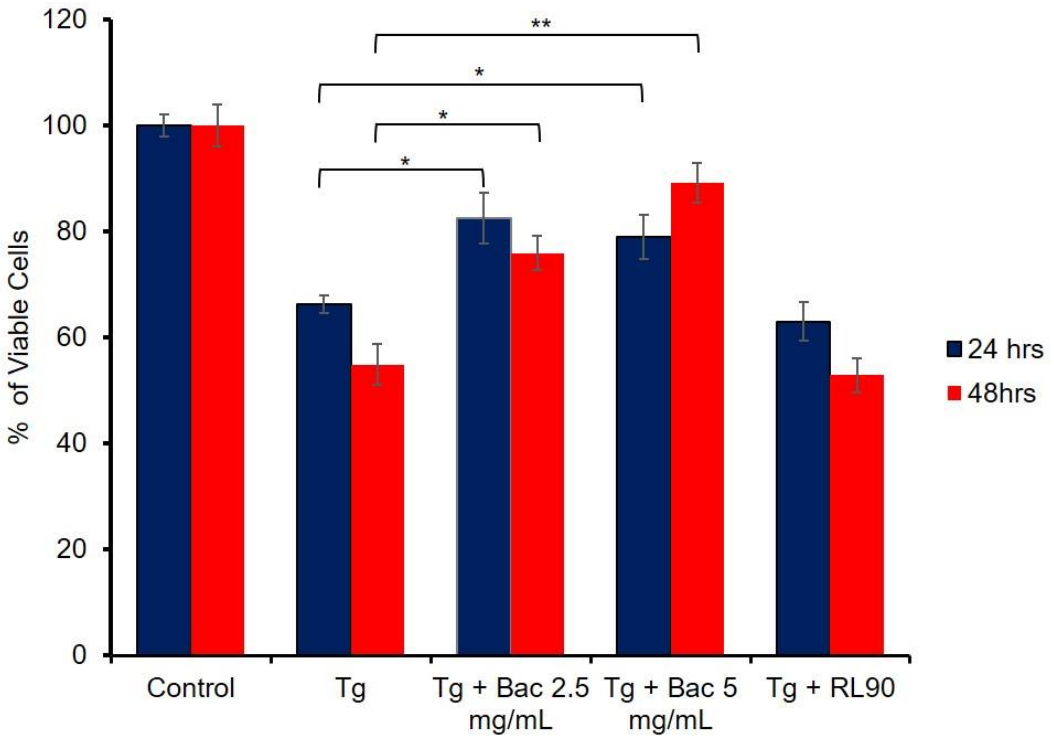

Figure 6.7. Effects of PDI inhibitors (Bac and RL90) on Tg-induced HepG2 cell death. The bar graph summarises the effect of Bac (2.5 mg/mL and 5 mg/mL) and RL90 (20 µg/mL) on Tg-induced HepG2 cell damage at 24 hrs (blue bars) and 48 hrs (red bars) post treatment. control = 0.1 % DMSO vehicle. Data represent mean±SEM (n=6 wells from 3 experiments performed in duplicate). (*p value ≤0.05, **p value ≤0.01).

6.3.8 Investigating whether the Vit C-mediated protection observed in HepG2 cells can be achieved in PHHs

We have demonstrated that Vit C protects against Tg-induced HepG2 cell damage (Figures 6.2, 6.4B). Using Rp-8-Br-cGMP, RL90 and Bac, we have also investigated whether the protection is cGMP/PKG-mediated, as well as the role of PDI. The data obtained with Rp-8-Br-cGMP and RL90 is consistent with the notion that the observed Vit C-mediated HepG2 cell protection against Tg-induced damage is cGMP/PKG-mediated and is modulated by PDI, whereas Bac, another PDI inhibitor appeared to protect HepG2 cells independent of Vit C.

Having made these observations in HepG2 cells, we then sought to investigate whether the Vit C-mediated protection against Tg-induced cell damage can be achieved in PHHs. To do this, we first performed a Tg concentration-response cytotoxicity assay on the PHHs. Our data revealed the concentration of Tg that reduced the viability of the cells to less than 50 % at the 2 different time points (24 and 48 hrs) as 4 µM (Figure 6.8), which we then used as our working concentration in our subsequent experiments.

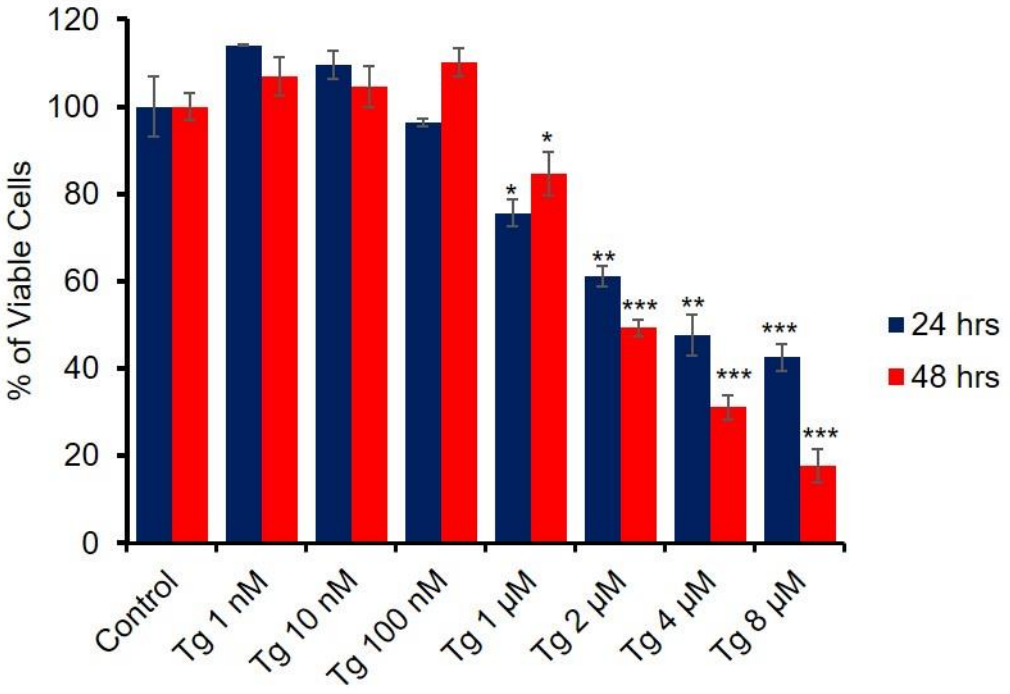

Figure 6.8. Concentration-response effect of Tg on PHH viability. The bar graph summarises cell death induced by different concentrations of Tg on PHHs at 24 hrs (blue bars) and 48 hrs (red bars) post Tg-treatment. Control = 0.1 % DMSO vehicle. Data represent mean±SEM (n=9 wells from 3 experiments performed in triplicate). (*p value ≤0.05, **p value ≤0.01, ***p value ≤0.001).

6.3.9 Concentration-response effect of Vit C on PHHs

Next, we sought to investigate whether Vit C would protect PHHs against Tg-mediated cell death similar to what was observed in HepG2 cells. Since our data on HepG2 cells revealed that higher concentration of Vit C (10 mM) was toxic to the cells (Figures 6.2 and 6.3), here we examined the concentration-response effect of Vit C on PHH survival. To do this, we treated the cells (PHHs) with different concentrations of Vit C (0 µM to 10 mM) and subsequently carried out a CellTitre Glo luminescent cell viability assay on the Vit C-treated cells at two different time points (24 and 48 hrs). The data revealed the safe concentration of Vit C that were not toxic to PHHs to be in the range of 50 µM to 500 µM. Concentrations of Vit C above 2 mM were toxic to PHHs at 24 and 48 hrs post treatment. At 24 hrs post treatment, 1 mM Vit C had no apparent cytotoxic effect on the cells, but at 48 hrs post-treatment, 1 mM Vit C was hepatotoxic to the PHHs (Figure 6.9).

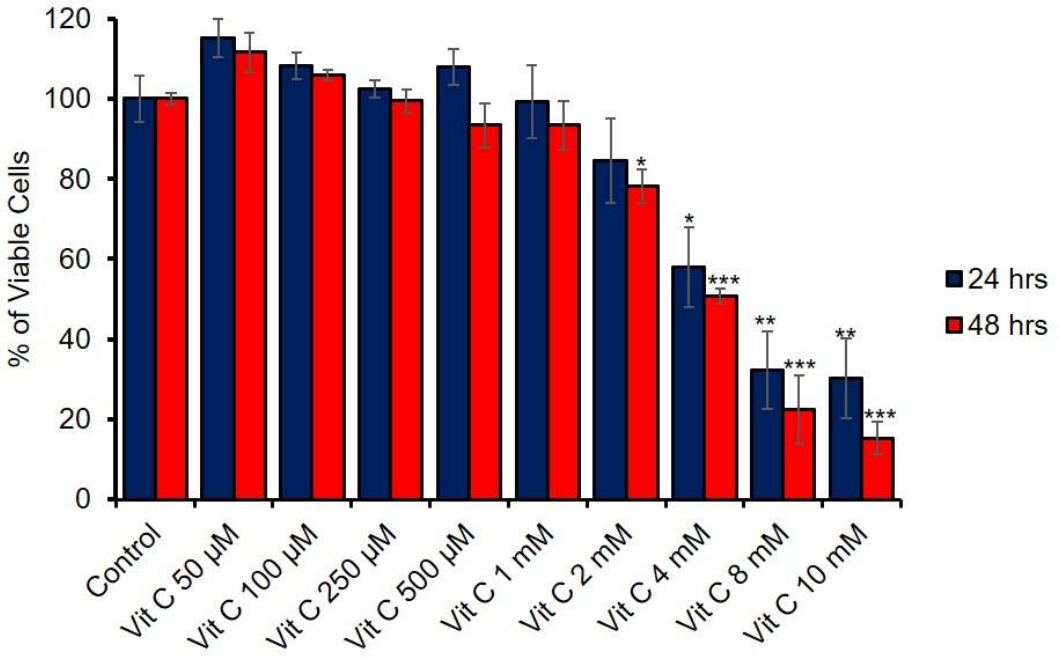

Figure 6.9. Concentration-response effect of Vit C on PHHs. The bar graph summarises the effect of different concentrations of Vit C on PHH viability at 24 hrs (blue bars) and 48 hrs (red bars) post Vit C treatment. Data represent mean±SEM (n=9 wells from 3 experiments performed in triplicate). (*p value ≤0.05, **p value ≤0.01, ***p value ≤0.001).

6.3.10 Vit C protects PHHs against Tg-induced cell damage

We have demonstrated that vit C protects HepG2 cells against Tg-induced cell death. We have also provided evidence that the mechanism is cGMP-mediated and is modulated by csPDI. We then sought to determine whether a similar hepatoprotective action of Vit C can be achieved in PHHs as this would provide more relevant results that would give a better representation of what is happening *in vivo*. We treated PHHs with Tg in combination with or without varying Vit C concentrations (50 µM to 1 mM). The data revealed that these concentrations of Vit C attenuated Tg-induced hepatotoxicity on PHHs (Figure 6.10). The hepatoprotective effect of Vit C was concentration dependent.

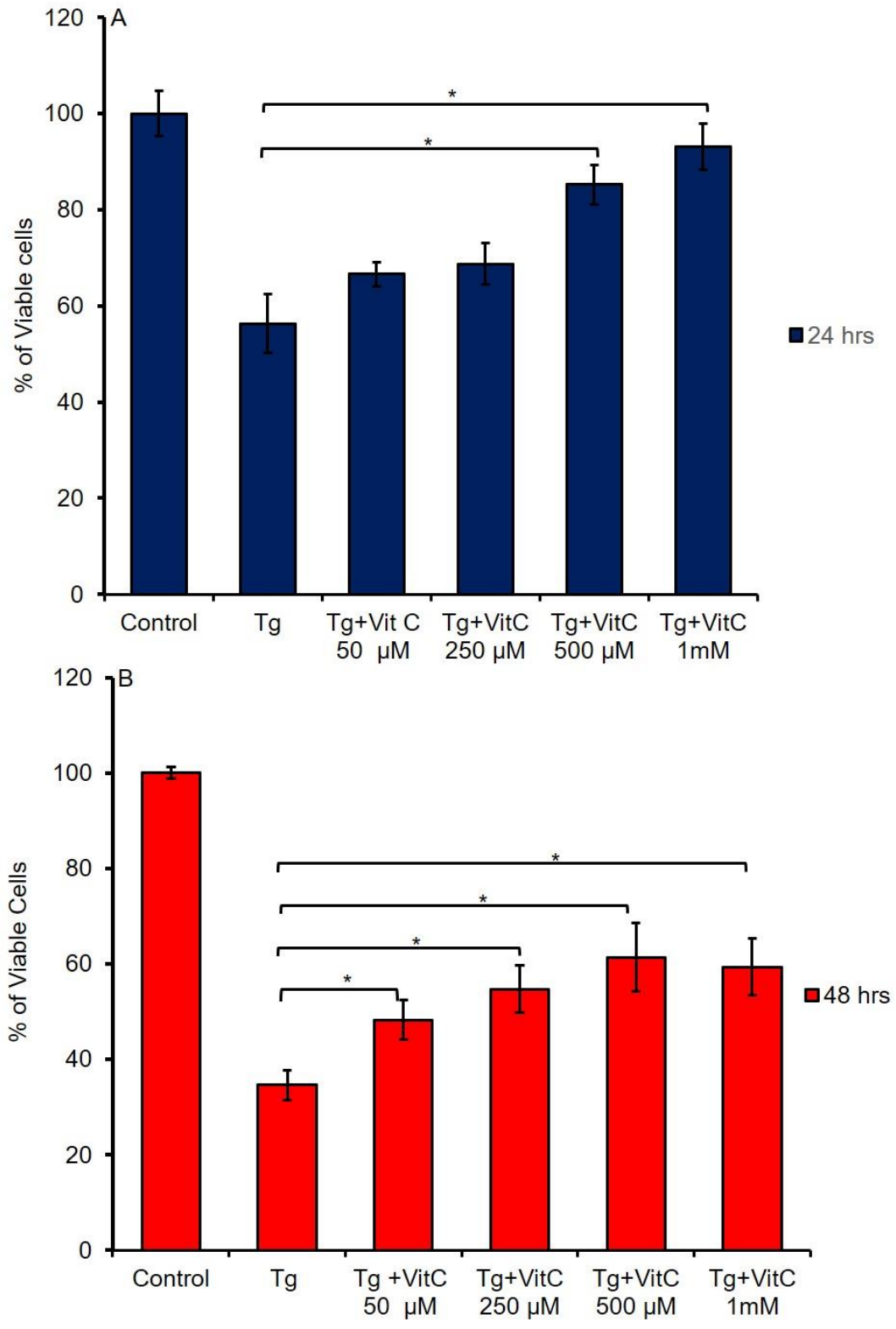

Figure 6.10. Vit C protects PHHs against Tg-induced hepatotoxicity. (A) The bar graph summarises the hepatoprotective effect of various concentrations of Vit C (50 µM to 1 mM) on Tg-induced PHH death at 24 hrs

post treatment. (B) The bar graph summarises the hepatoprotective effect of various concentrations of Vit C (50 µM to 1 mM) on Tg-induced PHH death at 48 hrs post treatment. Control = 0.1 % DMSO vehicle. Data represent mean±SEM (n=9 wells from 3 experiments performed in triplicate). (*p value ≤0.05).

6.3.11 NAPQI concentration response effect on PHHs

As acetaminophen is a major culprit in DILI and elevated $[Ca^{2+}]_i$ has been implicated in the acetaminophen-induced hepatotoxicity (203), we sought to investigate whether Vit C would atenuate acetaminophen-induced hepatocyte damage. In order to this this, we utilized N-acetyl-p-benzoquinone imine (NAPQI); a toxic metabolite released from the xenobiotic metabolism of acetaminophen. We first investigated the concentration-response for NAPQ-induced toxicity on PHHs. Surprisingly, the data revealed that NAPQI even at a concentration of 200 µM had no toxic effect on PHHs (Figure 6.11). Unfortunately, We could not continue with the NAPQI experiments as time and resources did not let us investigate whether higher concentrations of NAPQI would be hepatotoxic.

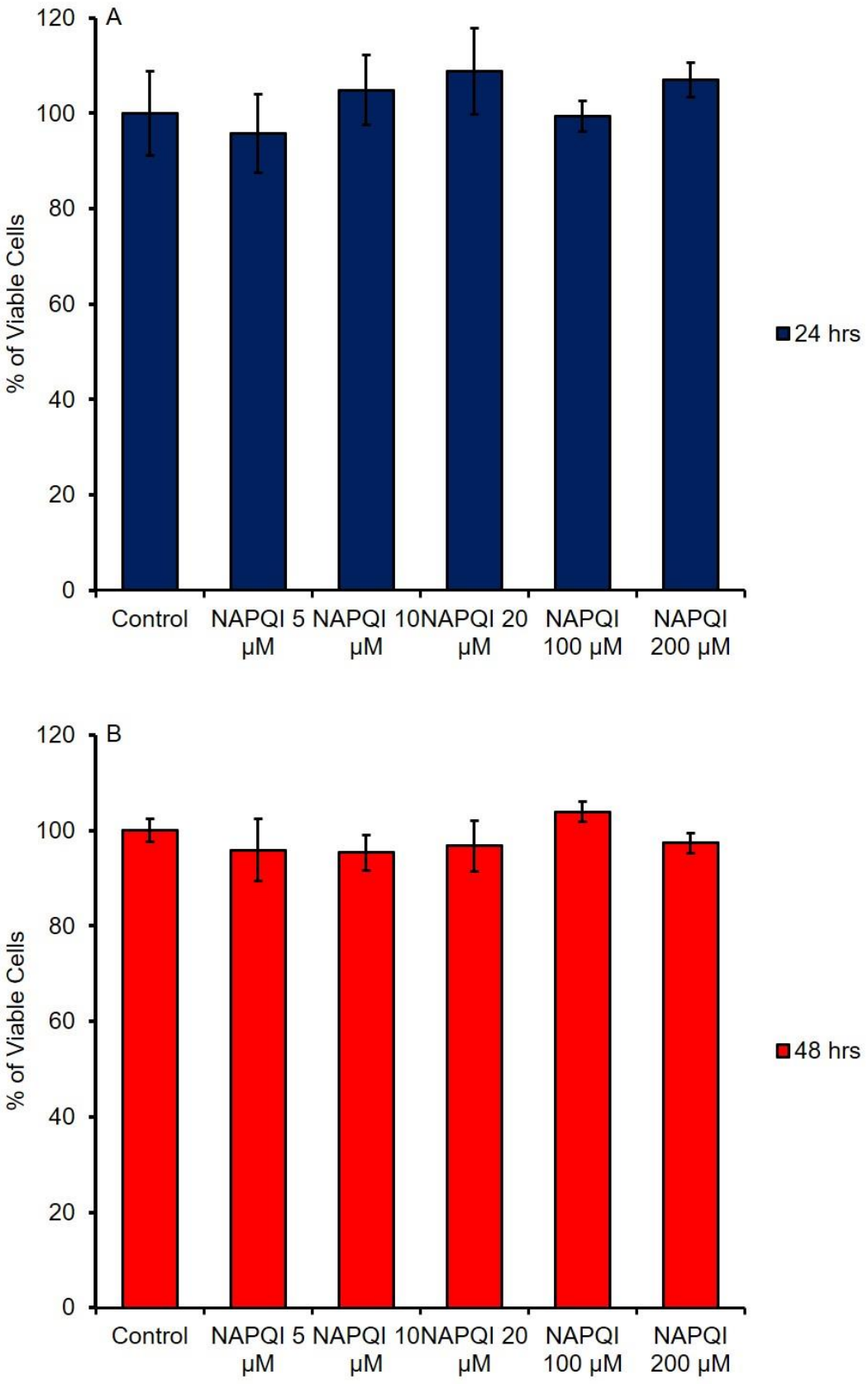

Figure 6.11. Concentration-response for NAPQI-induced toxicity on PHHs. (A) The bar graph summarises the effect of various concentrations of

NAPQI on PHH viability at 24 hrs post treatment. (B) The bar graph summarises the effect of various concentrations of NAPQI on PHH viability at 48 hrs post treatment. Control= 0.1 % DMSO. Data represent mean±SEM (n=9 wells from 3 experiments performed in triplicate).

6.3.12 Vit C protects against ethanol (EtOH)-induced PHHs damage

As alcohol is another major cause of liver damage, we curiously sought to investigate whether Vit C will confer any protection on human hepatocytes against alcohol-induced hepatotoxicity. To investigate this, we used ethanol (EtOH) to induce PHH damage. First, we performed a concentration-response experiment to determine the concentration of EtOH that would be toxic to PHHs. PHHs were treated with different concentrations of EtOH (0 mM to 800 mM) and a CellTitre Glo luminescent cell viability assay was carried out at 24 and 48 hrs post EtOH treatment. The data revealed that EtOH damaged PHHs in a concentration-dependent manner, and only 800 mM of EtOH was observed to reduce the viability of PHHs to less than 50 % (Figure 6.12). Upon treating PHHs with EtOH in combination with different concentrations of Vit C, the data showed that Vit C protected the cells against the hepatotoxic effect of EtOH and the effect of Vit C was concentration-dependent (Figure 6.13).

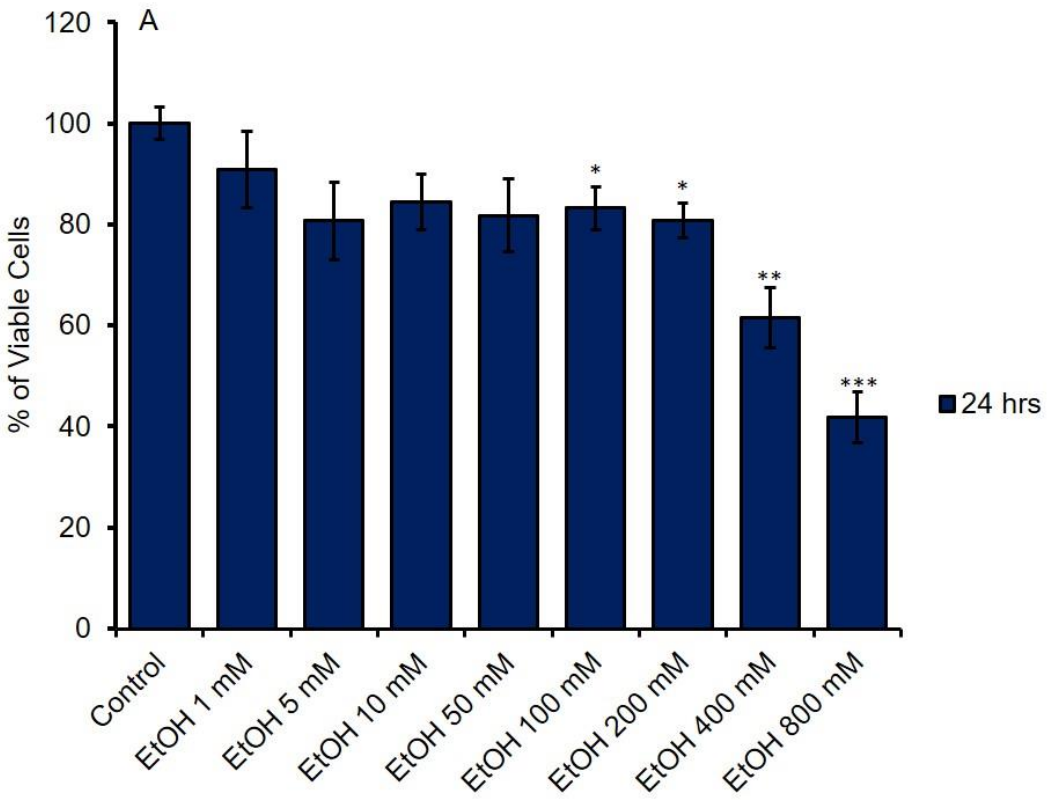
A
120
100
80
60
40
20
0
% of Viable Cells
*
*
**
***
24 hrs
Control
EtOH 1 mM
EtOH 5 mM
EtOH 10 mM
EtOH 50 mM
EtOH 100 mM
EtOH 200 mM
EtOH 400 mM
EtOH 800 mM

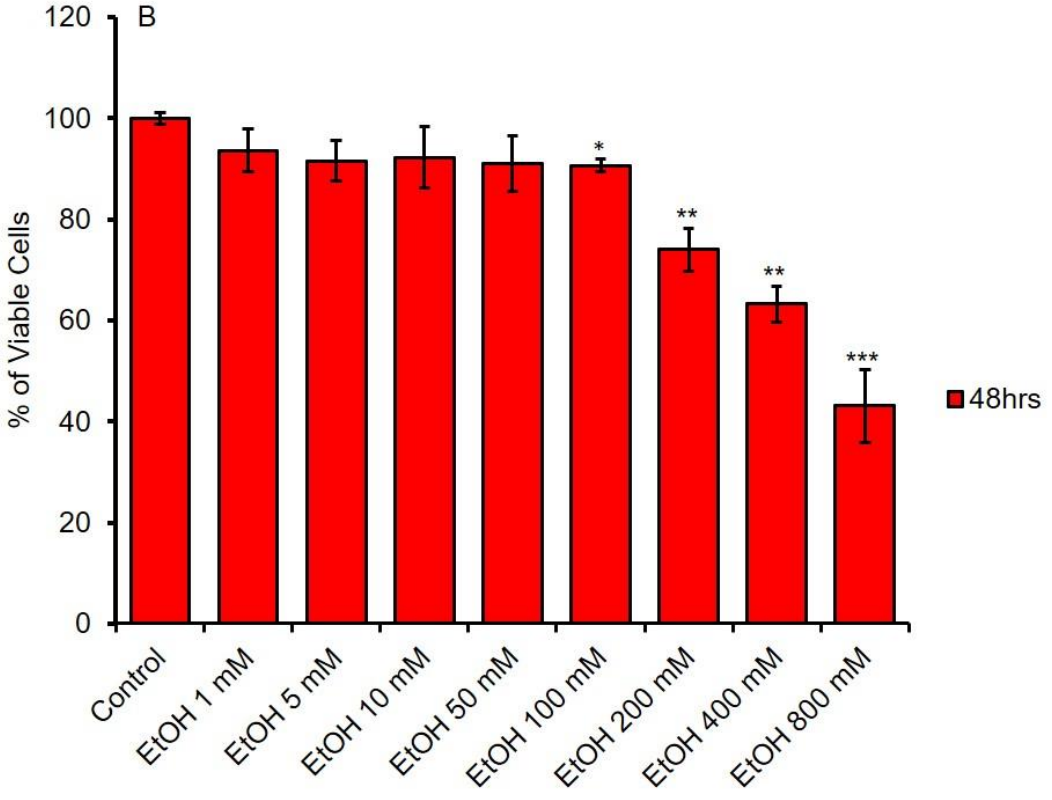
B
120
100
80
60
40
20
0
% of Viable Cells
*
**
**
***
48hrs
Control
EtOH 1 mM
EtOH 5 mM
EtOH 10 mM
EtOH 50 mM
EtOH 100 mM
EtOH 200 mM
EtOH 400 mM
EtOH 800 mM

Figure 6.12. Concentration-response for EtOH-induced toxicity on PHHs. (A) The bar graph summarises cell death induced by different concentrations of EtOH on PHHs at 24 hrs post EtOH-treatment. (B) The bar graph summarises cell death induced by different concentrations of EtOH on PHHs at 48 hrs post EtOH-treatment. Data represent mean±SEM (n=9 wells from 3 experiments performed in triplicate). (*p value ≤0.05, **p value ≤0.01, ***p value ≤0.001).

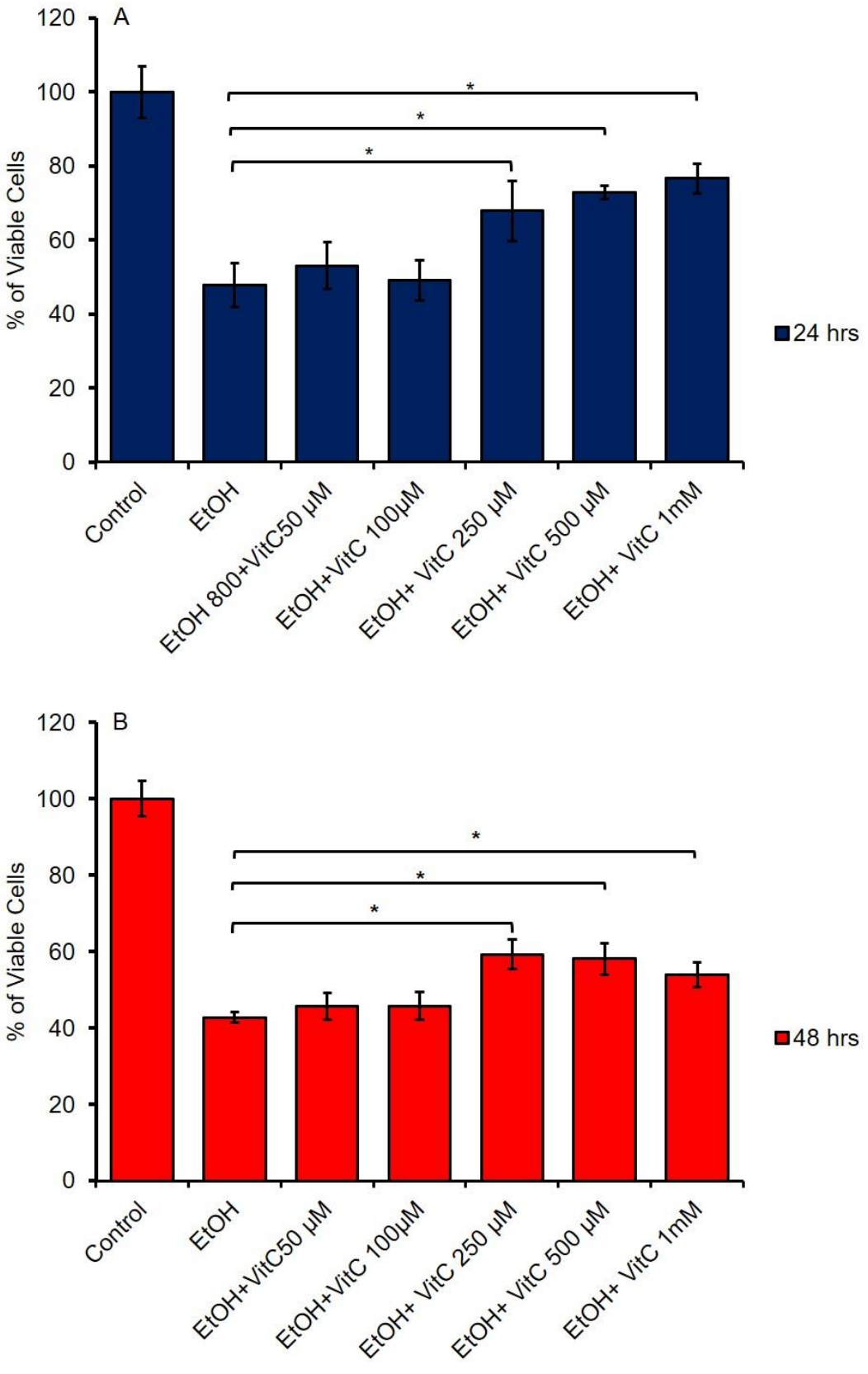

Figure 6.13. Vit C protects PHHs against EtOH-induced hepatotoxicity.

(A) The bar graph summarises the hepatoprotective effect of various

concentrations of Vit C (50 µM to 1 mM) on EtOH-induced PHH damage at 24 hrs post treatment. (B) The bar graph summarises the hepatoprotective effect of various concentrations of Vit C (50 µM to 1 mM) on EtOH-induced PHH damage at 48 hrs post treatment. Data represent mean±SEM (n=9 wells from 3 experiments performed in triplicate). (*p value ≤0.05).

6.4 Discussion

We present here that Vit C like ANP and SNP protects HepG2 cells against Tg-induced cell death, and this protection was cGMP/PKG-mediated. Importantly, this protection was also observed in PHHs. We also show for the first time in HepG2 cells that the Vit C-mediated hepatoprotection is downregulated in the presence of RL90 (an anti-PDI monoclonal antibody). Finally, we show in PHHs that Vit C protects against hepatotoxicity induced by high concentrations of EtOH.

We assessed the ability of Vit C, ANP and SNP to protect human hepatocytes against Ca^{2+}-mediated cell death by treating HepG2 cells with Tg alone and in combination with either Vit C or ANP or SNP. Tg elevates $[Ca^{2+}]_c$ by blocking SERCA pumps, thereby inhibiting sequestration of Ca^{2+} into the ER and depleting ER $[Ca^{2+}]$ (210, 384). Our data revealed that Vit C, SNP and ANP protected HepG2 cells against Tg-induced cell death (Figure 6.2). This is in agreement with previous studies that investigated the hepatoprotective effect of ANP in rat hepatocytes (225). The authors demonstrated that ANP protects rat hepatocytes against Ca^{2+}-mediated cell death by elevating cGMP, activating PKG and consequently lowering $[Ca^{2+}]_i$ (225). Of note, though at 24 hrs post treatment of HepG2 cells with Tg in combination with ANP, an apparent hepaprotective effect of ANP against the Tg-induced cytotoxicity was observed, this protection was however lost at 48 hrs post treatment (Figure 6.2). The reason for this loss of ANP-mediated HepG2 cell protection at 48 hrs post treatment is not clear, but temperature-dependent degradation of the peptide is one likely explanation. Another likely explanation is proteolytic

degradation of ANP as natriuretic peptides including ANP can be degraded by extracellular proteases (385). SNP, on the other hand, had no apparent hepaprotective effect against Tg-induced HepG2 cell damage at the 24 hrs post treatment, but at 48 hrs post treatment, a significant protection was observed.

An important observation made on the Vit C-mediated protection against Tg-induced HepG2 cell damage was that, although concentrations of Vit C in the range of 100 µM to 1.25 mM protected HepG2 cells against Tg-induced cytotoxicity (Figures 6.2 and 6.5), higher concentration of Vit C (10 mM) had an additional cytotoxic action with Tg on the cells (Figure 6.2). Interestingly, on treating the HepG2 cells with different concentrations of Vit C alone in order to determine the Vit C concentration range beyond which undesirable hepatotoxic effects would result, our data showed that concentrations of Vit C less than or equal to (≤) 1.25 mM had no significant cytotoxic effect on HepG2 cells (Figures 6.3 and 6.4), while 10 mM Vit C applied alone significantly damaged the HepG2 cells (Figure 6.3). The concentration of Vit C required to achieve HepG2 cell and PHH protection is consistent with the concentrations used in the previous studies that describe Vit C-mediated hepatocyte protection (322, 386).

We also wanted to determine whether the Vit C protection of hepatocytes against Tg-induced cell death was linked to its cGMP elevation action and consequent activation of PKG and reduction of $[Ca^{2+}]_i$. To do this, we focused on obstructing the cGMP/PKG downstream mechanisms using the PKG inhibitor Rp-8-Br-cGMP. Previous studies have shown that ANP protection of

rat hepatocytes against Ca^{2+}-mediated hepatotoxicity was cGMP/PKG-mediated (225, 283). Unpublished data from our group also showed that Vit C mimics the hepatoprotective action of ANP by elevating cGMP, and through PKG, attenuates ATP and TLC-induced $[Ca^{2+}]_i$ signal and consequently reducing ATP and TLC-induced cell death in rat hepatocytes. In line with this, our data revealed that the observed hepatoprotective effect of Vit C against Tg-induced cell death was abrogated by the PKG inhibitor Rp-8-Br-cGMP (Figure 6.5). Taking together, these data are consistent with the notion that Vit C-mediated protection of hepatocytes against the toxic effects of agents that elevates $[Ca]_i$ is mediated through the cGMP/PKG pathway, distinct from its direct free radical scavenging actions. The important similarities between our data on HepG2 cells and the previous unpublished data from our group on rat hepatocytes to some extent validate our findings.

Next, we sought to examine whether the Vit C protection of HepG2 cells is modulated by csPDI. To do this, we utilized the PDI inhibitors RL90 and Bac, both of which have been used in previous studies to inhibit csPDI (333). We showed in chapter 3 that inhibition of csPDI with RL90 and Bac attenuated Vit C-induced elevation of cGMP, and in chapter 4 we showed that inhibition of csPDI with RL90 and Bac downregulated the ability of Vit C to attenuate $[Ca^{2+}]_i$ signal. In the presence of RL90, the observed Vit C-mediated protection of HepG2 cells against Tg-induced cell damage was attenuated (Figure 6.6). This is consistent with inhibition of csPDI with RL90 attenuating Vit C elevation of cGMP, hence downregulating the ability of Vit C to reduce Tg-induced increases in $[Ca^{2+}]_i$ and consequent Ca^{2+}-mediated hepatotoxicity. Surprisingly, Bac had an opposite effect to that of RL90 on the HepG2 cells

viability. As our data from chapters 3 and 4 revealed that inhibition of csPDI with Bac downregulated the ability of Vit C to elevate cGMP and restored Tg-induced elevations in $[Ca^{2+}]_i$ even in the presence of Vit C, we therefore expected that Bac would attenuate the hepatoprotective effect of Vit C against Tg-induced cell damage. On the contrary, treating HepG2 cells with Tg, Vit C and Bac revealed that Bac potentiated the hepatoprotective effect of Vit C against the Tg-induced cell death (Figure 6.6). In quest of a possible explanation for the contradicting action of Bac on the cGMP, Ca^{2+} and HepG2 cell viability experiments, especially the opposing action it mediated on the HepG2 cell viability experiments compared to that of RL90, we investigated the effect of Bac and RL90 alone on the Tg-induced hepatotoxicity. Interestingly, our data revealed that Bac alone protected HepG2 cells against Tg-induced cell death, while RL90 alone had no apparent effect on Tg-induced hepatotoxicity (Figure 6.7). Interestingly, Bac is known to inhibit proteases (387, 388), including caspases (389). Zhao and colleagues have previously reported that Bac inhibits the activity of caspase 3/7 and alleviates the apoptotic effects of different inducers of cell death in mouse embryonic fibroblasts (MEFs) (389). Though the authors attributed the cytoprotective effect of Bac to its inhibition of PDI catalytic activity, which in turn results in the inhibition of the Caspase 3/7 activity. Moreover, Bac is a mixture of polypeptides and a non-specific PDI inhibitor compared to RL90 which is a specific anti-PDI monoclonal antibody (390, 391), it is therefore conceivable that the RL90 results represent more reliable inhibition of csPDI.

The observation that Bac protected HepG2 cells against Tg-induced damage, suggests a potential therapeutic role for it in hepatocyte/liver injury. However,

we must point out that the polypeptide antibiotic is toxic in some other tissues/organs. In particular, parenteral Bac application via intramuscular injection has been reported to be nephrotoxic (392).

We have shown that Vit C through cGMP/PKG protects HepG2 cells against Tg-induced hepatotoxicity (Figures 6.2, 6.4B and 6.5). Also, preliminary data from our group revealed that Vit C through cGMP/PKG protects primary rat hepatocytes against ATP and TLC-induced hepatocyte damage. Whether this Vit C-mediated protection against the hepatotoxic effect of these Ca^{2+} elevating agents can be achieved in PHHs had not been determined. Therefore, we investigated this by treating PHHs with Tg in combination with or without Vit C. The data revealed that Vit C protects PHHs against Tg-induced damage (Figure 6.10), in line with our observation in HepG2 cells. The consistency of the data in HepG2 cells and PHHs validates that Vit C have the ability to protect human hepatocytes against Tg-induced cell death. However, in the PHHs, we did not investigate whether the protection against Tg cytotoxic effect is cGMP/PKG-mediated.

Since acetaminophen and alcohol constitute some of the major agents that can induce liver injury, we sought to investigate whether Vit C would protect against their hepatotoxic effects. To do this, we utilized NAPQI (the reactive metabolite of acetaminophen) and Ethanol (EtOH). First, a concentration response of both NAPQI and EtOH was performed on the PHHs. The data revealed that EtOH resulted in PHHs damage in a concentration-dependent fashion (Figure 6.12). Surprisingly, NAPQI had no apparent cytotoxic effect on PHHs even at a concentration of 200 µM and a prolonged incubation time of

48 hrs (Figure 6.11), though the same concentration of NAPQI had previously been demonstrated to induce some observable hepatotoxicity on PHHs (393). Human interindividual differences in susceptibility to drug toxicity (394) is a likely explanation for the dissimilarity in the hepatotoxicity potential of NAPQI. Our next plan was to investigate the effect of higher concentrations of NAPQI, in the range of 300 µM to 1 mM, on PHHs, unfortunately, time and resources did not permit us. On treating PHHs with EtOH in combination with or without Vit C, we observed that Vit C protected PHHs against EtOH-induced damage in a concentration-dependent manner (Figure 6.13). The Vit C protection against EtOH-induced hepatoxicity have been widely studied, and indeed most of the existing data support our observation that Vit C is hepatoprotective against EtOH effect (320, 321, 395). In addition, several lines of evidence also support the cytoprotective effect of Vit C against ethanol mediated cytotoxicity in various other cell types/organs such as in prenatal rat hippocampal neurons, postnatal rat brain and human brain glial cells (396-398), suggesting that the cytoprotective effect of Vit C against ethanol toxicity is not hepatocyte/liver specific.

In conclusion, we have been able to show that Vit C is able to protect HepG2 cells and PHHs against Tg-induced cell death. We have also shown that Vit C protects PHHs against EtOH-induced cell death. Though previous studies attribute the hepatoprotective action of Vit C to its direct antioxidant effect and ability to scavenge free radicals, in HepG2 cells, we have established that the Vit C protection against Tg-induced damage is mediated by cGMP/PKG. This suggests that the observed protection of Vit C against the hepatotoxic effect of Tg might be occurring via a mechanism dependent on reduction of $[Ca^{2+}]_i$

and distinct from its direct free radical scavenging ability. Finally, we were able to show that inhibition of PDI with RL90 attenuated Vit C protection of HepG2 cells against Tg-induced cell death, consistent with csPDI modulating the ability of Vit C to protect hepatocytes against Tg-mediated damage.

Chapter 7

General discussion and concluding remarks

I present here for the first time that Vitamin C (Vit C), like ANP and SNP stimulates cGMP generation (chapter 3) and attenuates elevations in $[Ca^{2+}]_i$ (chapter 4) in HepG2 cells. Also, in HEK293 cells which we used as a non-hepatocyte model, the data showed that Vit C elevates cGMP and reduces $[Ca^{2+}]_i$ in HEK293 cells. Similar Vit C stimulation of cGMP and reduction of $[Ca^{2+}]_i$ has been reported in PC12 cells (329) and Molt-3 human lymphoblastoid cells (332) respectively, and in primary rat hepatocytes (unpublished data from our group). Vit C and ANP, but not SNP-induced cGMP generation in HepG2 cells was attenuated by the PDI inhibitor bacitracin (Bac) and the anti-PDI specific monoclonal antibody RL90. These inhibitory effects of Bac and RL90 were also observed in HEK293 cells. These data suggest that inhibition of csPDI activity downregulates cGMP stimulation by ANP and Vit C and their consequent reduction of $[Ca^{2+}]_i$. As a confirmation of these functional effects of csPDI, the immunofluorescence data revealed the presence of PDI on the plasma membrane of HepG2 and HEK293 cells, also called csPDI (chapter 5). Importantly, the csPDI is also expressed in PHHs, consistent with the notion that the PDI modulation of Vit C and ANP-induced cGMP generation can be achieved in PHHs, though we did not investigate this in this study. Furthermore, we show that Vit C, like ANP and SNP protects HepG2 cells against Tg-induced hepatotoxicity, and the Vit C-mediated HepG2 cell protection is mediated by PKG and modulated by PDI.

Our observation that Vit C through PKG attenuated Tg-induced HepG2 cell damage suggests that the hepatoprotective effect of Vit C may be mediated via the attenuation of harmful $[Ca^{2+}]_i$ elevations, mimicking the previously demonstrated actions of ANP (225), distinct from the direct free radical

scavenging property of the vitamin. Importantly, the Vit C-mediated hepatoprotection against Tg-induced damage was also observed in PHHs, and our data also demonstrates that the vitamin protects against EtOH-induced PHH damage.

The concentrations of Vit C required to stimulate cGMP generation, reduce $[Ca^{2+}]_i$ and achieve hepatoprotection in this study is consistent with the concentrations that have been used by majority of the previous studies (322, 329, 332, 399). Although the normal plasma concentration of Vit C is in the range of 50-60 µM (400, 401), this can increase up to 100 µM following long-term vegetarian diet and/or oral supplementation (400). Also, certain cells/tissues/organs can accumulate higher concentrations of Vit C in high micromolar range or even millimolar range (402-404) including human liver where Vit C concentration is in the range of 600-900 µM (401). Moreover, pharmacologic plasma Vit C concentrations (0.3 to 15 mM) can be achieved by intravenous administration (405-408). These pharmacologic concentrations are not maintained but are cleared from the body within hrs by renal filtration and excretion (408, 409). Oral administration have been shown to yield only a maximum of about 220 µM plasma Vit C concentration due to pharmacokinetic control processes which can be bypassed by intravenous administration (408, 410, 411). Treatment with such pharmacologic concentrations of Vit C has the potential to alleviate Ca^{2+}-mediated hepatocyte damage.

An important feature of the Vit C-mediated cGMP elevation, reduction of $[Ca^{2+}]_i$ and hepatoprotection against the Tg-induced HepG2 cell damage is the involvement of PDI, assessed through the modulatory action of the PDI inhibitor Bac and the anti-PDI monoclonal antibody RL90 (Discussed in

chapters 3, 4 and 6 respectively) and the apparent colocalization of PDI and NPRA on hepatocyte membrane (chapter 5). Our observation that the two PDI inhibitors (Bac and RL90) modulates the ability of Vit C to protect against Tg-induced HepG2 cell damage, suggest that PDI could be a potential therapeutic target in hepatocyte injury. Interestingly, similar emerging roles of PDI as a therapeutic target in various disease conditions have been demonstrated in previous studies (389, 412-414). For example, PDI has been implicated in the induction and progression of tumours/cancers in various organs such as kidney, ovary, lungs, brain and prostrate (415-417). Particularly, administration of the PDI inhibitor Bac and an anti-PDI monoclonal antibody were reportedly observed to inhibit the migration and invasion of glioma cells (413). In these disease states, PDI is thought to suppress apoptosis, resulting in tumour growth and metastasis. While the above studies demonstrate the anti-apoptotic effects of PDI, other studies have revealed that PDI can also be pro-apoptotic; inhibition of PDI catalytic activity reduces apoptosis induced by pro-apoptotic stimuli in MEFs and PC12 cells (389, 418). Together, these studies suggest that PDI has both detrimental and protective effects in specific disease states, hence, we suggest that there is need for further validation of the roles of the isomerase in various disease conditions. In this study, we have investigated the role of PDI in Vit C-mediated hepatoprotection using HepG2 cells, which is a liver cancer cell line, we therefore suggest that the mechanism should also be explored further in PHHs and possibly in primary human liver cancer cells as this would give a better representation of what is achievable *in vivo*, and also enable us to better understand the effect that would be mediated

by PDI both on normal (non-cancerous) hepatocytes and on cancerous hepatocytes as in the case of liver cancer patients.

In addition to Vit C mediating cytoprotection as shown in this study and previous studies (317, 419), recent evidence suggests that it has anti-cancer property, suggesting the possibility of a dual therapeutic role for the vitamin; at pharmacologic concentrations, Vit C is reported to be cytotoxic to cancer cells, but not to normal cells (407, 409, 420-422). Chen and colleagues demonstrated that pharmacologic Vit C concentrations (0.3 mM to 10 mM) reduced the viability of three different human cancer cell lines (lymphoma; JLP-119, breast; MCF7 and breast; MB231) and four mouse cancer cell lines (lung; KLN205, kidney; RAG, colon; CT26 and melanoma; B16) to less than 50%, whereas, 20 mM Vit C had no effect on the viability of different normal human cells (breast; Hs587Bst, fibroblast; CCD34SK, lymphocyte and monocyte) (409). Also, High-dose parenteral Vit C enhanced the effect of conventional chemotherapeutic agents in ovarian cancer in mouse models but protected normal cells/tissues from chemotherapy-associated toxicity, including hepatobiliary toxicity in cancer patients (420). These studies clearly demonstrate that high concentrations of Vit C kill different cancer cells, but not normal cells. In comparison, our data revealed that different concentrations of Vit C had similar effects on the viability of both the liver cancer cell line (HepG2 cells) and the normal liver cells (PHHs) used in this study. For example, concentrations of Vit C up to 1 mM protected both HepG2 cells and PHHs against Tg-induced cell death, and these concentrations did not cause any damage to either of the liver cell types, except for the 1 mM Vit C that was observed to be cytotoxic to the primary liver cells after 48 hrs incubation

(chapter 6). On the other hand, higher Vit C concentrations were toxic to both the HepG2 cells and PHHs. For example, 10 mM Vit C reduced the viability of both liver cell types to less than 50 %. The ability of Vit C to protect normal liver cells (PHHs) against the hepatotoxicity induced by harmful Ca^{2+} elevations, will be of enormous value. However, the observation that this protection is also achievable in HepG2 which is a liver cancer cell line raises some concern over its safety in liver cancer patients. Importantly, since Vit C protected HepG2 cells against the cytotoxic effect of Tg, it is necessary to investigate whether it would protect primary liver cancer cells against the toxic effects of chemotherapy, with a possible consequence of protecting liver cancer cells against cancer drugs *in vivo*, even though previous studies have demonstrated that it acts in synergy with chemotherapy in certain cancers such as ovarian cancer (420). We must reiterate that most of the mechanisms in this study have been demonstrated in HepG2 cells and less in normal PHHs, hence there is need to explore the mechanisms further in the PHHs as this would give a better representation of what would happen *in vivo*.

Also, the ability of Vit C to elevate cellular cGMP and reduce $[Ca^{2+}]_i$ could also have implications on other liver-related conditions such as portal hypertension and reduced blood pressure in the liver. Thrombosis is one of the causes of portal hypertension, in addition to liver cirrhosis, and increased platelet $[Ca^{2+}]$ is a major culprit in thrombus formation (423, 424). Data from this study and previous studies have demonstrated that Vit C reduces $[Ca^{2+}]_i$, in HepG2 cells and HEK293 cells (chapter 4), PRH (unpublished study from our group), and Molt-3 human lymphoblastoid cells (332), we therefore speculate that the Vit C reduction of $[Ca^{2+}]_i$, could be achieved in other cell types like platelets and

vascular smooth muscle cells (VSMCs). Ability of Vit C to reduce $[Ca^{2+}]_i$ in platelets might therefore have the benefit of attenuating Ca^{2+}-dependent thrombus formation, which could then ameliorate thrombosis-induced portal hypertension and its associated complications such as gastrointestinal bleeding from varices. Another important factor is the possibility of Vit C stimulating cGMP in VSMCs present in the hepatic and portal vessels. In VSMCs, elevation in cGMP would activate PKG, consequently resulting in vasodilation (425), which may also help reduce blood pressure within the liver. Therefore, in addition to Vit C protecting against Ca^{2+}-mediated cell death through the elevation of cGMP as demonstrated in this study, its cGMP stimulating ability might also have beneficial effect on blood pressure as described above. An investigation on the possibility of Vit C modulating cellular cGMP and Ca^{2+} in platelets and VSMCs is therefore of interest.

Our current study has shown that Vit C elevates cGMP and reduces $[Ca^{2+}]_i$ in HepG2 and HEK293 cells. Though the data does not demonstrate the exact mechanism of action, our observation that non-cell permeant inhibitors of PDI modulates the action of the vitamin, like that of ANP suggest that the Vit C-mediated elevation of cGMP occurs at the cell surface via the ANP/pGC route. We therefore speculate that Vit C could be mediating its cGMP generation action and consequent $[Ca^{2+}]_i$ reduction and hepatoprotective effect via two possible mechanistic pathways as listed below.

1) **First Speculation**: That Vit C could be acting directly on the membrane GC-linked receptor on the cell surface, consequently activating the membrane bound guanylyl cyclase, stimulating cGMP generation and cGMP/PKG-mediated $[Ca^{2+}]_i$ reduction and protection against Ca^{2+}-

mediated damage (Figure 7.1). Here we also adopt the hypothesis of Pan and group that csPDI by colocalizing with membrane GC-linked receptor, interacts with it and allosterically modulates cGMP generation action (333).

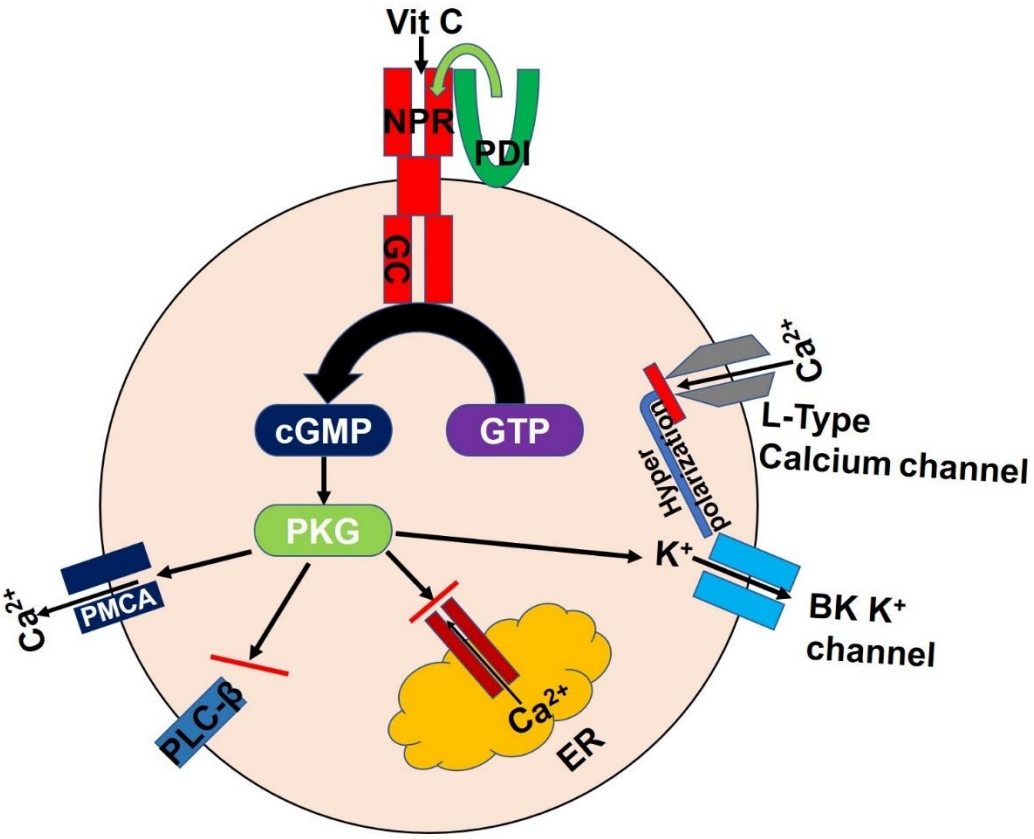

Figure 7.1: First hypothesized mechanism of Vit C elevation of cGMP and reduction of $[Ca^{2+}]_i$ in hepatocytes. Direct action of Vit C on NPR activates the cGMP generation action of the NPR-linked pGC, with an allosteric modification of the cGMP system by colocalized csPDI. The generated cGMP, through PKG, reduces $[Ca^{2+}]_i$ and protects against Ca^{2+}-mediated hepatocyte damage. Solid arrows without bars represent activation of the protein/channel the arrow is leading to, while arrows with red bar represent inhibition of the protein/channel the arrow is leading to.

2) **Second Speculation:** That Vit C through its redox property acts on and reduces csPDI. When reduced, csPDI interacts with colocalized GC-linked receptors on the cell membrane, catalysing changes in the disulphide bonds in the receptor. This would consequently result in a conformational change of the receptor and subsequent transmembrane signal transduction and activation of GC. GC activation would in return lead to cGMP generation, reduction in $[Ca^{2+}]_i$ and hepatoprotection (Figure 7.2).

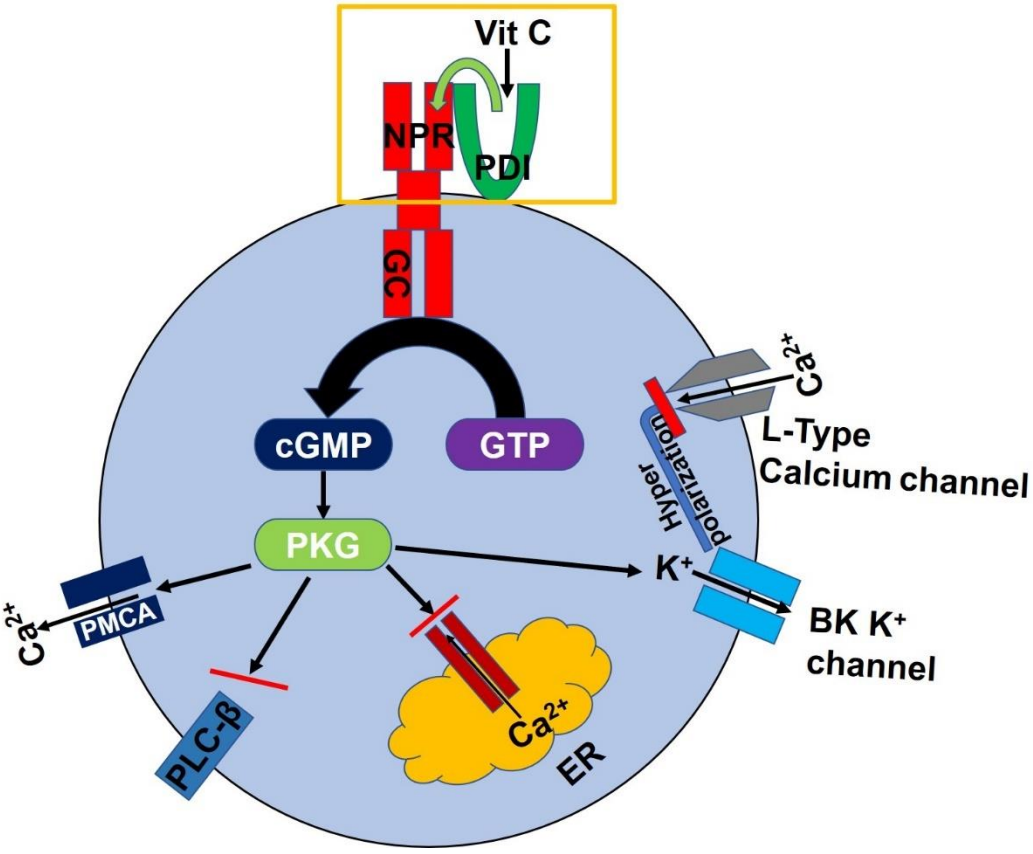

Figure 7.2: Second hypothesized mechanism of Vit C elevation of cGMP and reduction of $[Ca^{2+}]_i$ in hepatocytes. Vit C acts on and reduces csPDI. Reduced csPDI then catalyses changes in the disulphide bonds present in the colocalized NPR which results in a transmembrane signal transduction and

activation of the NPR-linked pGC and consequent generation of cGMP and reduction of $[Ca^{2+}]_i$.

Future experiments

In this study, we have shown that Vit C modulates both cGMP and $[Ca^{2+}]_i$ and protects hepatocytes against Ca^{2+}-mediated damage. However, we could not establish the exact target on which the vitamin acts to mediate these effects. To address this, we have made two possible speculations as stated above. To investigate these speculations, one important experiment that could be performed would be to utilize a cell line that lack csPDI, like LLC-PK1 which has previously been shown to lack PDI expression (333) and investigate whether Vit C would be able to stimulate cGMP in them. Ability of Vit C to stimulate cGMP generation in such cell types would suggest that the vitamin is not acting on csPDI, but directly on the pGC-linked NPR (first speculation). However, if Vit C does not elevate the cGMP level in such cell types that lack PDI, then that would suggest that the vitamin is acting on the isomerase, possibly by reducing it, which in turn catalyse changes in the colocalized pGC-linked NPRA, thus causing an activation of the pGC and subsequent cGMP generation (second speculation).

One key limitation of this study is that most of the mechanisms were investigated in the liver cancer cell line HepG2 with limited work carried out on PHHs. For example, Vit C elevation of cGMP and reduction of $[Ca^{2+}]_i$ was investigated only in HepG2 cells. Also, though we were able to establish that Vit C protects against Tg-induced hepatotoxicity in PHHs, the involvement of

cGMP/PKG and PDI in the protection was only investigated in HepG2 cells. Hence, it is important to further explore these in PHHs.

Other important experiments that could be performed in order to further improve the validity of this study include:

1) Since our current data shows that Vit C protects against Tg-induced hepatocyte damage, it would be useful to determine whether these protections can be achieved against other consumable Ca^{2+} elevators such as bile salts.
2) In this study, we have performed the cell viability assay by measuring the amount of ATP present in the cells using CellTitre Glo luminescent cell viability assay. Repeating these experiments using another assay such as propidium iodide staining would also help in improving the validity of our findings.
3) Here we have used Rp-8-Br-cGMP to investigate the involvement of cGMP/PKG in the Vit C protection against Tg-induced damage, but there is need to also utilize other inhibitors of PKG such as Rp-8-pCPT-cGMPS to further validate this experiment.

In conclusion, I have revealed that Vit C elevates cellular cGMP, reduces $[Ca^{2+}]_i$, and mediates hepatoprotection in HepG2 cells. With the aid of the PDI inhibitor Bac and the anti-PDI monoclonal antibody, I have also demonstrated that these functions of Vit C are modulated by PDI. As the intact membrane of living cells are generally impermeable to large proteins including antibodies (342, 343), our observation that RL90 which is an anti-PDI monoclonal antibody and a specific inhibitor of PDI attenuates these actions of Vit C,

including cGMP elevation, reduction of $[Ca^{2+}]_{i,}$ and hepatoprotection, particularly suggests the involvement of csPDI in these mechanisms. Also, the observation in chapter 3 that Bac and RL90 attenuated ANP-mediated cGMP elevation, like that of Vit C, but had no effect on SNP-mediated cGMP elevation is consistent with the notion that Vit C and ANP mediates their cGMP elevating action via the same route; i.e., the ANP/pGC pathway, as previously proposed by Chen and colleagues (329). This also implicates csPDI and not ER PDI in the mechanism. Our study therefore suggests a link between Vit C, cGMP, csPDI, intracellular Ca^{2+} signal and hepatoprotection and identifies a mechanism via which Vit C mediates hepatoprotection distinct from its direct free radical scavenging ability. These findings highlight pGC and csPDI as promising therapeutic targets to protect hepatocytes and other cell types against injury induced by harmful Ca^{2+} elevations. Since these mechanisms have been investigated in HepG2 cells which is a liver cancer cell line, with limited data in PHHs, I therefore suggest that these mechanisms should be further explored in PHHs and even in primary liver cancer cells as this would help verify the utility of this approach being achieved *in vivo*, and also the safety of administering Vit C and modulators of PDI as therapeutic agents in liver cancer patients.

References

1. Boyer JL. Bile formation and secretion. Comprehensive Physiology. 2013;3(3):1035-78.

2. Mitra V, Metcalf J. Metabolic functions of the liver. Anaesthesia & Intensive Care Medicine. 2012;13(2):54-5.

3. Racanelli V, Rehermann B. The liver as an immunological organ. Hepatology. 2006;43(2):54-62.

4. Rogers AB, Dintzis RZ. Comparative Anatomy and Histology. 2nd ed. Academic Press. 2018 Chapter 13 - Hepatobiliary System:229-39.

5. Jeschke MG, Lopez ON, Finnerty CC. Total Burn Care. 5th ed. Elsevier. 2018. Chapter 24 - The Hepatic Response to Thermal Injury:259-67.

6. Laskin DL. Parenchymal and Nonparenchymal Cell Interactions in Hepatotoxicity. Biological Reactive Intermediates IV: Molecular and Cellular Effects and Their Impact on Human Health. 2012:499.

7. Seo W, Jeong W. Hepatic non-parenchymal cells: Master regulators of alcoholic liver disease? World J Gastroenterol. 2016;22(4):1348-56.

8. Lu Z-, Wei-Chen, Ju C-, Jun-Den, Kuai S-, Pei H, et al. CD25 Is a Novel Marker of Hepatic Bile Canaliculus. INTERNATIONAL JOURNAL OF SURGICAL PATHOLOGY. 2012;20(5):455-61.

9. Gissen P, Arias IM. Structural and functional hepatocyte polarity and liver disease. J Hepatol. 2015;63(4):1023-37.

10. Treyer A, Müsch A. Hepatocyte polarity. Comprehensive Physiology. 2013;3(1):243-87.

11. Wang L, Boyer JL. The maintenance and generation of membrane polarity in hepatocytes. Hepatology. 2004;39(4):892-9.

12. Rogers AB, Dintzis RZ. Comparative Anatomy and Histology. Elsevier. 2012. Chapter 13 - Liver and Gallbladder:193-201.

13. Marieb EN, Hoehn K. Human anatomy & physiology. 10th ed. Pearson. 2016. Chapter 23: The Digestive System:876-933.

14. Wang Y, Zhang C. The Roles of Liver-Resident Lymphocytes in Liver Diseases. Frontiers in Immunology. 2019;10:1582-95.

15. Mehal WZ, Azzaroli F, Crispe IN. Immunology of the Healthy Liver: Old Questions and New Insights. Gastroenterology. 2001;120(1):250-60.

16. Bogdanos DP, Gao B, Gershwin ME. Liver immunology. Compr Physiol. 2013;3(2):567-98.

17. Balato A, Unutmaz D, Gaspari AA. Natural Killer T Cells: An Unconventional T-Cell Subset with Diverse Effector and Regulatory Functions. Journal of Investigative Dermatology. 2009;129(7):1628-42.

18. Gomes AQ, Correia DV, Silva-Santos B. Non-classical major histocompatibility complex proteins as determinants of tumour immunosurveillance. EMBO Rep. 2007;8(11):1024-30.

19. Wintermeyer P, Cheng C, Gehring S, Hoffman BL, Holub M, Brossay L, et al. Invariant Natural Killer T Cells Suppress the Neutrophil Inflammatory Response in a Mouse Model of Cholestatic Liver Damage. Gastroenterology. 2009;136(3):1048-59.

20. Naito M, Hasegawa G, Takahashi K. Development, differentiation, and maturation of Kupffer cells. Microsc Res Tech. 1997;39(4):350-64.

21. Knolle PA, Schmitt E, Jin S, Germann T, Duchmann R, Hegenbarth S, et al. Induction of Cytokine Production in Naive CD4^+ T Cells by Antigen-Presenting Murine Liver Sinusoidal Endothelial Cells but Failure to Induce Differentiation Toward T~h~1 Cells. GASTROENTEROLOGY. 1999;116(6):1428-40.

22. Lohse AW, Knolle PA, Bilo K, Ubrig A, Waldmann C, Ibe M, et al. Antigen-Presenting Function and B7 Expression of Murine Sinusoidal Endothelial CelLs and Kupffer CelLs. GASTROENTEROLOGY. 1996;110(4):1175-81.

23. Bernsmeier C, Albano E. Liver dendritic cells and NAFLD evolution: A remaining open issue. Journal of Hepatology. 2017 June 2017;66(6):1120-2.

24. Thomson AW, Lu L. Are dendritic cells the key to liver transplant tolerance? Immunol Today. 1999;20(1):27-32.

25. Thomson AW, Knolle PA. Antigen-presenting cell function in the tolerogenic liver environment. Nat Rev Immunol. 2010;10(11):753-66.

26. Lau AH, Thomson AW. Dendritic cells and immune regulation in the liver. Cellular and Molecular Immunology. 2003;52(2)307-14.

27. Matsuno K, Ezaki T, Kudo S, Uehara, Y. A life stage of particle-laden rat dendritic cells in vivo: their terminal division, active phagocytosis, and translocation from the liver to the draining lymph. The Journal of Experimental Medicine. 1996;183(4):1865-78.

28. Kudo S, Matsuno K, Ezaki T, Ogawa M. A Novel Migration Pathway for Rat Dendritic Cells from the Blood: Hepatic Sinusoids–Lymph Translocation. The Journal of Experimental Medicine.1997;185(4)777-84.

29. Paloma AV, Aguilar NE, Beatriz BF, Uribe M, Nahum MS. The Role of Dendritic Cells in Fibrosis Progression in Nonalcoholic Fatty Liver Disease. Biomed Research International. 2015; (2015): 768071. doi:10.1155/2015/768071

30. Rui L. Energy Metabolism in the Liver. Comprehensive Physiology. 2014;4(1):177-97.

31. Mitanchez D, Doiron B, Chen R, Kahn A. Glucose-Stimulated Genes and Prospects of Gene Therapy for Type I Diabetes. Endocrine Reviews. 1997;18(4):520-40.

32. Adeva-Andany M, Pérez-Felpete N, Fernández-Fernández C, Donapetry-García C, Pazos-García C. Liver glucose metabolism in humans. Bioscience Reports. 2016;36(6):e00416.

33. Aiston S, Andersen B, Agius L. Glucose 6-phosphate regulates hepatic glycogenolysis through inactivation of phosphorylase. DIABETES. 2003;52(6):1333-9.

34. Villar-Palasi C, Guinovart JJ. The role of glucose 6-phosphate in the control of glycogen synthase. FASEB JOURNAL. 1997;11(7):544-58.

35. Agius L. Glucokinase and molecular aspects of liver glycogen metabolism. Biochemical Journal. 2008;414(1):1-18.

36. Leclercq IA, Da Silva Morais A, Schroyen B, Van Hul N, Geerts A. Insulin resistance in hepatocytes and sinusoidal liver cells: Mechanisms and consequences. Journal of Hepatology. 2007;47(1):142-56.

37. Engelking LR. Textbook of Veterinary Physiological Chemistry. 3rd ed. Academic Press. 2015. Chapter 37 - Gluconeogenesis:225-30.

38. Abumrad N, Coburn C, Ibrahimi A. Membrane proteins implicated in long-chain fatty acid uptake by mammalian cells: CD36, FATP and FABPm. BIOCHIMICA ET BIOPHYSICA ACTA-MOLECULAR AND CELL BIOLOGY OF LIPIDS. 1999;1441(1):4-13.

39. Liu X, Wang H, Liang X, Roberts MS. Liver Pathophysiology: Therapies and Antioxidants. 1st ed. Academic Press. 2017. Chapter 30 - Hepatic Metabolism in Liver Health and Disease:391-400.

40. Ahmadian M, Duncan RE, Jaworski K, Sarkadi-Nagy E, Sul HS. Triacylglycerol metabolism in adipose tissue. FUTURE LIPIDOLOGY. 2007;2(2):229-37.

41. McGarry JD, Foster DW. Ketogenesis and its regulation. American Journal of Medicine. 1976;61(1):9-13.

42. Hostetler HA, Huang H, Kier AB, Schroeder F. Glucose Directly Links to Lipid Metabolism through High Affinity Interaction with Peroxisome

Proliferator-activated Receptor α. Journal of Biological Chemistry. 2008;283(4):2246-54.

43. Young-Cheul Shin, Yun H, Park HH. Structural dynamics of the transaminase active site revealed by the crystal structure of a co-factor free omega-transaminase from Vibrio fluvialis JS17. Scientific Reports. 2018;8(1): :11454.

44. Frayn KN. Metabolic regulation. a human perspective. 3rd ed. Wiley. 2010. Chapter 7-Integration of Carbohydrate, Fat and Protein Metabolism in Normal Daily Life:169-213.

45. Omiecinski CJ, Vanden Heuvel JP, Perdew GH, Peters JM. Xenobiotic Metabolism, Disposition, and Regulation by Receptors: From Biochemical Phenomenon to Predictors of Major Toxicities. TOXICOLOGICAL SCIENCES. 2011;120(1):49-75.

46. Ionescu C, Caira MR. Drug metabolism: current concepts. Springer. 2005. Chapter 3-Pathways of Biotransformation -Phase II Reactions:129-167.

47. Jancova P, Anzenbacher P, Anzenbacherova E. Phase II drug metabolizing enzymes. Biomedical Papers of the Medical Faculty of the University of Palacky Olomouc, Czech Repub. 2010;154(2):103-16.

48. Sipes IG, Wiersma DA, Armstrong DJ. The role of glutathione in the toxicity of xenobiotic compounds: metabolic activation of 1,2-dibromoethane by glutathione. Advances Experimental Medicine and Biology. 1986;197:457-67.

49. Gonzalez FJ, Kimura S. Understanding the role of xenobiotic-metabolism in chemical carcinogenesis using gene knockout mice. Mutation Research. 2001;477(1-2):79-87.

50. Gao B. Basic liver immunology. Cellular and Molecular Immunology. 2016;13(3):265-6.

51. Meldolesi J, Pozzan T. The endoplasmic reticulum Ca2+ store: a view from the lumen. Trends in Biochemical Sciences. 1998;23(1):10-14.

52. YAMAGUCHI Y, DALLE-MOLLE E, HARDISON WGM. Vasopressin and A23187 stimulate phosphorylation of myosin light chain-1 in isolated rat hepatocytes. American Journal of Physiology: Gastrointestinal & Liver Physiology. 1991;261(2):312-9.

53. Blackmore PF, Strickland WG, Bocckino SB, Exton JH. Mechanism of hepatic glycogen synthase inactivation induced by Ca2+-mobilizing hormones. Studies using phospholipase C and phorbol myristate acetate. Biochemical Journal. 1986;237(1):235-42.

54. Lin HV, Accili D. Hormonal regulation of hepatic glucose production in health and disease. Cell Metabolism. 2011;14(1):9-19.

55. Amaya MJ, Nathanson MH. Calcium signaling in the liver. Comprehensive Physiology. 2013;3(1):515-39.

56. Amaya MJ, Nathanson MH. Calcium Signaling and the Secretory Activity of Bile Duct Epithelia. Cell Calcium. 2014;55(6)317-24.

57. Berridge MJ(1), Irvine RF(2). Inositol trisphosphate, a novel second messenger in cellular signal transduction. Nature. 1984;312(5992):315-21.

58. Berridge MJ, Irvine RF. Inositol phosphates and cell signalling. Nature. 1989;341(6239):197-205.

59. Pinton P, Pozzan T, Rizzuto R. The Golgi apparatus is an inositol 1,4,5-trisphosphate-sensitive Ca2+ store, with functional properties distinct from those of the endoplasmic reticulum. EMBO Journal. 1998;17(18):5298-308.

60. Gerasimenko OV, Gerasimenko JV, Tepikin AV, Petersen OH. ATP-dependent accumulation and inositol trisphosphate- or cyclic ADP-ribose-mediated release of Ca2+ from the nuclear envelope. Cell. 1995(3):439-44.

61. Echevarría W, Leite MF, Guerra MT, Zipfel WR, Nathanson MH. Regulation of calcium signals in the nucleus by a nucleoplasmic reticulum. Nature Cell Biology. 2003;5(5):440-6.

62. Marchenko SM, Yarotskyy VV, Kovalenko TN, Kostyuk PG, Thomas RC. Spontaneously active and InsP3-activated ion channels in cell nuclei from rat cerebellar Purkinje and granule neurones. JOURNAL OF PHYSIOLOGY. 2005;565(3):897-910.

63. Gerasimenko OV, Gerasimenko JV, Belan PV, Petersen OH. Inositol trisphosphate and cyclic ADP-ribose-mediated release of Ca2+ from single isolated pancreatic zymogen granules. Cell. 1996;84(3):473-80.

64. Berridge MJ, Bootman MD, Roderick HL. Calcium signalling: dynamics, homeostasis and remodelling. Nature Reviews.Molecular Cell Biology. 2003;4(7):517-29.

65. Berridge MJ, Lipp P, Bootman MD. The versatility and universality of calcium signalling. Nature Reviews Molecular Cell Biology. 2000;1(1):11-21.

66. Bootman MD, Berridge MJ, Roderick HL. Calcium Signalling: More Messengers, More Channels, More Complexity. Current Biology. 2002;12(16):563-5.

67. Calcraft PJ, Ruas M, Pan Z, Cheng X, Arredouani A, Hao X, et al. NAADP Mobilizes Calcium from Acidic Organelles Through Two-Pore Channels. Nature. 2012;459(7246):596-600.

68. Ishibashi K, Suzuki M, Imai M. Molecular Cloning of a Novel Form (Two-Repeat) Protein Related to Voltage-Gated Sodium and Calcium Channels. Biochem Biophys Res Commun. 2000(2):370-6.

69. Berridge MJ. Inositol Trisphosphate and Calcium Signaling. Nature. 1993;361(6410)315-25.

70. Simon MI, Strathmann MP, Gautam N. Diversity of G Proteins in Signal Transduction. Science. 1991;252(5007):802-8.

71. Lev S, Moreno H, Martinez R, Canoll P, Peles E, Musacchio JM, et al. Protein tyrosine kinase PYK2 involved in Ca(2+)-induced regulation of ion channel and MAP kinase functions. Nature. 1995;376(6543):737-45.

72. Rosenbaum DM, Rasmussen SGF, Kobilka BK. The structure and function of G-protein-coupled receptors. Nature. 2009;459(7245):356-63.

73. Coleman JLJ, Ngo T, Smith NJ. The G protein-coupled receptor N-terminus and receptor signalling: N-tering a new era. Cell Signal. 2017;33:1-9.

74. Sengupta D, Prasanna X, Mohole M, Chattopadhyay A. Exploring GPCR-Lipid Interactions by Molecular Dynamics Simulations: Excitements, Challenges, and the Way Forward. J Phys Chem B. 2018;122(22):5727-37.

75. Wu DQ, Lee CH, Rhee SG, Simon MI. Activation of phospholipase C by the alpha subunits of the Gq and G11 proteins in transfected Cos-7 cells. J Biol Chem. 1992;267(3):1811-7.

76. Paweł Mystek, Rysiewicz B, Gregrowicz J, Marta Dziedzicka-Wasylewska, Polit A. Gγ and Gα Identity Dictate a G-Protein Heterotrimer Plasma Membrane Targeting. Cells. 2019;8(10):1246-60.

77. Caers J, Peymen K, Suetens N, Temmerman L, Janssen T, Schoofs L, et al. Characterization of G Protein-coupled Receptors by a Fluorescence-based Calcium Mobilization Assay. Journal of Visualized Experiments. 2014 89(89):e51516-e51516.

78. Hollmann MW, Strumper D, Herroeder S, Durieux ME. Receptors, G proteins, and their interactions. Anesthesiology. 2005;103(5):1066-78.

79. Rhee SG, Choi KD. Regulation of inositol phospholipid-specific phospholipase C isozymes. J Biol Chem. 1992;267(18):12393-6.

80. Gresset A, Sondek J, Harden TK. The phospholipase C isozymes and their regulation. Subcell Biochem. 2012;58:61-94.

81. Berridge MJ, Bootman MD, Roderick HL. Calcium: Calcium signalling: dynamics, homeostasis and remodelling. Nature Reviews Molecular Cell Biology. 2003;4(7):517-29.

82. Rhee SG. Regulation of Phosphoinositide-Specific Phospholipase C*. Annu Rev Biochem. 2001;70(1):281-312.

83. Cantley L. The Kidney: Physiology and Pathophysiology. 5th ed. Elsevier Inc. 2013. Chapter 13 - Principles of Cell Signaling:369-403.

84. Huang KP. The mechanism of protein kinase C activation. Trends Neurosci. 1989;12(11):425-32.

85. Maruyama IN. Mechanisms of Activation of Receptor Tyrosine Kinases: Monomers or Dimers. Cells. 2014;3(2):304-30.

86. Sarabipour S, Ballmer-Hofer K, Hristova K. VEGFR-2 conformational switch in response to ligand binding. ELIFE. 2016;(5)e13876.

87. Gomes DA, Rodrigues MA, Leite MF, Gomez MV, Varnai P, Balia T, et al. c-Met Must Translocate to the Nucleus to Initiate Calcium Signals. J Biol Chem. 2008;283(7):4344-51.

88. Rodrigues MA, Gomes DA, Andrade VA, Leite MF, Nathanson MH. Insulin induces calcium signals in the nucleus of rat hepatocytes. Hepatology. 2008;48(5):1621-31.

89. Hirata K, Pusl T, O'Neill AF, Dranoff JA, Nathanson MH. The type II inositol 1,4,5-trisphosphate receptor can trigger Ca2+ waves in rat hepatocytes. Gastroenterology. 2002;122(4):1088-100.

90. Hirata K, Dufour J, Shibao K, Knickelbein R, O'Neill AF, Bode H, et al. Regulation of Ca2+ Signaling in Rat Bile Duct Epithelia by Inositol 1,4,5-Trisphosphate Receptor Isoforms. 2002;36(2):284-96.

91. Nathanson, M.H. (1,4), Fallon MB(1), Padfield PJ(2), Maranto AR(3). Localization of the type 3 inositol 1,4,5-Trisphosphate receptor in the Ca2+ wave trigger zone of pancreatic acinar cells. J Biol Chem. 1994 ;269(7):4693-6.

92. Hirata K, Nathanson MH, Burgstahler AD, Okazaki K, Mattei E, Sears ML. Relationship between inositol 1,4,5-trisphosphate receptor isoforms and subcellular Ca2+ signaling patterns in nonpigmented ciliary epithelia. Invest Ophthalmol Vis Sci. 1999;40(9):2046-53.

93. Trauner M, Boyer JL. Bile Salt Transporters: Molecular Characterization, Function, and Regulation. Physiol Rev. 2003(2):633-71.

94. Cruz LN, Guerra MT, Kruglov E, Mennone A, Garcia CRS, Chen J, et al. Regulation of multidrug resistance-associated protein 2 by calcium signaling in mouse liver. Hepatology. 2010;52(1):327-37.

95. Kruglov EA, Gautam S, Guerra MT, Nathanson MH. Type 2 inositol 1,4,5-trisphosphate receptor modulates bile salt export pump activity in rat hepatocytes. HEPATOLOGY. 2011;54(5):1790-9.

96. Nathanson MH, Boyer JL. Mechanisms and regulation of bile secretion. Hepatology. 1991;14(3):551-66.

97. Franchitto A, Onori P, Renzi A, Carpino G, Mancinelli R, Alvaro D, et al. Recent advances on the mechanisms regulating cholangiocyte proliferation and the significance of the neuroendocrine regulation of cholangiocyte pathophysiology. Annals of Translational Medicine. 2013;1(3):27.

98. Hirata K, Nathanson MH. Bile Duct Epithelia Regulate Biliary Bicarbonate Excretion in Normal Rat Liver. GASTROENTEROLOGY. 2001;121(2):396-406.

99. Maroni L, Haibo B, Ray D, Zhou T, Wan Y, Meng F, et al. Functional and structural features of cholangiocytes in health and disease. 2015;1(4):368-380.

100. Kanno N, LeSage G, Glaser S, Alpini G. Regulation of cholangiocyte bicarbonate secretion. AMERICAN JOURNAL OF PHYSIOLOGY-GASTROINTESTINAL AND LIVER PHYSIOLOGY. 2001;281(3):612-25.

101. Lazaridis KN, Strazzabosco M, LaRusso NF. The Cholangiopathies: Disorders of Biliary Epithelia. GASTROENTEROLOGY. 2004;127(5):1565-77.

102. Hohenester, S. (1,2), Maillette de BW, Paulusma CC(1), Oude Elferink, R.P. (1), Beuers U(1), van Vliet, S.J. (3), et al. A biliary HCO 3- umbrella constitutes a protective mechanism against bile acid-induced injury in human cholangiocytes. Hepatology. 2012;55(1):173-83.

103. Beuers U, Hohenester S, de BW, Kremer AE, Jansen PL, Elferink RP. The biliary HCO(3)(-) umbrella: a unifying hypothesis on pathogenetic and therapeutic aspects of fibrosing cholangiopathies. Hepatology 2010;52(4):1489-96.

104. Masyuk AI, Masyuk TV, LaRusso NF. Physiology of the Gastrointestinal Tract. Elsevier. 2012. Chapter 56 - Physiology of Cholangiocytes:1531-57.

105. Minagawa N, Nagata J, Shibao K, Masyuk AI, Gomes DA, Rodrigues MA, et al. Cyclic AMP regulates bicarbonate secretion in cholangiocytes through release of ATP into bile. 2007;133(5)1592-602.

106. Alvaro D, Alpini G, Jezequel AM, Bassotti C, Francia C, Fraioli F, et al. Role and mechanisms of action of acetylcholine in the regulation of rat cholangiocyte secretory functions. 1997;100(6):1349-62.

107. Nathanson MH, Gautam A, Bruck R, Isales CM, Boyer JL. Effects of Ca2+ agonists on cytosolic Ca2+ in isolated hepatocytes and on bile secretion in the isolated perfused rat liver. Hepatology. 1992;15(1):107-16.

108. LOWE PJ, MIYAI K, STEINBACH JH, HARDISON WGM. Hormonal regulation of hepatocyte tight junctional permeability. American Journal of Physiology: Gastrointestinal & Liver Physiology. 1988;18(4):G454-61.

109. NATHANSON MH, GAUTAM A, OI CHENG NG, BRUCK R, BOYER JL. Hormonal regulation of paracellular permeability in isolated rat hepatocyte couplets. American Journal of Physiology: Gastrointestinal & Liver Physiology. 1992 06;25(6):G1079-86.

110. Erlinger S. Review: New insights into the mechanisms of hepatic transport and bile secretion. J Gastroenterol Hepatol. 1996(6):575-9.

111. Boyer JL. Tight Junctions in Normal and Cholestatic Liver: Does the Paracellular Pathway Have Functional Significance? Hepatology. 1983;3(4):614-7.

112. Bartlett PJ, Gaspers LD, Pierobon N, Thomas AP. Calcium-dependent regulation of glucose homeostasis in the liver. Cell Calcium. 2014;55(6):306-16.

113. Kraus-Friedmann N, Feng L(1). The role of intracellular Ca2+ in the regulation of gluconeogenesis. Metabolism: Clinical and Experimental. 1996;45(3):389-403.

114. Exton JH, Park CR. Control of gluconeogenesis in liver. I. General features of gluconeogenesis in the perfused livers of rats. J Biol Chem. 1967;242(11):2622-36.

115. Silva ACMD, Kelmer-Bracht A, Constantin J, Ishii-Iwamoto E, Yamamoto NS, Bracht A. The influence of Ca2+ on the effects of glucagon on hepatic glycolysis. Gen Pharmacol. 1998;30(5):655-62.

116. Kneer NM, Wagner MJ, Lardy HA. Regulation by calcium of hormonal effects on gluconeogenesis. J Biol Chem. 1979;254(23):12160-8.

117. Eugenín, E.A. (1), González, H. (1), Sáez, C.G. (1), Sáez, J.C. (1,2). Gap junctional communication coordinates vasopressin-induced glycogenolysis in rat hepatocytes. American Journal of Physiology - Gastrointestinal and Liver Physiology. 1998;274(37-6):G1109-16.

118. Peach MJ. Molecular actions of angiotensin. Biochem Pharmacol. 1981;30(20):2745-51.

119. Dixon CJ(1), White PJ(1), Hall JF(1), Boarder MR(1), Kingston S(2). Regulation of human hepatocytes by P2Y receptors: Control of glycogen

phosphorylase, Ca2+, and mitogen-activated protein kinases. J Pharmacol Exp Ther. 2005;313(3):1305-13.

120. Dixon CJ, Hall JF, Webb TE, Boarder MR. Regulation of Rat Hepatocyte Function by P2Y Receptors: Focus on Control of Glycogen Phosphorylase and Cyclic AMP by 2-Methylthioadenosine 5'-Diphosphate. J Pharmacol Exp Ther. 2004;311(1):334-41.

121. Freemark M, Handwerger S. Glycogenolytic Effects of the Calcium Ionophore A23187, but Not Vasopressin Or Angiotensin, in Fertalrat Hepatocytes. Pediatric Research. 1984;18(1):137A.

122. Stepniak E, Ricci R, Eferl R, Sumara G, Sumara I, Rath M, et al. c-Jun/AP-1 controls liver regeneration by repressing p53/p21 and p38 MAPK activity. Genes and Development. 2006;20(16):2306-14.

123. Michalopoulos GK. Principles of Liver Regeneration and Growth Homeostasis. Comprehensive Physiology. 2013;3(1) :485-513.

124. Kahl CR, Means AR. Regulation of Cell Cycle Progression by Calcium/Calmodulin-Dependent Pathways. Endocrine Reviews. 2003;24(6):719-36.

125. Lagoudakis L, Garcin I, Julien B, Nahum K, Gomes DA, Combettes L, et al. Cytosolic Calcium Regulates Liver Regeneration in the Rat. Hepatology. 2010; 52(2):602-11.

126. Whitfield JF(1), Boynton AL(1), MacManus JP(1), Rixon RH(1), Sikorska M(1), Tsang B(1), et al. The Roles of Calcium and Cyclic Amp in Cell Proliferation. 1980; 339(1):216-40.

127. Garcin I, Tordjmann T. Calcium Signalling and Liver Regeneration. International Journal of Hepatology. 2012; 2012: 630670-6.

128. Mine T, Kojima I, Ogata E, Nakamura T. Comparison of effects of HGF and EGF on cellular calcium in rat hepatocytes. Biochem Biophys Res Commun. 1991;181(3):1173-80.

129. Cruise, J.L. (1,2), Muga SJ(1), Lee Y-(1), Michalopoulos GK(1). Regulation of hepatocyte growth: Alpha-1 adrenergic receptor and ras p21 changes in liver regeneration. J Cell Physiol. 1989;140(2):195-201.

130. Pauls TL(1), Cox JA(2), Berchtold MW(3). The Ca2+-binding proteins parvalbumin and oncomodulin and their genes: New structural and functional findings. Biochimica et Biophysica Acta - Gene Structure and Expression. 1996;1306(1):39-54.

131. Rodrigues MA, Gomes DA, Leite MF, Grant W, Zhang L, Lam W, et al. Nucleoplasmic Calcium Is Required for Cell Proliferation. Cell Communication and Signalling. 2007:282(23):17061-8

132. Soliman EM, Rodrigues MA, Gomes DA, Sheung N, Yu J, Amaya MJ, et al. Intracellular calcium signals regulate growth of hepatic stellate cells via specific effects on cell cycle progression. Cell Calcium. 2009;45(3):284-92.

133. Clapham DE. Calcium signaling. Cell. 1995;80(2):259-68.

134. Machaca K. Ca 2+ signaling, genes and the cell cycle. Cell Calcium. 2011;49(5):323-30.

135. PARKASH J, ASOTRA K. Calcium wave signaling in cancer cells. Life Sciences. 2010;87(19-22)587-95.

136. Hajnóczky G, Davies E, Madesh M. Calcium signaling and apoptosis. Biochemical and Biophysical Research Communications. 2003;304(3):445-54.

137. Yang Z, Kirton HM, MacDougall DA, Boyle JP, Deuchars J, Frater B, et al. The Golgi apparatus is a functionally distinct Ca2+ store regulated by PKA and Epac branches of the ß1-adrenergic signaling pathway. Science Signaling. 2015;8(398): ra101

138. Yang J, Zhao Z, Gu M, Feng X, Xu H. Release and uptake mechanisms of vesicular Ca2+ stores. Protein & Cell. 2019;10(1):8-19.

139. Hacker K, Medler KF. Mitochondrial Calcium Buffering Contributes to the Maintenance of Basal Calcium Levels in Mouse Taste Cells. Jounral of Neurophysiology. 2008;100(4):2177-91.

140. Schwaller B. Cytosolic Ca2+ Buffers. Cold Spring Harbor Perspectives in Biology. 2010;2(11): a004051.

141. Harr MW, Distelhorst CW. Apoptosis and Autophagy: Decoding Calcium Signals that Mediate Life or Death. Cold Spring Harbor Perspectives in Biology. 2010;2(10): a005579.

142. Elmore S. Apoptosis: A Review of Programmed Cell Death. Toxicologic Pathology. 2007;35(4):495-516.

143. Ashkenazi A, Dixit VM. Death Receptors: Signaling and Modulation. Science. 1998;281(5381):1305-8.

144. Cardone MH, Roy N, Stennicke HR, Salvesen GS, Franke TF, Stanbridge E, et al. Regulation of Cell Death Protease Caspase-9 by Phosphorylation. Science. 1998;282(5392):1318-21.

145. Evan GI, Vousden KH. Proliferation, cell cycle and apoptosis in cancer. Nature. 2001;411(6835)342-8.

146. Luo X, Budihardjo I, Zou H, Slaughter C, Wang X. Bid, a Bcl2 Interacting Protein, Mediates Cytochrome c Release from Mitochondria in

Response to Activation of Cell Surface Death Receptors. Cell. 1998;94(4):481-90.

147. Tsujimoto Y. Role of Bcl-2 family proteins in apoptosis: apoptosomes or mitochondria? Genes to Cells. 1998;3(11):697-707.

148. Gross A, McDonnell JM, Korsmeyer SJ. BCL-2 family members and the mitochondria in apoptosis. Genes and Development. 1999;13(15):1899-1911.

149. Droin NM, Green DR. Role of Bcl-2 family members in immunity and disease. Biochemica Et Biophysica Acta- Molecular Cell Research. 2004;1644(2-3):179-88.

150. Bassik MC, Scorrano L, Oakes SA, Pozzan T, Korsmeyer SJ. Phosphorylation of BCL-2 regulates ER Ca2+ homeostasis and apoptosis. The Embo Journal. 2004;23(5):1207-16.

151. Li C, Fox CJ, Master SR, Bindokas VP, Chodosh LA, Thompson CB. Bcl-X(L) affects Ca(2+) homeostasis by altering expression of inositol 1,4,5-trisphosphate receptors. Proc Natl Acad Sci U S A. 2002;99(15):9830-5.

152. White C, Li C, Yang J, Petrenko NB, Madesh M, Thompson CB, et al. The endoplasmic reticulum gateway to apoptosis by Bcl-X(L) modulation of the InsP3R. Nat Cell Biol. 2005;7(10):1021-8.

153. Oakes SA, Scorrano L, Opferman JT, Bassik MC, Nishino M, Pozzan T, et al. Proapoptotic BAX and BAK Regulate the Type 1 Inositol Trisphosphate Receptor and Calcium Leak from the Endoplasmic Reticulum. Proc Natl Acad Sci U S A. 2005;102(1):105-110.

154. Klionsky DJ. Autophagy: from phenomenology to molecular understanding in less than a decade. NATURE REVIEWS MOLECULAR CELL BIOLOGY. 2007(11):931-37.

155. Lum JJ, Bauer DE, Kong M, Harris MH, Li C, Lindsten T, et al. Growth Factor Regulation of Autophagy and Cell Survival in the Absence of Apoptosis. Cell. 2005;120(2):237-48.

156. Onodera J, Ohsumi Y. Autophagy Is Required for Maintenance of Amino Acid Levels and Protein Synthesis under Nitrogen Starvation. J Biol Chem. 2005;280(36):31582-6.

157. Levine B, Kroemer G. Autophagy in the Pathogenesis of Disease. Cell. 2008;132(1):27-42.

158. Wirawan E, Vanden Berghe T, Lippens S, Agostinis P, Vandenabeele P. Autophagy: for better or for worse. Cell Res. 2012;22(1):43-61.

159. Mizushima N, Levine B. Autophagy in mammalian development and differentiation. Nat Cell Biol. 2010 09;12(9):823-30.

160. Singh R, Cuervo AM. Autophagy in the Cellular Energetic Balance. Cell Metabolism. 2011;13(5):495-504.

161. Cao Y, Klionsky DJ. Physiological functions of Atg6/Beclin 1: a unique autophagy-related protein. CELL RESEARCH -ENGLISH EDITION-. 2007(10):839-49.

162. Yue Z, Jin S, Yang C, Levine AJ, Heintz N. Beclin 1, an Autophagy Gene Essential for Early Embryonic Development, Is a Haploinsufficient Tumor Suppressor. Proc Natl Acad Sci U S A. 2003;100(25):15077-82.

163. Bootman MD, Chehab T, Bultynck G, Parys JB, Rietdorf K. The regulation of autophagy by calcium signals: Do we have a consensus? Cell Calcium. 2018;70:32-46.

164. Grinde B. Role of Ca2+ for protein turnover in isolated rat hepatocytes. Biochem J. 1983;216(3):529-36.

165. Hoyer-Hansen M, Bastholm L, Szyniarowski P, Campanella M, Szabadkai G, Farkas T, et al. Control of macroautophagy by calcium, calmodulin-dependent kinase kinase-beta, and Bcl-2. Mol Cell. 2007;25(2):193-205.

166. Wang SH, Shih YL, Ko WC, Wei YH, Shih CM. Cadmium-induced autophagy and apoptosis are mediated by a calcium signaling pathway. Cell Mol Life Sci. 2008;65(22):3640-52.

167. Gao W, Ding W-, Stolz DB, Yin X-. Induction of macroautophagy by exogenously introduced calcium. AUTOPHAGY. 2008;(6):754-61.

168. Criollo A, Maiuri MC, Tasdemir E, Vitale I, Fiebig AA, Andrews D, et al. Regulation of autophagy by the inositol trisphosphate receptor. Cell Death Differ. 2007;14(5):1029-39.

169. Sarkar S, Andres Floto R, Berger Z, Imarisio S, Cordenier A, Pasco M, et al. Lithium Induces Autophagy by Inhibiting Inositol Monophosphatase. J Cell Biol. 2005;170(7):1101-11.

170. Khan MT, Joseph SK. Role of Inositol Trisphosphate Receptors in Autophagy in DT40 Cells. J Biol Chem. 2010;285(22):16912-20.

171. Harr, M.W. (1,6), McColl KS(1), Zhong F(1), Distelhorst, C.W. (1,2,4,5), Molitoris JK(3). Glucocorticoids downregulate Fyn and inhibit IP3-mediated calcium signaling to promote autophagy in T lymphocytes. Autophagy. 2010;6(7):912-21.

172. Sun F, Xu X, Wang X, Zhang B. Regulation of autophagy by Ca2+. Tumor Biology. 2016;37(12):15467-76.

173. Jung CH, Ro S, Cao J, Otto NM, Kim D. mTOR regulation of autophagy. FEBS Lett. 2010;584(7):1287-95.

174. Hardie DG. AMP-activated/SNF1 protein kinases: conserved guardians of cellular energy. Nat Rev Mol Cell Biol. 2007;8(10):774-85.

175. Cárdenas C, Miller RA, Smith I, Bui T, Molgó J, Müller M, et al. Essential Regulation of Cell Bioenergetics by Constitutive InsP3 Receptor Ca2+ Transfer to Mitochondria. Cell. 2010;142(2):270-83.

176. Nomura, M. (1,2), Ueno A(1), Saga K(1), Kaneda Y(1), Fukuzawa M(2). Accumulation of cytosolic calcium induces necroptotic cell death in human neuroblastoma. Cancer Res. 2014;74(4):1056-66.

177. Dhuriya YK, Sharma D. Necroptosis: a regulated inflammatory mode of cell death. Journal of Neuroinflammation. 2018;15(1):1-9.

178. Micheau O, Tschopp Jü. Induction of TNF Receptor I-Mediated Apoptosis via Two Sequential Signaling Complexes. Cell. 2003;114(2):181-90.

179. Amin P(1), Florez M(1), Najafov A(1), Geng J(1), Ofengeim D(1), Dziedzic SA(1), et al. Regulation of a distinct activated RIPK1 intermediate bridging complex I and complex II in TNFα-mediated apoptosis. Proc Natl Acad Sci U S A. 2018;115(26):E5944-53.

180. Chen J, Kos R, Garssen J, Redegeld F. Molecular Insights into the Mechanism of Necroptosis: The Necrosome As a Potential Therapeutic Target. Cells. 2019;8(12):1486-1506.

181. Pasparakis M, Vandenabeele P. Necroptosis and its role in inflammation. Nature. 2015;517(7534):311-20.

182. Wang L, Du F, Wang X. TNF-[alpha] Induces Two Distinct Caspase-8 Activation Pathways. Cell. 2008;133(4):693-703.

183. Seifert L(1), Miller, G. (2,3). Molecular pathways: The necrosome-A target for cancer therapy. Clinical Cancer Research. 2017;23(5):1132-6.

184. Sun W, Wu X, Gao H, Yu J, Zhao W, Lu J, et al. Cytosolic calcium mediates RIP1/RIP3 complex-dependent necroptosis through JNK activation and mitochondrial ROS production in human colon cancer cells. Free Radical Biology and Medicine. 2017;108:433-44.

185. Nuria Oliva-Vilarnau, Hankeova S, Vorrink SU, Mkrtchian S, Andersson ER, Lauschke VM. Calcium Signaling in Liver Injury and Regeneration. Frontiers in Medicine. 2018;5:192-209.

186. Armand M, Pasquier B, Andre M, Borel P, Senft M, Peyrot J, et al. Digestion and absorption of 2 fat emulsions with different droplet sizes in the human digestive tract. The American Journal of Clinical Nutrition. 2013;70(6):1096-1106.

187. Kalakonda A, Jenkins BA, John S. Physiology, Bilirubin. StatPearls. [Internet]. StatPearls Publishing; Treasure Island (FL): 2018.

188. Pusl T, Nathanson MH. The role of inositol 1,4,5-trisphosphate receptors in the regulation of bile secretion in health and disease. Biochem Biophys Res Commun. 2004;322(4):1318-25.

189. SHIBAO K, HIRATA K, ROBERT ME, NATHANSON MH. Loss of Inositol 1,4,5-Trisphosphate Receptors from Bile Duct Epithelia Is a Common Event in Cholestasis. Gastroenterology. 2003;125(4):1175-87.

190. Guan L, Fu P, Li P, Li Z, Liu H, Xin M, et al. Mechanisms of hepatic ischemia-reperfusion injury and protective effects of nitric oxide. World J Gastrointest Surg. 2014;6(7):122-8.

191. Banerjee A, Banerjee V, Czinn S, Blanchard T. Increased reactive oxygen species levels cause ER stress and cytotoxicity in andrographolide treated colon cancer cells. Oncotarget. 2017;8(16):26142-53.

192. Deniaud A, Sharaf ed, Maillier E, Poncet D, Kroemer G, Lemaire C, et al. Endoplasmic reticulum stress induces calcium-dependent permeability transition, mitochondrial outer membrane permeabilization and apoptosis. Oncogene. 2008;27(3):285-99.

193. Halestrap Ap. Calcium, mitochondria and reperfusion injury: a pore way to die. Biochemical Society Transactions. 2006;34(2):232-7.

194. Baumgartner HK, Gerasimenko JV, Thorne C, Ferdek P, Pozzan T, Tepikin AV, et al. Calcium Elevation in Mitochondria Is the Main Ca2+ Requirement for Mitochondrial Permeability Transition Pore (mPTP) Opening. The Journal of Biological Chemistry. 2009;284(31):20796-803.

195. Smith DA, Schmid EF. Drug withdrawals and the lessons within. CURRENT OPINION IN DRUG DISCOVERY AND DEVELOPMENT. 2006;9(1):38-46.

196. Ostapowicz G, Fontana RJ, Schiødt F,V., Larson A, Davern TJ, Han SHB, et al. Results of a prospective study of acute liver failure at 17 tertiary care centers in the United States. Ann Intern Med. 2002;137(12):947-54.

197. Maddrey WC. Hepatotoxicity: The adverse effects of drugs and other chemicals on the liver. Gastroenterology. 2000 May 2000;118(5):984-5.

198. Yoon E, Babar A, Choudhary M, Kutner M, Pyrsopoulos N. Acetaminophen-Induced Hepatotoxicity: a Comprehensive Update. Journal of Clinical and Translational Hepatology. 2016;4(2):131-142.

199. Jaeschke H. Mechanisms of Hepatotoxicity. Toxicological Sciences. 2002;65(2):166-76.

200. Russmann S, Kullak-Ublick G, Grattagliano I. Current concepts of mechanisms in drug-induced hepatotoxicity. Current Medicinal Chemistry. 2009;16(23):3041-53.

201. Lauschke VM, Magnus Ingelman-Sundberg. The Importance of Patient-Specific Factors for Hepatic Drug Response and Toxicity. International Journal of Molecular Sciences. 2016;17(10):1714-41.

202. Thomas SHL. Paracetamol (acetaminophen) poisoning. Pharmacology and Therapeutics. 1993;60(1):91-120.

203. Kheradpezhouh E, Ma L, Morphett A, Barritt GJ, Rychkov GY. TRPM2 channels mediate acetaminophen-induced liver damage. Proc Natl Acad Sci U S A. 2014;111(8):3176.

204. Bessems JGM, Vermeulen NPE. Paracetamol (acetaminophen)-induced toxicity: Molecular and biochemical mechanisms, analogues and protective approaches. Crit Rev Toxicol. 2001;31(1):55-138.

205. Cohen SD, Khairallah EA. Selective Protein Arylation and Acetaminophen-Induced Hepatotoxicity. Drug Metab Rev. 1997;29(1):59-77.

206. Jaeschke H, Bajt ML. Intracellular Signaling Mechanisms of Acetaminophen-Induced Liver Cell Death. Toxicological Sciences. 2006;89(1):31-41.

207. Muriel P. Role of free radicals in liver diseases. Hepatology International. 2009;3(4):526-36.

208. Zhou L, McKenzie BA, Eccleston ED, J., Srivastava SP, Chen N, Erickson RR, et al. The covalent binding of [14C]acetaminophen to mouse hepatic microsomal proteins: the specific binding to calreticulin and the two forms of the thiol:protein disulfide oxidoreductases. Chem Res Toxicol. 1996;9(7):1176-82.

209. Shin N, Liu Q, Stamer SL, Liebler DC. Protein Targets of Reactive Electrophiles in Human Liver Microsomes. Chemical Research in Toxicology. 2007;20(6):859-67.

210. Sehgal P, Szalai P, Olesen C, Praetorius HA, Nissen P, Christensen SB, et al. Inhibition of the sarco/endoplasmic reticulum (ER) Ca2+-ATPase by thapsigargin analogs induces cell death via ER Ca2+ depletion and the unfolded protein response. J Biol Chem. 2017;292(48):19656-73.

211. Ridgway EB, Ashley CC. Calcium transients in single muscle fibers. Biochem Biophys Res Commun. 1967;29(2):229-34.

212. McBurney RN, Neering IR. The measurement of changes in intracellular free calcium during action potentials in mammalian neurones. Journal of Neuroscience Methods. 1985;13(1):65-76.

213. Simpson AWM. Fluorescent measurement of [Ca2+]c: Basic practical considerations. Calcium Signaling Protocols. 2013;937:3-36.

214. Grynkiewicz G, Poenie M, Tsien RY. A new generation of Ca2+ indicators with greatly improved fluorescence properties. J Biol Chem. 1985;260(6):3440-50.

215. Tsien RY. New Calcium Indicators and Buffers with High Selectivity Against Magnesium and Protons: Design, Synthesis, and Properties of Prototype Structures. Biochemistry. 1980;19(11):2396-404.

216. Tsien RY, Pozzan T, Rink TJ. Calcium Homeostasis in Intact Lymphocytes: Cytoplasmic Free Calcium Monitored with a New, Intracellularly Trapped Fluorescent Indicator. J Cell Biol. 1982;94(2):325.

217. Takahashi A, Camacho P, Lechleiter JD, Herman B. Measurement of intracellular calcium. Physiological Reviews. 1999;79(4):1089-125.

218. Paredes RM, Etzler JC, Watts LT, Lechleiter JD. Chemical Calcium Indicators. Methods (San Diego California). 2008;46(3):143-51.

219. Tsuji FI(1), Inouye, S. (1,5), Ohmiya Y(2), Fagan TF(3), Toh H(4). MOLECULAR EVOLUTION OF THE Ca2+-BINDING PHOTOPROTEINS OF THE HYDROZOA. Photochem Photobiol. 1995;62(4):657-61.

220. Bonora M, Giorgi C, Bononi A, Marchi S, Patergnani S, Rimessi A, et al. Subcellular calcium measurements in mammalian cells using jellyfish photoprotein aequorin-based probes. Nature Protocols. 2013;8(11):2105-18.

221. Shimomura O, Johnson FH, Saiga Y. Extraction, Purification and Properties of Aequorin, a Bioluminescent Protein from the Luminous Hydromedusan, Aequorea. J Cell Comp Physiol. 1962;59(3):223-39.

222. Helm R, Tsien RY. Engineering green fluorescent protein for improved brightness, longer wavelengths and fluorescence resonance energy transfer. CURRENT BIOLOGY. 1996;6(2):178.

223. Kotlikoff MI. Genetically encoded Ca2+ indicators: using genetics and molecular design to understand complex physiology. Journal of Physiology. 2007;578(1):55-67.

224. Wu J, Abdelfattah AS, Miraucourt LS, Kutsarova E, Ruangkittisakul A, Zhou H, et al. A long Stokes shift red fluorescent Ca2+ indicator protein for

two-photon and ratiometric imaging. Nature Communications. 2014;5:5262-88.

225. Green AK, Stratton RC, Squires PE, Simpson AWM. Atrial Natriuretic Peptide Attenuates Elevations in Ca2 and Protects Hepatocytes by Stimulating Net Plasma Membrane Ca2 Efflux. The Journal of Biological Chemistry. 2007;282(47):34542-54.

226. Potter LR. Guanylyl cyclase structure, function and regulation. Cell Signal. 2011;23(12):1921-1926.

227. Scheving LA, Russell WE. Guanylyl Cyclase C Is Up-Regulated by Nonparenchymal Cells and Hepatocytes in Regenerating Rat Liver. Cancer Res. 1996;56(22):5186-91.

228. Potter LR. Handbook of Cell Signaling. 2nd ed. Academic Press. Chapter 172 - Guanylyl Cyclases. 22010:1399-407.

229. Gao Y, Raj JU. Fetal and Neonatal Physiology. 5th ed. Chapter 78-Regulation of Pulmonary Circulation. 2017:786-794.

230. Theilig F, Bostanjoglo M, Pavenstädt H, Grupp C, Holland G, Slosarek I, et al. Cellular distribution and function of soluble guanylyl cyclase in rat kidney and liver. Journal of the American Society of Nephrology. 2001;12(11):2209-20.

231. Ma X, Sayed N, Beuve A, van dA. NO and CO differentially activate soluble guanylyl cyclase via a heme pivot-bend mechanism. EMBO J. 2007;26(2):578-88.

232. Stone JR, Marletta MA. Soluble guanylate cyclase from bovine lung: activation with nitric oxide and carbon monoxide and spectral characterization of the ferrous and ferric states. Biochemistry. 1994;33(18):5636-40.

233. Francis SH, Busch JL, Corbin JD. cGMP-Dependent Protein Kinases and cGMP Phosphodiesterases in Nitric Oxide and cGMP Action. Pharmacological Reviews. 2010;62(3):525-63.

234. Schlossmann J, Huettner JP, Wolfertstetter S. cGMP-Dependent Protein Kinase Inhibitors in Health and Disease. Pharmaceuticals (Basel Switzerland). 2013;6(2):269-86.

235. Gao Y, Dou D, Qin X, Qi H, Ying L. Protein Kinases. Open Acess Publisher. 2012. Chapter 15- cGMP-Dependent Protein Kinase in the Regulation of Cardiovascular Functions:338-56

236. Osborne BW, Wu J, McFarland CJ, Nickl CK, Sankaran B, Casteel DE, et al. Crystal Structure of cGMP-dependent Protein Kinase Reveals Novel Site of Interchain Communication. Structure. 2011;19(9):1317-27.

237. Vaandrager AB, Bot AG, Ruth P, Pfeifer A, Hofmann F, De Jonge,H.R. Differential role of cyclic GMP-dependent protein kinase II in ion transport in murine small intestine and colon. Gastroenterology. 2000;118(1):108-14.

238. el-Husseini A, Bladen C, Vincent SR. Molecular characterization of a type II cyclic GMP-dependent protein kinase expressed in the rat brain. J Neurochem. 1995;64(6):2814-7.

239. Gambaryan S, Haeusler C, Markert T, Poehler D, Jarchau T, Walter U, et al. Expression of type II cGMP-dependent protein kinase in rat kidney is regulated by dehydration and correlated with renin gene expression. J Clin Invest. 1996;98(3):662-70.

240. Chikuda H, Kugimiya F, Hoshi K, Ikeda T, Ogasawara T, Shimoaka T, et al. Cyclic GMP-dependent protein kinase II is a molecular switch from proliferation to hypertrophic differentiation of chondrocytes. GENES AND DEVELOPMENT. 2004;18(19):2418-29.

241. Reierson GW, Guo S, Mastronardi C, Licinio J, Wong M. cGMP Signaling, Phosphodiesterases and Major Depressive Disorder. Current Neuropharmacology. 2011;9(4):715-27.

242. Kaupp UB, Seifert R. Cyclic nucleotide-gated ion channels. Physiol Rev. 2002;82(3):769-824.

243. Matulef K, Zagotta WN. Cyclic Nucleotide-Gated Ion Channels. Annual Review of Cell & Developmental Biology. 2003;19(1):23-44.

244. Kraus-Friedmann N. Cyclic nucleotide-gated channels in non-sensory organs. CELL CALCIUM. 2000;27(3):127-38.

245. Hackos DH, Korenbrot JI. Divalent Cation Selectivity Is a Function of Gating in Native and Recombinant Cyclic Nucleotide–gated Ion Channels from Retinal Photoreceptors. Journal of General Physiology. 1999;113(6):799-818.

246. Craven KB, Zagotta WN. CNG and HCN Channels: Two Peas, One Pod. Annu Rev Physiol. 2006;68:375-401.

247. Kramer RH, Molokanova E. Modulation of cyclic-nucleotide-gated channels and regulation of vertebrate phototransduction. Journal of Experimental Biology. 2001;204(17):2921-31.

248. Li M, Zhou X, Wang S, Michailidis I, Gong Y, Su D, et al. Structure of a eukaryotic cyclic nucleotide-gated channel. Nature. 2017;542(7639):60-65.

249. Liu DT, Tibbs GR, Paoletti P, Siegelbaum SA. Constraining Ligand-Binding Site Stoichiometry Suggests that a Cyclic Nucleotide–Gated Channel Is Composed of Two Functional Dimers. Neuron. 1998;21(1):235-48.

250. Pollard TD, Earnshaw WC, Lippincott-Schwartz J, Johnson GT. Cell Biology. Elsevier. 3rd ed. Chapter 16 - Membrane Channels. 2017:261-84.

251. Biel M. Cyclic nucleotide-regulated cation channels. J Biol Chem. 2009;284(14):9017-21.

252. Sperelakis N. Cell Physiology Source Book. Essentials of Membrane Biophysics. Elsevier Science. 4th ed. Chapter 21-Structure and Mechanism of Voltage-Gated Ion Channels:383-408

253. Bender AT, Beavo JA. Cyclic Nucleotide Phosphodiesterases: Molecular Regulation to Clinical Use. Pharmacol Rev. 2006;58(3):488-520.

254. Francis SH, Blount MA, Corbin JD. Mammalian Cyclic Nucleotide Phosphodiesterases: Molecular Mechanisms and Physiological Functions. Physiol Rev. 2011;91(2):651-90.

255. Esposito K, Reierson GW, Luo HR, Wu GS, Licinio J, Wong M-. Phosphodiesterase genes and antidepressant treatment response: A review. Ann Med. 2009;41(3):177-85.

256. Olga AHR, Rutten K, Harry WMS, Blokl A, Prickaerts J, Blokland A. Selective phosphodiesterase inhibitors: a promising target for cognition enhancement. Psychopharmacology. 2008;202(1)419-33.

257. Mustafa HN(1), Hegazy, G.A. (2,3), Alamoudi AA(2), El Awdan, S.A. (4). Liver ischemia/reperfusion injury, a setting in which the functional mass is reduced and the role of PDE5 inhibitor. European Journal of Anatomy. 2019;23(5):325-32.

258. Soderling SH, Bayuga SJ, Beavo JA. Identification and Characterization of a Novel Family of Cyclic Nucleotide Phosphodiesterases. J Biol Chem. 1998;273(25):15553-8.

259. Rosman GJ, Martins TJ, Sonnenburg WK, Beavo JA, Ferguson K, Loughney K. Isolation and characterization of human cDNAs encoding a cGMP-stimulated 3',5'-cyclic nucleotide phosphodiesterase. GENE. 1997;191(1):89-95.

260. Liu H, Maurice DH. Expression of cyclic GMP-inhibited phosphodiesterases 3A and 3B (PDE3A and PDE3B) in rat tissues: Differential subcellular localization and regulated expression by cyclic AMP. British Journal of Pharmaology. 1998;125(7):1501-10.

261. Fawcett L, Baxendale R, Stacey P, McGrouther C, Harrow I, Soderling S, et al. Molecular Cloning and Characterization of a Distinct Human Phosphodiesterase Gene Family: PDE11A. Proc Natl Acad Sci. 2000;97(7):3702-7.

262. Yuasa K, Kotera J, Fujishige K, Michibata H, Sasaki T, Omori K. Isolation and characterization of two novel phosphodiesterase PDE11A variants showing unique structure and tissue-specific expression. J Biol Chem. 2000(40):31469-79.

263. Fisher DA, Smith JF, Pillar JS, St. Denis SH, Cheng JB. Isolation and Characterization of PDE9A, a Novel Human cGMP-specific Phosphodiesterase. J Biol Chem. 1998;273(25):15559-64.

264. Azevedo MF, Faucz FR, Bimpaki E, Horvath A, Levy I, de Alexandre RB, et al. Clinical and Molecular Genetics of the Phosphodiesterases (PDEs). Endocrine Reviews. 2014;35(2):195-233.

265. Huai Q, Wang H, Zhang W, Colman RW, Robinson H, Ke H, et al. Crystal Structure of Phosphodiesterase 9 Shows Orientation Variation of Inhibitor 3-Isobutyl-1-Methylxanthine Binding. Proc Natl Acad Sci. 2004;101(26):9624-29.

266. Beavo JA, Hardman JG, Sutherland EW. Stimulation of adenosine 3',5'-monophosphate hydrolysis by guanosine 3',5'-monophosphate. J Biol Chem. 1971;246(12):3841-6.

267. Erneux C, Couchie D, Dumont JE, Baraniak J, Stec WJ, Garcia Abbad E, et al. Specificity of Cyclic GMP Activation of a Multi-substrate Cyclic Nucleotide Phosphodiesterase from Rat Liver. European Journal of Biochemistry. 1981;115(3):503-10.

268. Beavo JA. Cyclic nucleotide phosphodiesterases: functional implications of multiple isoforms. Physiol Rev. 1995;75(4):725-48.

269. Rybalkin SD, Rybalkina IG, Beavo JA. Phosphorylation of cAMP hydrolyzing PDE (PDE3A) by cGMP-dependent protein kinase (PKG) in human platelets. BMC Pharmacology. 2007;7(1):1471-2210.

270. Turko IV, Francis SH, Corbin JD. Binding of cGMP to both allosteric sites of cGMP-binding cGMP-specific phosphodiesterase (PDE5) is required for its phosphorylation. Biochemical Journal. 1998;329(3):505-10.

271. Zoraghi R, Bessay EP, Corbin JD, Francis SH. Structural and Functional Features in Human PDE5A1 Regulatory Domain That Provide for Allosteric cGMP Binding, Dimerization, and Regulation. J Biol Chem. 2005;280(12):12051-63.

272. Yuasa K, Ohgaru T, Asahina M, Omori K. Identification of rat cyclic nucleotide phosphodiesterase 11A (PDE11A): comparison of rat and human PDE11A splicing variants. Eur J Biochem. 2001;268(16):4440-8.

273. Jorgensen TD, Dissing S, Gromada J. Cyclic GMP potentiates phenylephrine but not cyclic ADP-ribose-evoked calcium release from rat lacrimal acinar cells. FEBS Lett. 1996;391(1):117-20.

274. Camello PJ, Petersen OH, Toescu EC. Simultaneous presence of cAMP and cGMP exert a co-ordinated inhibitory effect on the agonist-evoked Ca2+ signal in pancreatic acinar cells. PFLUGERS ARCHIV-EUROPEAN JOURNAL OF PHYSIOLOGY. 1996;432(5):775-81.

275. Milbourne EA, Bygrave FL. Do nitric oxide and cGMP play a role in calcium cycling? Cell Calcium. 1995;18(3):207-13.

276. Cornwell TL, Lincoln TM. Regulation of intracellular Ca2+ levels in cultured vascular smooth muscle cells. Reduction of Ca2+ by atriopeptin and 8-bromo-cyclic GMP is mediated by cyclic GMP-dependent protein kinase. J Biol Chem. 1989;264(2):1146-55.

277. FURUKAWA K, NAKAMURA H. Cyclic GMP Regulation of the Plasma Membrane (Ca2+-Mg2+)ATPase in Vascular Smooth Muscle. Journal of Biochemistry. 1987;101(1):287-90.

278. Furukawa K-, Tawada Y, Shigekawa M. Regulation of the plasma membrane Ca2+ pump by cyclic nucleotides in cultured vascular smooth muscle cells. J Biol Chem. 1988;263(17):8058-65.

279. Pandol SJ, Schoeffield-Payne M. Cyclic GMP regulates free cytosolic calcium in the pancreatic acinar cell. Cell Calcium. 1990;11(7):477-86.

280. Tertyshnikova S, Yan X, Fein A. cGMP inhibits IP3-induced Ca2+ release in intact rat megakaryocytes via cGMP- and cAMP-dependent protein kinases. Journal of Physiology. 1998;512(1):89-96.

281. Schlossmann J, Ammendola A, Ashman K, Zong XG, Huber A, Neubauer G, et al. Regulation of intracellular calcium by a signalling complex of IRAG, IP3 receptor and cGMP kinase I beta. Nature. 2000;404(6774):197-201.

282. Guihard G, Combettes L, Capiod T. 3':5'-Cyclic guanosine monophosphate (cGMP) potentiates the inositol 1,4,5-trisphosphate-evoked Ca2+ release in guinea-pig hepatocytes. Biochem J. 1996;318(3):849-55.

283. Green AK, Zolle O, Simpson AWM. Atrial natriuretic peptide attenuates Ca2 oscillations and modulates plasma membrane Ca2 fluxes in rat hepatocytes. Gastroenterology. 2002;123(4):1291-303.

284. Rooney TA, Joseph SK, Queen C, Thomas AP. Cyclic GMP induces oscillatory calcium signals in rat hepatocytes. J Biol Chem. 1996;271(33):19817-25.

285. Dufour JF, Turner TJ, Arias IM. Nitric oxide blocks bile canalicular contraction by inhibiting inositol trisphosphate-dependent calcium mobilization. Gastroenterology. 1995;108(3):841-9.

286. Von Ruecker AA, Wild M, Rao GS, Bidlingmaier F, Clin Invest J. Atrial Natriuretic Peptide Protects Hepatocytes Against Damage Induced by Hypoxia and Reactive Oxygen Possible Role of Intracellular Free lonized Calcium. Journal of Clinical Chemistry and Clinical Biochemistry. 1989;27(9):531-7.

287. Guihard G, Combettes L, Capiod T. 3':5'-cyclic guanosine monophosphate (cGMP) potentiates the inositol 1,4,5-trisphosphate-evoked Ca2+ release in guinea-pig hepatocytes. Biochemical Journal. 1996;318(3):849-55.

288. BURGSTAHLER AD, NATHANSON MH. NO modulates the apicolateral cytoskeleton of isolated hepatocytes by a PKC-dependent, cGMP-independent mechanism. American Journal of Physiology: Gastrointestinal & Liver Physiology. 1995;32(5):G789-99.

289. Dzeja C, Hagen V, Kaupp UB, Frings S. Ca2+ permeation in cyclic nucleotide-gated channels. Embo Journal. 1999;18(1):131-44.

290. Gao T, Yatani A, Dell'Acqua M,L., Sako H, Green SA, Dascal N, et al. cAMP-Dependent Regulation of Cardiac L-Type Ca2+ Channels Requires Membrane Targeting of PKA and Phosphorylation of Channel Subunits. Neuron. 1997;19(1):185-96.

291. Wall ME, Francis SH, Corbin JD, Grimes K, Robyn Richie-Jannetta, Kotera J, et al. Mechanisms Associated with cGMP Binding and Activation of cGMP-Dependent Protein Kinase. Proc Natl Acad Sci. 2003;100(5):2380.

292. Xia C(1), Bao, Z. (1,2), Liu, M. (1,4), Yue C(3), Sanborn BM(3). Phosphorylation and Regulation of G-protein-activated Phospholipase C-ß3 by cGMP-dependent Protein Kinases. J Biol Chem. 2001;276(23):19770-7.

293. Haug LS, Jensen V, Hvalby O, Walaas SI, Oestvold AC. Phosphorylation of the inositol 1,4,5-trisphosphate receptor by cyclic nucleotide-dependent kinases in vitro and in rat cerebellar slices in situ. J Biol Chem. 1999;274(11):7467-73.

294. Geiger M. Fundamentals of vascular biology. Springer. 2019. Chapter 5-Vascular Smooth Muscle Cells: Regulation of Vasoconstriction and Vasodilation:97-110

295. White RE, Lee AB, Shcherbatko AD, Lincoln TM, Schonbrunn A, Armstrong DL. Potassium channel stimulation by natriuretic peptides through cGMP-dependent dephosphorylation. Nature. 1993;361(6409):263-6.

296. Zhou XB, Ruth P, Schlossmann J, Hofmann F, Korth M. Protein Phosphatase 2A Is Essential for the Activation of Ca2+-activated K+ Currents by cGMP-dependent Protein Kinase in Tracheal Smooth Muscle and Chinese Hamster Ovary Cells. J Biol Chem. 1996;271(33):19760-7.

297. Alioua A, Tanaka Y, Wallner M, Hofmann F, Ruth P, Meera P, et al. The large conductance, voltage-dependent, and calcium-sensitive K^+ channel, Hslo, is a target of cGMP-dependent protein kinase phosphorylation in vivo. J Biol Chem. 1998;273(49):32950-6.

298. Fukao M, Mason HS, Britton FC, Kenyon JL, Horowitz B, Keef KD. Cyclic GMP-dependent protein kinase activates cloned BKCa channels expressed in mammalian cells by direct phosphorylation at serine 1072. J Biol Chem. 1999;274(16):10927-35.

299. Hall SK, Armstrong DL. Conditional and unconditional inhibition of calcium-activated potassium channels by reversible protein phosphorylation. J Biol Chem. 2000;275(6):3749-54.

300. Carini R, DE Cesaris Mg, Splendore R, Domenicotti CM, Nitti M, Pronzato MA, et al. Mechanisms of hepatocyte protection against hypoxic injury by atrial natriuretic peptide. Hepatology. 2003;37(2):277-85.

301. Kim Y-, Talanian RV, Billiar TR. Nitric oxide inhibits apoptosis by preventing increases in caspase-3-like activity via two distinct mechanisms. J Biol Chem. 1997;272(49):31138-48.

302. Kobayashi H, Nonami T, Kurokawa T, Takeuchi Y, Harada A, Nakao A, et al. Role of Endogenous Nitric Oxide in Ischemia-Reperfusion Injury in Rat Liver. J Surg Res. 1995;59(6):772-9.

303. Galen F-(1), Cottart C-(1), Nivet V(1), Clot, J.-P. (1,4), Souil E(2), Dinh-Xuan A, et al. Implication of nitric oxide synthase-III and guanosine 3':5'-cyclic monophosphate in the cytoprotective effects of nitric oxide against hepatic ischemia-reperfusion injury. Comptes Rendus de l'Academie des Sciences - Serie III. 1999;322(10):871-7.

304. Nikolaev VO, Sprenger JU. Biophysical Techniques for Detection of cAMP and cGMP in Living Cells. International Journal of Molecular Sciences. 2013;14(4):8025-46.

305. Cawley SM, Sawyer CL, Brunelle KF, van der Vliet A, Dostmann WR. Nitric oxide-evoked transient kinetics of cyclic GMP in vascular smooth muscle cells. Cellular Signalling. 2007;19(5):1023-33.

306. Honda A, Adams SR, Sawyer CL, Lev-Ram V, Tsien RY, Dostmann W. Spatiotemporal dynamics of guanosine 3 ',5 '-cyclic monophosphate revealed by a genetically encoded, fluorescent indicator. Proc Natl Acad Sci. 2001;98(5):2437-42.

307. Nikolaev VO, Gambaryan S, Lohse MJ. Fluorescent sensors for rapid monitoring of intracellular cGMP. Nature Methods. 2006;3(1):23-5.

308. Russwurm M, Mullershausen F, Friebe A, Jäger R, Russwurm C, Koesling D. Design of fluorescence resonance energy transfer (FRET)-based cGMP indicators: a systematic approach. Biochem J. 2007;407(1):69-77.

309. Takimoto E, Champion HC, Belardi D, Moslehi J, Mongillo M, Mergia E, et al. cGMP Catabolism by Phosphodiesterase 5A Regulates Cardiac Adrenergic Stimulation by NOS3-Dependent Mechanism. Circ Res. 2005;96(1):100-9.

310. Mongillo M, Tocchetti CG, Terrin A, Lissandron V, Cheung Y-, Dostmann WR, et al. Compartmentalized Phosphodiesterase-2 Activity Blunts beta-Adrenergic Cardiac Inotropy via an NO/cGMP-Dependent Pathway. Circ Res. 2006;98(2):226-34.

311. Nausch LWM, Ledoux J, Bonev AD, Nelson MT, Dostmann WR. Differential patterning of cGMP in vascular smooth muscle cells revealed by single GFP-linked biosensors. Proceedings of the National Academy of Sciences of the United States of America (PNAS). 2008;105(1):365-70.

312. Mo E, Amin H, Bianco IH, Garthwaite J. Kinetics of a cellular nitric oxide/cGMP/phosphodiesterase-5 pathway. J Biol Chem. 2004;279(25):26149-58.

313. Roy B, Garthwaite J. Nitric Oxide Activation of Guanylyl Cyclase in Cells Revisited. Proc Natl Acad Sci. 2006;103(32):12185.

314. Bhargava Y, Hampden-Smith K, Chachlaki K, Wood KC, Vernon J, Allerston CK, et al. Improved genetically-encoded, FlincG-type fluorescent biosensors for neural cGMP imaging. Frontiers in Molecular Neuroscience. 2013;6(26): doi: 10.3389/fnmol.2013.00026.

315. Fadime EP. Vitamin C: An Antioxidant Agent. Intech Open Science. 2017;23-35. Doi:10.5772/intechopen.69660.

316. Pham-Huy L, He H, Pham-Huy C. Free Radicals, Antioxidants in Disease and Health. International Journal of Biomedical Science. 2008;4(2):89-96.

317. El-Ridi M, Rahmy T. Action of Vitamin C Against Acetaminophen-Induced Hepatorenal Toxicity in Rats. Journal of Toxicology-Toxin Reviews. 2000;19(3):275-304.

318. Eid RA, Zaki MSA, Alghamdi MA, Sideeg AM, Ali K, Z. M, Andarawi M, et al. Vitamin C Administration Attenuated Artemether Induced Hepatic Injury in Rats. International Journal of Morphology. 2020;38(1):48-55.

319. Nadia R.A. Abou-Zeid. Ameliorative effect of vitamin C against 5-fuorouracil-induced hepatotoxicity in mice: A light and electron microscope study. The Journal of Basic and Applied Zoology. 2014;67(4):109-18.

320. Okamura Y, Omori A, Asada N, Ono A. Effects of vitamin C and E on toxic action of alcohol on partial hepatectomy-induced liver regeneration in rats. Journal of Clinical Biochemistry and Nutrition. 2018;63(1):50-7.

321. Ramírez-Farías C, Madrigal-Santillán E, Gutiérrez-Salinas J, Rodríguez-Sánchez N, Martínez-Cruz M, Valle-Jones I, et al. Protective effect of some vitamins against the toxic action of ethanol on liver regeneration induced by partial hepatectomy in rats. World Journal of Gastroenterology. 2008;14(6):899-907.

322. Grajeda-Cota P, Rami´rez-Mares MV, González de Meji´a E. Vitamin C protects against in vitro cytotoxicity of cypermethrin in rat hepatocytes. Toxicology in Vitro. 2004;18(1):13-9.

323. Ahmadizadeh, Abdolkany, Afravy. The Preventive Effect of Vitamin C on Styrene-Induced Toxicity in Rat Liver and Kidney. Jundishapur Journal of Health Sciences. 2015;7(2):14-19.

324. Xu P, Li Y, Yu Z, Yang L, Shang R, Yan Z. Protective Effect of Vitamin C on Triptolide-induced Acute Hepatotoxicity in Mice through mitigation of oxidative stress. An Acad Bras Cienc. 2019;91(2):e20181257.

325. Bandara P, George J, McCaughan G, Naidoo D, Lux O, Salonikas C, et al. Antioxidant levels in peripheral blood, disease activity and fibrotic stage in chronic hepatitis C. Liver International. 2005;25(3):518-26.

326. Souza dS, De Bem AF, Colpo E, Bertoncello I, Nogueira CW, Rocha JBT. Plasmatic vitamin C in nontreated hepatitis C patients is negatively associated with aspartate aminotransferase. Liver International. 2008;28(1):54-60.

327. Boobis AR, Seddon CE, Nasseri-Sina P, Davies DS. Evidence for a direct role of intracellular calcium in paracetamol toxicity. Biochem Pharmacol. 1990;39(8):1277-81.

328. Cui R, Yan L, Luo Z, Guo X, Yan M. Blockade of store-operated calcium entry alleviates ethanol-induced hepatotoxicity via inhibiting apoptosis. Toxicology and Applied Pharmacology. 2015;287(1):52-66.

329. Chen Z, Che D, Chang C. Antioxidants, vitamin C and dithiothreitol, activate membrane-bound guanylate cyclase in PC12 cells. Journal of Pharmacy and Pharmacology: An international journal of pharmaceutical science. 2001;53(2):243-7.

330. Parker WH, Qu Z, May JM. Intracellular Ascorbate Prevents Endothelial Barrier Permeabilization by Thrombin*. Journal of Biological Chemistry. 2015;290(35):21486-97.

331. Grossmann M, Dobrev D, Himmel H.M, Ravens U, Kirch W. Ascorbic acid-induced modulation of venous tone in humans. Hypertension. 2001;37(3):949–54

332. Ozturk G, Mulholland CW, Hannigan M. Vitamin C decreases intracellular calcium level in human lymphoid cells. JOURNAL OF PHYSIOLOGY AND PHARMACOLOGY. 2001;52(2):285-92.

333. Pan S, Chen HH, Correia C, Dai H, Witt TA, Kleppe LS, et al. Cell Surface Protein Disulfide Isomerase Regulates Natriuretic Peptide Generation of Cyclic Guanosine Monophosphate. PLoS One. 2014;9(11):1-14.

334. Araujo TLS, Fernandes CG, Laurindo FRM. Golgi-independent routes support protein disulfide isomerase externalization in vascular smooth muscle cells. Redox Biology. 2017;12:1004-10.

335. Araujo TLS, Zeidler JD, Oliveira PVS, Dias MH, Armelin HA, Laurindo FRM. Protein disulfide isomerase externalization in endothelial cells follows classical and unconventional routes. Free Radic Biol Med. 2017;103:199-208.

336. Terada K, Manchikalapudi P, Noiva R, Jauregui HO, Stockert RJ, Schilsky ML. Secretion, surface localization, turnover, and steady state expression of protein disulfide isomerase in rat hepatocytes. The Journal of Biological Chemistry. 1995;270(35):20410-6.

337. Turano C, Coppari S, Altieri F, Ferraro A. Proteins of the PDI family: Unpredicted non-ER locations and functions. Journal of Cell Physiology. 2002;193(2):154-63.

338. Rosenberg N, Mor-Cohen R, Sheptovitsky VH, Romanenco O, Hess O, Lahav J. Integrin-mediated cell adhesion requires extracellular disulfide exchange regulated by protein disulfide isomerase. Exp Cell Res. 2019;381(1):77-85.

339. Jain S, McGinnes LW, Morrison TG. Thiol/Disulfide Exchange Is Required for Membrane Fusion Directed by the Newcastle Disease Virus Fusion Protein. J Virol. 2007;81(5):2328-39.

340. Fenouillet E, Barbouche R, Jones IM. Cell Entry by Enveloped Viruses: Redox Considerations for HIV and SARS-Coronavirus. Antioxidants and Redox Signaling. 2007;9(8):1009-34.

341. Godin B, Touitou E. Mechanism of bacitracin permeation enhancement through the skin and cellular membranes from an ethosomal carrier. Journal of Controlled Release. 2004;94(2):365-79.

342. Marschall ALJ, Frenzel A, Schirrmann T, Schüngel M, Dubel S. Targeting antibodies to the cytoplasm. MAbs. 2011;3(1):3-16.

343. Yang NJ, Hinner MJ. Getting Across the Cell Membrane: An Overview for Small Molecules, Peptides, and Proteins. Site-Specific Protein Labeling. 2015;1266(1):29-53.

344. Felbel J, Trockur B, Ecker T, Landgraf W, Hofmann F. Regulation of cytosolic calcium by cAMP and cGMP in freshly isolated smooth muscle cells from bovine trachea. J Biol Chem. 1988;263(32):16764-71.

345. Goerbig MN, Gines P, Bataller R, Nicolas JM, Garcia-Ramallo E, Tobias E, et al. Atrial Natriuretic Peptide Antagonizes Endothelin-Induced Calcium Increase and Cell Contraction in Cultured Human Hepatic Stellate Cells. Hepatology. 1999;30(2):501-9.

346. Li S, Sun N. Regulation of intracellular Ca2+ and calcineurin by NO/PKG in proliferation of vascular smooth muscle cells. Acta Pharmacol Sin. 2005;26(3):323-8.

347. Ishikawa T, Hume JR, Keef KD. Regulation of Ca2+ channels by cAMP and cGMP in vascular smooth muscle cells. Circ Res. 1993;73(6):1128-37.

348. Chung JW, Schacht J. ATP and Nitric Oxide Modulate Intracellular Calcium in Isolated Pillar Cells of the Guinea Pig Cochlea. Journal of the Association for Research in Otolaryngology. 2001;2(4):399-407.

349. Seagrave J, Curry M, Ramsey RC, Martinez JR. Intracellular pH changes induced by exposure to weak acids and bases in submandibular cells of early postnatal rats. Archives of Oral Biology. 1992;37(9):699-703.

350. Dong QS, Wroblewska B, Myers AK. Inhibitory Effect of Alcohol on Cyclic Gmp Accumulation in Human Platelets. Thromb Res. 1995 Oct-15;80(2):143-51.

351. Fock EM, Lavrova EA, Bachteeva VT, Chernigovskaya EV, Parnova RG. Nitric oxide inhibits arginine-vasotocin-induced increase of water osmotic permeability in frog urinary bladder. Pflügers Archiv - European Journal of Physiology. 2004;448(2):197-203.

352. Jaeschke H. Mechanisms of Hepatotoxicity. Toxicological Sciences. 2002;65(2):166-76.

353. Zoeteweij JP, van de Water B, de Bont HJ, Mulder GJ, Nagelkerke JF. Involvement of intracellular Ca2 and K in dissipation of the mitochondrial membrane potential and cell death induced by extracellular ATP in hepatocytes. Biochem J. 1992;288(1):207-13.

354. Ray SD, Kamendulis LM, Gurule MW, Yorkin RD, Corcoran GB. Ca2 antagonists inhibit DNA fragmentation and toxic cell death induced by acetaminophen. FASEB Journal. 1993;7(5):453-63.

355. Hemmings SJ, Pulga VB, Tran ST, Uwiera RRE. Differential inhibitory effects of carbon tetrachloride on the hepatic plasma membrane, mitochondrial and endoplasmic reticular calcium transport systems: implications to hepatotoxicity. Cell Biochem Funct. 2002;20(1):47-60.

356. Sakon M, Ariyoshi H, Umeshita K, Monden M. Ischemia–Reperfusion Injury of the Liver with Special Reference to Calcium-Dependent Mechanisms. Surg Today. 2002;32(1):1-12.

357. Ray SD, Kamendulis LM, Gurule MW, Yorkin RD, Corcoran GB. Ca2 antagonists inhibit DNA fragmentation and toxic cell death induced by acetaminophen. FASEB Journal. 1993;7(5):453-63.

358. Hasegawa C, Yamada T, Ohara H, Nakazawa T, Sano H, Ando H, Kunimatsu M, Ozaki Y, Takahashi S, Nomura T, Joh T, Itoh M.

Taurochenodeoxycholic acid induced biphasic hepatotoxicity in isolated perfused rat liver: roles of Ca2+ and calpain. Hepatogastroenterology. 2003;50(52):972-8.

359. Hemmings SJ, Pulga VB, Tran ST, Uwiera RRE. Differential inhibitory effects of carbon tetrachloride on the hepatic plasma membrane, mitochondrial and endoplasmic reticular calcium transport systems: implications to hepatotoxicity. Cell Biochem Funct. 2002;20(1):47-60.

360. Stratton RC, Squires PE, Green AK. ANP stimulates hepatocyte Ca2 efflux via plasma membrane recruitment of PKGIα. Biochem Biophys Res Commun. 2008;368(4):965-70.

361. Matsunobu T, Schacht J. Nitric oxide/Cyclic GMP pathway attenuates ATP-evoked intracellular calcium increase in supporting cells of the guinea pig cochlea. J Comp Neurol. 2000;423(3):452-61.

362. Cornwell TL, Lincoln TM. Regulation of intracellular Ca2+ levels in cultured vascular smooth muscle cells. Reduction of Ca2+ by atriopeptin and 8-bromo-cyclic GMP is mediated by cyclic GMP-dependent protein kinase. Journal of Biological Chemistry. 1989;264(2):1146-55.

363. Matsunobu T, Schacht J. Nitric oxide/Cyclic GMP pathway attenuates ATP-evoked intracellular calcium increase in supporting cells of the guinea pig cochlea. J Comp Neurol. 2000;423(3):452-61.

364. Karala A, Ruddock LW. Bacitracin is not a specific inhibitor of protein disulfide isomerase. FEBS J. 2010;277(11):2454-62.

365. Cho J, Furie BC, Coughlin SR, Furie B. A critical role for extracellular protein disulfide isomerase during thrombus formation in mice. J Clin Invest. 2008;118(3):1123-31.

366. Dutta D. Mechanism of store-operated calcium entry. J Biosci. 2000;25(4):397-404.

367. Berridge MJ. Capacitative calcium entry. Biochem J. 1995;312(1):1-11.

368. Araujo TLS, Fernandes CG, Laurindo FRM. Golgi-independent routes support protein disulfide isomerase externalization in vascular smooth muscle cells. Redox Biology. 2017;12:1004-10.

369. Essex DW, Chen K, Swiatkowska M. Localization of protein disulfide isomerase to the external surface of the platelet plasma membrane. Blood. 1995;86(6):2168-73.

370. Kröning H, Kähne T, Ittenson A, Franke A, Ansorge S. Thiol-proteindisulfide-oxidoreductase (proteindisulfide isomerase): a new plasma membrane constituent of mature human B lymphocytes. Scand J Immunol. 1994;39(4):346-50.

371. Akagi S, Yamamoto A, Yoshimori T, Masaki R, Ogawa R, Tashiro Y. Localization of protein disulfide isomerase on plasma membranes of rat exocrine pancreatic cells. J Histochem Cytochem. 1988;36(8):1069-74.

372. Jordan PA, Gibbins JM. Extracellular disulfide exchange and the regulation of cellular function. Antioxid Redox Signal. 2006;8(3-4):312-24.

373. Kaiser BK, Yim D, Chow IT, Gonzalez S, Dai Z, Mann HH, et al. Disulphide-isomerase-enabled shedding of tumour-associated NKG2D ligands. Nature. 2007;447(7143):482-6.

374. Laurindo FRM, Pescatore LA, Fernandes DdC. Protein disulfide isomerase in redox cell signaling and homeostasis. Free Radic Biol Med. 2012;52(9):1954-69.

375. Dusterhoft S, Jung S, Hung C-, Tholey A, Sonnichsen FD, Grotzinger J, et al. Membrane-Proximal Domain of a Disintegrin and Metalloprotease-17 Represents the Putative Molecular Switch of Its Shedding Activity Operated by Protein-disulfide Isomerase. Journal American Chem Soc. 2013;135(15):5776-81

376. Uboh FE, Ebong PE, Akpan HD, Usoh IF. Hepatoprotective effect of vitamins C and E against gasoline vapor-induced liver injury in male rats. Turkish Journal of Biology. 2012;36(2):217-23.

377. Foufelle F, Fromenty B. Role of endoplasmic reticulum stress in drug-induced toxicity. 2016;4(1):e00211.

378. Lancaster EM, Hiatt JR, Zarrinpar A. Acetaminophen hepatotoxicity: an updated review. Arch Toxicol. 2015;89(2):193-9.

379. den Braver MW, den Braver-Sewradj SP, Vermeulen NPE, Commandeur JNM. Characterization of cytochrome P450 isoforms involved in sequential two-step bioactivation of diclofenac to reactive p-benzoquinone imines. Toxicol Lett. 2016;253:46-54.

380. Boelsterli UA. Diclofenac-induced liver injury: a paradigm of idiosyncratic drug toxicity. Toxicology and Applied Pharmacology. 2003;192(3):307-22.

381. Lim MS, Lim PLK, Gupta R, Boelsterli UA. Critical role of free cytosolic calcium, but not uncoupling, in mitochondrial permeability transition and cell death induced by diclofenac oxidative metabolites in immortalized human hepatocytes. Toxicology and Applied Pharmacology. 2006;217(3):322-31.

382. Maiuri AR, Breier AB, Turkus JD, Ganey PE, Roth RA. Calcium Contributes to the Cytotoxic Interaction Between Diclofenac and Cytokines. Toxicol Sci. 2016;149(2):372-84.

383. Grossmann M, Kirch W, Dobrev D, Himmel HM, Ravens U. Ascorbic acid-induced modulation of venous tone in humans. Hypertension. 2001;37(3):949-54.

384. Jones KT, Sharpe GR. Thapsigargin Raises Intracellular Free Calcium Levels in Human Keratinocytes and Inhibits the Coordinated Expression of Differentiation Markers. Experimental Cell Research. 1994;210(1):71-6.

385. Potter LR. Natriuretic peptide metabolism, clearance and degradation. FEBS J. 2011;278(11):1808-17.

386. Carvalho M, Remião F, Milhazes N, Borges F, Fernandes E, Carvalho F, et al. The toxicity of N-methyl-α-methyldopamine to freshly isolated rat hepatocytes is prevented by ascorbic acid and N-acetylcysteine. Toxicology. 2004;200(2):193-203.

387. Daly DJ, Maskrey P, Pennington RJT. Characterization of proline endopeptidase from skeletal muscle. International Journal of Biochemistry. 1985;17(4):521-4.

388. Vitkovic L, Sadoff HL. Purification of the extracellular protease of Bacillus licheniformis and its inhibition by bacitracin. J Bacteriol. 1977;131(3):891-6.

389. Zhao G(1), Li C(1), Lu H(2). Proapoptotic activities of Protein Disulfide Isomerase (PDI) and PDIA3 protein, a role of the Bcl-2 protein Bak. J Biol Chem. 2015;290(14):8949-63.

390. Jasuja R, Passam FH, Kennedy DR, Kim SH, van Hessem L, Lin L, et al. Protein disulfide isomerase inhibitors constitute a new class of antithrombotic agents. J Clin Invest. 2012;122(6):2104-13.

391. Vardanyan RS, Hruby VJ. Synthesis of essential drugs. 2006.

392. Miller JH, McDonald RK, Shock NW. The Effect of Bacitracin on Renal Function. J Clin Invest. 1950;29(4):389-95.

393. Tee LBG, Davies DS, Seddon CE, Boobis AR. Species differences in the hepatotoxicity of paracetamol are due to differences in the rate of conversion to its cytotoxic metabolite. Biochem Pharmacol. 1987;36(7):1041-52.

394. Hattis D. Human interindividual variability in susceptibility to toxic effects: from annoying detail to a central determinant of risk. Toxicology. 1996;111(1):5-14.

395. Abhilash PA, Harikrishnan R, Indira M. Ascorbic acid supplementation causes faster restoration of reduced glutathione content in the regression of alcohol-induced hepatotoxicity in male guinea pigs. Redox Rep. 2012;17(2):72-9.

396. Naseer MI, Ullah N, Ullah I, Koh PO, Lee HY, Park MS, et al. Vitamin C protects against ethanol and PTZ-induced apoptotic neurodegeneration in prenatal rat hippocampal neurons. Synapse. 2011;65(7):562-71.

397. Naseer MI, Najeebullah, Ikramullah, Zubair H, Hassan M, Yang BC, et al. Vitamin-C protect ethanol induced apoptotic neurodegeneration in postnatal rat brain. Pak J Med Sci. 2009;25(5):718-722.

398. Sánchez-Moreno C, Paniagua M, Madrid A, Martín A. Protective effect of vitamin C against the ethanol mediated toxic effects on human brain glial cells. 2003;14(10):606-13.

399. Taha MO, Souza HS, Carvalho CA, Fagundes DJ, Simo&tilde, es MJ, et al. Cytoprotective effects of ascorbic acid on the ischemia-reperfusion injury of rat liver. Transplant Proc. 2004;36(2):296-300.

400. Duarte TL, Lunec J. Review: When is an antioxidant not an antioxidant? A review of novel actions and reactions of vitamin C. Free Radic Res. 2005;39(7):671-86.

401. Padayatty SJ, Levine M. Vitamin C physiology: the known and the unknown and Goldilocks. 2016; 22(6): 463-493.

402. Rice ME. Ascorbate regulation and its neuroprotective role in the brain. Trends Neurosci. 2000;23(5):209-16.

403. Spector R. Vitamin Homeostasis in the Central Nervous System. N Engl J Med. 1977;296(24):1393-8.

404. Milby K, Oke A, Adams RN. Detailed mapping of ascorbate distribution in rat brain. Neurosci Lett. 1982;28(2):169-74.

405. Padayatty SJ, Riordan HD, Hewitt SM, Katz A, Hoffer LJ, Levine M. Intravenously administered vitamin C as cancer therapy: three cases. 2006;174(7):937-42

406. Wang F, Ming-Ming He, Zi-Xian Wang, Li S, Jin Y, Ren C, et al. Phase I study of high-dose ascorbic acid with mFOLFOX6 or FOLFIRI in patients with metastatic colorectal cancer or gastric cancer. BMC Cancer. 2019;19(1):460

407. Monti M, D., Mitchell E, Bazzan AJ, Littman S, Zabrecky G, Yeo CJ, et al. Phase I evaluation of intravenous ascorbic Acid in combination with gemcitabine and erlotinib in patients with metastatic pancreatic cancer. PLoS One. 2012;7(1):e29794.

408. Padayatty SJ, Sun H, Wang Y, Riordan HD, Hewitt SM, Katz A, et al. Vitamin C pharmacokinetics: implications for oral and intravenous use. Ann Intern Med. 2004;140(7):533-7.

409. Chen Q, Michael GE, Krishna MC, Mitchell JB, Corpe CP, Buettner GR, et al. Pharmacologic Ascorbic Acid Concentrations Selectively Kill Cancer Cells: Action as a Pro-Drug to Deliver Hydrogen Peroxide to Tissues. Proc Natl Acad Sci U S A. 2005;102(38):13604-9.

410. Levine M, Cathy Conry-Cantilena, Wang Y, Welch RW, Washko PW, Dhariwal KR, et al. Vitamin C Pharmacokinetics in Healthy Volunteers: Evidence for a Recommended Dietary Allowance. Proc Natl Acad Sci U S A. 1996;93(8):3704-9.

411. Levine M, Wang Y, Padayatty SJ, Morrow J. A New Recommended Dietary Allowance of Vitamin C for Healthy Young Women. Proc Natl Acad Sci U S A. 2001;98(17):9842-6.

412. Ping S, Liu S, Zhou Y, Li Z, Li Y, Liu K, et al. Protein disulfide isomerase-mediated apoptosis and proliferation of vascular smooth muscle cells induced by mechanical stress and advanced glycosylation end products result in diabetic mouse vein graft atherosclerosis. Cell Death Dis. 2017;8(5):e2818.

413. Goplen D, Wang J, Enger PO, Tysnes BB, Terzis AJA, Laerum OD, et al. Protein Disulfide Isomerase Expression Is Related to the Invasive Properties of Malignant Glioma. Cancer Res. 2006(20):9895-902.

414. Andreu CI, Woehlbier U, Torres M, Hetz C. Protein disulfide isomerases in neurodegeneration: From disease mechanisms to biomedical applications. FEBS Lett. 2012;586(18):2826-34.

415. Xu S, Sankar S, Neamati N. Protein disulfide isomerase: a promising target for cancer therapy. Drug Discovery Today. 2014;19(3):222-40.

416. Lovat PE, Corazzari M, Armstrong JL, Martin S, Pagliarini V, Hill D, et al. Increasing Melanoma Cell Death Using Inhibitors of Protein Disulfide Isomerases to Abrogate Survival Responses to Endoplasmic Reticulum Stress. Cancer Res. 2008;68(13):5363-9.

417. Xu S, Butkevich AN, Yamada R, Zhou Y, Debnath B, Duncan R, et al. Discovery of an orally active small-molecule irreversible inhibitor of protein disulfide isomerase for ovarian cancer treatment. Proc Natl Acad Sci U S A. 2012;109(40):16348-16353.

418. Hoffstrom BG, Kaplan A, Letso R, Schmid RS, Turmel GJ, Lo DC, et al. Inhibitors of protein disulfide isomerase suppress apoptosis induced by misfolded proteins. Nature Chemical Biology. 2010;6(12):900-6.

419. Yu SJ, Bae S, Kang JS, Yoon J, Cho EJ, Lee J, et al. Hepatoprotective effect of vitamin C on lithocholic acid-induced cholestatic liver injury in Gulo(−/−) mice. Eur J Pharmacol. 2015;762:247-55.

420. Ma Y, Chapman J, Levine M, Polireddy K, Drisko J, Chen Q. High-Dose Parenteral Ascorbate Enhanced Chemosensitivity of Ovarian Cancer and Reduced Toxicity of Chemotherapy. Science Translational Medicine. 2014;6(222):222ra18.

421. Chen Q, Michael GE, Sun AY, Je-Hyuk Lee, Krishna MC, Shacter E, et al. Ascorbate in Pharmacologic Concentrations Selectively Generates Ascorbate Radical and Hydrogen Peroxide in Extracellular Fluid in vivo. Proc Natl Acad Sci U S A. 2007;104(21):8749-54.

422. Chen Q, Michael GE, Sun AY, Pooput C, Kirk KL, Krishna MC, et al. Pharmacologic Doses of Ascorbate Act as a Prooxidant and Decrease Growth of Aggressive Tumor Xenografts in Mice. Proc Natl Acad Sci U S A. 2008;105(32):11105-9.

423. Ahn YS, Jy W, Harrington WJ, Shanbaky N, Fernandez LF, Haynes DH. Increased platelet calcium in thrombosis and related disorders and its correction by nifedipine. Thrombosis Research. 1987;45(2):135-43.

424. Nesbitt WS, Giuliano S, Kulkarni S, Dopheide SM, Harper IS, Jackson SP. Intercellular Calcium Communication Regulates Platelet Aggregation and Thrombus Growth. J Cell Biol. 2003;160(7):1151-61.

425. Feil R, Lohmann SM, de Jonge H, Walter U, Hofmann F. Cyclic GMP-Dependent Protein Kinases and the Cardiovascular System: Insights from Genetically Modified Mice. Circ Res. 2003;93(10):907-16.